MOLECULAR AND VIROLOGICAL ANALYSIS OF HIV-ASSOCIATED PERSISTENT GENERALISED LYMPHADENOPATHY (PGL)

Archana Reddy

PhD

University of Edinburgh

2001

DECLARATION

I declare that this thesis has been composed by myself and has not been submitted for any other degree. The work described herein is my own except where otherwise indicated and all work of other authors is duly acknowledged.

Archana Reddy

Faculty of Medicine
Department of Medical Microbiology,
University of Edinburgh Medical School
Teviot Place,
Edinburgh,
EH8 9AG

To Vinoo, my sister and parents

ACKNOWLEDGEMENTS

I would like to thank my supervisor Professor Dorothy Crawford for allowing me the opportunity to do this PhD and for all her help, generosity and support. I convey my deepest gratitude and regard to Dr. Tim Crook without whose continual motivation, friendship, guidance (and valuable reagents!) this project would not have been possible.

I am particularly indebted to Dr. Andrew Krajewsky for providing invaluable control material, Ian Bennet for all his patience with my endless sequencing requests and Dr. Louise Brooks for introducing me to SSCP.

It goes without saying that I could not have completed this project without the morale boosting hugs, kindness and support of my family and friends. A special thanks to Karen for her unstinting assistance, Jill and Maurice for their technical advice and expertise, and the rest of the herpesvirus group for providing help (and laughter!) at the times that I needed it the most.

Finally, I would like to acknowledge the financial support provided by the Overseas Research Scholarship Scheme and the University of Edinburgh.

ABSTRACT

Non-Hodgkin's lymphoma (NHL) represents the second most common cancer affecting individuals infected with Human Immunodeficiency virus (HIV). NHL is 60 to 100 times more likely to develop in AIDS patients than in the general population. The great majority (90-95%) of these are aggressive high-grade B cell lymphomas that respond poorly to chemotherapy, and are associated with a median survival, after diagnosis, of only 4-6 months. Approximately one-third of HIV-infected individuals present early in infection with a syndrome called Persistent generalised lymphadenopathy (PGL). The enlarged lymph nodes of this condition may represent pre-malignant lesions.

The aim of this study was to investigate genetic and virological variables in PGL and to identify early genetic lesions that might be predictive of future lymphoma development in these individuals. Lymph node biopsies from 23 individuals with PGL together with appropriate controls from HIV-uninfected individuals were analysed for alterations in the structure and expression of selected genes.

The results of the study were as follows: i) Mutations in *p53* were detected in 26% of HIV-infected individuals. ii) A distinct pattern of *p73* and *p63* gene expression was observed in the HIV-PGL samples compared to the controls. iii) Structural modifications of the genes on the *INK4* locus were absent. iv) Epigenetic silencing of the *INK4a*, *INK4b*, and *p73* genes was not observed. v) Mutations in *bcl-6* were detected in 48% of HIV-infected individuals and in 12.5% of healthy individuals, along with polymorphic substitutions at nucleotides, +753 and +875. vi) Rearrangements of c-*myc* t(8:14) and *bcl-2* t(14:18) were not observed in either the study or control groups except for a single t(8:14) in the lymph node of a healthy individual. vii) EBV DNA was detected in 100% of HIV-infected individuals and in 86% of healthy individuals. KSHV DNA was detected in 8.7% of HIV-infected individuals and in none of the healthy controls. Based on the findings in this study, a speculative model for the molecular pathogenesis of AIDS-NHL is proposed. This model hypothesises that *p53* and *bcl-6* mutations occur early in lymphomagenesis, whereas activation/deregulation of oncogenes such as c-*myc* and *bcl-2*, and/or inactivation of the tumour suppressor genes of the *INK4* family constitute later events in the development of AIDS-NHL.

CONTENTS

LIST OF FIGURES

LIST OF TABLES

ABBREVIATIONS

aa	Amino acid
AIDS	Acquired Immunodeficiency syndrome
AIDS-BL	AIDS-related Burkitt's lymphoma
AIDS-BLL	AIDS-related Burkitt's-like lymphoma
AIDS-DLCL	AIDS-related diffuse large cell lymphoma
AIDS-NHL	AIDS-related Non-Hodgkin's lymphoma
AIDS-PCNSL	AIDS-related primary central nervous system lymphoma
AIDS-SNCCL	AIDS-related small non-cleaved cell lymphoma
ALL	Acute lymphoblastic leukaemia
AML	Acute myeloid leukaemia
ARF	Alternate reading frame
ARL	AIDS-related lymphoma
ATM	Ataxia telangiectasia mutated gene
ATR	ATM-Rad51 related protein
BARTs	BamH1 A rightward transcripts
b/HLH/Z	Basic/Helix-loop-helix/zipper domain
BL	Burkitt's lymphoma
BLL	Burkitt's-like lymphoma
bp	Base-pair
BPB	Bromophenol blue
$CaCl_2$	Calcium chloride
CD	Cluster designation
CDC	Centers for Disease Control
CDK	Cyclin dependent kinase
cDNA	Complementary DNA
Ci	Curie
CML	Chronic myeloid leukaemia
cm^2	Centimeter squared
CNS	Central nervous system
CO_2	Carbon dioxide

CTL	Cytotoxic T lymphocyte
dATP	2'-Deoxyadenosine 5'-triphosphate
°C	Degrees Celsius
dCTP	2'-Deoxycytidine 5'-triphosphate
DEPC	Diethylpyrocarbonate
dGTP	2'-Deoxyguanosine 5'-triphosphate
dH_2O	Distilled water
DMF	Dimethylformamide
DMSO	Dimethylsulphoxide
DNA	Deoxyribonucleic acid
dNTPs	Deoxynucleoside 5'-triphosphates
DTT	Dithiothreitol
dTTP	2'-Deoxythymidine 5'-triphosphate
EBERs	Epstein-Barr encoded RNAs
EBNA	Epstein-Barr nuclear antigen
EBV	Epstein-Barr virus
EDTA	Ethylene diamine-tetraacetic acid
EtBr	Ethidium bromide
FCS	Fetal calf serum
FITC	Fluorescein isothiocyanate
FLICE	FADD homologous ICE/CED-3-like protease
FLIP	FLICE- inhibitory protein
g	G-number
GPCR	G protein-coupled receptor
HAART	Highly active antiretroviral therapy
HCl	Hydrochloric acid
HD	Hodgkin's disease
HEPES	N-2-Hydroxyethylpiperazine-N'-2-ethanesulfonic acid
HHV-6	Human herpesvirus 6
HIV	Human Immunodeficiency virus
hMDM2	human homologue of mouse double-minute
IBL	Immunoblastic lymphoma

IFN	Interferon
Ig	Immunoglobulin
IgH	Immunoglobulin heavy chain
IL	Interleukin
INK4	Inhibitors of cyclin dependent kinase 4
IPTG	Isopropylthio- β- D galactoside
kb	Kilobase
KCl	Potassium chloride
kDa	Kilodalton
Kg	Kilogram (10^3)
KS	Kaposi's sarcoma
KSHV	Kaposi's sarcoma-associated herpesvirus
L	Litre
LB	Luria Bertani medium
LCL	Lymphoblastoid cell line
LMP	Latent membrane protein
LNCCL	Large non-cleaved cell lymphoma
LTR	Long Terminal Repeat
m	Milli (10^{-3})
M	Molar (moles per litre)
MALT	Mucosa-associated lymphoma tissue
MCD	Multicentric Castleman's disease
MDM2	Mouse double-minute
mg	milligram
$MgCl_2$	Magnesium chloride
μ	Micro (10^{-6})
ml	millilitre
ML	Myeloid leukaemia
MM	Multiple myeloma
MMLV-RT	Moloney Murine Leukemia Virus reverse transcriptase
mRNA	Messenger RNA
n	Nano (10^{-9})

NaCl	Sodium chloride
$NaHCO_3$	Sodium bicarbonate
NaOH	Sodium hydroxide
NHL	Non-Hodgkin's lymphoma
NPC	Nasopharyngeal carcinoma
OD	Optical density
ORF	Open reading frame
p	Pico (10^{-12})
PBMCs	Peripheral blood mononuclear cells
PBS	Phosphate buffered saline
PEL	Primary effusion lymphoma
PGL	Persistent generalised lymphadenopathy
POZ	poxvirus and zinc finger domain
PTLD	Post-transplant lymphoproliferative disorder
PVP	Polyvinylpyrolidine
RNA	Ribonucleic acid
RNase	Ribonuclease
rpm	Revolutions per minute
RPMI	Roswell Park Memorial Institute
RT	Reverse transcriptase
SDS	Sodium dodecyl sulphate
SDW	Sterile distilled water
SSC	Standard saline citrate
TE	Tris-EDTA
TEMED	N,N,N',N', Tetramethylethylenediamine
TGFβ	Transforming growth factor β
Tris	Tris (hydroxymethyl) aminomethane
Tween20	Polyoxethylene(20)-sorbitan monolaurate
UV	Ultraviolet
v/v	Volume per volume
w/v	Weight per volume
X-Gal	5 bromo-4 chloro-3 indolyl-β-D galactoside

CHAPTER ONE

INTRODUCTION

1.1 Human Immunodeficiency virus (HIV)

The World Health Organisation (WHO) and the Joint United Nations Programme on HIV/Acquired Immunodeficiency Syndrome (UNAIDS) estimated that at the end of 2000 over 36.1 million people were living with the Human Immunodeficiency virus (HIV), with 5.3 million new infections occurring world-wide in that year alone (UNAIDS/WHO, 2000). HIV belongs to the family *Retroviridae* and subfamily *Lentivirinae*. Since its discovery, (Barre-Sinoussi *et al.*, 1983; Gallo *et al.*, 1984) this retrovirus, recognised because of its association with AIDS, has claimed more than 21 million lives (UNAIDS/WHO, 2000). However, with the inception of highly active antiretroviral therapy (HAART), or triple "cocktail" therapy in 1995, deaths from AIDS in the United States have declined by 44%, along with the frequency of hospitalisations and the incidence of major AIDS-related opportunistic infections (Palella *et al.*, 1998). However, in developing countries the full impact of HAART has not been realised due to cost implications, and hence HIV continues to be a major cause of infectious death in these countries.

1.1.1 Structure and genome organisation of the virus

The structure of the virus is depicted in Figure 1 and reviewed in (Levy, 1993; Luciw, 1996; see figure 1). The HIV genome is about 9.8kb in length and is comprised of nine genes that are flanked by long terminal repeat (LTR) elements (figure 2). These include the *gag*, *pol* and *env* genes that are common to all replication-competent retroviruses as well as the regulatory genes *Tat* and *Rev* and the accessory genes *Nef, Vif, Vpr and Vpu*. The protein products of these genes are translated from different RNAs produced through the use of ribosomal frame-shifting and alternative splice sites (reviewed in Luciw, 1996; see figure 2).

1.1.2 Tropism and spread

HIV primarily infects activated $CD4^+$ cells (T-cell tropic) through binding of viral gp120 to the CD4 molecule, and terminally differentiated cells of the macrophage lineage (M-tropic). The virus however, has a diverse cellular host range (reviewed in Levy, 1993). Sequence variation within a region of the gp120 molecule, called the

Figure 1. Structure of HIV

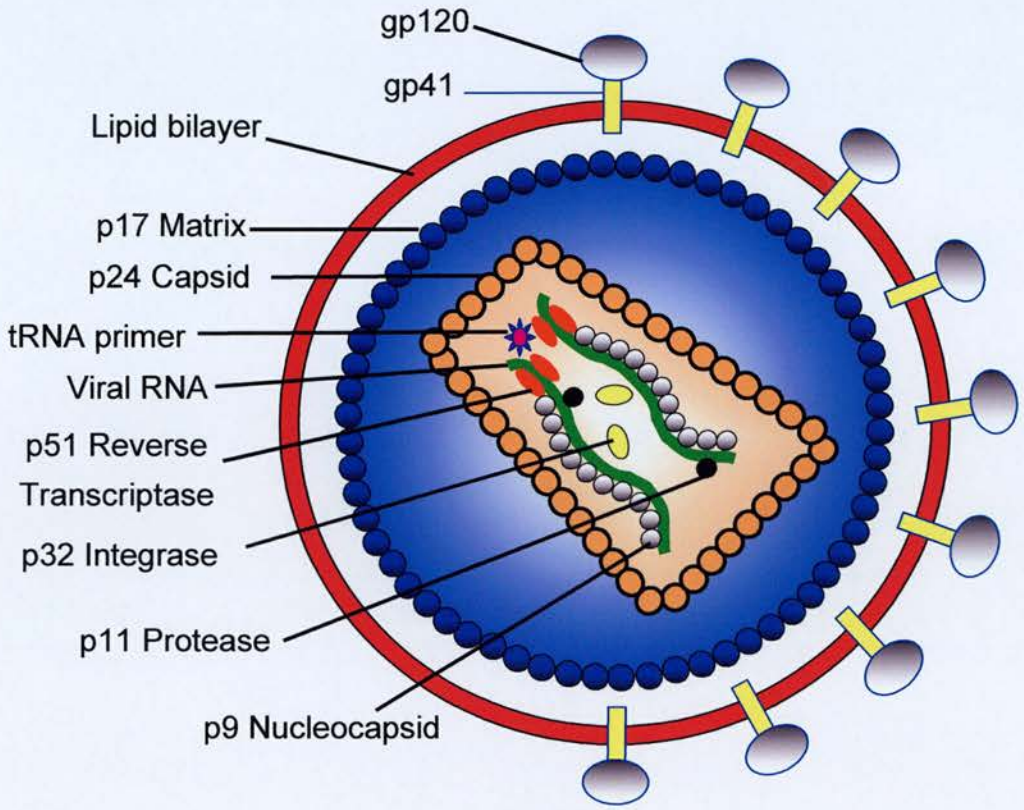

The HIV virion is spherical with a diameter of approximately 110nm. A lipid bilayer envelope encapsulates a cone-shaped core. Projecting from the envelope surface are 72 knob-like structures, which are heterodimers of the envelope glycoproteins, gp120 and gp41. The core contains two identical molecules of single-stranded RNA, with which the virally encoded enzymes, RNA-dependent DNA polymerase or reverse transciptase (RT), integrase (IN) and protease (PR), are associated. The protein products of the *gag* polyprotein gene provide the structure and integrity of the virion. They include the matrix protein (MA), located between the nucleocapsid and the envelope, the capsid protein (CA), and the nucleocapsid protein (NC) that is closely coupled with the RNA genome.

Adapted from *Fields Virology*, Edited by Fields *et al.*, 1996, Philadelphia:Lipincott-Raven.

Figure 2. Genome organisation of HIV-1

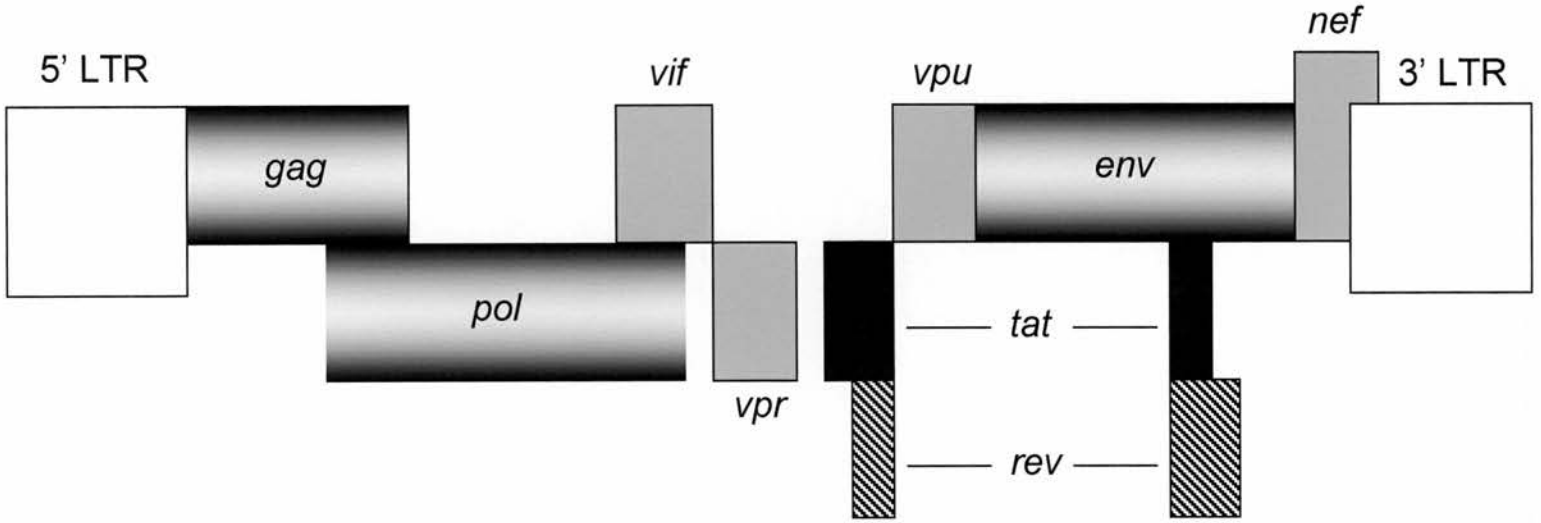

The *gag*, *pol* and *env* genes constitute the virion structural genes and are heavily shaded. The accessory genes *vif*, *vpu*, *vpr* and *nef* are shown in grey and the regulatory genes include *tat* (black boxes) and *rev* (striped boxes). The 5' and 3' LTR regions are shown as open boxes.
LTR: Long terminal repeat

Adapted from *Fields Virology*, Edited by Fields *et al.*, 1996, Philadelphia:Lipincott-Raven

V3 loop plays an important role in influencing biological properties of the virus such as cell tropism, syncytium formation, infectivity and cytopathicity (Stamatatos and Cheng-Mayer 1993; Willey *et al.*, 1994)

HIV can be transmitted both vertically (mother to child) and horizontally through sexual exposure, contaminated blood and blood products, or sharing of needles by intravenous drug users (IVDUs) (reviewed in Levy, 1993).

1.1.3 Clinical course of HIV infection

Primary infection provokes an acute mononucleosis-like illness with fever, sore throat, headache, rash, lymphadenopathy and malaise, which lasts between 1-3 weeks. This phase is characterised by high-level virus replication in the activated lymphocytes in the lymph nodes, simultaneous with a transient decrease in $CD4^+$ cell counts and increase in $CD8^+$ cell numbers.

A marked reduction in viremia due to a highly active cytotoxic T cell (CTL) immune response and a rise in $CD4^+$ T cell numbers coincide with the clinically latent or asymptomatic period, which averages around 10 years (Bacchetti and Moss, 1989). Neutralising antibodies, particularly against the V3 loop of gp120 are detectable after seroconversion, although they are not as effective as the cellular response in the control of viral infection. During this period equilibrium is established between the virus and host immunity, and the set point of this steady state predicts clinical outcome. Thus, low viral load correlates with long clinical latency whereas a high viral burden predicts a short latent period (Mellors *et al.*, 1996). Viral replication, however, continues over the entire course of infection (Ho *et al.*, 1995) with proviral load in the lymphoid tissues being 5-10 times greater than in peripheral blood, suggesting that the lymphoid germinal centres serve as important reservoirs of viral RNA (Pantaleo *et al.*, 1993).

The terminal phase of HIV infection, characterised by the onset of AIDS, is marked by a sudden increase in viremia due to decline in host CTL immune responses. Progressive depletion of $CD4^+$ T cells is the defining feature of immunodeficiency (Lang *et al.*, 1989). At this stage opportunistic infections and/or malignancies occur and death ensues in an average of 15 months.

1.1.4 HIV-associated Persistent Generalised Lymphadenopathy (PGL)

PGL is a frequent finding of early HIV infection, and is present in more than one-third of infected patients in some studies (Gerstoft *et al.*, 1987; Metroka *et al.*, 1983). PGL is defined by the Centers for Disease Control (CDC) as "unexplained lymphadenopathy of longer than 3 months duration, in two or more extrainguinal sites, in the absence of any intercurrent illnesses known to cause adenopathy".

1.1.4.1 Morphology of lymph nodes in PGL

Morphologically the abnormal lymph nodes exhibit a characteristic B cell hyperplasia and dysplasia (Meyer *et al.*, 1984). Distinct histological stages (I to III) have been described, although the change may be gradual, with lack of clear markers of transition from one stage to the next.

Stage I is characterised by florid follicular hyperplasia, with mantle zone depletion and lymphocyte infiltration, particularly $CD8^+$ T cells, which frequently invade and fragment the follicular centres. The lymph node sinuses frequently contain clusters of monocytoid B cells, which represent reactive B lymphocytes derived from the marginal zone. Stage II is characterised by a decrease in the number of follicles with the remainder showing involution. This is accompanied by a decrease in lymphocytes and an increase in plasma cells in the interfollicular areas. In Stage III there is complete destruction of lymph node architecture with remnants of the dendritic reticulum cells. The "burned-out" lymph nodes are usually small and depleted of both T and B lymphocytes.

Follicular hyperplasia, with follicular fragmentation and disruption are non-specific changes commonly seen in a number of benign conditions and immunodeficiencies. However, thinning of the mantle zone and marked depletion of the lymphocytes is pathognomonic of HIV lymphadenitis, and may be used in the differential diagnosis of this syndrome (Chadburn *et al.*, 1989; Jaffe *et al.*, 1985; Pallesen *et al.*, 1987). A further distinguishing feature of lymphadenopathy in HIV-infected individuals is the increased production of interferon γ (IFN-γ) by the $CD8^+$ cells of these lymph nodes, which is believed to promote B cell proliferation (Boyle *et al.*, 1993).

The clinical and immunological status at the time of biopsy in HIV-infected PGL individuals correlates significantly with histological lymph node changes. In the

study by Gerstoft *et al.*, all patients with opportunistic infections and AIDS-related complex were found to have Stage III histology. Furthermore, they also had significantly fewer $CD4^+$ cells and inverted $CD4^+$: $CD8^+$ ratios compared to Stage I individuals. Consistent with the polyclonal hypergammaglobulinemia observed in these patients, serum IgA and IgM levels were significantly higher in Stage III individuals compared with Stage I individuals, perhaps reflecting secondary infection with opportunistic pathogens (Gerstoft *et al.*, 1987).

1.1.4.2 Role of viruses in the pathogenesis of PGL

Only limited studies have been carried out to investigate the role of B cell tropic viruses such as Epstein-Barr virus (EBV) in the germinal centre B cell activation and hyperproliferation that is characteristic of PGL. Using molecular and *in situ* techniques, some investigators have suggested that the B cells of these abnormal nodes are very rarely infected with EBV or HIV (Boyle *et al.*, 1992; Uccini *et al.*, 1989). These findings however, were contradicted by the detection of EBV and HIV in PGL lymph nodes using sensitive PCR techniques (Ometto *et al.*, 1997; Shibata *et al.*, 1991; Armstrong and Horne 1984; Tenner-Racz *et al.*, 1986). Despite detection of these viruses in the lymph nodes of individuals with PGL, there is no direct evidence suggesting that they contribute to the B cell proliferation observed.

1.1.5 AIDS-related lymphomas (ARL)

1.1.5.1 Incidence

Lymphoma was incorporated into the CDC case definition of AIDS in 1985, and is now recognised as the second most common malignancy affecting HIV-positive women and homosexual men (second only to Kaposi's sarcoma [KS]), and the most frequently diagnosed cancer in other HIV transmission groups (CDC, 1985; Beral and Newton 1998).

The National Cancer Institute (NCI) estimates that between 8% and 27% of the approximately 50,000 cases of Non-Hodgkin's lymphomas (NHL) diagnosed yearly in the United States are HIV-related (Gail *et al.*, 1991). HIV-infected individuals are 60 times more likely to develop NHL (Beral, 1991), and 10 times more likely to

to develop Hodgkin's disease (HD) than the general population (Beral, 1991; see Table 1). Although the advent of HAART has been associated with a significant decline in common HIV-1 associated opportunistic infections and KS, the effect of HAART on AIDS-related NHL (AIDS-NHL) is still unclear (Palella *et al.*, 1998).

Table 1

Relative risk of AIDS-related lymphoma compared with the general population

Lymphoma type	Relative risk (Fold-increase over general population)
Non-Hodgkin's lymphoma	60
Burkitt's	220
Diffuse large-cell	145
Immunoblastic	627
Primary central nervous system	1000
Hodgkin's disease	10

Adapted from Beral and Newton (1998) and Levine (2000).

1.1.5.2 Histopathological classification of AIDS-NHL

90-95% of AIDS lymphomas are of B cell origin, and comprise a spectrum of lesions ranging from polyclonal lymphoid hyperplasia to high-grade malignancies most frequently of the diffuse large-cell type (Levine *et al.*, 1985). The two most common histological types of AIDS-NHL are diffuse large-cell lymphomas (AIDS-DLCL) and small non-cleaved cell lymphomas (AIDS-SNCCL) that differ in regard to the time of onset, EBV positivity, molecular genetic features, and histogenetic derivation. Anaplastic $CD30^+$ large-cell lymphomas (Nosari *et al.*, 1996), as well as primary effusion lymphomas containing KSHV (Cesarman *et al.*, 1995) have also been described in the spectrum of AIDS-NHL, but are less frequently observed.

1.1.5.3 Clinical classification of AIDS-NHL

In addition to the histological classification described above, AIDS-NHL may also be broadly classified on the primary site of presentation as systemic lymphoma, constituting 80% of all AIDS-NHL, and central nervous system (CNS) lymphoma comprising the remaining 20%. Clinically, disease presentation is that of an aggressive tumour with frequent extranodal involvement and poor response to

chemotherapy. Prognosis of patients with AIDS-NHL has been associated with extent of disease and extranodal involvement, severity of underlying immunodeficiency (measured by $CD4^+$ lymphocyte count in the peripheral blood) and prior AIDS diagnosis (history of opportunistic infection or KS). Individuals with CNS lymphoma have more severe underlying disease than those with systemic lymphomas as shown by higher incidence of prior AIDS diagnoses (73% vs. 37%), lower median $CD4^+$ cell count (30/dL versus 189/dL), and a worse median survival time (2.5 months vs. 6.0 months) (Levine *et al.*, 1991).

1.1.5.3.1 AIDS-related systemic NHL

Systemic NHLs arise in patients with a wide range of immune function. 70% of cases occur in persons with a $CD4^+$ lymphocyte count higher than $50x10^6$/L and approximately 30% in persons with a $CD4^+$ count in excess of $200x10^6$/L (Levine *et al.*, 1991). Extranodal presentation commonly occurs (87-95% of individuals) at a variety of sites. The CNS, bone marrow, gastrointestinal tract and liver are involved in 42%, 33% 27% and 12% of cases respectively. The vast majority of patients present with systemic 'B' symptoms, which include unexplained fever, drenching night sweats and/or weight loss in excess of 10% of normal body weight (Kaplan *et al.*, 1989). Prognostic criteria predicting shorter survival in patients with AIDS-NHL constitute age greater than 35 years, $CD4^+$ count less than $100x10^6$/L, elevated serum LDH levels and history of intravenous drug use (Straus *et al.*, 1998). Treatment of systemic disease is problematic, although recently, combination chemotherapy in conjunction with HAART has been found to improve prognosis (Ratner *et al.*, 2001).

(i) AIDS-related small non-cleaved cell lymphoma (AIDS-SNCCL)

These lymphomas represent 20-30% of AIDS-NHL, and develop in the presence of relatively high $CD4^+$ counts (>$200x10^6$/L) (Boyle *et al.*, 1990). According to the Revised European American Lymphoma (REAL) classification, SNCCL is further categorised into Burkitt's lymphoma (BL) or high-grade Burkitt's-like lymphoma (BLL) (Chan *et al.*, 1994). AIDS-BLL is a distinct histological entity and morphologically intermediate between typical BL and DLCL, with immunoblastic features (Carbone *et al.*, 1995).

(ii) AIDS-related diffuse large cell lymphoma (AIDS-DLCL)

AIDS-DLCL is sub-divided into AIDS-related large non-cleaved cell lymphoma (LNCCL) and AIDS-related immunoblastic lymphoma (IBL), and constitutes approximately 70% of AIDS-NHL (Gaidano and Dalla-Favera 1995). These lymphomas arise in the setting of severe immunosuppression and are more heterogeneous than AIDS-SNCCL (Boyle *et al.*, 1990).

1.1.5.3.2 AIDS-related primary central nervous system lymphoma (AIDS-PCNSL)

These tumours predominantly have a large-cell histology (Camilleri-Broet *et al.*, 1997) and arise in the advanced stages of HIV infection when $CD4^+$ T lymphocyte counts fall below $50x10^6$/L. Up to 75% of these individuals exhibit a previous AIDS-defining diagnosis, in contrast to those with systemic lymphoma (37%) (Levine *et al.*, 1991).

PCNSL lesions usually occur as solitary or multiple parenchymal lesions in a perivascular cuffing pattern (Camilleri-Broet *et al.*, 1997). About half of the patients diagnosed with PCNSL present with focal neurological problems such as seizures, headache, memory loss, as well as systemic symptoms of diarrhoea, weight loss and fatigue (Rosenblum *et al.*, 1988). Symptoms are often indistinguishable from those of an opportunistic infection, central nervous system toxoplasmosis. Traditional treatment involves corticosteroids, followed by whole-brain radiation, but a key aspect of control is immune restoration in these patients through HAART (McGowan and Shah, 1998).

1.1.5.4 HIV-associated Hodgkin's disease (HIV-HD)

Unlike NHL and KS in the setting of HIV-associated immunodeficiency, Hodgkin's disease is not considered an AIDS-defining diagnosis by the CDC (CDC, 1993). Although most patients have not had an AIDS-defining diagnosis prior to the onset of HD, between 36-83% have had a history of PGL (Andrieu *et al.*, 1993). HIV-HD is usually aggressive, with widely disseminated disease and bone marrow involvement in up to 50% of cases (Rubio, 1994). Most patients present with mixed cellularity or lymphocyte-depleted Hodgkin's disease, systemic 'B' symptoms, and a

median $CD4^+$ count of $300x10^6$/L or less. Median survival time is between 8 and 18 months. Death in these patients is not due to Hodgkin's disease (most patients respond to chemotherapy regimens and granulocyte colony stimulating factor), but rather to opportunistic infections or other HIV-related malignancies (Levine, 1998).

1.1.5.5 Human herpes virus-6 (HHV-6) and AIDS-NHL

A causative role for HHV-6 in AIDS-NHL has been suggested (Corbellino *et al.*, 1993; Lusso and Gallo, 1994). Although low copy numbers of HHV-6 DNA have been found in lymphadenopathies associated with HIV infection, the prevalence of HHV-6 DNA in B cell AIDS-NHL was found to be lower or similar to that observed in lymphoproliferative disorders from HIV-uninfected individuals (Dolcetti *et al.*, 1996; Fillet *et al.*, 1995). These studies therefore argue against a strong association between HHV-6 infection and pathogenesis of AIDS-NHL.

1.2 The Cell Cycle

The cell cycle is typically characterised by four stages: **G1-S-G2-M**; G1 and G2 signify the gap phases of the cycle, S the phase of DNA synthesis and M the mitotic phase. In addition to these 4 phases there are two major control points: one towards the end of G1, known as the restriction point, and the other at the initiation of mitosis. G2 cells deprived of growth factors before the restriction point exit the cell cycle and enter G0.

Homeostasis in an organism is maintained by a fine balance between cell proliferation and cell death, both of which are controlled by the sequential assembly and activation/inactivation of crucial cell cycle regulators. Some of the genes encoding these growth regulators are directly involved in tumourigenesis and constitute the cancer-related genes such as the oncogenes, tumour suppressor genes, apoptosis regulators and DNA repair genes.

Tumour suppressor genes, refers to a group of growth regulators that are capable of suppressing tumour formation. Knudson's two-hit hypothesis for tumour suppressors requires inactivation of both alleles by deletion or mutation, before loss of function can occur (Knudson, 1971). A mutated tumour suppressor gene comprises one of

many selected genetic events found in cancer progression, and may serve either as an *initiator* (in the case of germline mutation) or a *progressor* in tumour progression. Sections 1.3 to 1.5 will focus on the tumour suppressor genes, *p53*, the *INK4* family (*INK4a*, *INK4b* and *ARF*), and the newly discovered *p53* family members, *p63* and *p73*, some of which are believed to contribute to the pathogenesis of AIDS-NHL.
p53 and *ARF* function both at the restriction point and at the mitotic checkpoint, whereas the *INK4a* and *INK4b* genes and their protein products $p16^{INK4a}$ and $p15^{INK4b}$ have a key role in regulating G1/S transition (see sections 1.3 to 1.5 and figure 3).

1.3 p53

TP53 is the most intensively studied gene in cancer biology. Its protein product, p53, was first identified (in 1979), as a cellular protein tightly complexed to simian virus 40 large T antigen (SV40T) (Lane and Crawford, 1979). p53 is now known to be a pivotal regulatory protein, a potent tumour suppressor and a multifunctional homotetrameric transcription factor (reviewed in Levine, 1997).

1.3.1 Structure of p53

TP53, found on chromosome 17p13 is 20kb in length and has 11 exons, the 1^{st} of which is non-coding. The gene gives rise to a 2.8kb mRNA transcript, which encodes a 53 kilodalton (kDa) nuclear phosphoprotein, of 393 amino acids (aa) (Lamb and Crawford, 1986). Sequence analysis has revealed the existence of five evolutionarily conserved domains in exons 1,4,5,7 and 8 (Soussi *et al.*, 1990 and see figure 4).
The protein is divided structurally and functionally into three domains: the transactivation domain, the sequence-specific DNA-binding domain and the oligomerisation domain. The first 42aa constitute the acidic N-terminal transcriptional activation domain that allows p53 to recruit basic transcriptional machinery and subsequently activate expression of target genes. This region is also critical for regulating the stability and activity of p53 via interactions with proteins such as the human form (hMDM2) of the mouse double-minute (MDM2) protein and viral oncoproteins (Lin *et al.*, 1995; Lohrum and Vousden, 1999). The core domain localised between aa residues 102 and 292 is principally involved in the sequence

Figure 3. The Cell Cycle

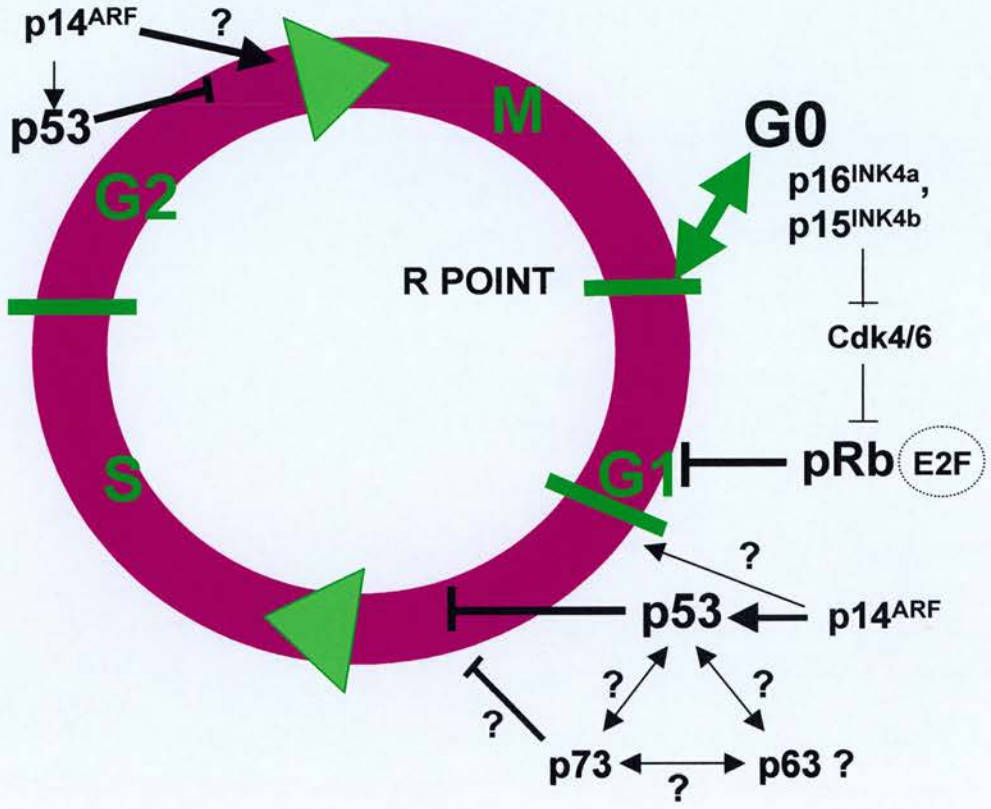

Schematic representation of the cell cycle indicating the points of action of p53 and its family members, p63 and p73, as well as members of the *INK4* gene family, $p16^{INK4a}$, $p14^{ARF}$ and $p15^{INK4b}$.

The 4 stages of the cell cycle are depicted as G1 (Gap phase 1), S (DNA synthesis), G2 (Gap phase 2) and M (mitosis). G0 represents point of exit of the cell from the cell cycle. The green triangles represent the direction of the cell cycle. The p53 and $p14^{ARF}$ tumour suppressor proteins function both at the G1/S and G2/M checkpoints. p53 acts to arrest the cell cycle at both these checkpoints by inducing either growth arrest or apoptosis, whereas $p14^{ARF}$ can arrest the cell cycle via p53-dependent and independent pathways. The INK4 proteins ($p16^{INK4a}$ and $p15^{INK4b}$) specifically bind to and inhibit the kinase activities of CDK4/6 and their association with the D-type cyclins. This interaction prevents the phosphorylation of pRb (and release of E2F), the primary substrate of the cyclin/CDK4 complex, with subsequent growth arrest at G1. Similar to p53, p73 can arrest cells at G1. The role of p63 in the progression of the cell through the cell cycle is presently unknown.

R point: Restriction point **pRb:** Retinoblastoma protein **?:** unclear

Figure 4. Structure of p53

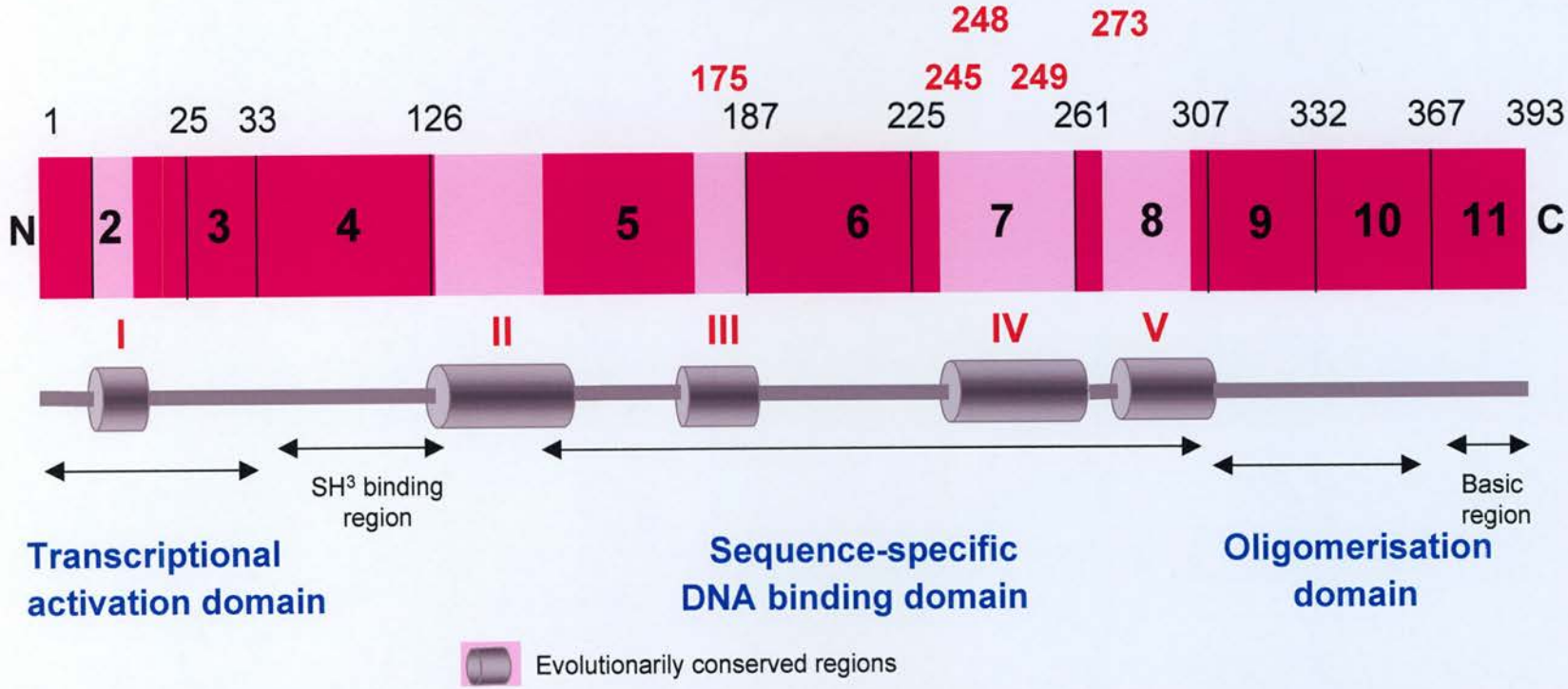

The p53 protein has 11 exons and is composed of 393 amino acids. The 1st exon, which is non-coding, is not shown. Amino acid numbers comprising each exon are shown above the protein. The protein is divided functionally into 3 domains: the N-terminal transactivation domain, the core sequence-specific DNA-binding domain and the C-terminal oligomerisation domain. The five evolutionarily conserved regions (I-V) of the protein are indicated by grey cylinders and pale pink boxes. Mutation "hot-spots" within regions III-V, are shown in red. The SH^3 binding region, separating the N-terminus and the core domain, and a 30 amino acid region rich in basic residues at the extreme C-terminus are also indicated.

specific DNA binding function of p53. The minimal p53 binding site consists of 2 copies of the consensus sequence 5'-PuPuPuC(A/T) (T/A)GPyPyPy-3', separated by 0-13 base pairs (el Deiry *et al.*, 1992). A region of proline repeats that allows interactions with signal transduction molecules containing a *src*-homology binding region, separates this domain from the N-terminus (Gorina and Pavletich, 1996; see figure 4).

Sequence-specific binding by the core domain is negatively regulated by the C-terminus, which can bind DNA non-specifically (Wang *et al.*, 1993). Such inhibitory activity is relieved upon exposure to stress, which results in increased DNA binding (Hupp and Lane, 1995). The C-terminus is further sub-divided into three regions; a flexible linker connecting the DNA binding domain to the oligomerisation domain, the oligomerisation domain (aa residues 320 to 360) and a regulatory region (30aa) composed predominantly of basic residues. The basic region can allosterically regulate conversion of p53 from the latent form (with respect to DNA binding) to one that is active for sequence-specific DNA binding (Hupp and Lane, 1994). This region also serves to recognise DNA damage and promote DNA strand re-annealing (Gottlieb and Oren, 1996).

1.3.2 Physiological role of p53

In unstressed cells, p53 is expressed at low levels and has a short half-life due to rapid turnover mediated by ubiquitination and proteolysis. The protein is stabilised following various cellular stresses, including ionising and ultraviolet radiation, DNA damage, hypoxia, ribonucleotide depletion, binding of viral proteins (SV40T, Adenovirus E1B) and deregulated expression of oncogenes (e.g *ras*, c-*myc* and *E2F*) (Lohrum and Vousden, 1999). The activation of p53 allows it to carry out its growth regulatory function(s) such as cell-cycle arrest, apoptosis, DNA repair, inhibition of DNA replication, senescence, differentiation, and anti-angiogenesis (Levine, 1997).

A major regulator of p53 levels in normal cells is hMDM2, which functions as an E3 ubiquitin ligase (Kubbutat *et al.*, 1997) and negatively regulates p53 in an autoregulatory feedback loop (Wu *et al.*, 1993). This protein mediates shuttling of p53 from the nucleus to the cytoplasm where it is degraded by ubiquitin-mediated proteolysis (Haupt *et al.*, 1997; Kubbutat *et al.*, 1997), and this requires the

interaction of hMDM2 with a transcriptional co-activator p300 (Grossman *et al.*, 1998). Proteolysis of p53 by this mechanism can be rescued by an alternative protein product of the *INK4a* locus, $p14^{ARF}$ (ARF), which binds and represses hMDM2 (Pomerantz *et al.*, 1998; Ko and Prives, 1996; see below).

1.3.3 The p53 signalling pathway

p53 functions to integrate cellular responses to stress and effects growth arrest and apoptosis through transactivation of target genes (see below and figure 5).

(i) Upstream events that signal to p53

There is now accumulating evidence that DNA damage and stress stimuli lead to the phosphorylation of p53 at both the N- and C-termini. Such modifications both stabilise the wild-type protein and increase its activity. These phosphorylation events are effected by serine and threonine kinases, including ATM, ATR, and CHK2 (Canman *et al.*, 1998; Tibbetts *et al.*, 1999; Hirao *et al.*, 2000). N-terminal phosphorylation is believed to induce conformational changes that affect the interaction of p53 with other proteins, including hMDM2 (Shieh *et al.*, 1997). In addition, covalent modification at regulatory sites within the C-terminus, such as phosphorylation, *O*-glycosylation and acetylation, is known to stimulate DNA binding by the central core region (Jayaraman and Prives, 1999). Furthermore, p53 appears to be connected to DNA repair processes through non-covalent modification of the C-terminus by components of the DNA repair machinery such as Rad51 and Ref1 (Jayaraman and Prives, 1999; Prives and Hall, 1999).

(ii) Downstream effectors of p53 function

p53 functions primarily as a transcriptional regulator (Crook *et al.*, 1994) and its activity is profoundly influenced by several co-activator and co-repressor proteins. Considerable complexity and cell-type differences exist in the spectrum of genes that are regulated by p53. The diverse biological functions of p53 (Levine, 1997; Ko and Prives, 1996 and see above) are beyond the scope of this thesis and this section will focus primarily on the growth arrest and apoptotic functions of this protein.

Figure 5. Signalling to and from p53

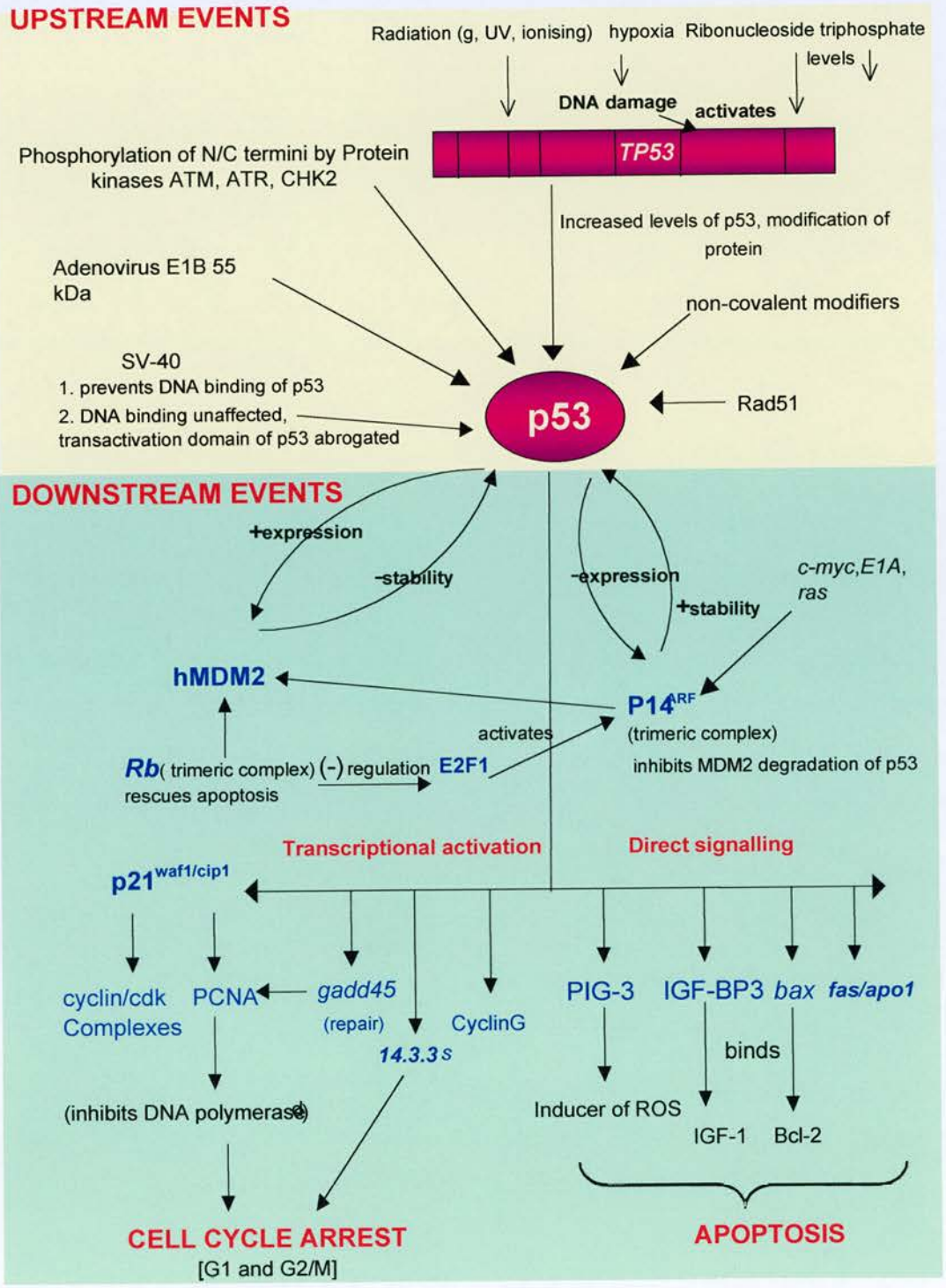

Figure 5. Signalling to and from p53. Events that signal to p53 and those that act downstream of the protein to effect growth arrest and apoptosis are shown in the yellow and green boxes, respectively.

The protein is activated in response to DNA damage that is induced by stress signals (e.g radiation, hypoxia and reduction in triphosphate levels). This leads to the stabilisation of the protein through modification by phosphorylation at the N- and C-termini by kinases, ATM, ATR, CHK2, or by non-covalent modification of the C-terminus by components of the DNA repair machinery (e.g. Rad51). Furthermore, stabilisation is also effected by expression of viral proteins such as SV40 Large T and Adenovirus E1B.

The hMDM2 and $p14^{ARF}$ proteins function in negative and positive feedback loops with p53 respectively. The expression of these proteins is regulated by p53, and they in turn control the stability of p53. $p14^{ARF}$ can induce p53 accumulation by inhibiting hMDM2-mediated degradation of p53. In addition, the transcription factor E2F-1, the retinoblastoma protein (pRb), and viral and cellular oncogenes (e.g. adenoviral E1A c-*myc* and *ras*) can stabilise p53 through the upregulation of $p14^{ARF}$.

Events occurring downstream of p53 to effect growth arrest and apoptosis include transcriptional activation of the $p21^{waf1}$, which induces growth arrest either by inhibiting the function of the CDK4/cyclin D complex, or by binding to the proliferating cell nuclear antigen (PCNA). Other genes that mediate G1 and G2 growth arrest include growth arrest and DNA-damage inducible gene #45 (GADD45), *14-3-3*σ, and cyclin G.

Apoptosis is induced via the upregulation of a number of pro-apoptotic proteins. These include Bax (*bcl-2* gene family), death receptors such as CD95/Fas and DR5/Killer, the insulin growth factor-binding protein 3 (*IGF-BP3*) gene and the p53-inducible genes (*PIGs*).

The choice between effecting cell-cycle arrest or apoptosis by p53, upon sensing DNA damage, is dependent on the cell-type, intensity of the DNA damage inducer, efficiency of DNA repair mechanisms, growth and survival factors, and the levels of p53 protein itself (Gottlieb and Oren, 1998). p53 mediates arrest of cells at the G1/S boundary mainly by transactivating the wild-type p53-activated fragment-1 (WAF1) gene or p21 which inhibits the function of the CDK4-cyclin D complex. p21 also binds to the proliferating cell nuclear antigen (PCNA) and can inhibit the processivity of DNA replication. Other genes, including the growth arrest and DNA-damage inducible gene #45 (*gadd45*), *14-3-3σ*, and *cyclin G*, have emerged as potential mediators of p53-dependent G1 and G2 arrest (reviewed in el Deiry, 1998; see figure 5).

Overexpression of wild-type p53 causes apoptosis in a wide variety of cell types, and this occurs both by sequence-specific, transactivation-dependent (SST) and independent mechanisms (Caelles *et al.*, 1994). *Bax*, a pro-apoptotic protein, was first identified as a candidate effector of p53-mediated apoptosis, although its induction is cell-type specific (Miyashita and Reed, 1995). Subsequently, death receptors such as CD95/Fas and DR5/Killer and genes containing p53-binding sites such as the insulin growth factor-binding protein 3 (*IGF-BP3*) gene, p53-inducible genes (*PIGs*), and the *c-fos* gene have been identified as mediators of p53-dependent apoptosis (reviewed in Gottlieb and Oren, 1998; Bates and Vousden, 1999; see figure 5). Viral proteins such as SV40T, adenovirus E1B and HPV E6 can antagonise the apoptotic function of p53 by targeting it for degradation or repressing its transcriptional ability (Mietz *et al.*, 1992; reviewed in Gottlieb and Oren, 1996).

1.3.4 The role of p53 in carcinogenesis

Mutations involving *p53* are the most common genetic alteration yet described in human cancer, occurring in approximately 50% of all human cancers (Hollstein *et al.*, 1991). More than 90% of mutations occur in the DNA-binding domain of p53. Such mutations either alter critical residues involved in DNA contact or modify the structural conformation of the protein, with subsequent loss of ability to function as a transcription factor. More than 40% of all mutations in *p53* occur in residues R175, G245, R248, R249, R273, and R282 ('hot-spots'), which play a critical role in the

structural integrity of this domain (Hollstein *et al.*, 1991, 1994).

The contribution of wild-type p53 to tumour suppression has been clearly demonstrated in p53 null mice which develop normally but are highly prone to spontaneous tumours later in life (Donehower *et al.*, 1992). A similar propensity for spontaneous tumours has also been observed in an inherited cancer syndrome, Li-Fraumeni syndrome, wherein affected individuals carry a mutated p53 allele in their germline in addition to a wild-type allele (Srivastava *et al.*, 1990).

p53 commonly conforms to Knudson's two-hit hypothesis (Knudson, 1971), wherein heterozygous loss of the short arm of chromosome 17 (LOH) containing p53 is often accompanied by point mutations in the remaining allele and vice-versa (Vogelstein *et al.*, 1988; Takahashi *et al.*, 1989). The spectrum of mutations is strongly biased in favour of missense point mutations, which produce a stable protein lacking the transactivating function of the wild-type protein (el Deiry *et al.*, 1992; Kern *et al.*, 1992). 3 classes of mutant p53 exist, which have distinct biological activities (Halevy *et al.*, 1990), according to the site of mutation and the relative levels of wild-type (wt) and mutant p53 in the cell:

(i) *Dominant mutants*: protein from the single mutant allele can form hetero-tetramers with wild-type p53, resulting in complexes that are defective for DNA binding (Kern *et al.*, 1992; Milner and Medcalf, 1991).

(ii) *Recessive mutants*: mutant p53 is unable to inactivate the function of wild-type p53.

(iii) *Gain-of-function mutants*: mutant protein is capable of conferring increased tumourigenicity or metastatic potential. Although the mechanism is uncertain it may involve stimulation of the transcription of cellular genes with oncogenic or angiogenic functions (Kern *et al.*, 1992), or, alternatively abrogation of the function of the p53 family member, p73 (Di Como *et al.*, 1999; Marin *et al.*, 2000 and see below).

1.4 The p53 gene family: Recent additions - p73 and p63

In 1997, the widely held belief that p53 was indeed part of a family of proteins was finally vindicated, when the structural homologue p73 was identified by Caput and

co-workers (Kaghad *et al.*, 1997). Shortly thereafter, several groups identified a third member of the family, variously termed p63, Ket, p40, p51, p73L (Osada *et al.*, 1998; Schmale and Bamberger 1997; Trink *et al.*, 1998; Yang *et al.*, 1998). Phylogenetic analysis of these proteins suggests that p63 is the evolutionary ancestor of the p53 gene family (Yang *et al.*, 1998).

1.4.1 Structural organisation of p73 and p63

The exon/intron organisation of the p53 family members is similar. Exon 1 is invariably non-coding and each gene is characterised by the presence of very large introns (Schmale and Bamberger 1997). The p73 gene is approximately 65kb with 14 exons (Kaghad *et al.*, 1997), whereas the p63 gene contains 15 exons (Yang *et al.*, 1998). The sequences of p73 and p63 are more similar to each other than either is to p53, with the highest degree of homology in the central DNA-binding domain, and least homology in the N-terminal transactivation domain (Kaghad *et al.*, 1997; Osada *et al.*, 1998; see figure 6). Akin to p53, both p73 and p63 can bind to canonical p53 binding sites, and activate transcription from a range of p53-responsive promoters (Kato *et al.*, 1999; Zhu *et al.*, 1998). Although *bax* and several redox-related genes (*PIGs 2, 3, 6* and *11*) induced by p53, are not significantly induced by p73, *in vitro* studies in human keratinocytes indicate that both p63 and p73 can transactivate the expression of markers of epidermal differentiation, namely loricrin, involucrin and transglutaminase (De Laurenzi *et al.*, 2000). Each can also induce apoptosis when overproduced in cells (Jost *et al.*, 1997; Osada *et al.*, 1998) and recently it has been shown that E2F1 can induce cell death in the absence of p53, through the activation of p73 (Irwin *et al.*, 2000).

The diversity in biological activity among p53 family members stems, at least in part, from differences in mRNA processing. In striking contrast to p53, both p63 and p73 undergo complex alternative splicing at the C-termini to generate multiple mRNA transcripts. To date, recognised variants of p63 include the (TA p63) α, β, and γ isoforms that retain the coding sequence for the N-terminal transactivation domain (TA) with additional N-terminal truncated transcripts being generated through the utilisation of a cryptic promoter located in intron 3, (ΔN p63) α, β, and γ. The ΔN isoforms are known to act in a dominant-negative manner with respect to wild-type

Figure 6. Structural comparison of p53, p63 and p73

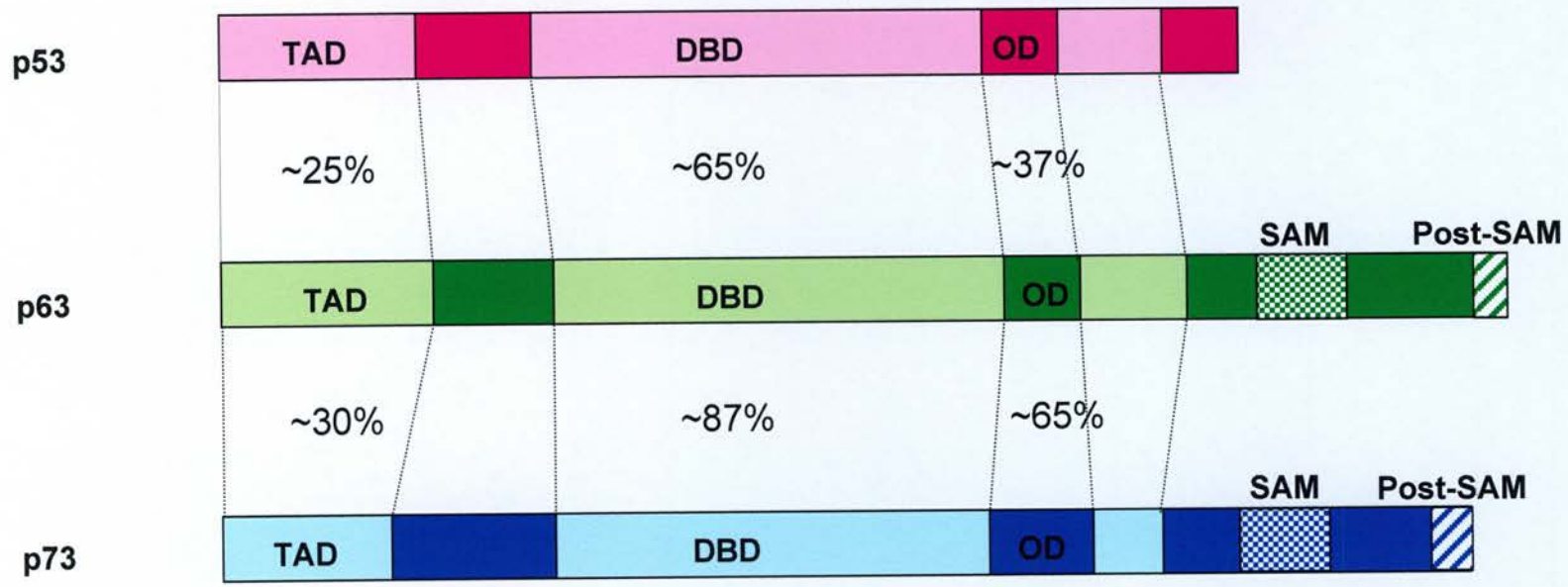

Schematic representation of the structure of p53 (pink boxes), p63 (green boxes) and p73 (blue boxes).
p63 and p73 are more similar to each other than either is to p53. The greatest sequence homology is observed in the central DNA-binding domain. The transactivation domains (TAD), DNA-binding domains (DBD) and oligomerisation domains (OD) are indicated in the paler shades of each colour representing the respective proteins. The SAM domains are shown as stippled boxes and the Post-SAM domains as hatched boxes. Both these domains are present only in the α isoforms of p63 and p73. **SAM:** Sterile alpha motif
Adapted from Ikawa *et al.*, 1999.

TA p63 and wild-type p53 (Yang *et al.*, 1998). Splicing of p73 generates at least 6 isoforms at the C-terminus, α, β, γ, δ, ε and ζ (De Laurenzi *et al.*, 1998, 1999; see figure 7). Similar to the ΔN variants of p63, investigators have recently reported the expression of p73 variants lacking exon 2 (Δ2 p73) in neuroblastomas and ovarian cancers (Casciano *et al.*, 1999; Ng *et al.*, 2000). Moreover, Pozniak and colleagues have recently ascribed an anti-apoptotic role for ΔN p73 in developing mouse neurons (Pozniak *et al.*, 2000), and suggest that this variant might act in a dominant negative fashion, analogous to ΔN p63.

p63 and p73 diverge from p53 predominantly in the C-terminus. In addition to the multiple splice variants generated at this terminus, a second transactivation domain between residues 382 and 491, not found in p53, has been described in p73 (Takada *et al.*, 1999). Furthermore, both p73α and p63α contain potential SAM (sterile alpha motif) domains (protein-protein interaction domains found in proteins involved in developmental regulation), underscoring the importance of these genes in differentiation (Bork *et al.*, 1999; see figure 7). The presence of a SAM structure suggests the existence of binding proteins that modulate p63 and p73 activities. In addition, a post-SAM domain, namely the last 70 amino acids, is necessary for inhibiting the transactivation function of TA p63α and TA p73α (Ozaki *et al.*, 1999; see figure 7).

1.4.2 Homo- and hetero-oligomerisation of the p53 family

p53 binds DNA as a homo-tetramer. The oligomerisation domains (OD) of p63 and p73 can bind weakly to each other but they are unable to form stable hetero-oligomers with wild-type p53 (Davison *et al.*, 1999). Moreover, the different C-termini of the various isoforms of p63 and p73 directly or indirectly influence the ability of these molecules to form productive oligomers, and may also influence their ability to activate p53-responsive promoters (De Laurenzi *et al.*, 1998; Kaghad *et al.*, 1997). There is evidence that certain p53 mutants can bind p73 and p63 and reduce its transcriptional activation function, with subsequent decrease in its ability to induce apoptosis (Di Como *et al.*, 1999; Gaiddon *et al.*, 2001). The existence of mutant p53-p73 complexes *in vivo* has also been established (Marin *et al.*, 2000).

Figure 7. Comparison of the *p53*, *p63* and *p73* genes

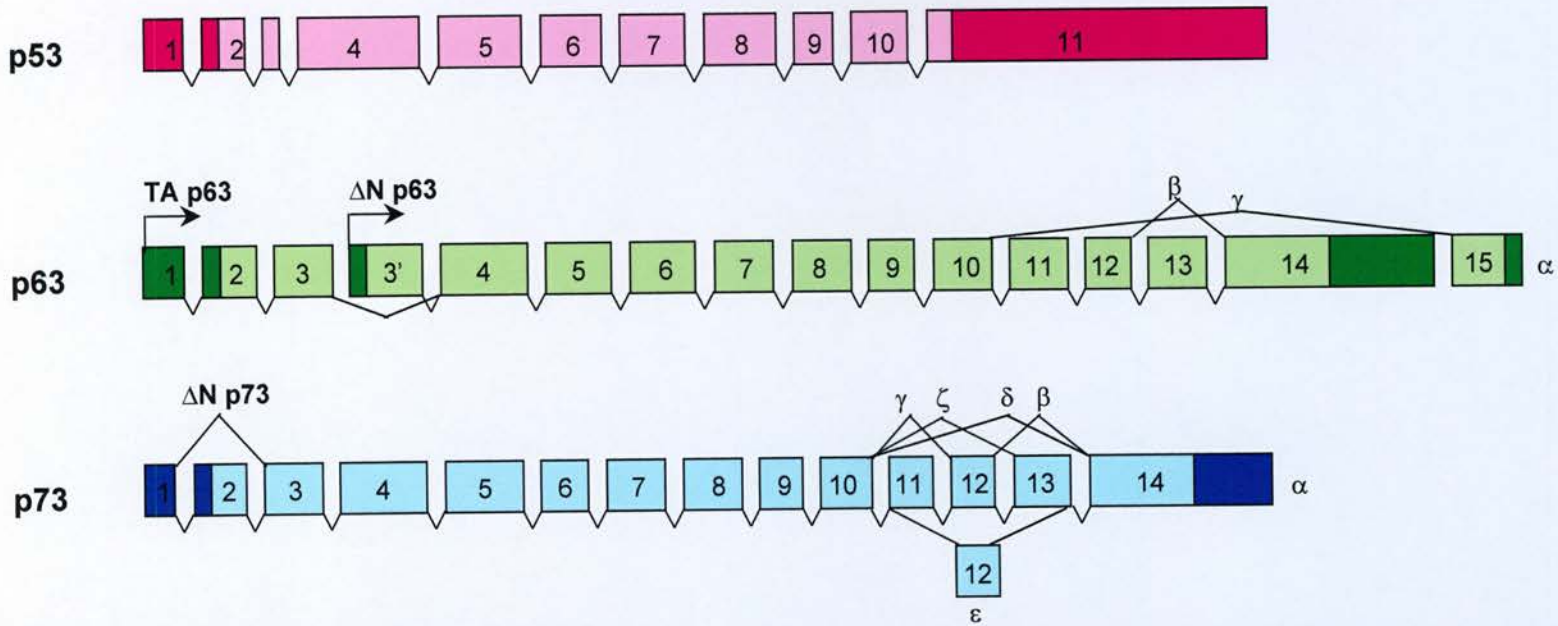

The *p53* gene, indicated as pink boxes, is composed of 11 exons. The *p63* gene (green boxes) is composed of 15 exons. Full-length transcription of the gene gives rise to the α transcript. However, splicing at the C-terminus gives rise to variants β (splices out exon 13) and γ (splices out exons 11, 12,13 and 14). Transcription at the N-terminus is either initiated in exon 1, giving rise to the TA variant, or through the use of a cryptic promoter located in intron 3, giving rise to the ΔN variant. Altogether, the *p63* gene encodes at least 6 isoforms of p63. The *p73* gene (blue boxes) is composed of 14 exons. Similar to *p63,* the gene is multiply spliced at its C-terminus to generate 6 isoforms, α (full length), β (splices out exon 13), γ (splices out exon 11), δ (splices out exon 11, 12 and 13), ε (splices out exon 11 and 13) and ζ (splices out exons 11 and 12). Furthermore, a variant of p73, ΔN p73 is generated through the deletion of exon 2. Coding regions are indicated in the paler shades of each colour representing the respective proteins. **Adapted from Levrero *et al.*, 1999.**

1.4.3 Activation of p63 and p73 by cellular stress signals

p73 is activated only by specific forms of DNA damage such as γ-irradiation and cisplatin. Treatment with these agents results in activation of c-*abl* tyrosine kinase activity, which in turn leads to increased p73 protein levels and subsequent apoptosis (Agami *et al.*, 1999; Gong *et al.*, 1999). More recently, it has been demonstrated that p73 can be induced by E2F-1, c-Myc and E1A, and activate apoptosis in the absence of functional p53 (Irwin *et al.*, 2000; Zaika *et al.*, 2000). The upstream events that activate p63 are not known.

1.4.4 Role of the p53 family members in development and cancer

(i) Role in differentiation and development

Although p53 is not indispensable for survival and growth, p63 and p73 have been shown to be essential for development and differentiation. p73 null mice have severe neurological, pheromonal and inflammatory defects but do not develop spontaneous tumours (Yang *et al.*, 2000), whereas $p63^{-/-}$ mice have major defects in limb, cranofacial and epithelial development (Yang *et al.*, 1999).

(ii) Role in carcinogenesis

The p73 gene maps to chromosome 1p36, a region frequently deleted in human cancers including neuroblastomas (Kaghad *et al.*, 1997). To concur with Knudson's two-hit hypothesis for tumour suppressor genes (Knudson, 1971), the remaining p73 allele is expected to be mutated in such cases. However, mutations in p73 are exceedingly rare in human cancers (Ichimiya *et al.*, 1999). A possible explanation for this is the monoallelic expression of p73 (due to genomic imprinting) in these tumours, such that loss of the transcribed allele would be sufficient to promote tumourigenesis (Kaghad *et al.*, 1997). This however does not account for the absence of mutations in those tumours where both alleles are expressed. Conflicting reports exist as to the biallelic and monoallelic expression of this gene, which varies with the tissue type as well as between different individuals. Perhaps surprisingly, p73 mRNA levels are frequently increased rather than decreased in tumour tissue relative to surrounding normal tissue (Kovalev *et al.*, 1998).

Recently, transcriptional silencing of p73 has been observed in specific haematological malignancies by aberrant hypermethylation of the promoter region (Corn *et al.*, 1999; Kawano *et al.*, 1999). Interestingly, a methylation-independent silencing mechanism of this gene has been proposed in neuroblastomas (Banelli *et al.*, 2000). Despite the above evidence, confirmation of p73's role as a tumour suppressor requires further investigation.

The role of p63 as a tumour suppressor presently remains unclear. This gene located on chromosome 3q27-29 is very similar to p73 in that it is rarely mutated in human cancers (Osada *et al.*, 1998). Recently, Sidransky and co-workers have shown that this gene is over-amplified in lung and head and neck squamous cell carcinomas and thereby behaves as an oncogene rather than a tumour suppressor (Yamaguchi *et al.*, 2000). Evidence in support of its oncogenic role also comes from studies that demonstrate the ability of ΔN isoforms of p63 (see above) to act as oncoproteins, by virtue of their ability to antagonise p53 function (Crook *et al.*, 2000; Yang *et al.*, 1998). More recent evidence indicates that wild-type p53 can regulate the stability of certain ΔN isoforms of p63 through caspase-mediated degradation, thus possibly counterbalancing the ability of these isoforms to precipitate tumourigenesis or induce epithelial proliferation (Ratovitski *et al.*, 2001). Further studies however, are needed to clarify the exact role of this gene in human neoplasia.

1.5 The INK4 locus

Orderly execution of the various stages of the cell-cycle is governed by the expression and interaction of three types of molecule; a family of enzymes called the *cyclin-dependent kinases (CDKs),* which are activated by a group of positive regulators, the *cyclins*, and inhibited by the *CDK inhibitors (CKIs)*. The CKIs include two distinct families; the *INK4* (**In**hibitors of cyclin dependent **k**inase **4**) family whose four members ($p16^{INK4a}$, $p15^{INK4b}$, $p18^{INK4c}$ and $p19^{INK4d}$) exclusively bind to and inhibit CDK4 and CDK6, and the *CIP/KIP* family whose three members ($p21^{CIP1/WAF1}$, $p27^{KIP1}$, $p57^{KIP2}$) are able to inhibit the activity of all CDKs (Sherr and Roberts 1995).

The remainder of this section will focus on the *INK4a* and *INK4b* genes and their protein products, $p16^{INK4a}$ and $p15^{INK4b}$, and a second protein product of the *INK4a*

locus, $p14^{ARF}$ [**a**lternative **r**eading **f**rame (ARF)].

1.5.1 Discovery and structure of $p16^{INK4a}$ and $p15^{INK4b}$

Serrano and co-workers were the first to isolate the cDNA encoding $p16^{INK4a}$ in 1993 (Serrano *et al.*, 1993). Soon after, low stringency screening of a cDNA library from transforming growth factor β (TGF-β)-arrested human keratinocytes using a $p16^{INK4a}$ probe, led to the isolation of $p15^{INK4b}$ (Hannon and Beach, 1994).

The *INK4a* and *INK4b* genes are tandemly linked on chromosome 9p21 within 30kb of one another in the same transcriptional orientation. The $p15^{INK4b}$ and the $p16^{INK4a}$ proteins are encoded by 2 and 3 exons respectively, with greater than 95% amino acid sequence identity in exon 2. All the INK4 proteins are characterised by the presence of anykrin repeat motifs that are used as structural scaffolds to facilitate protein-protein interactions. Both $p16^{INK4a}$ and $p15^{INK4b}$ contain 4 anykrin-like repeats, and studies suggest that the third anykrin repeat is crucial for interaction of the INK4 proteins with CDK4 and CDK6 (Roussel 1999; Ruas and Peters, 1998).

The principal function of the INK4 proteins is to specifically bind to and inhibit the kinase activities of CDK4 and CDK6 and their association with the D-type cyclins. This interaction prevents the phosphorylation of pRb, which is the primary substrate of the cyclin/CDK4 complex (Ewen, 1994). Hypophosphorylated pRb then forms DNA complexes with members of the E2F and DP transcription factor families, genes that are necessary for DNA synthesis, with subsequent growth arrest at G1 (Sherr and Roberts, 1995).

1.5.2 Alternative product of the *INK4a* locus: $p14^{ARF}$/$p19^{ARF}$ (ARF)

The *INK4* locus in mouse and man contains two independent but overlapping genes, *INK4a* and *ARF*, which encode functionally distinct proteins (Quelle *et al.*, 1995; see figure 8). The initiator codon in exon 1β is not in frame with sequences encoding $p16^{INK4a}$ in exon 2, and thus a novel 14 kDa polypeptide (19 kDa in the mouse, hence $p19^{ARF}$) is translated from an alternative reading frame in exon 2 (Quelle *et al.*, 1995; see figure 8).

Unlike $p16^{INK4a}$ and the other INK4 proteins, ARF does not bind the CDKs. It interacts with hMDM2 and arrests cells in the G1 and G2 phases of the cell cycle

Figure 8. The *INK4a/ARF* locus

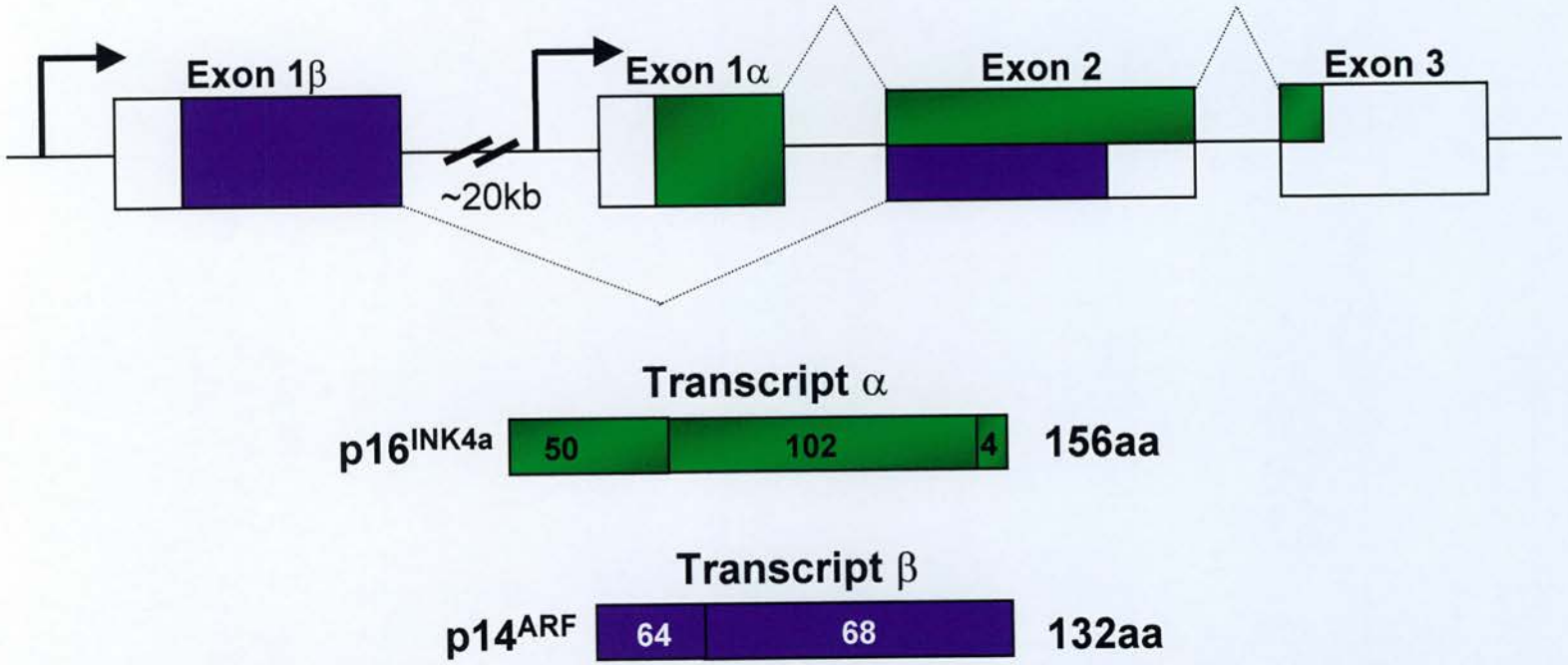

The *CDKN2a* locus on human chromosome 9p21 encodes 2 transcripts that initiate at unique first exons that are spliced to a common exon 2. Genomic sequences encoding $p16^{INK4a}$ (the α transcript) are shown as green shaded areas within the boxes designated exons 1α, 2 and 3, whereas the blue areas shaded in exons 1β and 2 encode $p14^{ARF}$ (β transcript). Unfilled portions of the exons correspond to non-coding 5' and 3' regions. Hatched lines indicate splicing between the exons. Exons 1α and 1β are indicated to have separate promoters (→). In the human genome, the alternative first exons are separated by approximately 20kb of intervening sequences. Note that exon 2 sequences are translated in different reading frames and the proteins are structurally unrelated. The β transcript however is terminated within exon 2, with exon 3 comprising an untranslated 3' exon. Amino acids contributed by each exon are indicated within the boxes. **ARF: Alternative Reading Frame. Adapted from James and Peters, 2000**

through the stabilisation of p53 (Pomerantz *et al.*, 1998), but does not seem to be required for p53's response to DNA damage (Kamijo *et al.*, 1997, 1998). Stabilisation of p53 by ARF can occur by several mechanisms, namely re-localising hMDM2 to the nucleolus, preventing hMDM2-p53 shuttling and accumulation of ARF-hMDM2-p53 'nuclear bodies' in the nucleoplasm, although the precise mechanism/s are yet to be established (Weber *et al.*, 1999; reviewed in Sherr and Weber, 2000). ARF is also believed to negatively regulate the cell cycle in a p53-independent manner (Carnero *et al.*, 2000; Weber *et al.*, 2000).

1.5.3 Expression and regulation of the INK4 proteins and ARF

INK4 and ARF transcripts are differentially expressed during murine embryogenesis and adulthood, suggesting that they have tissue-specific functions (Roussel, 1999).

Regulation of $p16^{INK4a}$ levels is primarily at the transcriptional level. In most tissues $p16^{INK4a}$ mRNA is very low, although it is extremely stable (half-life >24 hours) (Hara *et al.*, 1996). Accumulation of $p16^{INK4a}$ mRNA and proteins occurs in response to cellular senescence, expression of oncogenic *ras*, and inactivation of pRb (Hara *et al.*, 1996; Okamoto *et al.*, 1995; Li *et al.*, 1994a).

$p15^{INK4b}$ is more abundantly and ubiquitously expressed than $p16^{INK4a}$. Its transcription is induced in most cells, and in particular epithelial cells, by TGF-β (Hannon and Beach, 1994), and there is evidence to indicate its upregulation by interferon-α in lymphoid cell lines (Sangfelt *et al.*, 1997). Its expression is not affected by pRb status and is generally constant throughout the cell cycle (Stone *et al.*, 1995).

Not only does ARF directly interfere with the p53-hMDM2 feedback loop but it is also subjected to negative regulation by p53 (Stott *et al.*, 1998). Furthermore, ARF is known to link two important tumour suppressor pathways in cancer- namely the p53 and the pRb pathways, through direct induction by E2F-1 (Bates *et al.*, 1998; see figure 9). Furthermore, ARF is believed to be a link between viral (E1A) and cellular (c-*myc*, *ras*) oncogene signalling and p53 accumulation, through its interaction with hMDM2 (de Stanchina *et al.*, 1998; Zindy *et al.*, 1998; Palmero *et al.*, 1998; see figure 5, page 17).

Figure 9. Regulatory mechanisms involving $p14^{ARF}$ and $p16^{INK4a}$

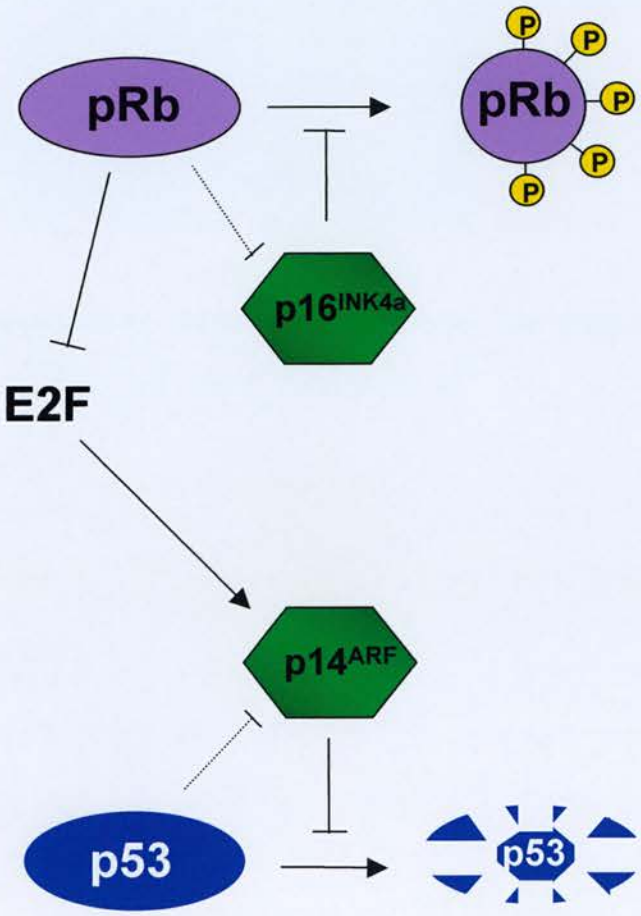

$p16^{INK4a}$ prevents the phosphorylation and inactivation of pRb by CDK4/6, whereas, $p14^{ARF}$ prevents the hMDM2-mediated degradation of p53. Both $p16^{INK4a}$ and $p14^{ARF}$ are themselves negatively regulated by pRB and p53 respectively. The release of E2F by the phosphorylation and ablation of pRb leads to the upregulation of $p14^{ARF}$, providing a direct connection between the pRb and p53 pathways.

Adapted from James and Peters, 2000.

1.5.4 Involvement of $p16^{INK4a}$, $p15^{INK4b}$ and ARF in cancer

The evidence to validate *INK4a* as a tumour suppressor came from research in two different fields, cancer genetics and cell cycle regulation. Search for a melanoma susceptibility gene resulted in the discovery that the region on chromosome 9p21 containing the $p16^{INK4a}$ gene is homozygously deleted in approximately 75% of melanoma cell lines (Kamb *et al.*, 1994). Its role in familial melanoma is now firmly established and is defined by the presence of germline mutations, typically point mutations or small intragenic deletions within the first or second exon (Hussussian *et al.*, 1994).

The ability of $p16^{INK4a}$ and $p15^{INK4b}$ to induce growth arrest by inhibiting phosphorylation of pRb suggests that loss of function could contribute to tumourigenesis, further endorsing their role as tumour suppressors. The importance of this cell cycle regulatory pathway has been underscored by alterations in other components of this pathway, such as inactivation of pRb, overexpression of D-type cyclins and CDKs, or CDK4 mutations that abrogates binding of $p16^{INK4a}$. These genetic lesions often appear to be mutually exclusive within tumours, suggesting that they have functionally equivalent consequences (Sherr, 1996). In contrast, an inverse correlation is not strictly observed between *INK4a/ARF* and p53 genetic alterations at least in some human cancers, further denoting a p53-independent function for ARF (Iida *et al.*, 2000; Sanchez-Cespedes *et al.*, 1999).

Inactivation of the INK4 locus has been shown in a range of cancers (Kamb *et al.*, 1994; Ruas and Peters, 1998). Essentially three modes of inactivation have been observed: i) homozygous deletion, ii) intragenic mutation and iii) promoter silencing by methylation.

(i) Homozygous deletion

Deletion of 9p21 is the most common method of inactivation, which generally involves the entire *INK4a*/ARF locus and frequently, but not always, *INK4b*. It affects up to 14% of all tumours analysed to date including gliomas, melanomas, leukaemias, head and neck tumours and carcinomas of the bladder, lung, kidney, pancreas and ovary (Ruas and Peters, 1998). Deletions of *INK4a* and *INK4b* have been consistently observed in children with acute lymphoblastic leukaemia (ALL)

(>30%), especially in leukaemias of the T-cell lineage (>50%) (Siebert *et al.*, 1996). In contrast, incidence of *INK4a* deletions is low in other haematological malignancies such as NHL, chronic and acute myeloid leukaemia (CML and AML, respectively) and primary breast cancers (<3%). Furthermore, deletions are consistently absent in cancers of the colon, cervix and liver (Kamb, 1995; Ruas and Peters, 1998).

Deletion of exon 1β in mice is associated with the development of lymphomas, sarcomas, carcinomas and gliomas, similar to that observed in *INK4a/ARF*-null mice, suggesting that ARF on its own is an important regulator of cell growth. The sensitivity of *ARF*-null mouse embryonic fibroblasts to oncogenic transformation further establishes a vital tumour suppressor function for this protein (Kamijo *et al.*, 1997).

(ii) Intragenic mutations

Mutations in the *INK4a/ARF* locus is much higher in permanently growing cell lines than in the primary tumours from which they are derived (Spruck *et al.*, 1994; Zhang *et al.*, 1994). Most point missense mutations occur in exon 2, common to both *INK4a* and *ARF*, and usually affect the amino acid sequence of both proteins (Quelle *et al.*, 1997; Kubo *et al.*, 1997; Sanchez-Cespedes *et al.*, 1999). Mutations occurring in *INK4a* affects residues that are crucial for interactions between $p16^{INK4a}$ and CDK4 or CDK6 leading to phosphorylation of pRb, E2F release and G1/S progression (Lilischkis *et al.*, 1996). Exon 2 mutations do not seem to affect the ability of ARF to induce cell cycle arrest, although they might affect nucleolar localisation of the protein (Quelle *et al.*, 1997). A fraction of mutations have been found to exclusively target exon 1α of *INK4a*, while mutations in *INK4b* are rare (Okamoto *et al.*, 1995). Mutations in exon 1β of *ARF* are rare (Burri *et al.*, 2001; Poi *et al.*, 2001; Tanaka *et al.*, 1997). Overall, point mutations in the *INK4a/ARF* coding regions have been detected in 5% of all human tumours analysed (Ruas and Peters, 1998).

(iii) Promoter silencing by methylation

Methylation of the *INK4* genes, in particular exon 1α of the $p16^{INK4a}$ gene, has been observed in a significant fraction of human tumours, which results in a complete loss

of its transcriptional activity. Hypermethylation has been proposed as an alternative to intragenic mutation in silencing the residual allele of tumours showing LOH at 9p21, although this has not yet been proven in primary tumours (Merlo *et al.*, 1995). Silencing of the *INK4a* promoter has been found in 19% of all human tumours studied (Ruas and Peters, 1998). Interestingly, methylation-induced silencing of the $p16^{INK4a}$ gene has been found in cancers of the breast and colon that do not show homozygous deletions of the gene, and might represent an alternative to deletion as a mode of inactivating $p16^{INK4a}$.

In murine T-cell lymphomas, loss of $p15^{INK4b}$ expression by methylation is more common than inactivation of the *INK4a/ARF* locus (Malumbres *et al.*, 1997), and recent studies by the same group reveal that in addition to promoter region hypermethylation, the 3' untranslated region of $p15^{INK4b}$ is also sensitive to methylation (Malumbres *et al.*, 1999). Furthermore, the *INK4b* gene is hypermethylated without silencing of the *INK4a* promoter in certain haematological malignancies (AML, T cell NHL and ALL) and gliomas. Hence, this suggests an independent contribution and a tumour suppressor role for $p15^{INK4b}$, at least in some human cancers (Herman *et al.*, 1997). Methylation of both *INK4a* and *INK4b* is a common occurrence in Burkitt's lymphomas, multiple myeloma and B cell NHL (Herman *et al.*, 1997).

Aberrant methylation of the *ARF* promoter has been recently reported in human colorectal and gastric cancers (25-45%) independently of *INK4a* promoter methylation (Esteller *et al.*, 2000; Iida *et al.*, 2000). However, the promoter is infrequently methylated in murine primary T-cell lymphomas (Melendez *et al.*, 2000).

1.6 Oncogenes

By definition, an oncogene typically refers to any gene that produces a malignant phenotype when introduced into a normal cell (Bishop, 1991; Weinberg, 1994). Oncogenes are derived from proto-oncogenes, cellular genes that function in various aspects of cell cycle regulation, including growth, proliferation, differentiation and apoptosis. Changes in the structure of the proto-oncogene, attributed to translocation,

mutation, and/or amplification resulting in the synthesis of an abnormal gene product (oncoprotein), or changes in the regulation of gene expression resulting in enhanced or inappropriate production of the normal protein, contributes to tumourigenesis. Table 2 highlights selected oncogenes and their mode of activation in associated human tumours.

Table 2

Mode of activation of selected oncogenes in human cancer

Proto-oncogene	Mechanism	Associated human tumour
ras	Point mutation	Variety of cancers, including lung, colon, pancreas, leukaemias, some AIDS-BL
c-*myc*	Translocation	BL, some DLCL
	Amplification	breast, lung, colon, prostate cancer and MM, ML
N-*myc*	Amplification	Neuroblastoma, small cell lung carcinoma
L-*myc*	Amplification	Small cell lung carcinoma
bcl-1	Translocation	Mantle zone lymphomas
	Amplification	Breast, liver and oesophageal cancers
bcl-2	Translocation	FL, DLCL
bcl-6	Translocation/ point mutations	DLCL, FL
bcl-10	Translocation/ point mutation	MALT lymphomas/ FL

BL, Burkitt's lymphoma; FL, Follicular lymphoma; DLCL, diffuse large cell lymphoma; MM, multiple myeloma; ML, myeloid leukaemia

The following sections describe three genes, c-*myc*, *bcl-2* and *bcl-6*, each of which have a distinct function in growth and proliferation (c-*myc*), apoptosis regulation (*bcl-2*) and differentiation (*bcl-6*). These genes have been investigated in the present study due to their implied role in the pathogenesis of certain AIDS-NHL (Dalla-Favera *et al.*, 1982b; Tsujimoto *et al.*, 1984; Ye *et al.*, 1993).

1.7 c-Myc

1.7.1 Discovery of c-*myc*

In 1979, an oncogene which caused carcinomas, sarcomas, endotheliomas and the leukaemic disorder **my**elo**c**ytomatosis (hence the acronym, ***myc***), was identified from the MC29 avian leukaemia retrovirus (ALV) (Sheiness and Bishop, 1979). In 1982, the human c-*myc* gene was isolated as the cellular homologue of the chicken retroviral v-*myc* gene (Dalla-Favera *et al.*, 1982a). Subsequently, its potent

oncogenicity was realised by the presence of chromosomal translocations involving the *myc* gene in animal and human tumours, such as murine plasmacytomas and Burkitt's lymphomas (Shen-Ong *et al.*, 1982; Dalla-Favera *et al.*, 1982b).

c-*myc* belongs to a family of genes including B-*myc*, L-*myc*, N-*myc* and s-*myc*. Besides c-*myc*, only N-*myc* and L-*myc* are involved in neoplastic transformation (Schwab *et al.*, 1985).

1.7.2 Structure of the c-*myc* gene and protein

The c-*myc* locus maps to chromosome 8q24 and consists of 3 exons. Exon 1 is untranslated, while exons 2 and 3 providing the major coding regions. The 2.4kb and 2.2kb transcripts initiated from promoters P_1 and P_2, account for 10-25% and 75-90% of steady-state c-*myc* RNAs in normal cells respectively, and contain the open reading frame (ORF) for the two major c-*myc* polypeptides, p67 and p64 (Taub *et al.*, 1984; Hann *et al.*, 1988; Bentley and Groudine, 1986). It has been suggested that p67 may act as a negative regulator of p64 activity (Hann, *et al.*, 1988). Minor promoters P_0 (5' to P_1) and P_3 give rise to less than 5% of c-*myc* mRNAs (3.1kb and 2.3kb respectively) (Bentley and Groudine, 1986).

The structure of the c-Myc protein is illustrated in Figure 10. The C-terminal DNA-binding domain and N-terminal transactivation domain of c-Myc are required for its biological activities (Kato *et al.*, 1990). In addition, the conserved Myc box II (MBII) is critical for the biological activity of c-Myc and for oncogenic transformation (Li *et al.*, 1994b; Ingvarsson, 1990; Henriksson and Luscher, 1996).

1.7.3 c-Myc as a transcription factor

c-Myc is a nuclear phosphoprotein that functions primarily as a transcription factor. The ability of c-Myc to interact with the transcriptional machinery is modulated by its interaction with other transcription factors through both its C- and N-termini. In addition, the protein can activate and repress transcription of a number of target genes involved in cellular processes such as proliferation, differentiation and apoptosis and these functions of c-Myc are summarised in Figure 11. The c-Myc target genes are beyond the scope of this thesis and are reviewed in Dang (1999).

Figure 10. Structural and functional domains of c-Myc

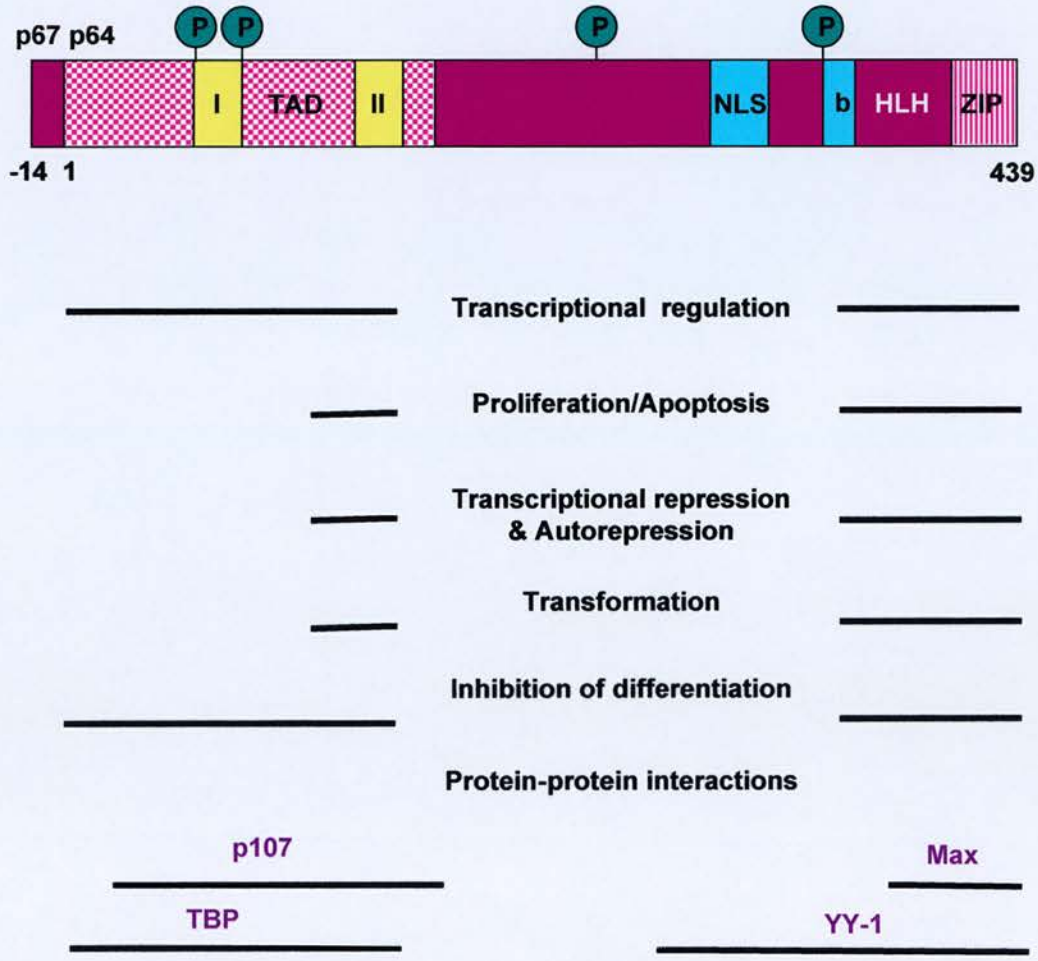

c-Myc harbors a transactivation domain (**TAD**; amino acids 1-143) at its N-terminus; a nuclear localisation signal (**NLS**; amino acids 320-328), a basic region (**b**; amino acids 355-368), a helix-loop-helix motif (**HLH**; amino acids 368-410) and a leucine zipper domain (**ZIP**; amino acids 411-439). The HLH/ZIP domains mediate protein-protein interaction while the basic region specifies DNA binding. Yellow boxes within the TAD represent Myc Box **I** (amino acids 45-63) and **II** (amino acids 129-141), two conserved regions found in all Myc family members. **P** indicates the localisation of the major in vivo phosphorylation sites. p67 contains an additional 14 amino acid residues at its N terminus, due to an initiation codon in exon 1, compared to p64 which initiates at the first AUG in exon 2. The functional and protein-protein interaction domains of Myc, along with a few examples of proteins (purple text) that interact with the C- and N-terminal domains are indicated.

Adapted from Henriksson and Luscher, 1996.

Figure 11. Functions of c-Myc

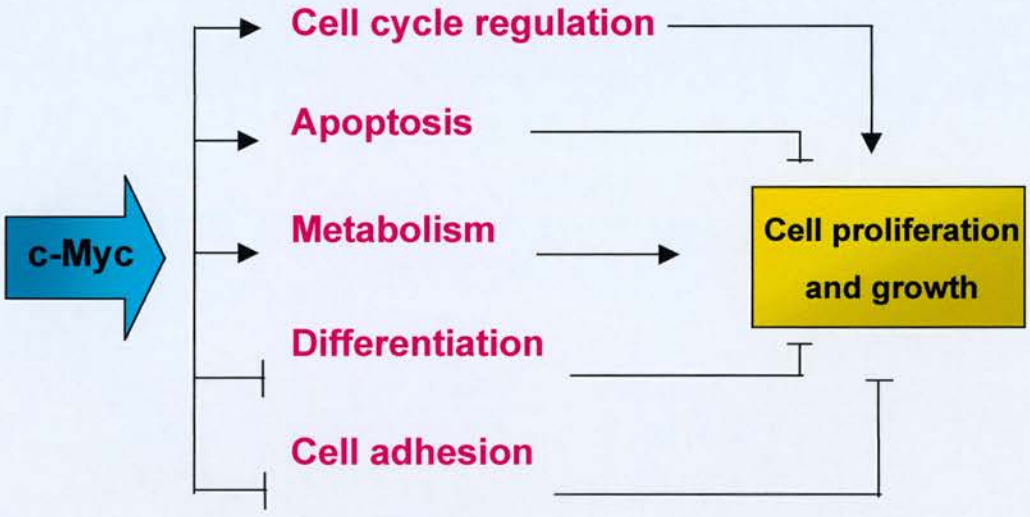

c-Myc has a number of biological functions. It positively affects cell cycle regulation, apoptosis and metabolism. c-Myc is absent is quiescent cells but is rapidly induced upon addition of growth factors. Ectopic c-Myc expression in quiescent cells promotes entry into S-phase and is growth factor-independent (Evan and Littlewood, 1993). c-Myc can also activate cellular apoptosis, which requires both the N-terminal transactivation domain and the b/HLH/Z domain (Evan et al., 1992). The proliferative and apoptotic activities of c-Myc are thought to be coupled, safeguarding against expansion of potentially malignant cells (Harrington et al., 1994). The protein sensitises the cell to apoptotic stimuli and death receptor signals from the CD95/Fas family in response to a variety of apoptotic stimuli such as hypoxia, DNA damage and glucose deprivation (Hueber et al., 1997; Evan and Littlewood, 1993).
c-Myc represses genes involved in cellular differentiation and cell adhesion through initiator or *Inr* elements. Transcriptional repression requires aa 106-143 within the TAD as well as the HLH domain (Li et al., 1994b; Lee et al., 1996). c-Myc mediated transformation thus requires both transactivation of growth-related genes and *Inr*-driven transcriptional repression of differentiation and cell adhesion genes.

Adapted from Dang *et al.*, 1999.

The CTD mediates c-Myc binding to physiological target genes that are involved in transcriptional regulation. Max, a b/HLH/Z protein, was first identified as a binding partner for c-Myc, which controls the access of c-Myc to physiological target sites (Blackwood and Eisenman, 1991). Hetero-dimerisation with Max is necessary for c-Myc to mediate proliferation, transformation and apoptosis (Amati *et al.*, 1993). Max in turn interacts with another b/HLH/Z protein family, Mad, which are implicated in transcriptional repression, cell growth inhibition and differentiation (Amati and Land, 1994).

1.7.4 Role of c-Myc in human neoplasia

c-*myc* is activated by a variety of genetic alterations such as chromosomal translocations, gene amplification, and somatic mutations. Beside its characteristic involvement in chromosomal translocations in BL (see below), the gene is also amplified in various cancers (Nesbit *et al.*, 1999, see Table 2). A common underlying feature of tumours with c-*myc* alterations is the deregulated or elevated expression of the gene (Cole, 1986; Spencer and Groudine, 1991).

1.7.4.1 c-*myc* alterations in BL

The juxtaposition of the c-*myc* gene on chromosome 8 with regulatory elements of the immunoglobulin (Ig) heavy chain (*IgH*), or light chains λ and κ on chromosomes 14, 22 or 2 respectively, is a characteristic feature of BL (Dalla-Favera *et al.*, 1982b). The most common translocation is t(8:14) (80% of cases) which involves a breakpoint on chromosome 14 in the switch region of μ (Sμ) in the majority of sporadic BL (sBL), and the *IgH* joining region in endemic BL. The site of chromosomal breakpoint observed in the different BL-types, is believed to reflect the stage of differentiation of the affected cell (Pelicci *et al.*, 1986a). On chromosome 8, the breakpoint is located at an undefined distance 5' to the c-*myc* locus in most eBL, whereas in sBL and AIDS-BL the break is usually within intron 1 or the immediate 5' non-transcribed region of the c-*myc* gene (Pelicci *et al.*, 1986a). These translocations place c-*myc* and the *IgH* gene in a head-to-head transcriptional configuration. In most sBL with t(8:14), the first exon of c-*myc* is removed from the coding portion of the gene (see figure 12).

Figure 12. c-*myc*/*IgH* t(8:14) translocation

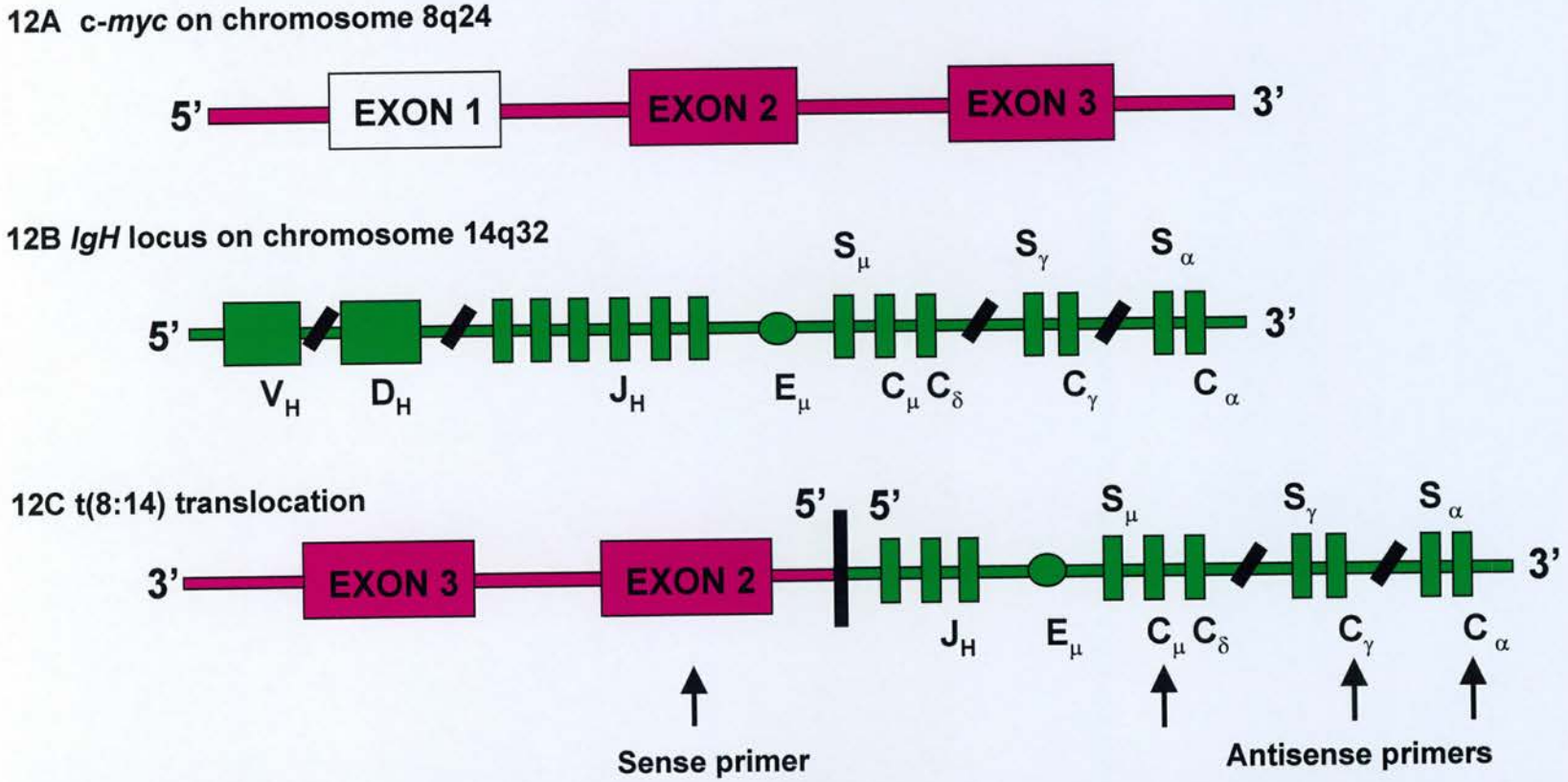

The gene rearrangement between *c-myc* and the *IgH* locus (represented in green), along with the approximate primer sites for Long Distance polymerase chain reaction (LD-PCR) are indicated. The 1st exon of c-*myc*, which is non-coding, is indicated as an unfilled box, and the 2 coding exons are indicated as solid pink boxes. The t(8:14) translocation between the two loci places them in a head-to-head orientation. The primers designed for the LD-PCR analysis of the t(8:14) breakpoint region are shown by black arrows. The sense primer is located in exon 2 of c-*myc* and the antisense primers are within the μ, γ, and α constant regions on the *IgH* locus. **VH:** variable **DH:** diversity **JH:** joining **E:** enhancer **S:** switch **C:** constant regions of the IgH locus. **Adapted from Basso *et al.*, 1999.**

In the less common 'variant' t(2:8) (15% of cases) and t(8:22) (5% of cases) translocations, the breakpoints on chromosome 8 occur up to 140kb downstream of the transcribed region of c-*myc*, and 5' of the variable region on the *Ig* light chains. The two loci are fused in the same transcriptional orientation (Cory, 1986).

Somatic mutation within the translocated c-*myc* allele, is another frequent structural feature of BL. Mutations mainly cluster in the 5' non-coding region either disrupting exon 1, intron 1 or the 5' flanking regions, and include insertions, deletions and single nucleotide substitutions (Pelicci *et al.*, 1986a; Wiman *et al.*, 1984). Additionally, the second exon of c-*myc* is also affected by mutations that modify key phosphorylation sites necessary for its transactivation function (Rabbitts *et al.*, 1983; Bhatia *et al.*, 1993). Furthermore, c-Myc mutants possess increased transforming activity, possibly due to their decreased responsiveness to the pRb family member, p107, which negatively regulates c-Myc (Hoang *et al.*, 1995) or by their resistance to ubiquitin-mediated degradation, resulting in increased stability (Bahram *et al.*, 2000).

1.7.4.2 Regulation of c-Myc in BL

The levels of c-*myc* RNA and protein expressed in BL are typically not strikingly higher than those seen in EBV-immortalised B cells, although they are elevated when compared to that observed in quiescent cells (Wiman *et al.*, 1984). Transcription of c-*myc* in BL predominantly arises from the translocated allele, while the unrearranged allele is repressed or expressed at very low levels (Croce and Nowell, 1985). Activation of the translocated allele is believed to occur by the influence of *cis*-acting *Ig* enhancer elements that are transcriptionally active in B cells. Thus, the rearranged allele escapes the repression mechanisms that usually inactivate the normal c-*myc* allele in the later stages of B cell maturation (Spencer and Groudine, 1991).

Alternatively, loss of regulation of c-*myc* from the translocated allele could occur by the truncation of exon 1 as seen in sporadic BL (see above), or by the presence of structural alterations in the 5' region of the translocated allele (Pelicci *et al.*, 1986a) and see above). This might inactivate important negative regulatory elements such as the block to transcriptional elongation near the 3' end of exon 1, leading to the constitutive transcriptional activation of c-*myc*, as seen in BL cells (Cesarman *et al.*,

1987). Cells that constitutively express c-Myc are maintained in a state of continuous proliferation, are highly apoptosis-prone (Evan *et al.*, 1992), and rarely undergo transformation unless they incur a second aberrant genetic event (Adams *et al.*, 1983). Thus additional changes that counteract apoptosis, such as activation of *bcl-2* (see section 1.8.7.2), mutations in *p53*, *RB* and *Bax* (Farrell *et al.*, 1991; Cinti *et al.*, 2000; Gutierrez *et al.*, 1999), or silencing of *INK4a* by methylation (Klangby *et al.*, 1998), are often present in primary BL and BL cell lines.

1.8 Bcl-2

1.8.1 Discovery of *bcl-2*

The **B** cell lymphoma/leukaemia-**2** (*bcl-2*) gene was so named because of its characteristic association with B cell malignancies. This proto-oncogene was originally identified by virtue of its involvement in the t(14:18) translocation breakpoint of follicular B cell NHL (Tsujimoto *et al.*, 1984). This discovery led to a new class of oncogenes whose primary function is regulation of programmed cell death (apoptosis) and cell survival, instead of promoting (c-*myc*) or inhibiting proliferation (*p53* and *RB*) (Korsmeyer, 1992).

1.8.2 Structure of the *bcl-2* gene and protein

The *bcl-2* gene is located on chromosome 18 (band q21), has three exons and utilises two different promoters to generate transcripts that encode two proteins namely p26α (Dittmer *et al.*, 1998) and p22β by alternative splicing (Reed *et al.*, 1988; Seto *et al.*, 1988). The Bcl-2 protein is an integral membrane protein, which is localised to mitochondrial, nuclear and endoplasmic reticulum membranes (Krajewski *et al.*, 1993). A stretch of 19 hydrophobic amino acids at the C-terminus of p26α, critical for its anti-apoptotic function, serves to anchor the protein into membranes, with a majority of the amino terminus exposed to the cytosol (Chen-Levy and Cleary, 1990; Hockenbery *et al.*, 1990). The truncated p22β form lacks this hydrophobic tail (Tsujimoto and Croce, 1986).

1.8.3 The Bcl-2 protein family

The Bcl-2 family comprises at least 16 members (Adams and Cory, 1998). All members possess sequence homology in one or more of four conserved motifs known as Bcl-2 homology domains (BH1 to BH4) that mediate protein-protein interactions (Yin *et al.*, 1994).

Although Bcl-2 (anti-apoptotic) and Bax (pro-apoptotic) are capable of functioning independently, dimerisation among Bcl-2 family members provides an important mechanism of regulating their activity (Knudson and Korsmeyer, 1997). The BH3 domain is critical for both hetero-dimerisation with anti-apoptotic proteins and for induction of apoptosis (Theodorakis *et al.*, 1996). The BH4 domain, which is found only in the anti-apoptotic members such as Bcl-2 and Bcl-X_L, is required for the binding and sequestration of *Caenorhabditis elegans*, Ced-4 homologues, thereby inhibiting apoptosis (Huang *et al.*, 1998; Korsmeyer, 1999 and see below).

1.8.4 Expression and physiological role of Bcl-2

Consistent with its role in cell survival, Bcl-2 is widely expressed during embryogenesis, notably in many neuronal populations, the retina and limb buds, although it is not absolutely required for embryonic development (Veis *et al.*, 1993). In the adult, expression is limited to T and B lymphocytes, haematopoietic cells, epithelia and peripheral neurons (Hockenbery *et al.*, 1991).

The physiological role of Bcl-2 has been elucidated by its topographical distribution in mature tissues, particularly the secondary germinal centres. The protein is expressed in early progenitor T and B cells, downregulated during the critical stage of lymphocyte development and selection, and re-expressed in mature T and B cells that have been selected for survival, thus implying a role in the selection and maintenance of plasma and memory B cells (Hockenbery *et al.*, 1991).

1.8.5 Role for the Bcl-2 family members in cell death regulation

A critical role for this gene as an intracellular apoptosis-suppressor came from the observation that overexpression of Bcl-2 increases the viability and survival of certain cytokine-dependent haematopoietic cell lines upon cytokine withdrawal (Vaux *et al.*, 1988). Furthermore, Bcl-2 prevents cell death in response to diverse

insults such as γ- and ultraviolet-radiation, growth factor withdrawal, oncogenes, viral proteins, oxidative stress and others (Yang and Korsmeyer, 1996).

Hetero-dimerisation with Bax is not essential for the anti-apoptotic function of Bcl-2. An important factor in determining susceptibility to apoptosis is the ratio of Bcl-2 to Bax that is present in the cell (Oltvai *et al.*, 1993). Bcl-2 exerts its anti-apoptotic activity through a variety of mechanisms, most of which involve prevention of cytochrome c release and subsequent activation of the apoptotic signal transduction pathway (Susin *et al.*, 1996; reviewed in Green and Reed, 1998). Pro-survival proteins can also inhibit apoptosis downstream of the release of cytochrome c by direct binding to the cytoplasmic pro-apoptotic protein, Apaf-1 (Ced-4 homologue), inhibiting its association with procaspase-9 and its activation (Hu *et al.*, 1998; Reed, 1997).

1.8.6 Bcl-2 and the cell cycle

Under sub-optimal growth conditions, Bcl-2 promotes exit of cells from the cell cycle and delays re-entry into cycle. This cell cycle inhibitory effect is genetically separable from its survival function (Huang *et al.*, 1997). Cell cycle inhibition by Bcl-2 is believed to have evolved to reduce its oncogenicity, and provide additional protection against apoptotic stimuli that proliferating cells encounter (Adams and Cory, 1998).

1.8.7 Involvement of *bcl-2* in cancer

1.8.7.1 *bcl-2* alterations in lymphomas

85% of follicular lymphomas (Yunis *et al.*, 1982) and 30% of diffuse B cell lymphomas (Aisenberg *et al.*, 1988) harbour the t(14:18) reciprocal translocation that juxtaposes the *bcl-2* gene and the *IgH* regulatory sequences. Nearly 70% of the breakpoints occur within the 3' untranslated region called the major breakpoint region (MBR) and 25% occur at a distance approximately 20kb 3' of the gene, called the minor cluster region (mcr) (Tsujimoto *et al.*, 1985; Cleary *et al.*, 1986). The corresponding breakpoints on chromosome 14 occur at or close to members of the joining region genes (JH) (Bakhshi *et al.*, 1987). Occasionally, the breakpoint may

occur 5' to the *bcl-2* gene (Yabumoto *et al.*, 1996), although these rearrangements involve not only *IgH* but also light chain genes as partners (see figure 13). These translocations are believed to occur as a result of endonucleolytic cleavages at the heavy chain diversity (D) and joining (J) segments by the enzyme recombinase during pre-B cell development, thus exposing sites of double-strand breaks to faulty recombinational events (Tsujimoto *et al.*, 1985).

The translocation places the *bcl-2* gene in the same transcriptional orientation as the *IgH* locus, thus giving rise to *bcl-2/IgH* chimeric transcripts (see figure 13). Since the protein-coding region of *bcl-2* is left intact, both normal and translocated alleles encode for a normal 25kDa Bcl-2 protein. Transcriptional deregulation and inappropriately elevated levels of the protein are commonly observed in lymphomas as a consequence of the translocation, which is thought to confer a survival advantage to the malignant B cells (Seto *et al.*, 1988).

Somatic mutations have been shown to accumulate in the translocated *bcl-2* allele in a subset of NHL, possibly due to the proximity of the gene to the hypermutable Ig region. The functional significance of these mutations is unclear (Tanaka *et al.*, 1992). Mutations near the amino-terminal BH4 domain of Bcl-2, a region responsible for the cell cycle inhibitory function of the protein, occurs in follicular lymphomas (Matolcsy *et al.*, 1996). It has been suggested that these mutations might relieve cell cycle inhibition without affecting the anti-apoptotic function of Bcl-2, thus contributing to the more aggressive phenotype characteristic of progressed follicular lymphoma (Huang *et al.*, 1997; Matolcsy *et al.*, 1996).

Healthy individuals frequently (20 to 60%) harbour the t(14:18) translocation (Limpens *et al.*, 1995; Aster *et al.*, 1992; Summers *et al.*, 2001), indicating that a translocation involving *bcl-2* is in itself insufficient to cause cancer, and additional events are necessary for malignant transformation to occur (McDonnell and Korsmeyer, 1991; see below). Nonetheless, detection of t(14:18) is a believed to be a marker for monitoring minimal residual disease and remission following therapy (Gribben and Nadler, 1995).

1.8.7.2 Co-operation between the *bcl-2* family and c-Myc and p53 in neoplasia

Synergistic interactions between *bcl-2* and c-*myc* resulting in an increased potential

Figure 13. *bcl-2/IgH* t(14:18) fusion

13 A Structure of *bcl-2*

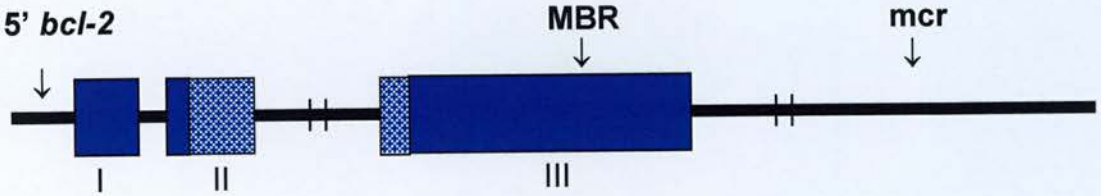

13 B MBR/*IgH* fusion

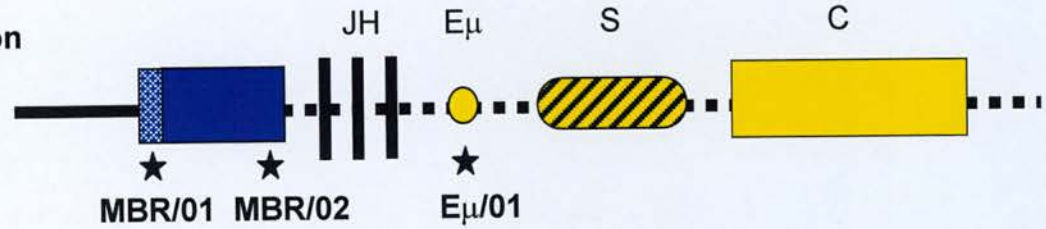

13 C mcr/*IgH* fusion

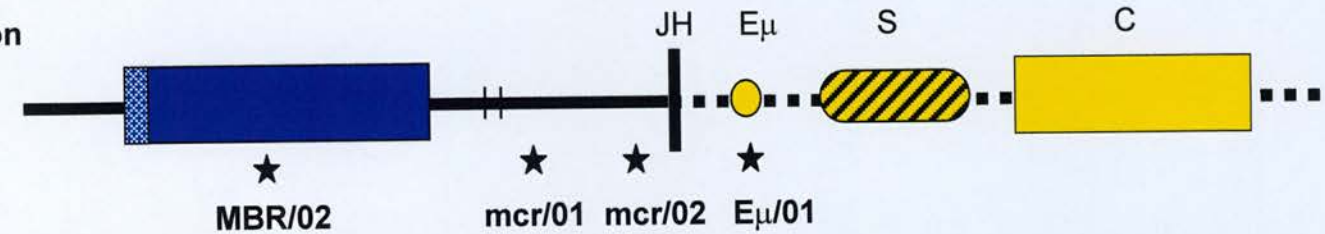

Gene rearrangement between *bcl-2* on chromosome 18 and the *IgH* locus (indicated in yellow) on chromosome 14 along with the approximate sites of the primers for the LD-PCR. The coding regions of *bcl-2* are indicated as stippled boxes and the non-coding regions as solid blue boxes. The three breakpoint cluster regions (5' *bcl-2*, MBR and mcr) are indicated. Primers for the *bcl-2* gene, indicated as stars, represent the sense strand in the forward direction, whereas those for the *IgH* gene represent the antisense strand in the reverse direction. **5' BCL-2:** 5' cluster region of *bcl-2* **MBR:** major breakpoint region, **mcr:** minor cluster region **JH:** joining region of the *IgH* **Eμ:** *IgH*-specific enhancer region **S:** switch region **C:** constant region. **Adapted from Akasaka *et al.*, 1998.**

for transformation (Strasser *et al.*, 1990), were first noted *in vitro* (Vaux *et al.*, 1988) and subsequently observed in naturally occurring lymphoid tumours *in vivo* (Lee *et al.*, 1989). This potent oncogenic combination probably reflects the ability of each gene to counter the anti-oncogenic properties of the other. In other words, Bcl-2 compensates the apoptotic function of deregulated c-Myc allowing unrestricted proliferation, whereas growth inhibition induced by Bcl-2 is overcome by the mitogenic effects of c-Myc (Cory *et al.*, 1999; Hueber and Evan, 1998; Fanidi *et al.*, 1992).

p53 is required for inducing apoptosis in response to genotoxic damage and often but not always upregulates expression of Bax (see section 1.3.3). Bcl-2 is capable of inhibiting both p53-dependent and independent mechanisms of cell death. Thymocytes from $p53^{-/-}$ mice are resistant to γ-irradiation and etoposide, but not glucocorticoids, interferon-γ and TGF-β. However, Bcl-2 is very effective at blocking cell death induced by these agents (Francis *et al.*, 2000; Strasser *et al.*, 1994).

1.8.7.3 Prognostic significance of *bcl-2* expression

Elevated expression of Bcl-2 is not restricted to B-lymphomas with a t(14:18) translocation, but is also common in lymphoproliferative disorders, and cancers of the lung, breast, colon and prostate, independent of the translocation (Pezzella *et al.*, 1990; reviewed in Jäättela, 1999). A distinct correlation between high Bcl-2 expression and poor prognosis has been reported in NHL and AML (Gascoyne *et al.*, 1997). In contrast, high levels of Bcl-2 are considered to be markers of favourable clinical outcome in breast cancer (Silvestrini *et al.*, 1994). Furthermore, loss of function mutations in Bax, and an elevated Bcl-2/Bax ratio is considered to be an indicator of poor prognosis, particularly in haematopoietic malignancies (Meijerink *et al.*, 1998; reviewed in Jäättela, 1999).

1.9 Bcl-6

1.9.1 Cloning and characterisation of *bcl-6*

Based on cytogenetic observations of recurrent chromosomal translocations affecting

band 3q27 in diffuse large cell lymphomas (DLCL), the genomic region within 3q27 was cloned from a lymphoma with a t(3:14) (q27:q32) breakpoint (Baron *et al.*, 1993). Subsequent nucleotide sequencing of the corresponding cDNA led to the identification of a novel putative proto-oncogene, *bcl-6*, for B cell lymphoma-6, also called *LAZ3* (lymphoma-associated zinc finger gene on chromosome 3) (Ye *et al.*, 1993).

1.9.2 Structure of the *bcl-6* gene and protein

The *bcl-6* gene has 10 exons spanning 26kb, with a 10kb intron between non-coding exons 1 and 2 (see figure 14A). Two transcription initiation sites have been mapped to exon 1. Exons 3 to 10 encode a 95 kDa phosphoprotein that contains six *krüppel*-type C_2H_2 zinc-finger (ZF) motifs typically found in sequence-specific transcription factors, and an evolutionarily conserved poxvirus and zinc finger (POZ) domain at the N-terminus (see figure 14B). This motif serves to mediate protein-protein interactions and is required for homo- or hetero-dimerisation, as well as transcriptional activation and repression. This region is also capable of regulating sequence-specific DNA binding by the zinc-finger domain. The POZ domain along with the central portion of the gene, which contains multiple phosphorylation sites embedded in PEST motifs, regulates its stability (Niu *et al.*, 1998; see figure 14).

1.9.3 Pattern and regulation of Bcl-6 expression

The pattern of *bcl-6* mRNA and protein expression is highly discordant, suggesting post-transcriptional and translational mechanisms of regulation (Allman *et al.*, 1996). The mRNA is expressed at variable levels in many tissues and organs, highest levels being in skeletal muscle. However protein expression is far more restricted. Within the B cell lineage, the protein is detected only within the germinal centre and not in the immature B cells or differentiated plasma cells (Yen-Moore *et al.*, 2000). In the T-cell lineage, it is expressed in a subset of $CD4^+$ T cells within the GC and cortical thymocytes (Cattoretti *et al.*, 1995). In non-lymphoid tissue, the protein can be found in proliferating chondrocytes, mature myocytes, and differentiating keratinocytes. This suggests that protein expression is tissue-specific and confined to cells at specific stages of differentiation (Knudson *et al.*, 2001).

Figure 14. Structure of the *bcl-6* gene and protein

14 A Structure of the *bcl-6* gene

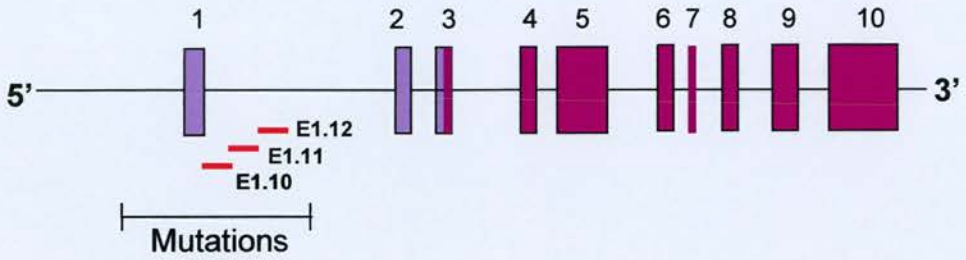

The dark purple boxes indicate the coding regions of the exons and the mauve boxes the non-coding regions. The mutation cluster region within the 5' non-coding region of the gene is indicated. A 740bp region encompassing the fragments E1.10, E1.11, and E1.12, wherein >90% of mutations reside, is indicated by bold red lines.

14 B Structure of the Bcl-6 protein

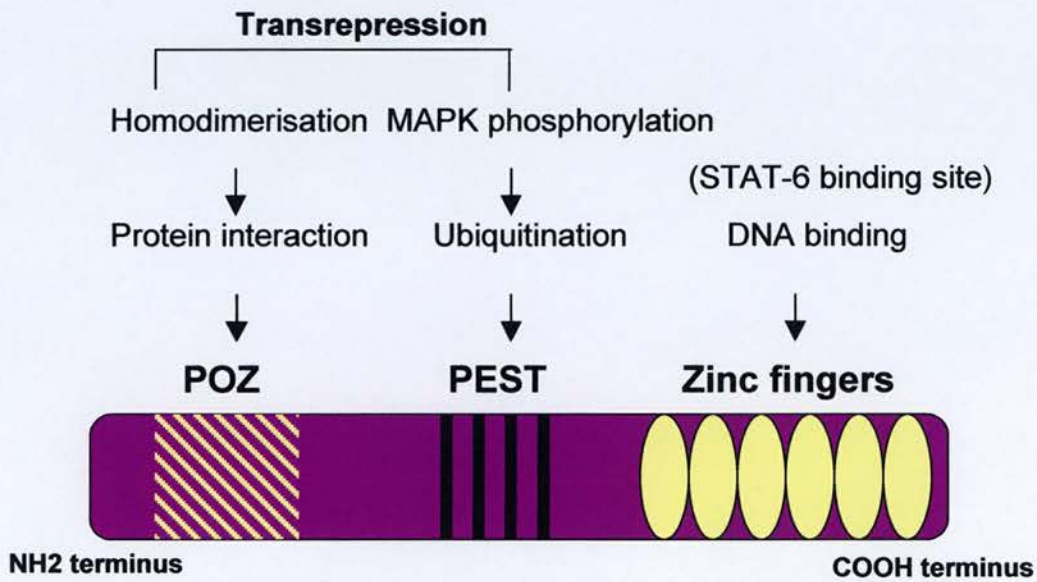

The Bcl-6 protein is a 95kDa nuclear phosphoprotein. The N-terminal POZ domain is responsible for protein-protein interactions, including homo-dimerisation and binding to nuclear co-repressors. The C-terminal domain, which is composed of six regularly spaced C_2H_2-type zinc fingers, mediates sequence-specific DNA recognition. The central region of the protein contains multiple phosphorylation sites embedded in PEST motifs. Trans-repression function of Bcl-6 requires both the POZ domain and the central PEST region. The STAT-6 binding site is indicated. **POZ:** poxvirus and zinc finger domain **PEST:** Proline (P), glutamic acid (E), serine (S) and threonine (T).

Adapted from Dalla-Favera *et al.*, 1999.

Relatively little is known about the upstream signals that induce Bcl-6. However, signalling pathways that downregulate the protein, have been identified. Antigen-receptor signalling in B cells can induce mitogen-activated protein kinase (MAPK)-mediated phosphorylation and subsequent degradation of the protein by the ubiquitin/proteosome pathway (Niu *et al.*, 1998). In addition, the protein can also be downregulated by CD40 signalling or by the CD40 functional homologue EBV LMP1 (Kenney *et al.*, 1998; Allman *et al.*, 1996; Ye *et al.*, 1997).

1.9.4 Transcriptional repression function of Bcl-6

The POZ domain mediates Bcl-6 transcriptional repression activity (Seyfert *et al.*, 1996) by interacting with nuclear co-repressors that recruit histone deacetylases, which in turn modify the activity of RNA polymerase II (Chang *et al.*, 1996). Target genes repressed by Bcl-6 are reviewed in Shaffer *et al* (2000). Inhibition of differentiation and enhanced proliferation through repression of target genes by deregulated or constitutively expressed Bcl-6, might have important consequences in the development of B cell lymphomas that harbour translocated *bcl-6* (Shaffer *et al.*, 2000).

1.9.5 Role for Bcl-6 in B and T cell development

The function of Bcl-6 in B and T cell development has been elucidated in studies carried out in *bcl-6* knockout mice. Mice deficient in Bcl-6 display normal B and T cell development but have a selective defect in T cell-dependent antibody responses with lack of affinity maturation, due to the inability of follicular B cells to proliferate and form germinal centres (Ye *et al.*, 1997). Further support for the function of Bcl-6 as a transcriptional switch in GC formation and post-GC differentiation comes from the observation that it is upregulated in B cells that enter the GC, and downregulated abruptly when they exit (Ye *et al.*, 1997).

Bcl-6 can modulate specific T cell-mediated responses. *bcl-6*$^{-/-}$ mice die at an early age of a severe inflammatory disease in multiple organs characterised by infiltrations of eosinophils and IgE-bearing B cells typical of a Th2-mediated hyperimmune response. This may be explained by the ability of Bcl-6 to bind and repress activation by STAT-6, a central mediator of IL-4-driven Th2 cell differentiation (Ye *et al.*,

1997).

1.9.5 Genetic alterations in *bcl-6*

1.9.5.1 *bcl-6* translocations in NHL

Rearrangements in *bcl-6* have been demonstrated in around 40% of DLCL, but are less frequently observed in follicular lymphoma (FL) (6 to 15%) and marginal zone B cell lymphoma (9%), and virtually absent in other lymphoid malignancies (Lo Coco *et al.*, 1994). In the setting of immunodeficiency, *bcl-6* alterations are detectable in 20% of AIDS-DLCL (Gaidano *et al.*, 1994).

An unusual feature of 3q27 reciprocal translocations is the heterogeneous nature of the partner chromosome. At least 33 different chromosomal loci have been described as participating in these translocations, including the *Ig* heavy and light chains and many non-Ig loci (Ye, 2000). 3q27 breakpoints are dispersed over a 10kb region (major translocation cluster, MTC) clustering mainly in the 5' flanking region within the first non-coding exon or intron of *bcl-6*. The 5' regulatory sequences which include the promoter in many cases, is removed, leaving the coding regions intact (Ye *et al.*, 1993). Thus, the germline promoter of the *bcl-6* gene is substituted by heterologous promoters fused in the same transcriptional orientation as the coding exons of *bcl-6* (Ye *et al.*, 1995a). The outcome of such promoter substitutions is usually a fusion transcript that translates a normal Bcl-6 protein (Chen *et al.*, 1998a; Ye *et al.*, 1995a). In B lymphoma cells, the germline *bcl-6* allele is transcriptionally inactive indicating that the cellular differentiation state of these cells is non-permissive for Bcl-6 expression and that translocation allows the expression of a gene that would normally be silenced (Ye *et al.*, 1995a). Therefore, the functional consequence of such translocations is transcriptional deregulation of *bcl-6*, resulting in a block to normal B cell differentiation and lymphomagenesis (Chen *et al.*, 1998a).

30% of cases that carry 3q27 abnormalities do not show a break in the MTC of *bcl-6* (Ye *et al.*, 1993). Recent studies indicate the possibility of an alternative breakpoint region (ABR) 200-270 kb telomeric and 5' to *bcl-6* (Chen *et al.*, 1998b).

An interesting observation that demonstrates the requirement for co-operative

interactions between genes to effect tumourigenesis is that *bcl-6* translocations are often accompanied by alterations in other genes, such as *bcl-2*, *bcl-1* and *p53* (Butler *et al.*, 1997). Concomitant rearrangements in *bcl-6* and *bcl-2* are observed in transformed lymphomas with a prior history of FL (Butler *et al.*, 1997), and a subset of high-grade mucosa-associated lymphoma tissue (MALT)-derived tumours display rearrangements in *bcl-6*, along with p53 mutations (Gaidano *et al.*, 1997a).

1.9.5.2 Somatic mutations in *bcl-6*

In contrast to the coding region of *bcl-6*, its 5' non-coding region displays extensive structural instability, which can result in deregulated expression (Capello *et al.*, 2000; Ye *et al.*, 1993). In addition to translocations and small intragenic deletions (Nakamura *et al.*, 1999; Ye *et al.*, 1995b), this region is frequently targeted by somatic mutations, both in GC derived tumours ($1.4x10^{-3}$ to $1.6x10^{-2}$ per bp) as well as normal B cells ($6.8x10^{-4}$ to $1.9x10^{-3}$ per bp) (Migliazza *et al.*, 1995; Shen *et al.*, 1998; see figure 14A). These 5' bcl-6 mutations are detectable in about 70% of DLCL and 45% of FL. Multiple biallelic mutations are present in both the germline and translocated *bcl-6* alleles. Furthermore, it is known that mutations in *bcl-6* can occur independently of translocation, as observed in 70% of AIDS-NHL (excluding DLCL), certain B-NHL without a 3q27 abnormality, and 28 to 50% of non-AIDS BL without detectable gross rearrangements (Capello *et al.*, 1997; Gaidano *et al.*, 1997c). More recently Zan *et al* have demonstrated that such mutations can occur out-with the *Ig* locus, and suggest the existence of *cis*-acting regulatory elements, similar to those in the *Ig* locus, in *bcl-6* (Zan *et al.*, 2000).

Of considerable interest is the observation that somatic mutations in *bcl-6* can also occur in normal GC and memory B cells, although at a much lower frequency (see above), indicating that *bcl-6* mutations may reflect a GC-related physiological process rather than a lymphoma specific phenomenon (Pasqualucci *et al.*, 1998).

1.9.5.3 Prognostic and histogenetic implications of *bcl-6* gene alterations and expression

bcl-6 mutations are more likely to reflect the GC or post-GC origin of tumours, since they are regarded as a marker of transition of a given B cell through the GC. This is

further corroborated by the fact that rare neoplasms of precursor B cells are significantly devoid of mutations in this gene, although they are frequently detected in DLCL, FL, BL and AIDS-NHL (Migliazza *et al.*, 1995).

Analysis of Bcl-6 protein expression has also contributed substantially to the histogenesis of AIDS-NHL and Hodgkin's disease. Analysis of AIDS-NHL shows that 100% of AIDS-BL express Bcl-6, whereas in AIDS-DLCL, expression is restricted to the cases displaying LNCCL morphology and generally absent in the immunoblastic type (Carbone *et al.*, 1997, 1998).

The significance of *bcl-6* rearrangement as a useful prognostic marker is controversial (Pescarmona *et al.*, 1997; Offit *et al.*, 1994). As a disease-specific diagnostic marker however, the persistence of tumour cells with *bcl-6* translocations after treatment can be used to monitor minimal residual disease. Somatic mutations in *bcl-6* have been considered as a reliable indicator of the more aggressive forms of post-transplant lymphoproliferative disorder, such as NHL and multiple myeloma, (Cesarman *et al.*, 1998).

1.10 Tumour-associated viruses

The first evidence of the tumour-inducing potential of viruses came in 1911, from the observation that a virus (Rous-sarcoma virus) could cause sarcomas in fowl (Rous, 1911). Since then viruses belonging to the retro-, herpes-, hepadna- papova- and adeno-virus families have been shown to be associated with a diverse range of neoplasias in humans and other hosts (for review see Wyke, 1997).

Three viruses associated with cancer both in immunocompetent and compromised (AIDS patients and organ transplant recipients) hosts are Epstein-Barr virus (EBV) (in Burkitt's lymphoma, AIDS-NHL and post-transplant lymphoproliferative disorder) (see below); Kaposi's sarcoma-associated herpesvirus (KSHV) (in Kaposi's sarcoma and primary effusion lymphoma) (see below); and human papillomavirus (HPV) (in anogenital, and cervical carcinoma) (Goedert *et al.*, 1998). However, only a small number of infected people develop virus-associated malignancy, reflecting the multi-step nature of carcinogenesis, with viral infection representing only one of these steps.

1.11 Epstein-Barr Virus (EBV)

EBV, a prototype gamma (γ) herpesvirus (Family *Herpesviridae*, genus *Lymphocryptovirus*), was first identified by Epstein and colleagues in cultured tumour biopsy cells from a case of endemic (African) Burkitt's lymphoma (BL) (Epstein *et al.*, 1964). Subsequently, the virus has been linked to diseases of both epithelial and lymphoid origin, in immunocompetent and immunocompromised hosts (reviewed in Brooks and Thomas, 1995, see Table 3).

Table 3

EBV-associated diseases

Association	Disease	Cell of origin	References
Causative agent	Acute infectious mononucleosis (IM)	Lymphoid	Niederman *et al.*, 1970
Etiologic association	Burkitt's lymphoma (BL)	Lymphoid	Epstein *et al.*, 1964
	Nasopharyngeal carcinoma (NPC)	Epithelial*	Wolf *et al.*, 1973
	Post-transplant lymphoproliferative disorder (PTLD)	Lymphoid	Crawford *et al.*, 1980 Hanto *et al.*, 1985
	AIDS-related lymphomas (ARL)	Lymphoid	Hamilton-Dutoit *et al.*, 1991
	Oral Hairy Leukoplakia (OHL)	Epithelial*	Greenspan *et al.*, 1985
	X-linked lymphoproliferative disease (XLPD)	Lymphoid	Purtilo *et al.*, 1975
	Hodgkin's disease (a subset)	Lymphoid	Weiss *et al.*, 1989
	T-cell lymphoma (a subset)	Lymphoid	Jones *et al.*, 1988
Suspected association	Gastric carcinoma (~10%)	Epithelial*	Imai *et al.*, 1994
	Carcinoma of the parotid gland	Epithelial*	Raab-Traub *et al.*, 1991
	Breast cancer	Epithelial	Bonnet *et al.*, 1999
	Leiomyosarcomas	smooth muscle	McClain *et al.*, 1995

* Epithelial cell infection/lesions are included for completion but are not discussed further.

1.11.1 Genome organisation

EBV is an enveloped virus, with a 172kb double-stranded linear DNA genome enclosed in an icosahedral capsid. The genome contains dispersed regions of repeat (internal repeats {IR} 1-4) and unique (U) sequences (short {US} and long {UL}) along its entire length, and is flanked by reiterated 500bp terminal direct repeats that are required for covalent circularisation of the genome in latently infected cells. The genome has the coding capacity for approximately 70 proteins. The latent and lytic

cycle genes are described in Table 4 (reviewed in Epstein and Crawford, 1998; Rickinson and Kieff, 1996).

Table 4

Classification and function of selected EBV genes

Class	Gene*	Function
LATENT	EBNA LP	Immortalisation, binds p53 and pRb
	EBNA1[a]	Episome maintenance
	EBNA2	Immortalisation, Transactivates viral & cellular genes (p21 and hMDM2)
	EBNAs 3a, 3b and 3c	3a and 3c, immortalisation 3c, viral transactivator, binds pRb
	LMP1[a]	Immortalisation, upregulates anti-apoptotic bcl-2 and A20, tumourigenic in nude mice
	LMP2a and 2b	Facilitate immortalisation. LMP2a inhibits EBV reactivation from latency
	EBERs	bind and inhibit protein kinase, PKR
	BARTs	role in signal transduction and growth control
LYTIC		
Immediate early	BRLF1 and BZLF1 (Zta)	switch from latent to lytic infection; Zta, effects growth arrest by inducing p53, p21 and p27; BRLF1, activates E2F1 and viral replication
Early	Early antigen (EA)	Viral replication
Late	Membrane antigen (MA)	Viral infectivity and spread
	Viral capsid antigen (VCA)	Viral structural protein

*, Only selective genes have been mentioned; [a], expressed during both latent and lytic infection; EBNA, Epstein-Barr nuclear antigen; LMP, latent membrane protein; EBERs, EBV-encoded RNAs; BARTs, BamH1 A rightward transcripts; LP, Leader protein; PKR, double stranded RNA protein kinase

1.11.2 EBV infection of B lymphocytes

EBV infects B cells (rarely T lymphocytes and epithelial cells) both *in vitro* and *in vivo*. Latent infection results in the expression of viral latent genes without virus production. Viral infection of lymphocytes is mediated by binding of the viral envelope glycoprotein (gp350/220) to the C3d/CR2 complement receptor (CD21), which is found on all mature B lymphocytes, peripheral T cells and thymocytes (Fingeroth *et al.*, 1984). *In vitro* infection of B cells leads to the activation and immortalisation of these cells resulting in the generation of continuously proliferating lymphoblastoid cell lines (LCL) (Pope *et al.*, 1968). The linear genome enters the nucleus and circularises to form an episome, which amplifies and then replicates concurrently with, but does not integrate, into, host cell DNA. Between 0.1 to 5% of LCL cells enter the lytic cycle at any one time resulting in infectious virus

production and cell death.

1.11.3 Models of EBV latency

EBV can establish three different patterns of latency in infected cells - Latency I, II and III, both *in vitro* and *in vivo*, with each pattern being characterised by the expression of a specific set of latent genes (Rowe *et al.*, 1992; reviewed in Rickinson and Kieff, 1996; see Table 5).

Table 5

Pattern of EBV latency in EBV-associated malignancies

Latency	BARTs	EBERs	EBNA						LMP		Cancer type
			1	2	3a	3b	3c	LP	1	2a/b	
I	+	+	+	-	-	-	-	-	-	-	Burkitt's lymphoma AIDS-associated SNCCL
II	+	+	+	-	-	-	-	-	+	+	Hodgkin's disease T cell NHL NPC AIDS-associated DLCL
III	+	+	+	+	+	+	+	+	+	+	PTLD AIDS-associated DLCL

Adapted from Niedobitek *et al.*, 1997.

BARTs, BamH1 A rightward transcripts; EBERs, Epstein-Barr encoded RNAs; EBNA, Epstein-Barr nuclear antigen; LMP, Latent membrane protein; NHL, Non-Hodgkin's lymphoma; DLCL, diffuse large-cell lymphoma; SNCCL, small non-cleaved cell lymphoma; PTLD, Post-transplant lymphoproliferative disorder; NPC, Nasopharyngeal carcinoma

1.11.4 EBV infection *in vivo*

EBV has a world-wide distribution and more than 90% of adults show evidence of past infection (Henle and Henle, 1966). The virus is transmitted predominantly through saliva (Yao *et al.*, 1985). In a majority of individuals primary infection occurs in the first 2 years of life and is usually asymptomatic. However, delayed primary infection in adolescence often manifests clinically as infectious mononucleosis (IM) (Diehl *et al.*, 1968; reviewed in Steven, 1996).

Following primary infection, life-long persistence is established, with 5-500 cells in every 10 million circulating B cells carrying the virus in a latent form (Miyashita *et al.*, 1995). Low level viral replication in the pharynx and intermittent shedding of infectious virus into saliva is observed during the carrier-state (Yao *et al.*, 1985).

1.11.5 Malignancies in immunosuppressed individuals

In immunocompetent individuals, EBV persistence is controlled by both cellular and humoral mechanisms. An antibody response to EBV antigens (mainly the lytic cycle antigens) is detectable during primary infection and convalescence, with IgG antibodies to the viral capsid antigen and EBNA-1 persisting in the serum throughout life (Henle *et al.*, 1987). Antibodies against gp350/220 are neutralising, and are present in both the serum and saliva of carriers (Yao *et al.*, 1991). However, it is the EBV-specific $CD8^+$ cytotoxic T cells (CTLs) that are primarily responsible for maintaining a stable virus-host balance (Moss *et al.*, 1978). Displacement of this equilibrium is classically seen in immunodeficient states, which leads to enhanced virus replication, increase in the number of EBV-carrying B cells, and elevated serum antibody levels to EBV lytic cycle antigens (Birx *et al.*, 1986; Thomas *et al.*, 1991).

1.11.5.1 AIDS-related Non-Hodgkin's lymphoma (NHL)

Unlike post-transplant lymphoproliferative disorders (PTLDs), AIDS-associated lymphomas are not uniformly associated with EBV, questioning whether the virus is involved in the development and pathogenesis of these lesions, or merely a passenger.

Among systemic AIDS-NHL, EBV is associated with around 70 to 80% of diffuse large cell lymphomas (DLCLs), and a similar proportion of Burkitt's-like lymphoma (BLL). The majority of DLCLs have a latency II or III phenotype and frequently, though not always, express the transforming antigens LMP-1 and EBNA-2, suggesting that the virus has a pathogenic role in the genesis of these tumours (Carbone *et al.*, 1993; Hamilton-Dutoit *et al.*, 1993).

At a frequency similar to sporadic BL, around 30% of AIDS-BL carry EBV and have a latency I phenotype (Ballerini *et al.*, 1993). Virus in BL is generally monoclonal, consistent with the hypothesis that the virus was present before clonal expansion, and might therefore contribute to lymphoma development (Neri *et al.*, 1991). Furthermore, positive identification of EBV DNA in the lymph nodes of HIV-infected individuals is considered to be a predisposing factor for subsequent development of lymphomas (Shibata *et al.*, 1991). However, EBV-positive AIDS-BL

fail to express EBNA-2 and LMP-1, which are key inducers of the transformed phenotype in other B cell tumour models (Carbone *et al.*, 1993). Moreover, the absence of EBV in around 70% of AIDS-BL challenges the contribution of the virus to the pathogenesis of these lesions.

AIDS-related PCNSL are consistently associated with EBV (MacMahon *et al.*, 1991) and display a latency III EBV phenotype, similar to that of systemic immunoblastic NHL. Expression of EBV-LMP-1 is detected in approximately 50% of cases, suggesting a transforming role for the virus in the pathogenesis of these lymphomas (Larocca *et al.*, 1998)

1.12 Kaposi's Sarcoma-associated Herpes Virus (KSHV)

Kaposi's sarcoma (KS) was first noted in 1872 by a Hungarian dermatologist, Moriz Kaposi, as purplish skin lesions (frequently accompanied by lymphoedema) that appeared on the lower extremities. Much later, these pigmented sarcomas were re-described in elderly men of Eastern European and Mediterranean descent (classic KS), African men and children (endemic KS) and organ transplant recipients (iatrogenic KS). With the onset of the AIDS epidemic a vast increase in KS cases was noted. Now AIDS-associated KS (AIDS-KS) is the most common neoplasm observed in AIDS patients (particularly young homosexual men), whose risk of developing the disease is 20,000 fold above that of the general population (Beral, 1991; Antman and Chang, 2000). In 1994, Chang and colleagues identified a previously unrecognised herpesvirus in the skin lesions of an individual with AIDS-KS, which came to be known as Kaposi's sarcoma-associated herpesvirus (KSHV) or human herpesvirus-8 (HHV-8) (Chang *et al.*, 1994).

1.12.1 Genome structure

KSHV is a γ-herpes virus, which is more similar to the simian herpesvirus saimiri (HVS) than it is to EBV. It consists of a double-stranded 165 to 172kb genome with a long unique region (LUR, ~140kb) flanked by terminal repeats. The LUR comprises the entire coding region for the virus and encodes over 80 genes. Genes that are conserved among all herpesvirus subfamilies are present along the length of

the genome and include those that code for structural proteins and DNA synthetic enzymes. Interspersed between these conserved gene blocks are regions unique to KSHV (open reading frames (ORFs) *K1-15*) and other rhadinoviruses, some of which can mimic cell cycle regulatory genes, cytokines and signal transduction proteins (Russo *et al.*, 1996, reviewed in Moore and Chang, 1998).

1.12.2 Gene expression and function

Taking into account tissue-specific differences in transcription patterns, KSHV gene expression has been broadly classified into 3 classes based on their ability to be stimulated by 12-*O*-tetradecanoylphorbol-13-acetate (TPA) or sodium butyrate in body cavity cell lines (BC-1) *in vitro* (Sarid *et al.*, 1998, and see Table 6).

Table 6

KSHV gene expression

Class*	Inducible by TPA	Selected genes
I	-	v-cyclin (v-cyc), v-FLIP, LNA
II	+	v-IL6, v-GPCR, v-Bcl2
III	++	K12 (kaposin)

*, Pattern of gene transcription examined in a body cavity lymphoma cell line (BC-1). -, Constitutive and not induced by TPA (latent mRNAs); +, constitutive and inducible by TPA; ++, only inducible by TPA (late lytic genes). Only selective Class I, II and III transcripts have been shown due to space constraints (for a detailed list refer Sarid *et al.*, 1998). LNA, latency associated nuclear antigen; FLIP, FLICE inhibitory protein; GPCR, G-protein coupled receptor; IL6, Interleukin-6

1.12.3 *In vitro* infection of B cells

KSHV can persistently infect primary peripheral blood B cells *in vitro* in the presence of EBV, and such infection leads to the outgrowth of continuously growing $KSHV^+/EBV^+$ LCLs. KSHV latent viral transcripts were expressed in non-stimulated $KSHV^+/EBV^+$ LCLs, and induction with phorbol ester and *n*-butyrate resulted in lytic expression (Kliche *et al.*, 1998).

1.12.4 Latent infection

Similar to other herpesviruses, KSHV persists as a covalently closed circular

episome in latently infected cells with limited viral gene expression. Two latency-associated Class I transcripts are encoded at the right hand end of the genome. A 5.32kb transcript (latent transcript 1) encodes *ORF73* (*LNA*), *ORF72* (*vCYC*) and *ORF71* (*vFLIP*), while splicing of the 5.32kb transcript yields a 1.7kb transcript (latent transcript 2) that encodes only *ORF72* and *ORF71* (Talbot *et al.*, 1999; see figure 15). *ORF73* encodes an immunoreactive latent nuclear antigen (LNA), analogous to the EBNA1 protein of EBV, and is constitutively expressed in cells latently infected with KSHV (Kellam *et al.*, 1997). This protein has been shown to be necessary and sufficient for viral episome maintenance, persistence and segregation during mitosis, by tethering the KSHV genome to the chromosome (Ballestas *et al.*, 1999). Recent evidence demonstrates that LNA can interact with p53 and inhibit transcriptional activation and apoptosis mediated by p53 (Friborg *et al.*, 1999). In addition, the virus can interact with the pRb tumour suppressor both *in vitro* and *in vivo* and transactivate E2F regulatory sequences (Radkov *et al.*, 2000).

1.12.5 KSHV transmission and seroprevalence

KSHV can be transmitted sexually, and is thought to be more readily transmissible through homosexual than heterosexual practices (Martin *et al.*, 1998). In areas where KS is endemic vertical transmission accounts for a portion of childhood cases, although the precise mode of transmission in late childhood and adolescence is still unknown (Bourboulia *et al.*, 1998). Viral DNA can be detected in the saliva, oral tissues, semen, peripheral blood and lymphoid tissue of seropositive people as well as in the gastrointestinal (GI) mucosa of HIV-infected individuals, suggesting other routes of transmission (Koelle *et al.*, 1997; Thomas *et al.*, 1996).

Unlike EBV, KSHV is not ubiquitous (Gao *et al.*, 1996a). The seroprevalence of KSHV in the general population, is highest in Africa (50%) where KS is endemic, whereas it is between 5 and 10% in the United States and 0.2% in Japan where KS is rare (Lennette *et al.*, 1996). In the American HIV-infected population, the incidence is 30% in homosexual men and 3 to 4% in women and haemophiliacs.

1.12.6 KSHV-associated diseases in HIV infection

KSHV has a tropism for B lymphocytes and has been detected in lymph nodes and

Figure 15. Transcription pattern of ORFs 71-73 of KSHV

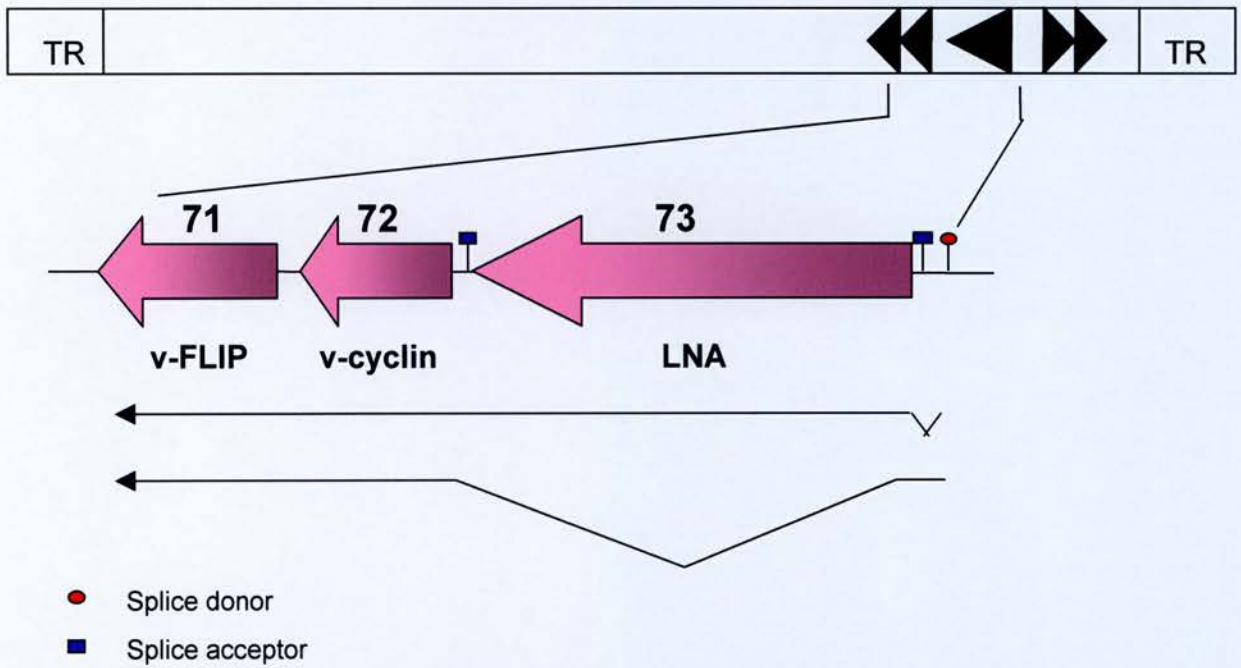

The LNA, v-cyclin and v-FLIP genes are part of a polycistronic transcript (5.32kb). Splicing of this transcript yields a bicistronic message (1.7kb) encoding v-cyclin and v-FLIP. The numbers above the arrows indicate the corresponding open reading frames. Splice donor and splice acceptor sites are indicated as red circles and blue squares respectively. **LNA:** Latent nuclear antigen **FLIP:** FLICE inhibitory protein **TR:** Terminal repeat.

Adapted from Talbot *et al.*, 1999.

peripheral blood B cells (Whitby *et al.*, 1995). However, the virus also has a predilection for spindle cells of endothelial origin (Boshoff *et al.*, 1995), as seen in KS, and primary human keratinocytes in culture (Cerimele *et al.*, 2001). KSHV has been etiologically linked to diseases with prominent vasculature such as KS and multicentric Castleman's disease, as well as a rare B cell lymphoma, primary effusion lymphoma, in both individuals who have a preserved immune function and those with AIDS (reviewed in Cannon and Cesarman, 2000 and see below).

(i) AIDS-associated KS (AIDS-KS)

A causal relationship between KSHV and KS has been established by studies that have demonstrated evidence of infection prior to the development of KS, as well as the presence of KSHV sequences in all forms of KS (Dupin *et al.*, 1995). Seroconversion to KSHV is a prognostic indicator of KS development (Whitby *et al.*, 1995; Gao *et al.*, 1996b).

KS lesions are histologically complex containing proliferating spindle cells of endothelial origin, but which often express markers characteristic of endothelial, macrophage and smooth muscle cells. Infiltrating plasma and mononuclear cells as well as abundant slit-like neovascular spaces are present in these lesions. AIDS-KS is particularly aggressive and frequently fatal, due to disseminated infection involving the lung, GI tract, liver and spleen (Friedman-Kien and Saltzman, 1990). The highly aggressive phenotype of AIDS-KS is believed to be induced by extracellular HIV-Tat, which synergises with, and mobilises sequestered basic fibroblast growth factor (bFGF), increasing endothelial cell growth and invasion in response to bFGF, by mimicking extracellular matrix proteins (Barillari *et al.*, 1999; Ensoli *et al.*, 1994). Most infected cells in a KS lesion are latently infected with lytic expression being limited to only 0.5 to 1% of cells. Productive infection occurs in the peripheral blood B cells of individuals with KS (Decker *et al.*, 1996).

(ii) Primary effusion lymphoma (PEL)

KSHV-associated lymphomas represent a distinct diagnostic entity, called body cavity-based lymphoma or PEL (Nador *et al.*, 1996). This malignancy accounts for 3 to 5% of AIDS-related NHL and has unique morphological and genetic

characteristics that distinguish it from other AIDS-NHL (Carbone *et al.*, 1996a). Clinically, PEL is an aggressive lymphoma that presents as lymphomatous effusions in the pleural, peritoneal and/or pericardial cavity without a contiguous tumour mass. However, 15% of KSHV-associated lymphomas present as solid extranodal tumours, with half of these developing a subsequent lymphomatous effusion. These lymphomas are B cell in origin and histologically comprise a mixture of anaplastic and immunoblast-like cells. Co-infection with EBV occurs in 90% of PELs (Fassone *et al.*, 2000); (Nador *et al.*, 1996). Apart from 5' non-coding mutations in *bcl-6* in 20% of cases (Gaidano *et al.*, 1997d), these lesions lack molecular defects commonly associated with B cell neoplasia, such as rearrangement of c-*myc*, activation of *bcl-2*, and mutations in *p53* and *ras* (Nador *et al.*, 1996; Carbone *et al.*, 1996a; Cesarman and Knowles, 1999).

(iii) Multicentric Castleman's disease (MCD)

MCD is an atypical lymphoproliferative disorder, which is characterised by a vascular proliferation in the germinal centres, and clinical presentation of multiple lymphadenopathies, autoimmune phenomena, skin rashes and intercurrent infection. Patients with MCD frequently develop other malignancies, most commonly KS and NHL (Soulier *et al.*, 1995). KSHV is consistently detected in MCD associated with AIDS, although it has also been identified in 40% of MCD cases in HIV-negative individuals (Soulier *et al.*, 1995). MCD in HIV positive patients frequently occurs in conjunction with KS (75%), although the virus is also present independent of KS in these individuals (Oksenhendler *et al.*, 1996). Elevated serum levels of IL-6 are thought to contribute to the characteristic polyclonal plasmacytosis and hypergammaglobulinemia observed. Notably, vIL6 of KSHV is expressed in a few B cells surrounding the lymphoid follicles, suggesting a paracrine mechanism to drive proliferation and differentiation of B cells in KSHV-associated MCD (Parravicini *et al.*, 2000; Staskus *et al.*, 1999).

1.13 Molecular features of AIDS-NHL

1.13.1 AIDS-SNCCL

AIDS-BL typically harbour translocations between the c-*myc* oncogene on chromosome 8 and one of the Ig gene loci on chromosomes 14,22 or 2 (Ballerini *et al.*, 1993; Subar *et al.*, 1988; Gaidano *et al.*, 1997b). Furthermore, the translocated c-*myc* alleles are frequently affected by mutations in exon 2, which alter the amino-acid sequence of the c-Myc protein (Bhatia *et al.*, 1994).

Inactivating mutations of the *p53* tumour suppressor gene were reported in 37% of AIDS-NHL, although the majority (60%) of these occur in the AIDS-BL sub-type (Ballerini *et al.*, 1993). This figure is twice as high as that observed in NHL of the immunocompetent host (Gaidano and Dalla-Favera, 1993). In contrast to sporadic and endemic BL, AIDS-BLs are consistently devoid of molecular lesions in *bax* (Gaidano *et al.*, 2000), a proapoptotic gene that is transcriptionally activated by p53 (Miyashita and Reed, 1995).

The molecular pathogenesis of AIDS-BLL is different from that of AIDS-BL, in that *p53* mutation is rare and c-*myc* translocations less frequent in the former than the latter (20-60% versus 100%) (Davi *et al.*, 1998; see Table 7). However, similar to AIDS-BL, approximately 70% of AIDS-BLL harbour *bcl-6* mutations (Gaidano *et al.*, 1997b). Furthermore, although rearrangements of *bcl-2* have been detected in a fraction of BLL in the immunocompetent host (Yano *et al.*, 1992), such abnormalities have not been detected across the spectrum of AIDS-NHL in the small number of studies that have been carried out (Gaidano *et al.*, 1997b).

1.13.2 AIDS-DLCL

Mutations and rearrangements of c-*myc* are observed less frequently (20-50%) in AIDS-DLCL than in AIDS-SNCCL (Ballerini *et al.*, 1993; Gaidano *et al.*, 1997b; Delecluse *et al.*, 1993a; see Table 7). However molecular alterations affecting *bcl-6* are associated with a significant fraction of these tumours (Strasser *et al.*, 1994). Rearrangements of *bcl-6* are detected in 20% of AIDS-DLCL and in 40% of DLCLs in the immunocompetent host (Gaidano *et al.*, 1994, 1997c). Mutations in the 5' regulatory region of the gene occurs in 70% of these tumours, similar to that

observed in the immunocompetent host (Capello *et al.*, 2000; Gaidano *et al.*, 1997d). Mutations in *p53* are rarely observed among this subset of tumours (Ballerini *et al.*, 1993; see Table 7).

Table 7

Molecular lesions associated with AIDS-NHL

AIDS-NHL type	p53 mutation	c-*myc* rearrangement/ mutation	bcl-6		bcl-2	EBV
			rearrangement	mutation		
DLCL						
LNCCL	rare	20-50%	20%	70%	-	40%
IBL	rare	20%	-	70%	-	>90%
SNCCL						
BL	60%	100%	-	60%	-	30%
BLL	-	20-60%	-	70%	-	30%
PCNSL	nd	-	-	70%	+	100%

nd, not done; +, positive expression; -, absence of genetic lesion/expression; DLCL, diffuse large-cell lymphoma; LNCCL, large non-cleaved cell lymphoma; IBL, immunoblastic lymphoma; SNCCL, small non-cleaved cell lymphoma; BL, Burkitt's lymphoma; BLL, Burkitt-like lymphoma; PCNSL, primary central nervous system lymphoma; EBV, Epstein-Barr virus

1.13.3 AIDS-PCNSL

Although the Bcl-6 protein is expressed by all PCNSLs in the immunocompetent host, AIDS-PCNSL are classified as Bcl-6-expressing or non-expressing cases (Carbone *et al.*, 1998). The IBL variants are characterised by an absence of Bcl-6 expression and rearrangement, and almost consistent expression of Bcl-2 and EBV LMP-1 (Kenney *et al.*, 1998; Carbone *et al.*, 1997). Conversely, the LNCCL variants express Bcl-6 and include rearranged and non-rearranged *bcl-6*. These tumours fail to express Bcl-2 and LMP-1, when infected with EBV (Larocca *et al.*, 1998). Mutations in *bcl-6* are relatively frequent among AIDS-PCNSLs, similar to that observed in the other subsets of AIDS-NHL (Larocca *et al.*, 1998; see Table 7).

1.13.4 Other genetic lesions associated with AIDS lymphomas

Besides the genetic alterations involving the c-*myc*, *p53* and *bcl-6* genes, structural

changes in other genes have been reported, albeit less frequently. Mutations in the *ras* oncogene occur predominantly in the AIDS-SNCCL subtype (approximately 15% of cases analysed) (Ballerini *et al.*, 1993) despite being absent in NHL of the immunocompetent host (Neri *et al.*, 1988). Furthermore, extensive structural analysis of the functional domains of the retinoblastoma gene (*RB*) locus in AIDS-NHL has indicated an absence of alterations (Ballerini *et al.*, 1993).

Deletions of the long arm of chromosome 6 (Vitolo *et al.*, 1998), a frequent genetic alteration of B-NHL in the immunocompetent host, has been reported in a fraction of AIDS-DLCL (around 20%), whereas it is consistently absent among other types of AIDS-NHL (Pastore *et al.*, 1996). In addition, AIDS-BL particularly those that are EBV-positive, demonstrate recurrent 1q21-25 chromosome abnormalities, suggesting that this genomic site harbours an unknown gene with relevance to AIDS-related lymphomagenesis (Polito *et al.*, 1995).

AIMS OF THE PROJECT

The aim of this project was to define the molecular genetic and virological characteristics of persistent generalised lymphadenopathy (PGL) in HIV-infected individuals, in an attempt to identify early lesions that might be predictive of future lymphoma development in these individuals. This was achieved by genetic (structural), epigenetic and/or expression analysis of selected tumour suppressor genes (*p53*, *p63*, *p73* and *INK4* genes), oncogenes (c-*myc*, *bcl-2* and *bcl-6*) and viruses (EBV and KSHV).

CHAPTER TWO

MATERIALS AND METHODS

2.1 Reagents

All cell culture reagents were supplied by Life Technologies unless otherwise stated. General reagents, unless specified, were supplied by Merck Ltd. Radiolabelled isotopes were supplied by ICN Biomedicals Ltd. and Amersham Pharmacia Biotec. Unless otherwise stated, Roche Diagnostics and Biochemicals Ltd. supplied restriction endonucleases and buffers. All oligonucleotides were synthesised by Life Technologies. Commercial suppliers are listed in appendix 3.

Reagent	**Supplier**
1Kb DNA ladder	Life Technologies
100bp DNA ladder	Life Technologies
λ DNA restricted with Hind III	Roche
Agarose	ICN
Ammonium persulphate	Bio-rad Laboratories
Ampicillin	Sigma
AmpliTaq Gold® polymerase	Roche
BPB	Sigma
BSA	Sigma
Chloroform	Sigma
DMF	Sigma
DMSO	Sigma
DNA Polymerization Mix	Amersham Pharmacia
Ethidium bromide	Life Technologies
FCS	Harlan Sera Lab
Ficoll™ 400	Amersham Pharmacia
Formamide	Life Technologies
ϕX-174 DNA/*Hinf* I dephosphorylated markers	Promega
Glycerol	Sigma
Isopropanol	Sigma
Kanamycin	Sigma
LA Taq polymerase	BioWhittaker

Mineral oil	Sigma
NICK™ column	Amersham Pharmacia
NuSieve® 3:1 agarose	Flowgen
PBS tablets	Oxoid
Pfx polymerase	Life Technologies
Polynucleotide kinase	Promega
PVP	Sigma
Proteinase K	Promega
RNAzol™ B	Biogenesis
RT-PCR Kit	Stratagene
Sheared salmon sperm DNA	CP Labs
Sequagel® MD	National Diagnostics Ltd
Taq DNA Polymerase	Promega
TaqStart™ Antibody	Clontech
TEMED	Bio-rad Laboratories
Triton® X-100	Sigma
Trypan Blue	ICN
Ultrapure dH_2O	Sigma
X Ray Developer and Fixer	Jet X-Ray

2.2 Equipment

Benchtop centrifugation was carried out using a Mistral 3000E MSE (Sanyo). Thermal cycling was carried out using the Hybaid Touchdown, Hybaid Omnigene (Hybaid) and the Robocycler Gradient 96 (Stratagene). Hybridisations were done in Shake N' Stack cabinets (Hybaid). General plastic-ware was supplied by SLS and Anachem. Tissue culture plastic-ware was supplied by Fred Baker, SLS and Life Technologies, unless specified otherwise.

2.3 General Solutions

All solutions were prepared in sterile distilled water (SDW)

Freezing Medium

90% v/v Fetal calf serum, 10% v/v DMSO

Culture Medium

2mM L-glutamine, 100 IU/ml Penicillin, 100 μg/ml Streptomycin, 5 or 10% v/v FCS, made up in 1×RPMI 1640

Phosphate buffered saline (PBS)

1 PBS tablet dissolved in 100ml of dH_2O

TaqStart Antibody [1.1μg/μl]

(in 10mM Tris-HCl pH7.0, 50mM KCl, 50% glycerol)

10×Tris-Borate-EDTA (TBE) Buffer

10.8% v/v Tris, 5.5% w/v Boric acid, 4% v/v 0.5M EDTA (pH 8.0)

20×Standard Saline Citrate (SSC)

3M sodium chloride, 0.3M trisodium citrate (pH 7.0)

Tris-EDTA (TE)

10mM Tris-HCl (pH 8.0), 1mM EDTA pH 8.0

Denaturing Solution

1.5 mM NaCl, 0.5M NaOH

Neutralising Solution

1.5mM NaCl, 0.5M Tris-HCl (pH 7.2), 0.001M EDTA (pH 8.0)

10% w/v Sodium Dodecyl Suphate (SDS)

made up in dH_2O

10×DNA Loading Buffer

100mM EDTA (pH 8.0), 6% w/v Sucrose, 0.1% v/v BPB, 0.1% Xylene cyanol

Stop solution

95% formamide, 20mM EDTA, 0.05% w/v BPB, 0.05% w/v Xylene cyanol

Formamide

Deionised in 10% w/v Mixed-bed resin.

100×Denhardt's solution

2% w/v BSA, 2% w/v Ficoll™, 2% w/v PVP

Pre-Hybridisation Solution

50% v/v Formamide, 25% v/v 20×SSC, 10% v/v 50×Denhardt's solution, 5% w/v SDS, 1% v/v sheared salmon sperm DNA

Sheared Salmon Sperm DNA

10mg/mL 1% v/v

Hybridisation solution

Prehybridisation solution with ^{32}P-labelled probe and fresh 1% v/v sheared salmon sperm DNA

T4 Polynucleotide Kinase [5U/mL] (from a recombinant *E. coli* bacterium strain)

10×Kinase buffer

700mM Tris-HCl (pH 7.6), 100mM $MgCl_2$, 50mM DTT

Membrane wash solutions

2×SSC/ 0.1% w/v SDS and 1×SSC/ 0.1% w/v SDS

Luria-Bertani medium (LB, supplied by Veterinary Pathology Media service)

1% bacto-tryptone, 0.5% Bacto-yeast extract, 1% sodium chloride adjusted to pH 7.2 using 1M sodium hydroxide

LB agar

LB supplemented with 1.5% agar

SOC medium

2% tryptone, 0.5% yeast extract, 10mM sodium chloride, 2.5mM potassium chloride, 10mM magnesium chloride, 10mM magnesium sulphate and 20mM glucose

2.3.1 DNA Size Markers

0.5µg of the DNA markers were used on each gel.

100bp DNA ladder [50µg/ml]

(in 10mM Tris-HCl pH7.5, 1mM EDTA)

1kb DNA ladder [200µg/ml]

(in 10mM Tris-HCl, pH7.5, 50mM NaCl, 0.1mM EDTA)

ϕX174 DNA/*Hinf* I dephosphorylated markers [50µg/ml]

(in 10mM Tris-HCl, pH7.5, 1mM EDTA)

λDNA restricted with *Hin*d III [250µg/ml]

(in 10mm Tris-HCL, 1mM EDTA pH8.0)

2.3.2 Bacterial Strains

JM109 (Promega, UK); *TOP10* (Invitrogen, Holland)

2.3.3 Plasmids

pGEM®-T	Promega, UK
pCR®-BLUNT	Invitrogen, Holland (Bernard *et al.*, 1994)
pCR®4-TOPO®	Invitrogen, Holland (Shuman, 1994)

2.4 Cell culture techniques

All cell culture techniques were carried out in an aseptic manner inside microbiological (class II) safety cabinets using sterile equipment and solutions.

2.4.1 Control Cell Lines

A store of control cell lines was kept under liquid nitrogen, and is shown in Table 8.

Table 8

Control Cell Lines

Cell line	Cell type	EBV/KSHV status	Reference
BCP-1	Body cavity lymphoma	-/+	Boshoff *et al.*, 1998
BJAB	BL	-/-	Menezes *et al.*, 1975
Namalwa	BL	+/-	Klein and Dombos, 1973
P3HR1	BL	+/-	Hinuma *et al.*, 1967
Raji	BL	+/-	Pulvertaft, 1965
Ramos	BL	-/-	Klein *et al.*, 1975

BL, Burkitt's lymphoma

2.4.2 Thawing cells

Cells were recovered from liquid nitrogen by thawing in a 37°C water bath for a few minutes and then slowly adding 9 times the volume of wash medium (HBSS). The cells were then spun down at 400g (g-number = $11.2 \times r \times n^2 \times 10^{-6}$, where r is the centrifugal radius in cm from axis to middle of tube and n is the speed in rpm) for 7 minutes in a bench centrifuge. This was followed by re-suspension of the cell pellet

in 5ml of tissue culture medium in a $25cm^2$ culture flask, and incubation at 37°C.

2.4.3 Culturing cells

All cells were cultured in a humidified 5% CO_2 incubator (Heraeus) at 37°C and fed every 2-3 days, as required, with tissue culture medium.

2.4.4 Counting cells

10µl of cell suspension was mixed with 10µl of 0.5% w/v trypan blue in PBS. 10µl of the mixture was placed on a haemocytometer (Weber Improved Neubauer, Merck). Cells were counted using a light microscope (Leitz). The cells that excluded the dye (viable cells) were counted.

2.4.5 Freezing cells

Around 10^7 cells were spun at 400g for 7 minutes in a bench centrifuge, followed by two washes with wash medium at 400g for 7 minutes. The cells were then re-suspended in 1 ml of freezing medium in a cryotube (Nunc, Life Technologies) which was placed at –70°C. 24 hours later the cells were transferred to a liquid nitrogen tank (Jencons).

2.5 Processing and storing of tissue

2.5.1 Processing of lymph nodes

Hyperplastic lymph node tissue, biopsied from 23 HIV-infected individuals with lymphadenopathy, was kindly provided by Prof. Ian Weller, UCL, London. 9 reactive control lymph nodes frozen in OCT (Optimum Tissue Cutting medium) compound were kindly provided by Dr. Andrew Krajewsky, Department of Pathology, Edinburgh University.

Tissue was recovered from liquid nitrogen and thawed briefly on ice. The tissue was placed on a petri dish and cut into smaller pieces with a sterile scalpel. The cut tissue was placed in clean eppendorfs, snap-frozen in isopentane and stored at –70°C or liquid nitrogen.

2.5.2 Processing of tonsillar tissue

7 fresh tonsils obtained from routine tonsillectomies performed at the City Hospital, Edinburgh, were collected in 10ml of saline. The specimen was placed on a petri dish and lymphoid tissue was dissected from the surrounding fibrous connective tissue. The tissue was then cut and stored as described in section 2.5.1.

2.6 DNA Extraction and Methods

2.6.1 Extraction of DNA from tissue

(i) Extraction of DNA using the Invitrogen Easy DNA Kit (Invitrogen)

DNA was extracted from snap-frozen PBMCs using the Invitrogen Easy-DNA kit according to the manufacturer's instructions (Invitrogen). Briefly 10^3-10^7 cells were thawed on ice and resuspended in 200µl of PBS (2.3). Tissue kept frozen at -70°C was thawed on ice, homogenised using sterile homogenisers (SLS), and resuspended in 200µl of PBS. 350µl of solution A (lysis solution) was added, the solution vortexed and incubated at 65°C for 10 minutes. 150µl of solution B (precipitation solution) was added and the solution vortexed vigorously, followed by the addition of 500µl of chloroform. The phases were separated by spinning the solution at 10000g for 20 minutes in a microfuge. The upper aqueous layer was carefully transferred to a clean eppendorf. 1ml of 100% ethanol was added to the solution and left at –20°C overnight, to precipitate the DNA. The DNA was pelleted by centrifugation, washed with 70% ethanol, air-dried and re-suspended in 30-50µl of sterile distilled water. Ribonuclease (RNase) was then added to a final concentration of 40µg/ml and incubated at 37°C, to remove contaminating RNA.

(ii) Extraction of DNA by the microfuge method

This method was used for the extraction of genomic DNA using autoclaved 1.5ml centrifuge tubes. 10^6 to $5x10^6$ cells were washed twice in cold PBS, and transferred to a microfuge tube in 1ml of PBS. The cells were then spun at 2000g for 1 minute and re-suspended in 500µl of DNA lysis buffer (10mM Tris pH 8.0, 1mM EDTA pH 8.0, 5mM NaCl and 0.5% SDS w/v). 100µg/ml of Proteinase K was added and the

lysate incubated at 37°C overnight. The aqueous layer of DNA was extracted with the addition of 500µl of TE-equilibrated phenol (pH 7.5) to remove proteins. The solutions were mixed, and then separated by spinning at 10000g for 10 minutes in the microfuge. The aqueous layer was carefully transferred to a fresh tube and further extractions were performed by adding an equal volume of phenol chloroform (1:1), using the same procedure until the interface of the organic and aqueous phase was clear. To ensure the complete removal of phenol (which would co-precipitate with DNA), a final extraction was performed with chloroform alone.

For ethanol precipitation of the DNA 0.1 volumes of 3M sodium acetate and 2.5 volumes of ice-cold absolute ethanol were added to the DNA solution, mixed well, and left at -20°C overnight or at -70°C for 1 hour. The DNA was pelleted by centrifugation for 10 minutes at room temperature in a microfuge. The precipitate was washed in 70% ethanol, dried and re-suspended in 50-100µl of sterile distilled water (SDW).

2.6.2 Extraction and purification of DNA from agarose gels

The QIAquick Gel Extraction Kit commercially available from Qiagen™ was used to extract DNA from agarose gels. The solutions and protocol were supplied with the kit.

The DNA fragment of interest was excised from the gel with a clean scalpel and weighed in a microfuge tube. Binding buffer QG was added to the gel in the ratio of 3:1 and incubated at 50°C for 10 minutes until the gel slice was completely dissolved. 1 gel volume of isopropanol was added to the solution and mixed. The solution was applied to a Qiaquick column and centrifuged for 1 minute at 10000g. The flow through was discarded and 500µl of binding buffer QG was added to the column and centrifuged for a further minute. The flow through was discarded and 750µl of wash buffer PE containing ethanol was added to the column and centrifuged at 10000g for one minute. The column was spun for an additional minute at 10000g to remove any residual ethanol. 30µl of buffer EB (10mM Tris-HCl, pH 8.5) was added to the centre of the column, allowed to stand for one minute and then centrifuged at 10000g for a further minute to elute the DNA.

2.6.3 Measurement of DNA/RNA concentration

The amount of DNA or RNA present in the sample is directly proportional to the amount of UV radiation absorbed by the sample. The concentration of nucleic acid was determined by spectrophotometry (GeneQuant II, Amersham Pharmacia Biotec). Absorbance was measured at wavelengths of 260 and 280nm.

DNA concentration = Absorption at 260nm (A^{260}) × 50 × dilution factor

RNA concentration = Absorption at 260nm (A^{260}) × 40 × dilution factor

where an A^{260} of 1.0 is equivalent to 50mg/ml of DNA and 40mg/ml of RNA. The purity of DNA was calculated as a ratio of OD_{260}/OD_{280}.

A value greater than 1.8 for DNA and 1.9 for RNA indicates that the sample is free of protein contamination.

2.7 RNA extraction and methods

Precautions were taken to preserve the integrity of RNA throughout the following procedures. Particular emphasis was placed on avoiding contamination with RNases. Sterile disposable plastic-ware was used, and all glassware was autoclaved prior to use. Gloves were changed frequently. Ultrapure (molecular biology grade) distilled water was used to prepare solutions, all of which were autoclaved prior to use.

2.7.1 Isolation of RNA by the RNAzol method

Total RNA was isolated using RNAzol™B, which is commercially available from Biogenesis Ltd., based on the acidic guanidinium-phenol-chloroform method described by Chomczynski and Sacchi (1987).

(i) Homogenisation

Tissue, which was kept frozen at –70°C, was placed on ice and 0.8-1ml of RNAzol B was added depending on the amount of tissue present. The tissue was homogenised using sterile homogenisers. RNA was extracted by the addition of 80-100µl of chloroform. The samples were shaken vigorously, left on ice for 5 minutes to allow the phases to separate, and then centrifuged at 10000g for 15 minutes at 4°C.

(ii) RNA precipitation

The aqueous phase was carefully transferred to a clean Eppendorf tube and an equal volume of isopropanol was added. The solutions were mixed well and allowed to precipitate at –20°C overnight. The RNA was pelleted by centrifugation as above.

(iii) RNA wash

The supernatant was removed and the pellet was washed once with 500µl of 75% ethanol, followed by centrifugation for 8 minutes (7500g, 4°C). At the end of the centrifugation the ethanol was removed carefully and briefly spun to remove any residual ethanol. The precipitated RNA was re-suspended in 30-50µl of RNase/DNase free water and the concentration of RNA was measured by UV spectrophotometry (see section 2.6.3).

2.7.2 First strand cDNA synthesis using Reverse Transcriptase (RT)

cDNA was synthesised using the Pro-Star First Strand RT-PCR Kit (Stratagene) according to the manufacturer's instructions. RNA was reverse transcribed using random primers and RT to give a heterogeneous population of cDNA templates, which were subsequently used as the starting template for RT-PCR. Briefly 1µg of RNA was dissolved in DEPC-treated water to give a final volume of 38µl. 3µl of random hexamer oligonucleotides was added to the RNA and incubated at 65°C for 5 minutes, followed by cooling at room temperature to allow annealing of the primers. The following reagents were then added to the reaction in the stated order:

10×1st strand buffer	5µl
RNase block ribonuclease inhibitor (40U/µl)	1µl
100 mM dNTPs	2µl
Mouse Moloney LV reverse transcriptase (MMLV-RT) (50U/µl)	1µl

The reactions were gently mixed and incubated for 1 hour in a 37°C water bath. The cDNA was heated for 5 minutes at 90°C prior to its use in PCR reactions.

2.8 Polymerase chain reaction (PCR)

2.8.1 Safe PCR Practice

Care was taken throughout the preparation of PCR reactions to avoid contamination of samples with amplified products, or unwanted DNA. Amplifications were carried out in a room designated for PCR work only. Gloves were worn and changed regularly, and sterile tubes and aerosol resistant tips were used throughout the procedure. All PCR reagents were aliquotted and stored in smaller volumes.

2.8.2 Genomic PCR

PCR was carried out essentially as described by (Saiki *et al.*, 1985, 1988).

2.8.2.1 Primers for the detection of viral DNA and human β-globin

The EBV W-repeat PCR detects the BamH1 W repeat sequence of the EBV genome. The KSHV PCR detects a 376bp fragment of open reading frame 73 (ORF-73), which encodes the latent nuclear antigen (LNA). PCR for detecting the human β-globin gene was carried out on all samples to check for amplifiable DNA. The sequences of the oligonucleotides are shown in Table 9.

2.8.2.2 Reaction mixture

Amplification was carried out in a final volume of 100μl for the β-globin and Bam H1 W PCRs and 50μl for the KSHV LNA PCR, using 500ng of genomic DNA as template. For every run, appropriate positive and negative controls were included. Sterile distilled water was always included as a control for DNA contamination.

Each reaction mixture consisted of 50mM KCl, 10mM Tris-HCl (pH 9.0), 0.1% Triton X-100, 1.5mM $MgCl_2$, 1μM each primer (0.4μM for the LNA PCR), 200μM each dNTP and 2.5 units of *Taq* (*Thermus aquaticus* strain YT1) DNA polymerase.

2.8.2.3 Amplification

The DNA template was initially denatured at 94°C for 5 minutes. The reaction mixture was overlaid with two drops of mineral oil, and cycled using the conditions shown in Table 10 (see Table 26, page 114 for optimised conditions).

Table 9

Primers and probes for the amplification of EBV, KSHV and human β-globin

Gene	Primer and Probe Sequences 5'→3'	Genome coordinates[1]	Product size (bp)	Reference
EBV Bam H1				
W1	CTT TAG AGG CGA ATG GGC GC	14068-14087	298	Faulkner *et al.*, 1999
W2	AGG ACC ACT TTA TAC CAG GG	14365-14346		
Probe	TGA CTT CAC CAA AGG TCA GG	14226-14245		
KSHV LNA				
LNA-5'	TGA GTG TGG AGG TGT AGT CTG	126776-126796	376	This study
LNA-3'	GCC GAC TCC ATC GAC GGC CG	127153-127134		
Probe	ATG GAG AAT GAG TAT CCG TGG	126907-126927		
β-Globin				
G1	ACA CAA CTG TGT TCA CTA GC	117-136	110	Saiki *et al.*, 1985
G2	CAA CTT CAT CCA CGT TCA CC	226-207		
Probe	GTT ACT GCC CTG TGG G	187-202		

[1]Genbank accession numbers are as follows: EBV BamH1 W (V01555), KSHV LNA (U75698) and β-globin (V00499)

Table 10

PCR Amplification Programs for the EBV, KSHV and β-globin PCR

Gene	Denaturation		Annealing		Extension		Final Extension		Number of Cycles
	Temp. (°C)	Time (secs)	Temp. (°C)	Time (secs)	Temp. (°C)	Time (secs)	Temp. (°C)	Time (mins)	
EBV BamH1	94	60	57	120	72	120			28
KSHV LNA	94	30	60	30	72	60			30
							72	10	1
β-Globin	94	60	49	120	72	120			28

Temp. , Temperature

2.8.3 Semi-quantitative analysis of EBV load

A ten-fold dilution series from 1-10^6 cells of the Burkitt's lymphoma cell line Namalwa (which contains 1-2 copies of the EBV genome per cell) in a background of 10^6 cells from an EBV negative cell line BJAB was carried out. BamH1 W PCR

was performed on DNA at each dilution. The dilution series was run alongside each set of patient samples, and the band intensity measured using scanning densitometric analysis. The density of the test sample was compared with the densities of the dilution series to obtain a semi-quantitative value of EBV genome copy number in each of the samples.

2.8.4 KSHV LNA-1 dilution series

To test the sensitivity of the KSHV PCR, a ten-fold dilution series of the body cavity-based lymphoma cell line BCP-1 (which contains 30-50 copies of the KSHV gene per cell) was made in a background of KSHV negative cell line BJAB. The dilution series, which ranged from 10^5 to 1 BCP-1 cell in a background of 10^6 negative cells, was run alongside the patient and control samples.

2.8.5 Reverse Transcriptase (RT)-PCR

RT-PCR was carried out essentially as described by Saiki *et al.*, 1985, 1988 and Hart *et al.*, 1988. cDNA was made from the samples on 2 separate occasions and analysed twice for the expression of a particular gene, using β-actin to confirm the presence of amplifiable cDNA on each occasion. For each RT-PCR a positive control (see Table 12, page 81) and SDW as a cDNA template-free negative control were included.

2.8.5.1 Primer pairs and probes for RT-PCR

The oligonucleotides primer pairs and probes used for RT-PCR were from published primer sequences and are shown in Table 11. The primer pairs for the $p15^{INK4b}$ and the KSHV LNA genes were designed from gene sequences deposited in Genbank (accession number L36844 and U75698 respectively) (Table 11) as was the probe for the exon 2 deleted variant of p73 (Δ2 p73) (accession number AF079082). cDNA plasmids for the detection of $p16^{INK4a}$ and $p14^{ARF}$ transcripts were kindly supplied by Dr. Gordon Peters (ICRF, London) and Dr. Tim Crook (LICR, London) respectively.

Table 11

Primer and probe sequences for RT-PCR

Gene	Primer and Probe sequences 5'→3'	Product size (bp)	Genome Coordinates	Reference
β-Actin				
5'	GTG GGG CGC CCC AGG CAC CA		144-163	Yamamura *et al.*, 1991
3'	CTC CTT AAT GTC ACG CAC GAT TTC	540	683-660	
Probe	GGA TAG CAA CGT ACA TGG CT		450-431	
TA p63				
5'	ATG TCC CAG AGC ACA CAG	629	145-162	Yang *et al.*, 1998
3'	AGC TCA TGG TTG GGG CAC		773-756	
Probe	AAC AGC CTA TAT GTT CAG TTC AGC CC		215-240	
ΔN p63				
5'	CAG ACT CAA TTT AGT GAG		25-42	Yang *et al.*, 1998
3'	AGC TCA TGG TTG GGG CAC	440	464-447	
Probe	TAT AAC ACA GAC CAC GCG CAG AAC AGC GTC AC		118-149	
p73				
5'	ACT TTG AGA TCC TGA TGA AG	535	1201-1220	De Laurenzi *et al.*, 1998
3'	CAG ATG GTC ATG CGG TAC TG		1735-1716	
Probe	TAT CGG CAG CAG CAG CAG CTC CTA CA		1275-1300	
Δ2 p73				
5'	ACG CAG CGA AAC CGG GGC CCG	(344)*	6-26	Ng *et al.*, 2000
3'	GCC GCG CGG CTG CTC ATC TGG	242	349-329	
Probes	GGA TTC CAG CAT GGA CGT CTT CC		245-267	
	CAC GTT TGA GCA CCT CTG GAG		149-169	
$p16^{INK4a}$				
5'	AGC CTT CGG CTG ACT GGC TGG	139	69-89	Gonzalez-Zulueta *et al.*, 1995
3'	CTG CCC ATC ATC ATG ACC TGG A		207-186	
$p14^{ARF}$				
5'	TAC TGA GGA GCC AGC GTC TA	188	287-306	Gazzeri *et al.*, 1998
3'	AGC ACC ACC AGC GTG TC		474-458	
$p15^{INK4b}$				
5'	GTT TAC GGC CAA CGG TGG		275-292	This study
3'	AGC ACC ACC AGC GTG TCC	346	620-603	
Probe	AAG GTG CGA CAC TCC TGG GAA		409-429	
ORF 71-73				
5'	TGG AGG CAG CTG CGC CAC		127882-865	Talbot *et al.*, 1999
3'	CTT GCC AGC TGA GGA ACT AC	956	122891-910	
Probe	AGC AGC TTG GTC CGG CTG ACT		127841-127	

The Genbank accession numbers used for the primer and probe sequences are as follows: β-actin (X00351); TAp63 (NM003722); ΔN p63 (AF075431); p73 (Y11416); Δ2 p73 (NM005427); $p16^{INK4a}$ (L27211); $p14^{ARF}$ (S78535); $p15^{INK4b}$ (L36844) and KSHV ORF 71-73 (U75698); *, full length p73 (344bp), Δ2 p73 (242bp).

2.8.5.2 Controls for RT-PCR

Positive control cDNA known to express the transcript under investigation, are summarised in Table 12. Positive controls for all RT-PCR experiments, except where mentioned, were kindly provided by Dr. Tim Crook (LICR, London) and Ms. Jenny O'nions (LICR, London). The H-358 lung cancer cell line was provided by Dr. Scott Bader (Molecular Medicine Centre, Western General Hospital), and the lymphoblastoid cell line (LCL) KB, by Dr. Ingo Johannessen (Clinical and Diagnostic Virology, University of Edinburgh). The LCLs (kindly provided by Ms. O'nions and Dr. Johannessen) were generated by infection of human primary B cells, isolated from buffy coat residues, with an EBV-preparation from a B95-8 EBV-positive marmoset cell line. A template cDNA-free reaction was included in each RT-PCR run as a negative control, where sterile distilled water, replaced target DNA.

Table 12

Positive controls for RT-PCR

Gene	cDNA from Cell line or tumour biopsy
TA p63	Lymphoblastoid cell line (PD-LCL)
ΔN p63	Squamous cell cancer (S1)
p73	Vulval squamous carcinomas (T1 and T2)
Δ2 p73	Vulval squamous carcinoma (5T and 11T)
$p16^{INK4a}$	Lymphoblastoid cell lines (PD-LCL and OTIS) Breast adenocarcinomas
$p15^{INK4b}$	BL cell line (BL-41)
$p14^{ARF}$	Vulval squamous cancer (T1 and T2)
	Lung cancer cell line (H358)
KSHV ORF 71-73	Body cavity lymphoma cell line (BCP-1)

BL, Burkitt's lymphoma; LCL, Lymphoblastoid cell line

2.8.5.3 Reaction mixture

cDNA synthesised from 40-100ng of RNA from each sample was used as the template in each reaction. Amplification of KSHV ORF 71-73, p73, Δ2 p73, TA p63, and ΔN p63 transcripts was carried out in a total volume of 50μl; amplification of $p16^{INK4a}$, $p15^{INK4b}$ and $p14^{ARF}$ transcripts was carried out in a volume of 30μl and

that for β-actin in 100μl. Each reaction mixture consisted of 50mM KCl, 10mM Tris-HCl (pH 9.0), 0.1% Triton X-100, and 0.5-1μM of each primer. Additionally, the amplification reactions for $p16^{INK4a}$, $p15^{INK4b}$ and $p14^{ARF}$ included 10% DMSO. Each reaction was over-laid with 2 drops of sterile mineral oil to prevent evaporation during amplification.

The concentrations of $MgCl_2$, primer and *Taq* DNA polymerase that were used for each individual RT-PCR is summarised in Table 26 (page 114). The reaction conditions for each primer pair were optimised (Table 26, page 114) using published conditions as a reference point (Table 25, page 107).

2.8.5.4 Amplification

PCR amplification was carried out in a Hybaid thermal cycler, and a summary of the PCR programmes is shown in Table 13. Optimisation of PCR reaction conditions for each primer pair (Table 26, page 114) was carried out using published conditions as a reference point (Table 25, page 107). For the β-actin and the ΔN p73 primer pairs, the annealing and extension temperatures were the same (1-step).

2.8.6 PCR amplification for sequencing using Platinum *Pfx* DNA Polymerase

To overcome the inherent errors and mis-incorporations of nucleotides by *Taq* polymerase ($0.2\text{-}2\times10^{-4}$ errors per bp per cycle) (Smith *et al.*, 1997; Cline *et al.*, 1996), Platinum *Pfx* DNA polymerase (Life Technologies) was used for the amplification of PCR products that were to be subsequently sequenced. *Pfx* polymerase is a high fidelity, proofreading enzyme with 3' to 5' exonuclease activity and is supplied in an inactive form bound to an antibody. The enzyme is rendered active at 94°C providing an automatic "hot start" for PCR. The high specificity and accuracy offered by the enzyme makes it very suitable for cloning and sequencing.

The following components were added to an eppendorf on ice, in a total reaction volume of 50μl; 1×Pfx amplification buffer, 300μM each dNTP, 1mM $MgSO_4$, 0.3μM each primer, 300ng of template DNA and 1.25 units of *Pfx* DNA polymerase. The template was denatured initially for 2 minutes at 94°C, followed by 30 cycles of denaturation at 94°C for 30 seconds, annealing at 63-66°C for 45 seconds and extension at 68°C for 90 seconds.

Table 13

RT-PCR Amplification Programs

Gene	Denaturation		Annealing		Extension		Final Extension		Number of Cycles
	Temp. (°C)	Time (secs)	Temp. (°C)	Time (secs)	Temp. (°C)	Time (secs)	Temp. (°C)	Time (mins)	
β-actin[1]	94	60	65	120	-	-	-	-	28
	-	-	-	-	-	-	72	10	1
P73	95	60	59	55	72	45	-	-	35
Δ2 p73[1]	94	720	-	-	-	-	-	-	1
	94	30	72	120	-	-	-	-	35
TA p63	94	30	52	30	72	60	-	-	28
ΔN p63	94	30	52	30	72	60	-	-	28
$p16^{INK4a}$	94	180	-	-	-	-	-	-	1
	94	60	56	30	72	40	-	-	25
	-	-	-	-	-	-	72	1	1
$p15^{INK4b}$	95	120	-	-	-	-	-	-	1
	95	30	58	60	72	60	-	-	25
							72	3	1
$p14^{ARF}$	94	60	56	30	72	40	-	-	22
KSHV ORF 71-73	94	30	57	30	72	60	-	-	35

[1], The annealing and extension steps are performed at the same temperature (1-step)

2.8.7 Long Distance PCR (LD-PCR)

LD-PCR is a recent advancement in PCR technology, which gives efficient amplification of DNA fragments >10kb (Cheng *et al.*, 1994), by incorporating a mixture of thermostable and proofreading polymerases, improved buffers and thermal cycling profiles. The Long and accurate (LA) PCR Kit Ver 2.1 (BioWhittaker) which includes the improved enzyme *TaKaRa LA Taq*™ was used effectively for the amplification of targets between 4 and 20 kb.

2.8.7.1 Primers for LD-PCR

The primers and probes used for the amplification of the c-*myc* t(8:14) and *bcl-2* t(14:18) translocations were derived from published sequences and are shown in Table 14.

Due to the head-to-head orientation of the c-*myc* gene with the *IgH* locus the sense primer is located in exon 2 of c-*myc* (external to exon1/intron). Since the breakpoints within the *IgH* locus are located preferentially in the switch regions, the antisense primers are located in the constant regions of the *IgH* locus (Cα, Cγ and Cμ) (figure 12, page 39). The c-*myc* probe recognises a sequence in exon 2 of the c-*myc* gene (Table 14).

The *bcl-2* and *IgH* genes are fused in the same transcriptional orientation. The sense primers were located in the MBR or mcr regions of *bcl-2* and upstream of these regions (Table 14), whereas the antisense primer was located in the *IgH* specific enhancer region (Eμ) (figure 13, page 45).

The oligonucleotide probe for the identification of the t(14:18) translocation (Eμ probe, Table 14) was designed in this study from a published sequence of the IgH region (Neale and Kitchingman, 1991), and lies just internal to the Eμ primer within the *IgH* locus.

2.8.7.2 Control cell lines and templates for LD-PCR

The control cell lines and templates that were used to detect translocations involving the c-*myc* and *bcl-2* genes, by LD-PCR is shown in Table 15, page 86. The P3HR1 cell line obtained from an endemic Burkitt's lymphoma was used as a negative control for the c-*myc* LD-PCR. The breakpoint on chromosome 8 is located around 190kb upstream of the c-*myc* gene, and hence outside the region amplified by the primers used in this study (Joos *et al.*, 1992). For the *bcl-2*/*IgH* LD-PCR analysis, lymph node biopsy 761 was used as the negative control and lymph nodes 1119 and 1143 as the positive controls (translocations confirmed by Andrew Krajewsky, personal communication).

Table 14

LD-PCR primers for the amplification of the c-*myc* t(8:14) and *bcl-2* t(14:18) translocations

Primer	Primer and probe sequences 5'→3'	Specificity	Strand/ Orientation	Reference
MYC/01	ACA GTC CTG GAT GAT GAT GTT TTT GAT GAA GGT CT	c-*myc*, exon 2	A/R	Battey *et al.*, 1983
Cμ	TGC TGC TGA TGT CAG AGT TGT TCT TGT ATT TCC AG	Cμ constant region	A/R	Akasaka *et al.*, 1996
Cγ	AGG GCA CGG TCA CCA CGC TGC TGA GGG AGT AGA GT	Cγ constant region	A/R	Akasaka *et al.*, 1996
Cα	TCG TGT AGT GCT TCA CGT GGC ATG TCA CGG ACT TG	Cα constant region	A/R	Akasaka *et al.*, 1996
Myc probe	TCG CTC TGC TGC TGC TGC TGG	c-*myc*, exon 2	A/F	Battey *et al.*, 1983
Eμ	CTA GGC CAG TCC TGC TGA CGC CGC ATC GGT GAT TC	Enhancer region of *IgH*	A/R	Neale and Kitchingman, 1991
MBR- 1	CAC AAG TGA AGT CAA CAT GCC TGC CCC AAA CAA AT	bcl-2, exon 3 coding region	S/F	Cleary *et al.*, 1986
MBR- 2	CTA TGG TGG TTT GAC CTT TAG AGA GTT GCT TTA CG	bcl-2, exon 3 immediately upstream of MBR	S/F	Cleary *et al.*, 1986
mcr- 1	GGT AGA GGT GAA TAC CCC AGG GCT GAG CAG GAA GG	bcl-2, 10 kb upstream of mcr	S/F	Akasaka *et al.*, 1998
mcr-2	TGT TGG TTG ACA TTT GAT GGC TTT GCT GAG AGG TA	bcl-2, mcr	S/F	Ngan *et al.*, 1989
Eμ probe	TAA GGT GTC TCC ACA GTC CT	Enhancer region of IgH	A/R	This study

A/R, antisense strand in reverse direction; S/F, sense strand in forward direction; MBR, major breakpoint region; mcr, minor cluster region.

Table 15

Control cell lines and templates for LD-PCR

Cell line/Template	Type	Translocation	Primers
Raji	BL cell line	c-*myc*/ Sγ	c-*myc*/ Cγ
Ramos	BL cell line	c-*myc*/ Sμ	c-*myc*/ Cμ
BL-41	BL cell line	c-*myc*/ Sα	c-*myc*/ Cα
P3HR1	BL cell line	190kb 5' of c-*myc*	*
1119[a]	Lymph node biopsy	*bcl-2* MBR	MBR-1 and MBR-2/ Eμ
1143[a]	Lymph node biopsy	*bcl-2* mcr	mcr-1 and mcr-2/ Eμ
761[a]	Lymph node biopsy	None	**

BL, Burkitt's lymphoma; Sγ and Cγ, switch and constant regions γ of the *IgH* locus respectively; Sμ and Cμ, switch and constant regions μ of the IgH locus respectively; Sα and Cα, switch and constant regions α of the IgH locus respectively; MBR, major breakpoint region; mcr, minor cluster region; *, negative control for t(8:14) using primers used in this study; **, negative control for t(14:18); [a], Personal communication from A. Krajewsky

2.8.7.3 Reaction mixture and amplification

Briefly, the reaction mixture was prepared by combining the following reagents to a total volume of 50μl in thin-walled PCR tubes. 1×LA PCR Buffer II with 2.5mM $MgCl_2$, 400μM each dNTP, 0.4μM of each primer, 200ng genomic DNA, and 2.5 units of *TaKaRa LA Taq*™. The reaction was overlaid with mineral oil and subjected to the following thermal cycling profile:

1 cycle of denaturation at 94°C for 1 minute

14 cycles of denaturation at 98°C for 20 seconds, primer annealing and DNA extension at 68°C for 20 minutes

16 cycles of denaturation at 98°C for 20 seconds, annealing and extension at 68°C for 20 minutes with 15-second increments per cycle (auto-segment extension)

1 cycle of final extension at 72°C for 10 minutes.

2.8.8 "Hot-Start" PCR

An automatic hot-start was employed for PCR, to prevent mis-priming and

amplification of non-specific products. The TaqStart™ Antibody was used to "hot-start LD-PCR amplification of t(8:14) and t(14:18) translocations. This monoclonal antibody which binds to, and blocks *Taq* polymerase activity at ambient temperature, dissociates from the enzyme above 70°C, thus providing an automatic "hot-start". The antibody is mixed with *Taq* at a micromolar ratio of 28:1, and incubated for 5 minutes at room temperature before its use in PCR.

"Hot-start" was also employed for the amplification of the Δ2 p73 transcript using the enzyme *AmpliTaq* Gold® polymerase (Roche). The enzyme was heat-inactivated for 12 minutes at 95°C before thermal cycling. This enzyme was also used as a "hot-start" for the methylation-specific PCR assay (see section 2.19.2).

2.9 Agarose gel electrophoresis

2.9.1 Preparation of agarose gels

The range of efficient separation of linear DNA molecules in agarose gels of different concentration is shown in Table 16 (Sambrook *et al.*, 1989).

Table 16

Percentage of Agarose for optimal resolution of DNA

Percentage agarose in the gel	Efficient range of separation of linear DNA molecules
0.7	0.8-10 kb
0.9	0.5-7 kb
1.2	0.4-6 kb
1.5	0.2-3 kb

The appropriate amount of Nusieve® 3:1 agarose (3 parts Nusieve agarose, 1 part SeaKem® agarose) as determined using Table 16 (page 87) was dissolved in 1×TBE and heated while stirring until the agarose was completely dissolved. 1μg/ml of EtBr was added to the gel solution to visualise the DNA. The molten gel was poured into the appropriate casting tray and allowed to set at room temperature.

2.9.2 Running agarose gels

The cast gel was submerged in 1×TBE. Samples and DNA markers (see section 2.3.1) were mixed with loading buffer in a ratio of 10:1, and loaded into the wells. Electrophoresis was carried out at 70mA until sufficient resolution of the DNA was achieved.

2.9.3 Imaging of the gel

The DNA was visualised and photographed using an UV Gel Documentation System (Ultra Violet Products Ltd., Cambridge, UK).

2.10 Southern transfer of DNA to nylon membranes

DNA was transferred to positively charged nylon membranes (Hybond-N^+, Amersham Pharmacia) by the method of Southern (1975).

After electrophoresis the gels were rinsed with dH_2O and washed in denaturing and neutralising solutions (section 2.3) for 20 minutes each. The prepared gel was placed on a 'wick' consisting of a sheet of pre-wet Whatman (3MM) paper placed on a plate over a tray containing 2×SSC (section 2.3), such that the ends of the paper were immersed in the solution. A piece of nylon membrane, cut to the size of the gel, was placed on top of the gel carefully to avoid any air-bubbles. The exposed area of the paper and tray were covered with cling-film to prevent any evaporation. 3 pieces of 3MM paper were placed on top of the membrane, followed by 3-4 inches of absorbent towels, a glass plate and a 400gram weight. The transfer was allowed to take place overnight at room temperature. After the transfer the membrane was washed briefly in 2×SSC, air-dried and UV cross-linked using a Stratalinker (Stratagene).

2.11 Pre-Hybridisation of Membranes

Nylon membranes were prehybridised in a hybridising oven for at least 3 hours in pre-hybridisation solution (see section 2.3) at 42°C (end-labelled probes) or 65°C (random-labelled probes) (see section 2.12).

2.12 Preparation of radioactive probes

(i) End-labelled oligonucleotide probes

Oligonucleotides were labelled with [γ^{32}P] ATP as follows:

1µl oligonucleotide (5pmol/µl)

2µl 10×Kinase buffer

5µl [γ ^{32}P] ATP (50µCi)

1µl T4 polynucleotide kinase (10U/µl)

dH_2O to a total volume of 20µl

The reaction was incubated at 37°C for 30 minutes.

(ii) Random-labelled probes

Random labelled probes were prepared using the Multiprime DNA labelling system (Amersham Pharmacia), by the method described by (Feinberg and Vogelstein 1983). The protocol and materials were supplied with the kit.

25ng DNA dissolved in dH_2O was heated at 95-100°C for 5 minutes and cooled rapidly on ice. The following were then added:

10µl of Buffer	(containing dATP, dGTP and dTTP in a solution containing Tris-Hcl, pH7.8, $MgCl_2$ and 2-mercaptoethanol)
5µl of primer	(Random hexanucleotides)
5µl of [α^{32}P] dCTP	(10µCi/µl)
1µl Klenow enzyme	(1 unit/µl in 50mM potassium phosphate, pH6.5, 10mM 2-mercaptoethanol and 50% glycerol)

This reaction was gently mixed and incubated at 37°C for 30 minutes.

Labelled probes were purified by fractionation on Sephadex G-50 NICK™ columns (Amersham Pharmacia) according to the manufacturer's instructions, to remove unincorporated label.

2.13 Hybridisation of ^{32}P-labelled probes to DNA

The eluate from the column was collected and added to 25ml of prehybridisation solution (2.3). For random labelling, probes were denatured at 95°C for 5 minutes before being added to the prehybridisation solution. 100µg/ml of denatured salmon sperm DNA was added to the mix, and incubated for at least 12 hours at

temperatures appropriate for end-labelled (42°C) or random-labelled (65°C) probes.

2.14 Washing and autoradiography

(i) End-labelled probes

The hybridisation mix was discarded and the non-specifically bound probe was washed off the nylon membrane by 2 washes in 2×SSC, 0.1% w/v SDS for 30 minutes each.

(ii) Random-labelled probes

25 ml washes at 65°C for 10 minutes each were used. Initial washes were in 2×SSC, 0.1% w/v SDS increasing to a stringency of 1-0.5×SSC, 0.1% w/v SDS over a series of twice repeated washes.

Monitoring the filter with a β-monitor was used to assess the adequacy of the washes and to determine whether a more stringent wash was required. The filter was then wrapped in cling-film and exposed to Hyper-MP film (Amersham Pharmacia) in a cassette with intensifying screens for up to a week at –70°C.

2.15 Stripping a membrane for re-probing

The membrane to be re-probed was placed in a hybridisation tube at 65°C, containing 100ml of 0.4M sodium hydroxide. After 30 minutes the sodium hydroxide solution was replaced with 100ml of a neutralising solution (0.1×SSC, 0.1% w/v SDS, 200mM Tris-HCl, pH 7.5) for two 15-minute incubations at 65°C. The membrane was exposed overnight to ensure all signals had been stripped.

Alternatively the membrane was stripped by boiling in a 0.5% w/v SDS solution and then allowed to cool to room temperature for approximately 2 hours.

2.16 Single strand conformation polymorphism (SSCP)

Single strand conformation polymorphism is a technique used to detect sequence changes in DNA and cDNA. The technique is based on the effect of sequence on the folding (intramolecular secondary structure) of single-stranded DNA, which affects its conformation and hence its migration through a non-denaturing polyacrylamide gel.

2.16.1 Primers for PCR-SSCP analysis of *p53*, *INK4* genes and *bcl-6*

The sequences and genome co-ordinates of the published oligonucleotide primer pairs used for SSCP-PCR in this study are shown in Tables 17 to 19.

Table 17

SSCP-PCR primers for *p53*

Exon	Sequence (5'→3')	Size (bp)	Coordinates[1]
2/3			
PU2	TCC TCT TGC AGC AGC CAG ACT GC	267	11678-11700
PD3	ACC CCT TGT CCT TAC CAG AAC GTT G		11942-11919
4			
PU4	CAC CCA TCT ACA GTC CCC CTT GC	307	12008-12030
PD4	CTC AGG GCA ACT GAC CGT GCA AG		12394-12372
5			
PU5	CTC TTC CTG CAG TAC TCC CCT GC	211	13042-13065
PD5	GCC CCA GCT GCT CAC CAT CGC TA		13253-13231
6			
PU6	GAT TGC TCT TAG GTC TGG CCC CTC	185	13308-13331
PD6	GGC CAC TGA CAA CCA CCC TTA ACC		13489-13466
7			
PU7	GTG TTG TCT CCT AGG TTG GCT CTG	139	13986-14009
PD7	CAA GTG GCT CCT GAC CTG GAG TC		14124-14102
8			
PU8	ACC TGA TTT CCT TAC TGC CTC TGG C	200	14404-14428
PD8	GTC CTG CTT GCT TAC CTC GCT TAG T		14603-14579
9			
PU9	GCC TCT TTC CTA GCA CTG CCC AAC	102	14668-14691
PD9	CCC AAG ACT TAG TAC CTG AAG GGT G		14769-14746
10			
PU10	TGT TGC TGC AGA TCC GTG GGC GT	131	17561-17583
PD10	GAG GTC ACT CAC CTG GAG TGA GC		17690-17668
11			
PU11	TGT GAT GTC ATC TCT CCT CCC TGC	153	18560-18583
PD11	GGC TGT CAG TGG GGA ACA AGA AGT		18712-18689

[1], Genbank accession number U94788. Primer sequences from Visscher *et al.*, 1996

Table 18

SSCP-PCR primers for *INK4 Locus*

Gene	Sequence (5'→3')	Size (bp)	Coordinates[1]
INK4a Exon 1α			
5'	TCT GCG GAG AGG GGG AGA GCA GGC A	278	28512-28531
3'	GCG CTA CCT GAT TCC AAT TC		28790-28767
ARF Exon 1β*			
5'	TAC TGA GGA GCC AGC GTC TA	188	287-306
3'	AGC ACC ACC AGC GTG TC		474-458
Exon 2a			
5'	CCA GGC ATC GCG CAC GTC CA	243	24943-24962
3'	ACA AGC TTC CTT TCC GTC ATG CCG		25186-25163
Exon 2b			
5'	TCT GAC CTT TGG AAG CTC TCA G	241	24764-24785
3'	TTC CTG GAC ACG CTG GTG GT		25005-24986

[1], Genbank accession numbers for exon 1α, exon 2a and exon 2b is AC000048, and S78535 for exon 1β. Primer sequences from (Zhang *et al.*, 1994); *, Exon 1β was amplified from cDNA (Gazzeri *et al.*, 1998)

Table 19

SSCP-PCR primers for *bcl-6*

Gene	Sequence (5'→3')	Size (bp)	Coordinates[1]
E1.10			
5'	CTC TTG CCA AAT GCT TTG	267	1749-1766
3'	TAA TTC CCC TCC TTC CTC		2013-1996
E1.11			
5'	AGG AAG GAG GGG AAT TAG	215	1997-2014
3'	AAG CAG TTT GCA AGC GAG		2210-2193
E1.12			
5'	TTC TCG CTT GCA AAC TGC	295	2191-2208
3'	CAC GAT ACT TCA TCT CAT C		2483-2465

[1], Genbank accession number Z79581. Primer sequences from Migliazza *et al.*, 1995

2.16.2 Controls for SSCP-PCR

Appropriate positive and negative controls for each exon/fragment were used and are described in Table 20. Biopsy material was kindly provided by Mr. Robert Morris, Western General Hospital, Edinburgh and Dr. Tim Crook, LICR, London. Nasopharyngeal carcinoma (NPC) cell lines, C17 and C18, were kindly provided by Dr. Louise Brooks, LICR, London.

Table 20

Controls for *p53*, *INK4 locus* and *bcl-6* SSCP-PCR

Gene	Exon/Fragment	DNA from biopsy[1] or cell line[2]	
		Positive control	**Negative control**
p53	2/3	-	Human genomic DNA[3]
	4	BCT R/R	BCN R/R
			BCN1 R/P
	5	C18	C17
		28697T	28697N
	6	03157T	03157N
		13758T	13758N
	7	00997T	00997N
	8	05747T	05747N
	9	C17 and C18	Human genomic DNA[3]
	10	C17	Human genomic DNA[3]
	11	C17	Human genomic DNA[3]
INK4 locus	Exon 1α	-	Human genomic DNA[3]
	Exon 1β	-	Human genomic DNA[3]
	Exon 2	-	Human genomic DNA[3]
bcl-6	E1.10	P3HR1	Raji
	E1.11	Raji	Namalwa
	E1.12	Raji	Namalwa

[1], Biopsies with a suffix T indicates tumour tissue and with a suffix N indicates normal tissue; [2], Cell lines C17 and C18 are nasopharyngeal carcinoma cell lines and Raji, Namalwa and P3HR1 are Burkitt's lymphoma cell lines; [3], Human genomic DNA obtained from normal diploid fibroblasts; R, Arginine; P, Proline (codon 72); BC, breast cancer

2.16.3 Amplification

PCR was initially performed without radioactivity for exons 2-11 of *p53*, exons 1α,

1β and 2 (2a, 2b) of the *INK4* locus, and a 735bp region in the first intron of *bcl-6* to assess the efficiency of the PCR conditions, along with β-globin amplification to check for amplifiable DNA. Amplification of *p53* and *INK4* was carried out in a total volume of 100μl, each reaction containing 10mM Tris-HCl, 50mM KCl, 1.5mM $MgCl_2$, 200μM of each dNTP, 1μM of each primer, 500ng of DNA and 1.25-2.5 units of *Taq* polymerase. The reaction mixture for the amplification of the *INK4* locus also contained 5% DMSO. Amplification of *bcl-6* was carried out in a final volume of 10μl, with the reaction containing 10mM Tris-HCl, 50mM KCl, 1.5mM $MgCl_2$, 0.2μM of each primer, 10μM each dNTP, 100ng of DNA and 0.5 units of *Taq* polymerase. The template was initially denatured at 94°C for 5 minutes. The reaction mixture was overlaid with mineral oil, and subjected to the amplification conditions shown in Table 21. The amplified products were run on a 2% agarose gel containing EtBr and visualised under UV light (see section 2.9).

Table 21

SSCP-PCR Amplification Programs for *p53*, *INK4* locus and *bcl-6*

Gene	Denaturation		Annealing		Extension		Number of Cycles
	Temp. (°C)	Time (secs)	Temp. (°C)	Time (secs)	Temp. (°C)	Time (secs)	
p53 Exons 2-11	95	30	70	45	72	90	5
	95	30	66	45	72	90	30
INK4 Locus							
Exons 1α, 2a, 2b	94	50	62	50	72	50	35
Exon 1β	95	30	50	30	72	30	30
bcl-6							
E1.10	94	30	56	15	72	45	35
E1.11	94	30	58	15	72	45	35
E1.12	94	30	54	15	72	45	35

Temp, Temperature

2.16.4 SSCP-PCR using radioactive ^{32}P and ^{33}P

SSCP-PCR was performed initially for exons 5 and 6 of p53, in a 50μl reaction

containing 10mM Tris-HCl, 50mM KCl, 1.5mM $MgCl_2$, 200μM each dNTP, 1μM of each primer and 1 unit of *Taq* polymerase. 2μCi of [α^{32}P] dCTP was added to each reaction and cycled at the conditions shown in Table 21. ^{32}P is a high-energy beta emitter, with a maximum range of 6m in air, whereas ^{33}P is a low-energy beta emitter, with a maximum range of only 50cm in air. Because of its lower average energy (0.08MeV vs. 0.69MeV for ^{32}P), ^{33}P is a considered a safer alternative to ^{32}P. Therefore, it was decided to use [α^{33}P] dCTP for SSCP-PCR. The reactions and cycling conditions were carried out exactly as described above, except that 10μCi of ^{33}P was substituted for ^{32}P in each reaction.

2.16.5 SSCP Gel running

The PCR products were separated on a polyacrylamide gel containing 10% v/v glycerol, 25% v/v Sequagel® MD and 6% v/v 10×TBE. 0.6×TBE (2.1.6) was used as the running buffer. 400μl of a 10% ammonium persulfate (APS) solution and 40μl of TEMED was added to polymerise the gel. The gel was cast between a pair of plates (380mm×170mm) separated by 0.3mm spacers.

The samples were heated at 94°C for 5 minutes and immediately placed on ice to keep the DNA denatured. 3μl of the PCR product was mixed with 3μl of stop solution (2.3), loaded into wells created by insertion of a "sharks tooth" comb and run slowly overnight at 3-4 W.

The gel was allowed to cool for 15 minutes before the plates were separated. The gel was blotted onto a sheet of Whatman 3MM paper, covered with cling-film and dried for 2 hours. The gel was then placed in an autoradiograph cassette and exposed to Hyperfilm AP (Amersham Pharmacia) at –70°C from 3 days up to a week, with intensifying screens.

2.17 Cloning

Cloning of PCR products was carried out using various commercially available systems. The pGEM®-T Vector Systems (Promega), and the TOPO TA Cloning® kit (Invitrogen), utilise the nontemplate-dependent activity of *Taq* polymerase which adds a single deoxyadenosine ('A') to the 3' ends of PCR products. The supplied,

linearised vectors have a single 3' deoxythymidine ('T') residue, which allows the PCR inserts to ligate efficiently to the vector.

The pGEM®-T vectors contain a multiple cloning region with the α-peptide coding region of the enzyme β-galactosidase fused to the *lacZ* gene. Insertional inactivation of the α-peptide allows recombinant clones to be directly identified by colour screening on IPTG-X-Gal plates.

The TOPO TA Cloning® exploits the ligation reaction of topoisomerase I by providing an "activated" linearised TA vector using proprietary technology (Shuman, 1994). Ligation of the vector with a PCR product containing 3' 'A' overhangs is very efficient and occurs spontaneously within 5 minutes at Room temperature.

The Zero Blunt™ PCR cloning kit is designed to clone blunt-ended PCR fragments. Recombinants are directly selected via disruption of a lethal gene. The system is based on vectors containing the lethal *Escherichia coli* gene, *ccd*B (Bernard *et al.*, 1994). The vector pCR®-BLUNT is supplied linearised and blunt-ended with the *ccd*B gene fused to the C-terminus of *lacZ*α. When a PCR product is cloned it disrupts expression of the *lacZ*α-*ccd*B fusion gene, permitting growth only of positive recombinants after transformation.

2.17.1 Ligation reactions

Typically 25-50ng of vector was ligated to the insert at a range of molar ratios, in the range of 3:1 to 10:1 (insert: vector). Vector and insert DNA were added to 10×ligation buffer (500mM Tris-HCl pH 7.5, 100mM magnesium chloride, 100mM DTT, 10mM ATP) and T4 DNA ligase. Reactions were incubated at 16°C for an hour or overnight at 4°C.

2.17.1.1 *pGEM®-T Vector Systems*

Whenever possible, fresh PCR products were used for cloning. However, if old PCR products were being used, then the PCR product was incubated at 72°C for 15 minutes with 1 unit of *Taq* DNA polymerase and 200μM dNTP, followed by inactivation of *Taq* at 97°C for 10 minutes, for the addition of an 'A' overhang.

10μl ligation reactions were set up as follows:

PCR product	1-2µl
2×Rapid ligation buffer (300mM Tris-HCl, pH 7.8, 100mM $MgCl_2$, 100mM DTT, 10mM ATP)	5.0µl
50ng/µl pGEM®-T Easy vector	1.0µl
Sterile water	to a total volume of 10µl
T4 DNA ligase (3 Weiss units)	1.0µl

The ligation reaction was incubated overnight at 4°C.

(i) Transformation

2µl of the ligation reaction was added to 50µl of JM109 High Efficiency competent cells and incubated on ice for 20 minutes. The cells were heat-shocked for 45 seconds at 42°C and then placed back on ice for a further 2 minutes. 950µl of SOC medium (section 2.3) was added to the cells and incubated at 37°C for 1.5 hours in a shaking water bath. 100µl of the transformation was spread on a LB agar (section 2.3) plate containing ampicillin (100µg/ml), 200µM IPTG and 0.004% X-Gal in DMF. The plates were incubated at 37°C overnight and then placed at 4°C to allow colour development. White colonies were tested for the presence of insert (section 2.17.4).

2.17.1.2 *TOPO TA® Cloning Kit for sequencing*

5µl TOPO-Cloning reaction was set up as follows:

PCR product	0.5-2µl
Salt solution	1µl
Sterile water	to a total volume of 5µl
pCR®4-TOPO® vector	1µl

The TOPO-Cloning reaction was incubated for 30-60 minutes at room temperature.

(i) Transformation

2µl of the TOPO-Cloning reaction were added to 50µl of TOP10 competent cells and incubated on ice for 30 minutes. The cells were heat-shocked for exactly 30

seconds at 42°C and then placed back on ice for a further 2 minutes. 250µl of SOC medium was added to the cells and incubated at 37°C for 30 minutes (ampicillin selection) or 1 hour (kanamycin selection) while being agitated by rotation. 50µl and 100µl of the transformation were spread on LB agar plates containing kanamycin or ampicillin. The plates were incubated at 37°C overnight and colonies were analysed for the presence of insert (section 2.17.4).

2.17.1.3 *The Zero-Blunt™ PCR Cloning Kit.*

10µl ligation reaction was set up as follows:

Linearised, pCR®-BLUNT (25ng)	1µl
Blunt PCR product	1-5µl
10×ligation buffer (with ATP) (60mM Tris-HCl, pH 7.5, 60mM $MgCl_2$, 50mM NaCl, 1mg/ml BSA, 70mM β-mercaptoethanol, 1mM ATP, 20mM DTT, 10mM spermidine)	1µl
Sterile water	to a total volume of 10µl
T4 DNA ligase (4U/µl)	1µl

The ligation reaction was incubated at 16°C for one hour.

(i) Transformation

2µl of the ligation reaction were added to 50µl of TOP10 competent cells and incubated on ice for 30 minutes. The cells were heat-shocked for exactly 45 seconds at 42°C and then placed back on ice for a further 2 minutes. 250µl of pre-warmed SOC medium was added to the cells and incubated at 37°C for 1 hour in a shaking water bath. 50-100µl of the transformation was spread onto LB plates containing 50µg/ml kanamycin. The plates were incubated at 37°C overnight and colonies tested for the presence of the insert (section 2.17.4).

2.17.2 Colony screening

Where PCR cloning was inefficient, colonies were screened using this protocol for

the ease of subsequently selecting positive clones. Using autoclaved toothpicks, individual colonies were scratched across the surface of a Hybond-N^+ membrane (Amersham Pharmacia), which had been stamped with a 50-square matrix, and placed on a selective media plate. The same colony was also scratched on a selective media plate at the same position as indicated from a matrix stuck to the underside of the plate. Both plates were incubated overnight at 37°C. The membranes were placed colony side up on blotting paper soaked in 2×SSC, 5% SDS for 2 minutes. The membranes were microwaved at full power for 45 seconds, which lyses the cells and denatures and fixes the DNA. The membranes were then available for prehybridisation (section 2.11) and subsequent hybridisation with a radioactively labelled probe (sections 2.12 and 2.13).

2.17.3 Minipreparation of plasmid DNA

The QIAprep Spin Miniprep Kit commercially available from Qiagen™ was used to extract plasmid DNA on a small scale. The solutions and protocol were supplied with the kit. A single colony was used to inoculate 5ml of LB (supplemented with an appropriate antibiotic) and grown overnight at 37°C with shaking. 1.5ml of the cells were pelleted using a microcentrifuge (10000g, 4 minutes) and re-suspended in 250µl of cell suspension buffer P1 containing RNase. The cells were lysed by the addition of 250µl of buffer P2 and then neutralised by the addition of 350µl of buffer N3. The cell debris was pelleted by microcentrifugation (10000g, 10 minutes). The supernatant was decanted into a QIAprep column and after centrifugation (10000g, 60 seconds) the flow through was discarded. The column was washed with 500µl of buffer PB, followed by a second wash with 750µl of Buffer PE containing ethanol, and centrifuged as above. The flow through was discarded and the column centrifuged for an additional 1 minute to remove residual ethanol. The DNA was eluted from the column by the addition of 50µl of buffer EB.

2.17.4 Endonuclease restriction digest

DNA restrictions were typically carried out for 2-3 hours at 37°C using commercially available restriction endonucleases. 3-10 units of enzyme were usually used to restrict 1µg of DNA in a 20µl volume of the recommended buffer.

Restriction endonuclease buffers were supplied at 10× the final concentration. The Roche incubation buffer range was used for single enzyme restrictions (Table 22).

Table 22

Composition of Roche restriction endonuclease buffers (Final concentration in mM)

Component	Buffer	
	B	**H**
Tris-HCl	10	50
Magnesium chloride	5	10
Potassium acetate	100	100
Dithioerythritol (DTE)	-	1
β-mercaptoethanol	1	-
pH at 37°C	8.0	7.5

2.18 DNA sequencing and analysis

2.18.1 Automated sequencing of double-stranded DNA templates

(i) Sequencing using the Sequitherm Excel™ II Kit

Cloned DNA was sequenced using the LICOR 4000L automated sequencer (MWG Biotech, Milton Keynes, UK), and the Sequitherm Excel™ II kit (Cambio, Cambridge, UK). Labelled M13 forward and reverse primers were purchased from MWG Biotech. Sequencing was kindly performed by Mr. Ian Bennet (Department of Veterinary Pathology, Edinburgh).

2.18.2 Isolation of DNA for sequencing following PCR using [α^{32}P] dCTP

The following procedure was used to isolate and identify DNA fragments of interest that could not be detected by ethidium bromide staining of agarose gels and subsequent visualisation under UV light.

(i) Radioactive PCR using [α^{32}P] dCTP

PCR was carried out using either genomic or cDNA as a template and 10μCi of [α^{32}P] dCTP per reaction, using reaction conditions and cycling profiles as described for the individual PCRs (see sections 2.8.2 and 2.8.5).

(ii) Polyacrylamide gel electrophoresis

5μl of PCR product was mixed with 5μl of loading dye, containing formamide and resolved on a 6% polyacrylamide gel. The gel was run at 80W for 2 hours, transferred onto Whatman 3MM paper and finally dried under vacuum at 80°C. Dried gels were then exposed to 2 films overnight at room temperature, one of which served as a template for excising the bands of interest and the other which was retained as a record. To allow accurate alignment of the developed autoradiograph with the dried gel, luminescent autoradiograph markers, Glogos® II (Stratagene) were placed on the four corners of the gel.

(iii) Isolation of DNA fragments

The autoradiograph was positioned on top of the dried gel as accurately as possible using the markers as a guide. The area surrounding the band of interest was cut out using a sterile scalpel blade making a window in the autoradiograph. The excised band from the dried gel was then placed in a sterile 1.5ml eppendorf containing 100μl of sterile distilled water. The DNA was eluted by incubating the tube at 65°C for 30 minutes and then at 4°C overnight.

(iv) Re-amplification of DNA

2μl of eluted DNA was re-amplified in a PCR using the same reaction and thermal cycling conditions used to initially amplify the DNA product of interest, but omitting the [α^{32}P] dCTP from the reaction mix. 20μl of the re-amplified product was resolved on a 2% w/v NuSieve® agarose gel containing 1μg/ml EtBr and visualized under UV light (see section 2.9).

(v) Cloning and sequencing of the re-amplified DNA

The re-amplified PCR products containing the DNA of interest were ligated into the pCR®4-TOPO® vector (2.17.1.2) and up to 5 clones recovered from each transformation were sequenced using the Sequitherm Excel™ II kit (2.18.2).

2.19 Methylation analysis

Methylation specific PCR (MSP) is a rapid inexpensive method for the analysis of the methylation status of CpG islands (cytosines located 5' to guanines) that are present in the regulatory regions of many genes. It is therefore an important technique for the study of abnormally methylated genes in neoplasia and of imprinted genes. The procedure takes advantage of the sequence difference between methylated and unmethylated alleles following sodium bisulphite treatment of DNA, which converts unmethylated, but not methylated, cytosines to uracil. The modified DNA is then used as a template for amplification using primers for a given locus, which are designed to distinguish methylated DNA from unmethylated DNA.

2.19.1 Bisulphite modification of DNA

Modification of DNA using sodium bisulphite was performed using reagents and protocols supplied with the CpGenome™ Modification Kit (Intergen, U.S.A). Briefly, 1μg of DNA was denatured with 3M NaOH at 37°C for 10 minutes, before the addition of 550μl of DNA Modification Reagent I containing sodium bisulphite and hydroquinone, and incubation at 50°C for 20 hours. This was followed by the addition of 5μl and 750μl of DNA Modification Reagents III and II containing NaOH and incubation at room temperature for 10 minutes to complete the chemical conversion. DNA purification was carried out by 3 washes in 70% ethanol followed by the addition of 50μl of 20mM NaOH/90% ethanol and incubation at room temperature for 5 minutes. The DNA pellet recovered after 2 washes in 90% ethanol was resuspended in 25μl of TE (10mM Tris/0.1mM EDTA, pH 7.5) and incubated at 50°C for 15 minutes to elute the DNA. The samples were centrifuged at 10000g for 3 minutes and the supernatant containing the eluted DNA transferred to a fresh eppendorf and stored at -20°C until used for PCR.

2.19.2 Methylation specific PCR (MSP)

2.19.2.1 Primers and reaction mixture

Following bisulphite modification of DNA, MSP was carried out using primers that could distinguish methylated from unmethylated DNA (Table 23, page 104). The CpG WIZ™ Amplification kit (Intergen, U.S.A) was used for the methylation analysis of $p16^{INK4a}$ and $p15^{INK4b}$, according to the manufacturer's instructions. Methylated and unmethylated control DNA (Intergen), chemically modified, was used as positive and negative controls respectively. Briefly, a hot-start PCR, using *AmpliTaq* Gold (section 2.8.8), was employed to eliminate mis-priming and PCR-related artefacts. Separate reaction mixes were made up using primers specific for the methylated (M) and unmethylated (U) reactions and were as follows:

10×Universal buffer	2.5µl
2.5mM dNTP mix	2.5µl
U or M primers	1.0µl
AmpliTaq Gold Polymerase	1 unit
Modified template DNA	50-100ng
dH_2O	Up to 25 µl

2.19.2.2 Amplification

The reactions were then subjected to the following thermal cycling conditions:

1 cycle for	
Activation of *AmpliTaq* Gold	95°C for 12 minutes
35 cycles of	
Denaturation	95°C for 45 seconds
Annealing	60°C for 45 seconds
Extension	72°C for 60 seconds

For the p73 MSP reaction, the reaction mix was made up to a total volume of 25µl, using primers specified in Table 23, and were as follows:

10x GeneAmp PCR Buffer II (100mM Tris-HCl, pH8.3, 500mM KCl)	2.5µl
25mM $MgCl_2$	2.5µl

5mM dNTP mix	4μl
U or M primers	0.4μM each
AmpliTaq Gold Polymerase	1 unit
Modified template DNA	50-100ng

The reactions were then subjected to the following thermal cycling conditions:

1 cycle for

Activation of *AmpliTaq* Gold	95°C for 12 minutes

35 cycles of

Denaturation	95°C for 30 seconds
Annealing	60°C for 45 seconds
Extension	72°C for 30 seconds

25μl of PCR-amplified products were resolved on 3% w/v NuSieve® agarose gels containing 1μg/ml EtBr and visualized under UV light (2.9).

Table 23

Primers for methylation analysis of $p16^{INK4a}$, $p15^{INK4b}$ and p73

Gene	Primer	Sequence	Product size (bp)
$p16^{INK4a}$	M	Primer sequences proprietary (Intergen, U.S.A) Accession number X94154	145
	U		154
$p15^{INK4b}$	M	Primer sequences proprietary (Intergen, U.S.A) Accession number SL5756	154
	U		162
p73*	M F	GGA CGT AGC GAA ATC GGG GTT C	60
	M R	ACC CCG AAC ATC GAC GTC CG	
	U F	AGG GGA TGT AGT GAA ATT GGG GTT T	69
	U R	ATC ACA ACC CCA AAC ATC AAC ATC CA	

M, methylated; U, unmethylated; F, forward; R, reverse; *, Primer sequences from Corn *et al.*, 1999

2.20 Statistical analysis

The statistical tests used in this study were (i) The Fisher's exact test for calculating *p* values from small sample numbers using 2x2 contingency tables and (ii) the Mann-Whitney test (non-parametric) for comparison of the medians of two unpaired groups.

CHAPTER THREE

RESULTS

3.1 Standardisation of study and control material

3.1.1 Study and Control Population

Frozen lymph node tissue from 23 HIV-infected individuals with persistent generalised lymphadenopathy (PGL) obtained in 1983-84, were used as the study population.

Tissue from nine HIV-negative reactive lymph nodes (coded 2425, 2435, 2437, 2462, 2478, 2495, 2498, 2499 and 2512), was obtained from the Department of Pathology, University of Edinburgh. 7 tonsils (numbered T1-T7), removed at routine tonsillectomy, were kindly provided by the ENT Department, City Hospital, Edinburgh. Both lymph nodes and tonsils from the HIV-uninfected individuals served as negative controls.

3.1.2 Standardisation of starting material

The aim of these preliminary studies was to determine the most efficient method of extracting DNA free from contaminating RNA and proteins, from the lymph node and tonsil material used in this study. A tonsil (T1) from an HIV-uninfected individual was used as the prototype for this experiment.

A fresh frozen tonsil was processed by cutting a small piece of tissue from the main block or cutting it into 10, 10-micron sections. DNA was then extracted using either the microfuge phenol-chloroform method, or the Invitrogen Easy DNA Kit (see section 2.6.1).

The purity of the DNA, as determined by the OD 260/280 ratio was 1.79 using the phenol-chloroform extraction method, irrespective of whether the tissue was cut or sectioned. Using the Invitrogen method, the OD 260/280 ratio of the DNA extracted from the cut and sectioned tissue was 1.8 and 1.76 respectively (see Table 24).

The purity of the DNA was unaffected by the way in which the tissue was processed or the protocol used (Table 24). Furthermore, no significant difference in DNA yield was observed using either experiment (Table 24). Therefore, it was decided to use the Invitrogen Easy DNA Kit to extract DNA from cut tissue, since it is a more rapid and convenient method of DNA extraction than the phenol-chloroform method.

Table 24

Standardisation of genomic DNA extraction method

Method of DNA extraction	Type of tissue processed	Ratio (OD 260/280)	Concentration of DNA (μg/ml)
Phenol-chloroform	small cut piece	1.79	247.2
	Ten 10 micron sections	1.79	203
Invitrogen	small cut piece	1.8	344
	Ten 10 micron sections	1.76	204

OD, optical density

3.2 Optimisation of PCR parameters

Specificity and yield of PCR amplified products is influenced by (i) $MgCl_2$ (ii) Annealing temperature (iii) dNTPs (iv) *Taq* polymerase and (v) number of cycles (see below). To establish optimal conditions (specificity and sensitivity) for PCR amplification with each primer pair, reaction conditions were standardised for the above parameters. Published reaction conditions were used as reference points (see Table 25).

Table 25

Summary of published conditions for genomic and RT-PCR

Gene[1]	$MgCl_2$ (mM)	Ann. Temp (°C)	Taq (U)	Primer (μM)	Cycle number
β-actin	*	65[2]	*	*	35
P63 (TA and ΔN)	*	52	*	*	40
p73	1.5	59	2.5[a]	0.4	35
Δ2 p73	*	72[2]	*	*	25
$p16^{INK4a}$	*	56	*	*	22
$p14^{ARF}$	*	60	*	*	35
KSHV ORF 71-73	*	57	*	*	30
BamH1 W	1.5	45	2.5[b]	1	35

Ann. Temp, annealing temperature; [1], References for the primer pairs used are given in Tables 9 and 11; [2], annealing and extension as 1-step; *, conditions not published; [a], U/50μl; [b], U/100μl

(i) Optimisation of magnesium concentration

Taq polymerase is dependent on the presence of free Mg^{2+} ions for its enzymatic function. A high concentration inhibits the enzyme whereas the product yield is reduced if the Mg^{2+} concentration is too low (Linz *et al.*, 1990).

cDNA synthesised from 40ng of RNA from a LCL, KB, was subjected to a 35-cycle amplification for β-actin mRNA. The $MgCl_2$ concentration was varied from 0.5mM to 4mM and included the established concentration of 1.5mM (see Table 25).

Figure 16 shows the results obtained with the primer pair for human β-actin. A 540bp PCR fragment was detected following amplification of cDNA from a human tonsil, with Mg^{2+} concentrations of 0.5mM to 3mM in 0.5mM increments (lanes 2 to 7), and 4mM (lane 8). The efficiency of amplification was reduced and non-specific bands were observed with Mg^{2+} concentrations above 1.5mM (lanes 6 to 8). The efficiency of amplification was similar at a Mg^{2+} concentration of 1.0 and 1.5mM. The optimal Mg^{2+} concentration was taken as the published value of 1.5mM for the human β-actin primer pair. The optimal Mg^{2+} concentration for the other primer pairs was established in a similar fashion. The results are shown in Table 26, page 114.

(ii) Optimisation of annealing temperature

The efficiency of primer annealing to the target and the outcome of the PCR reaction is dependent on accurate annealing temperatures (Kocher and Wilson, 1991).

cDNA synthesised from 40ng of RNA from the BL-41 Burkitt's lymphoma cell line was subjected to a 35-cycle amplification for $p15^{INK4b}$ mRNA, containing the established optimal $MgCl_2$ concentration (see Table 26, page 114). The annealing temperature (Tm) of the $p15^{INK4b}$ primer pair was calculated to be 59°C using the formula [(2×A/T)+(4×G/C)]. The PCR run included annealing temperatures of 54°C to 62°C in 2°C increments.

Figure 17 shows the results obtained with the primer pair for human $p15^{INK4b}$. A 346bp PCR fragment was detected following amplification at annealing temperatures of 54, 56°C, 58°C and 60°C (lanes 1 to 4). The efficiency of the amplification and quality of the product (as judged by the intensity of bands on the gel) was found to be similar at 56°C and 58°C, but no amplification was noted at 62°C. The optimal annealing temperature was taken as 58°C for the $p15^{INK4b}$ primer pair.

Figure 16. Optimisation of Mg^{2+} concentration for PCR using β-actin primers

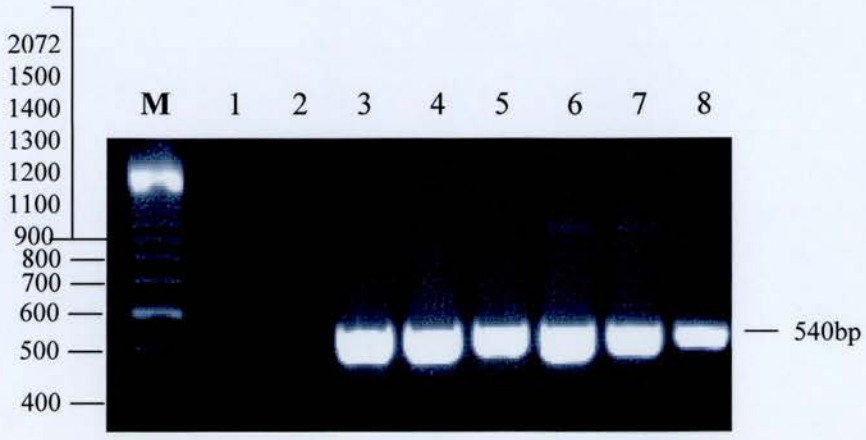

cDNA synthesised from 40ng of RNA was subjected to amplification (35 cycles) in a 50μl reaction using β-actin primers. 20μl of the amplified product was resolved on a 2% w/v agarose gel. The bands were visualised under UV light. **M:** 100bp DNA size marker (fragment sizes in bp). **Lane 1:** Sterile distilled water **Lanes 2-8:** 0.5mM, 1.0mM, 1.5mM, 2.0mM, 2.5mM, 3.0mM, and 4.0mM Mg^{2+} per reaction, respectively. The β-actin PCR product (540bp) is indicated.

Figure 17. Optimisation of annealing temperature for PCR using $p15^{INK4b}$ primers

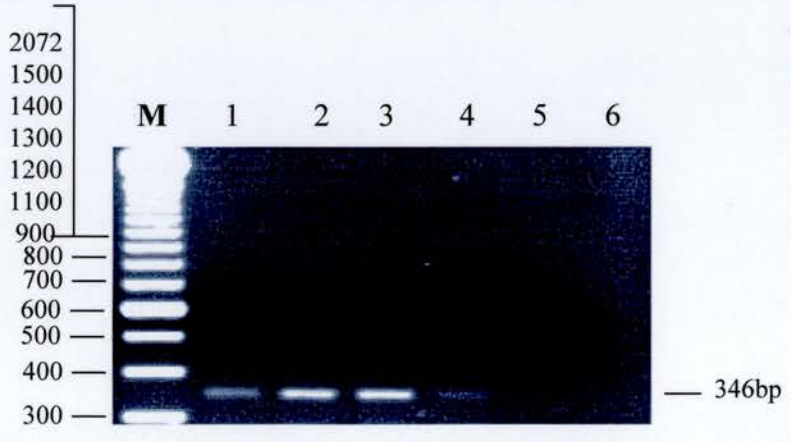

cDNA synthesised from 40ng of RNA was subjected to amplification (35 cycles) in a 30μl reaction using $p15^{INK4b}$ primers. 20μl of the amplified product was resolved on a 2% w/v agarose gel and the bands were visualised under UV light. **M:** 100bp DNA size marker (fragment sizes in bp). **Lanes 1-5:** Annealing temperatures of 54°C, 56°C, 58°C, 60°C, and 62°C respectively **Lane 6:** Sterile distilled water. The $p15^{INK4b}$ PCR product (346bp) is indicated.

The optimal annealing temperature for the other primer pairs was established in a similar fashion, either using published conditions (Table 25, page 107) or calculated Tm as starting values. The results are shown in Table 26 on page 114.

(iii) Optimisation of primer concentration

An excess of primers can lead to the amplification of non-target sequences, while too low a concentration can limit the efficiency of the PCR (Sambrook *et al.*, 1989).

cDNA synthesised from 40ng of RNA from a human lung cancer cell line (H-358) was subjected to a 35-cycle amplification for $p14^{ARF}$ mRNA containing established optimal Mg^{2+} concentration and annealing temperature (Table 26, page 114).

Figure 18 shows the amplification of a 188bp PCR product with the primer pair for $p14^{ARF}$. The PCR run included primer concentrations of 0.25, 0.5, 1, 1.25 and 1.5μM (lanes 2 to 6 respectively). The efficiency of the amplification was reduced, and increasing non-specific products were observed, with primer concentrations above 0.5μM. Amplification was completely inhibited at a primer concentration of 1.5μM. The optimal primer concentration was taken to be 0.5μM for the $p14^{ARF}$ primer pair. The optimal primer concentration for the other primer pairs was established in a similar fashion. The results are shown in Table 26 on page 114.

(iv) Optimal *Taq* DNA polymerase concentration

The amount of *Taq* polymerase required in a reaction is dependent on the target DNA, the primers and the volume of the reaction. Insufficient enzyme results in a poor yield, whereas excess causes nucleotide misincorporation and amplification of non-target sequences (Sambrook *et al.*, 1989; Kocher and Wilson, 1991).

cDNA synthesised from 40ng of RNA from a LCL, KB, was subjected to a 35-cycle amplification for $p16^{INK4a}$ mRNA, in a reaction volume of 30μl, containing the established optimal Mg^{2+} and primer concentration and annealing temperature (see Table 26, page 114). The PCR run included reactions containing 0.5-4.5 units (U) of *Taq* polymerase, in 1U increments.

Figure 19 shows the results obtained with the primer pair for $p16^{INK4a}$. A 139bp PCR fragment was detected following amplification of the LCL, KB, with the concentration of *Taq* polymerase enzyme in the range of 0.5-3.5 U (lanes 2 to 5), but

Figure 18. Optimisation of primer concentration for PCR using $p14^{ARF}$ primers

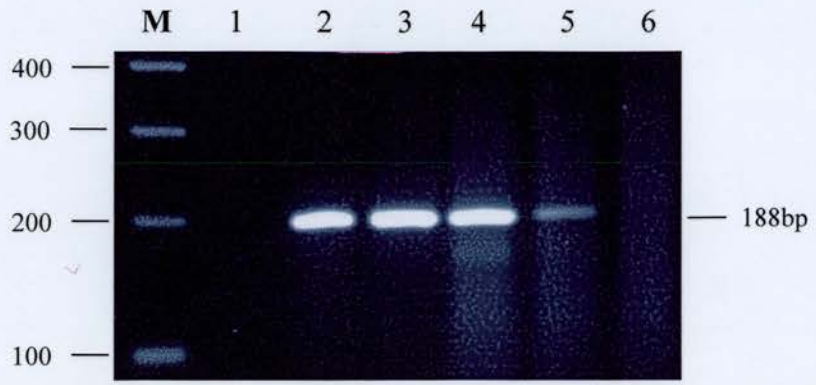

cDNA synthesised from 40ng of RNA was subjected to amplification (35 cycles) in a 30μl reaction using $p14^{ARF}$ primers. 20μl of the amplified product was resolved on a 2% w/v agarose gel. The bands were visualised under UV light. **M:** 100bp DNA size marker (fragment sizes in bp). **Lane 1:** Sterile distilled water **Lanes 2-6:** 0.25μM, 0.5μM, 1μM, 1.25μM and 1.5μM primers per reaction, respectively. The $p14^{ARF}$ PCR product (188bp) is indicated.

Figure 19. Optimisation of *Taq* polymerase concentration for PCR using $p16^{INK4a}$ primers

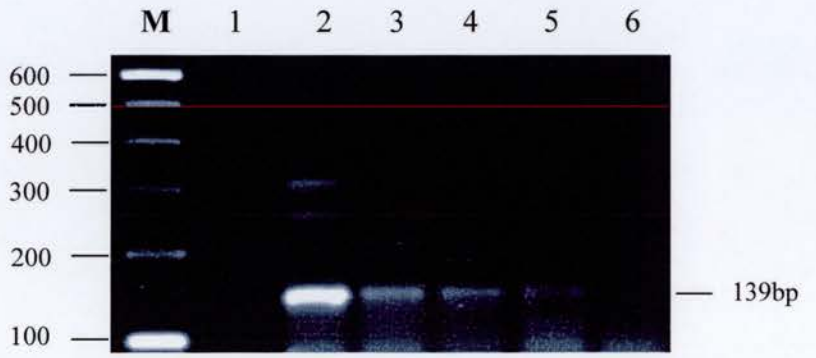

cDNA synthesised from 40ng of RNA was subjected to amplification (35 cycles) in a 30μl reaction using $p16^{INK4a}$ primers. 20μl of the amplified product was resolved on a 2% w/v agarose gel. The bands were visualised under UV light. **M:** 100bp DNA size marker (fragment sizes in bp). **Lane 1:** Sterile distilled water **Lanes 2-6:** 0.5U, 1.5U, 2.5U, 3.5U, and 4.5U of *Taq* DNA polymerase per 30 μl reaction, respectively. The $p16^{INK4a}$ PCR product (139bp) is indicated.

amplification was completely inhibited with 4.5 U of the enzyme (lane 6). The efficiency of the amplification and quality of the product (as judged by the intensity of bands on the gel) decreased with enzyme concentrations above 0.5 U. The optimum *Taq* polymerase concentration was therefore taken to be 0.5 U/30µl for the $p16^{INK4a}$ primer pair. The optimum enzyme concentration for the other primer pairs was established in a similar fashion. The results are shown in Table 26 on page 114.

(v) Optimisation of cycle number

The number of PCR cycles required for amplification of target sequence depends on the amount of available target DNA and the efficiency of the PCR reaction (Taylor, 1991).

cDNA synthesised from 40ng of RNA from a tonsil was subjected to a 35-cycle amplification for β-actin mRNA at the established optimal annealing temperature, primer, *Taq* and Mg^{2+} concentrations (see Table 26, page 114). The PCR run included reactions carried out in increments of 5 cycles from 15 cycles to 40 cycles and included the published cycle number of 35 cycles (Table 25, page 107).

Figures 20A and 20B show the results obtained with the primer pair for β-actin. A 540bp PCR fragment was detected using 20 to 40 cycles of amplification (lanes 3 to 7), but was not detectable at 15 cycles (Figure 20A, lane 2). Following hybridisation with a ^{32}P-labelled oligonucleotide, a 540bp fragment could be detected at a cycle number of 15 (figure 20B, lane 2). The intensity of the bands was measured using scanning densitometry (UVP Gel Works) and a graph was plotted of cycle number against band volume. From the graph, the intensity of the amplified fragments was found to be similar when using 30 or more cycles (figure 20C). Therefore, the optimum number of PCR cycles for the β-actin primer pair was taken to be 28 cycles (between 25 and 30 cycles), which is on the linear slope of the curve (figure 20C). However, lower number of cycles is appropriate for semi-quantitative PCR analysis. The optimum cycle number for the other primer pairs was established in a similar fashion. The results are shown in Table 26 on page 114.

Figure 20. Determination of optimal number of PCR cycles using β-actin primers

20 A

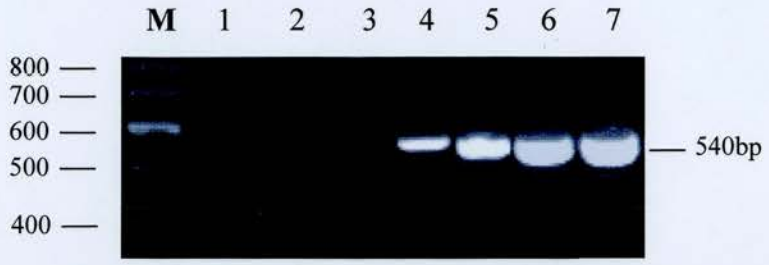

cDNA synthesised from 40ng of RNA was subjected to amplification in a 50μl reaction for 35 cycles using β-actin primers. 20μl of the amplified product was resolved on a 2%w/v agarose gel. The bands were visualised under UV light. **M:** 100bp DNA size marker (fragment sizes in bp). **Lane 1:** Sterile distilled water **Lanes 2-7:** 15, 20, 25, 30, 35 and 40 PCR cycles respectively. The β-actin PCR product (540bp) is indicated.

20 B

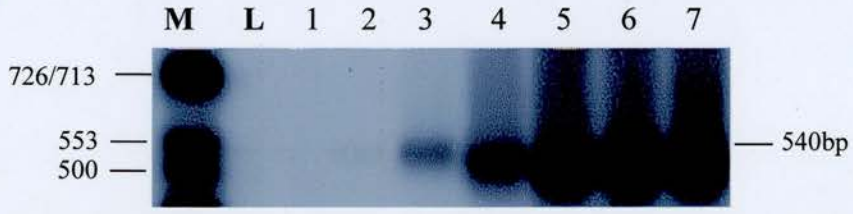

PCR products were Southern transferred to a Hybond N^+ membrane and hybridized with a ^{32}P-labelled oligonucleotide probe specific for the amplified fragment. **M:** *Hinf1* digested ϕX-174 DNA size marker (fragment sizes in bp). **L:** 100bp DNA size marker. **Lane 1:** Sterile distilled water **Lanes 2-7:** 15, 20, 25, 30, 35 and 40 PCR cycles respectively. The β-actin PCR product (540bp) is indicated.

20 C

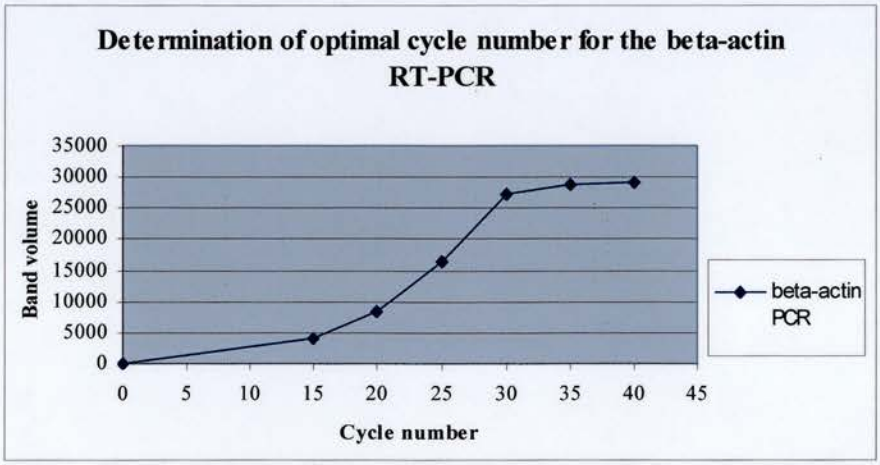

The intensity of the bands, obtained after hybridization of the β-actin PCR products with a ^{32}P-labelled oligonucleotide probe, was measured using scanning densitometry (UVP Gel Works). A graph was then plotted with the cycle number on the X-axis and the band volume on the Y-axis. The optimal cycle number for the β-actin PCR was determined to be 28 cycles, which is on the exponential portion of the amplification curve.

3.2.1 Summary of optimisation experiments for genomic and RT-PCR

A summary of the optimised PCR conditions for each primer pair is shown in Table 26. dNTPs were used at concentrations of 200μM each (Sambrook *et al.*, 1989). Reaction conditions for the β-globin PCR were kindly optimised by Dr. Tanzina Haque.

Table 26

Summary of optimisation experiments for genomic and RT-PCR

Gene	$MgCl_2$ (mM)	Ann. Temp (°C)	*Taq* (U)	Primer (μM)	Cycle number
β-actin	1.5	65	1.5[b]	1	28
p63 (TA and ΔN)	1.5	52	1[c]	0.5	28
p73	1.5	59	2.5[c]	0.25	35
Δ2 p73	1.5	72[1]	1[c]	0.5	35
$p16^{INK4a}$	2	56	0.5[d]	0.5	25
$p14^{ARF}$	2	56	0.5[d]	0.5	22[a]
$p15^{INK4b}$	2	58	0.5[d]	0.5	25
LNA	1.5	60	2.5[c]	0.4	30
KSHV ORF 71-73	1.5	57	1.0[c]	0.4	35
BamH1 W	1.5	57	2.5[b]	1	28

Ann. Temp, annealing temperature; [1], annealing and extension as 1-step; [a], cycle number for semi-quantitative PCR; [b], U/100μl; [c], U/50μl; [d], U/30μl

3.3 Determination of primer sensitivity for Methylation-specific PCR (MSP)

Aberrant methylation of CpG islands in the promoter region of a gene is an important mechanism of inactivation of the function of some tumour suppressor genes. In preliminary work, primers and conditions for MSP were evaluated. These experiments were designed to assess the sensitivity of the assay in detecting methylated alleles present in a background of unmethylated DNA. Serial 10-fold

dilutions of DNA from the BL cell lines, Raji (with documented methylation in the $p16^{INK4a}$ and $p15^{INK4b}$ genes) and Namalwa (with methylation in *p73* as assessed in this study), in a total of 1μg of lymphoblastoid cell DNA was carried out. The DNA from each dilution series was chemically modified using the CpGenome™ Modification Kit (Intergen) and 40ng of DNA was subjected to MSP analysis using primers specific for methylated and unmethylated alleles.

Figures 21A and 21B demonstrate the sensitivity of the MSP analysis for detecting methylated alleles of $p16^{INK4a}$ and p73 genes respectively using the primers specified in Table 23, page 104. In the case of the $p16^{INK4a}$ gene a band of 145bp could be detected at a dilution of 10^{-3} (4pg of methylated DNA) (figure 21A, lane 4). A similar result was obtained with the MSP for the p73 gene using the Namalwa cell line. A band of 60bp could be detected at a dilution of 10^{-3} (~ 4pg of methylated DNA) (figure 21B, lane 4). The sensitivity of the $p15^{INK4b}$ primer pair was similarly established, and methylated alleles could be detected at a dilution of 10^{-3} (~ 4pg of methylated DNA).

3.4 Optimisation of conditions for Long-Distance (LD)-PCR

Junctional sequences created by the fusion of two genes occur in particular subtypes of lymphomas and leukaemias, and hence detection of such sequences can provide valuable information for diagnosis and subsequent management of haematological neoplasms (Dalla-Favera *et al.*, 1982b; Tsujimoto *et al.*, 1984; Ye *et al.*, 1993). The breakpoint on the partner chromosome can be distributed over a large region, such that the region enclosed by the primers is too large to yield a PCR product by standard PCR techniques. Therefore, a long-distance PCR strategy (Akasaka *et al.*, 1996; see section 2.8.7) was used in this study to investigate chromosomal translocations involving the c-*myc* and *bcl-2* genes.

Figure 21. Sensitivity of MSP analysis for the detection of methylated alleles

21 A

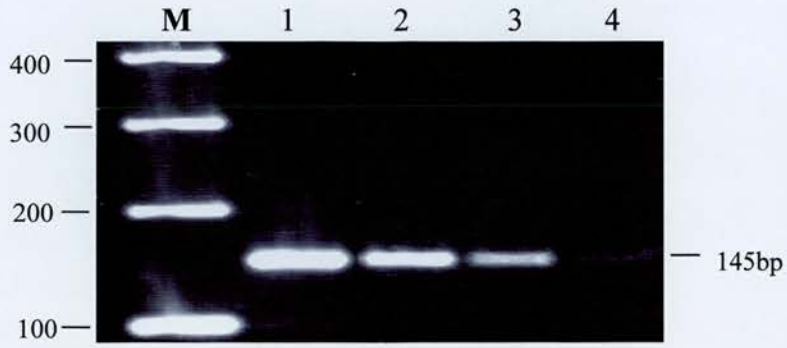

A ten-fold dilution series of the BL cell line, Raji, in a total of 1μg of lymphoblastoid cell line (LCL) DNA was prepared and subjected to sodium bisulfite modification. 40ng of each dilution was subjected to amplification in a 35-cycle hot-start PCR for $p16^{INK4a}$ using the appropriate primers for the methylated reaction. 25μl of PCR product was resolved on a 2.5% w/v agarose gel. The bands were visualised under UV light. **M:** 100bp DNA size marker (fragment sizes in bp). **Lanes 1,2,3 and 4:** 1, 10^{-1}, 10^{-2}, and 10^{-3} dilutions respectively of Raji DNA in LCL DNA. The $p16^{INK4a}$ methylated product (145bp) is indicated.

21 B

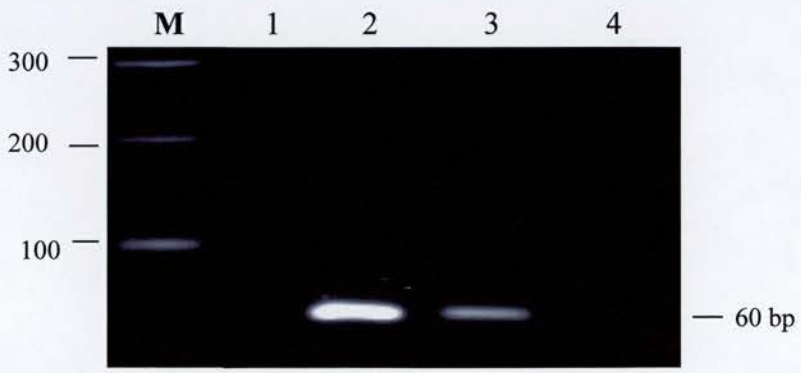

A ten-fold dilution series of the BL cell line, Namalwa, in a total of 1μg of lymphoblastoid cell line (LCL) DNA was prepared and subjected to sodium bisulfite modification. 40ng of each dilution was subjected to amplification in a 35-cycle hot-start PCR for p73 using the appropriate primers for the methylated reaction. 25μl of PCR product was resolved on a 2.5% w/v agarose gel. The bands were visualised under UV light. **M:** 100bp DNA size marker (fragment sizes in bp). **Lane 1:** Sterile distilled water. **Lanes 2,3 and 4:** 10^{-1}, 10^{-2}, and 10^{-3} dilutions respectively of Namalwa DNA in LCL DNA. The p73 methylated product (60bp) is indicated.

3.4.1 Optimisation of LD-PCR conditions for the detection of translocations involving the c-*myc* and *bcl-2* genes

The specificity, sensitivity, optimal magnesium concentration and annealing temperature for each primer pair used in the LD-PCR analysis of the c-*myc* and *bcl-2* translocations was established, and representative experiments are shown below.

3.4.1.1 Specificity of primers used for LD-PCR analysis

To test the specificity of the primers used for the c-*myc* LD-PCR analysis (Table 14, page 85), genomic DNA from cell lines that have been shown to harbour translocations specific to a primer set (Akasaka *et al.*, 1996; Table 15, page 86) was amplified (Figure 22, page 119).

A 7.6kb fragment from the Raji cell line was amplified with the c-*myc*/Cγ primer set (figure 22, lane 1).

A 4.0kb fragment from the BL-41 cell line was amplified with the c-*myc*/Cα primer set (figure 22, lane 2).

A 4.9kb fragment from the Ramos cell line was amplified with the c-*myc*/Cμ primer set (figure 22, lane 3).

No amplification was observed when the Raji cell line, which has a c-*myc*/Sγ translocation, was tested with the c-*myc*/Cμ primer set (figure 22, lane 4). Negative amplification with the P3HR1 cell line, wherein the breakpoint on chromosome 8 is located around 190kb upstream of the c-*myc* gene (Joos *et al.*, 1992), further confirmed the specificity of the primers (figure 22, lane 5).

The specificity of the primer pairs for the analysis of *bcl-2*/*IgH* translocations (Table 14, page 85) was established in a similar fashion. Lymph nodes with known translocations between the MBR (1119) and mcr (1143) regions on chromosome 18 and the JH region of chromosome 14 (Krajewsky, A, personal communication), amplified with the MBR/Eμ and mcr/Eμ primer pairs respectively. A lymph node with no known t(14:18) translocation did not amplify with any of the primer pairs (Table 15, page 86).

3.4.1.2 Optimisation of Mg^{2+} concentration for LD-PCR

Since sub-optimal concentrations of Mg^{2+} can inhibit *Taq* polymerase activity (Linz *et al.*, 1990), the following experiment was carried out to optimise Mg^{2+} ion concentration for the LD-PCR.

Figure 23 shows a 7.6kb region, which was amplified from DNA extracted from the BL cell line, Raji, in a 35-cycle RT-PCR reaction using the c-*myc*/Cγ primer pair and Mg^{2+} concentrations of 2.0mM, 2.5mM and 3.0mM (lanes 1 to 3 respectively). The efficiency of amplification was reduced at a Mg^{2+} concentration of 2.0mM, and non-specific bands were observed with increasing concentrations of Mg^{2+}. From the above experiment the optimum Mg^{2+} concentration was taken as the published concentration of 2.5mM for the c-*myc*/Cγ primer pair (figure 23, lane 2).

The optimum $MgCl_2$ concentration for the other primer pairs was established in a similar fashion and found to be 2.5mM.

3.4.1.3 Optimisation of annealing temperature for LD-PCR

The following experiment was carried out to ascertain the optimal annealing temperature for the LD-PCR amplification of the c-*myc* and *bcl-2* translocations.

Figure 24 shows the results obtained when genomic DNA from the BL-41 cell line was amplified in a 35-cycle LD-PCR reaction using the c-*myc*/Cα primer pair and at annealing temperatures of 63°C, 68°C and 73°C (figure 24, lanes 1,2 and 3 respectively). A 4.0kb product was amplified at annealing temperatures of 63°C and 68°C (figure 24 lanes, 1 and 2 respectively), although the efficiency of amplification, as judged by the intensity and size of the band, was greater at an annealing temperature of 68°C. Amplification was not observed at an annealing temperature of 73°C. The optimum annealing temperature was taken as the published value of 68°C for the c-*myc*/Cα primer pair.

The optimum annealing temperature for all the other primer pairs was established in a similar fashion and was found to be 68°C in each case.

Figure 22. Specificity of primers used for LD-PCR

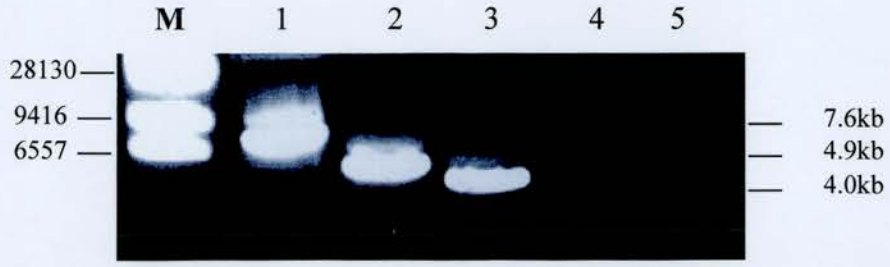

200ng of genomic DNA from the BL-41, Raji and Ramos cell lines were subjected to amplification in a 35-cycle LD-PCR reaction using the c-*myc*/Cα, c-*myc*/Cγ and c-*myc*/Cμ primer pairs respectively. DNA from the Raji cell line was similarly subjected to amplification using the c-*myc*/Cα primer set. 20μl of the PCR product was resolved on a 0.8% w/v agarose gel and the bands were visualised under UV light. **M:** Lambda (λ) DNA digested with Hind III DNA size marker (fragment sizes in bp). **Lane 1:** Raji cell line (7.6kb translocation) **Lane 2:** Ramos cell line (4.9kb translocation) **Lane 3:** BL-41 cell line (4.0kb translocation) **Lane 4:** Raji cell line (*c-myc*/Cμ primer set) **Lane 5:** P3HR1 cell line.

Figure 23. Optimisation of Mg^{2+} concentration for LD-PCR

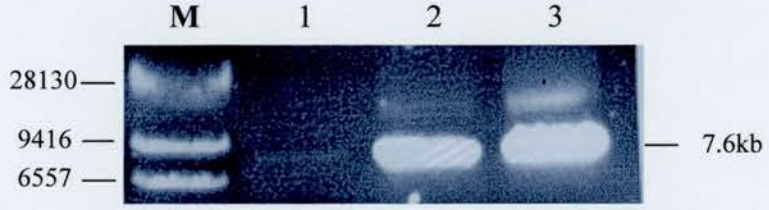

200ng of genomic DNA from the Raji cell line was subjected to amplification in a 35-cycle LD-PCR reaction using the c-*myc*/Cγ primer set. 20μl of the PCR product was resolved on a 0.8% w/v agarose gel and the bands were visualised under UV light. **M:** Lambda (λ) DNA digested with Hind III DNA size marker (fragment sizes in bp). **Lanes 1-3:** 2.0mM, 2.5mM and 3mM Mg^{2+} per reaction respectively. The c-*myc*/Sγ (7.6kb) translocation is indicated.

Figure 24. Optimisation of annealing temperature for LD-PCR

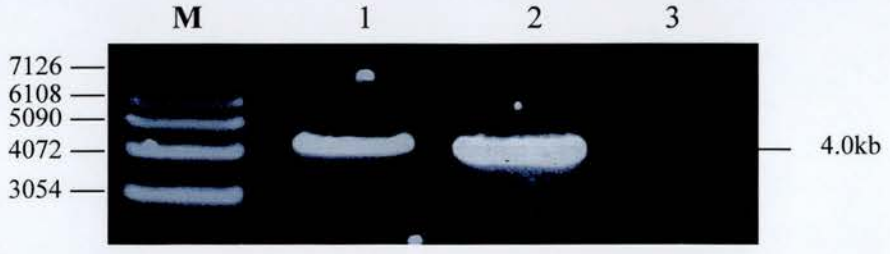

200ng of genomic DNA from the BL-41 cell line was subjected to amplification in a 35-cycle LD-PCR reaction using the c-*myc*/Cα primer set. 20μl of the PCR product was resolved on a 0.8% w/v agarose gel and the bands were visualised under UV light. **M:** 1kb DNA size marker (fragment sizes in bp). **Lanes 1-3:** Annealing temperatures of 63°C, 68°C and 73°C respectively. The c-*myc*/Sα (4.0kb) translocation is indicated.

3.4.1.4 Sensitivity of the primers used for LD-PCR analysis

To ascertain the sensitivity of the primers used to detect the c-*myc* and *bcl-2* translocations, the Raji cell line and DNA from lymph node biopsy 1119 were used respectively.

(i) Sensitivity of the primers used for the c-*myc* LD-PCR

Serial ten-fold dilutions of Raji cells (which harbour a c-*myc*/Sγ translocation) in increasing numbers of cells from a lymphoblastoid cell line were prepared. 100ng of DNA extracted from each dilution was then subjected to LD-PCR analysis using the c-*myc*/Cγ primer set. A band of 7.6kb could be detected at a dilution of 10^{-2} (figure 25A, lane 3). Hybridisation of the amplified products with a [γ^{32}P] ATP-labelled c-*myc* probe increased the sensitivity of detection by one order of magnitude and a 7.6kb band could be detected at a dilution of 10^{-3} (figure 25B, lane 4). Since 100ng of DNA is equivalent to 10^4 cells on average, the sensitivity of detection was estimated to be 10 copies of the c-*myc*/*IgH* translocation.

The sensitivity of detection of the t(8:14) translocations using the other primer pairs was established in a similar fashion, and in each case was found to be 10 copies.

(ii) Sensitivity of the primers used for the *bcl-2* LD-PCR

Since the accurate cell number could not be determined with the lymph node biopsy, serial ten-fold dilutions of genomic DNA from a lymph node biopsy (1119) which has a MBR/JH fusion, in increasing amounts of DNA from a lymphoblastoid cell line were prepared. 100ng of DNA extracted from each dilution was then subjected to LD-PCR analysis using the MBR-1/Eμ primer set. Hybridisation of the amplified products with a [γ^{32}P] ATP-labelled Eμ probe identified a 4.2kb band at a dilution of 10^{-3} (figure 26, lane 7). Since 100ng of DNA is equivalent to 10^4 cells on average, the sensitivity of detection was estimated to be 10 copies of the MBR/JH fusion.

The sensitivity of detection of *bcl-2*/*IgH* fusions using the other primer pairs was established in a similar manner, and in all cases was found to be 10 copies.

Figure 25. Sensitivity of the primers used for the c-*myc* LD-PCR

25 A

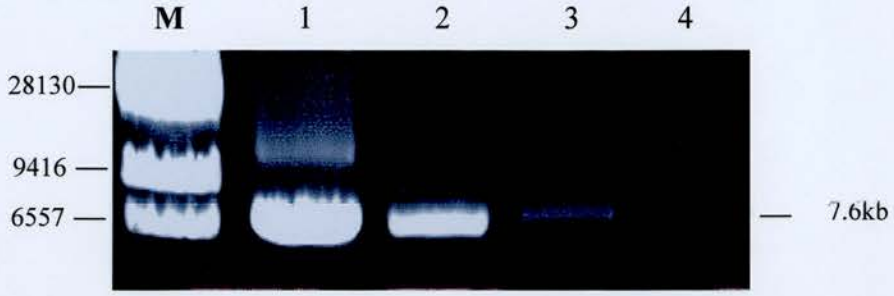

Serial ten-fold dilutions of Raji cells (which harbor a c-*myc*/Sγ translocation) in increasing numbers of cells from a lymphoblastoid cell line (LCL) were prepared. 100ng of DNA from each dilution was then subjected to LD-PCR analysis using the c-*myc*/Cγ primer set. 20μl of the PCR product was resolved on a 0.8% w/v agarose gel. **M:** Lambda (λ) DNA digested with Hind III DNA size marker (fragment sizes in bp). **Lanes 1 to 4:** 1, 10^{-1}, 10^{-2}, and 10^{-3} dilutions of Raji cells in cells from an LCL, respectively. The c-*myc*/Sγ (7.6kb) translocation is indicated.

25 B

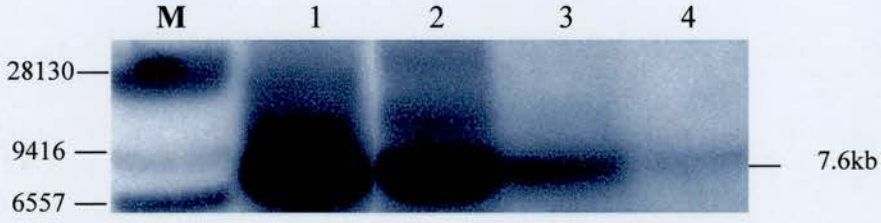

PCR products were transferred to a Hybond N^+ membrane, and hybridised with a [γ^{32}P] ATP-labelled c-*myc* probe. **M:** Lambda (λ) DNA digested with Hind III DNA size marker (fragment sizes in bp). **Lanes 1 to 4:** 1, 10^{-1}, 10^{-2}, and 10^{-3} dilutions of Raji cells with cells from an LCL, respectively. The c-*myc*/Sγ (7.6kb) translocation is indicated.

Figure 26. Sensitivity of the primers used for the *bcl-2* LD-PCR

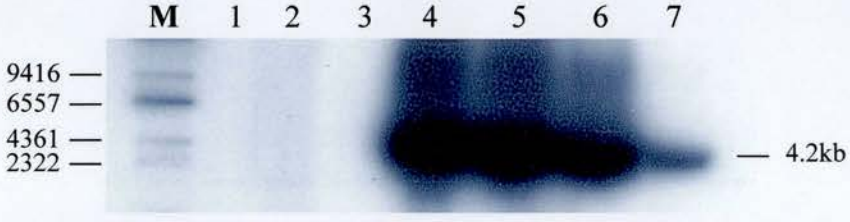

Serial ten-fold dilutions of DNA from a lymph node (1119) in increasing amounts of DNA from a lymphoblastoid cell line, was prepared. 100ng of DNA from each dilution was then subjected to LD-PCR analysis using the MBR-1/Eμ primer set. 20μl of the PCR product was resolved on a 0.8% w/v agarose gel, transferred to a Hybond N^+ membrane, and hybridised with a [γ^{32}P] ATP-labelled Eμ probe. **M:** Lambda (λ) DNA digested with Hind III DNA size marker (fragment sizes in bp). **Lanes 1:** Blank **Lane 2:** Sterile distilled water **Lane 3:** Lymph node without t(14:18) translocation (761) **Lanes 4 to 7:** 1, 10^{-1}, 10^{-2}, and 10^{-3} dilutions of lymph node (1119) DNA in cells from a LCL, respectively. The MBR-1/JH (4.2kb) translocation is indicated.

3.5 Screening for amplifiable DNA using β-Globin primers

DNA prepared from PGL tissue, as well as HIV-negative control tonsil and lymph node, was amplified using β-globin primers (Table 9, page 78) to check for the presence of amplifiable DNA. A band of 110bp was detected in all the PGL samples (figures 27A and 27B) as well as in all the control tonsils (figure 28A) and lymph nodes (figure 28B). A lymphoblastoid cell line (LCL), KB, was used as a positive control for amplification and sterile water was used as a control for PCR contamination.

Figure 27. Screening for amplifiable DNA in PGL tissue using human β-globin primers

27 A

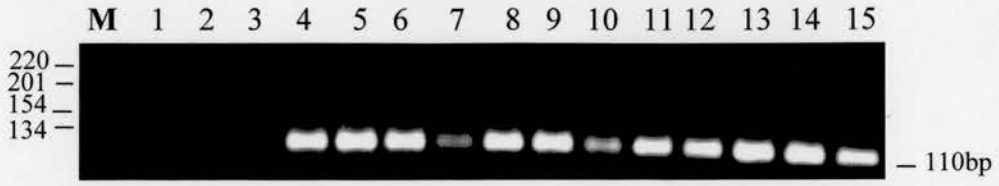

1μg of DNA prepared from PGL tissue was subjected to amplification in a 28-cycle PCR reaction using human β-globin primers. 20μl of PCR product was resolved on a 2% w/v agarose gel and visualised under UV light. **M:** 1kb DNA size marker (fragment sizes in bp). **Lane 1:** Blank **Lane 2:** Sterile water **Lane 3**: Blank **Lanes 4-15:** PGL samples. The 110bp β-globin product is indicated.

27 B

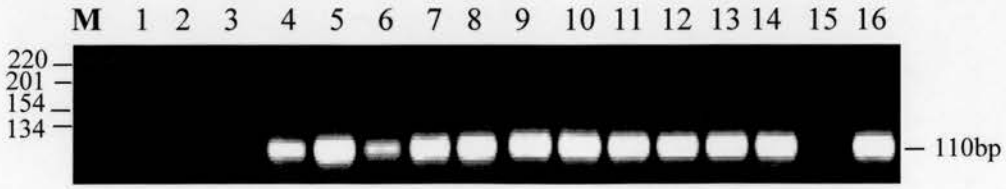

1μg of DNA prepared from PGL tissue was subjected to amplification in a 28-cycle PCR reaction using human β-globin primers. 20μl of PCR product was resolved on a 2% w/v agarose gel and visualised under UV light. **M:** 1kb DNA size marker (fragment sizes in bp). **Lane 1:** Blank **Lane 2:** Sterile water **Lane 3**: Blank **Lanes 4-14:** PGL samples **Lane 15:** Blank **Lane 16:** Lymphoblastoid cell line (LCL). The 110bp β-globin product is indicated.

Figure 28 A **Screening for amplifiable DNA in normal tonsil tissue preparations using human β-globin primers**

1μg of DNA prepared from tonsil tissue was subjected to amplification in a 28-cycle PCR reaction using human β-globin primers. 20μl of PCR product was resolved on a 2% w/v agarose gel and visualised under UV light. **M:** 1kb DNA size marker (fragment sizes in bp). **Lane 1-3:** Blank **Lane 4:** LCL **Lane 5:** Sterile water **Lanes 6-12:** Tonsils. The 110bp β-globin product is indicated.

Figure 28 B **Screening for amplifiable DNA in normal lymph node tissue preparations using human β-globin primers**

1μg of DNA prepared from lymph node tissue was subjected to amplification in a 28-cycle PCR reaction using human β-globin primers. 20μl of PCR product was resolved on a 2% w/v agarose gel and visualised under UV light. **M:** 1kb DNA size marker (fragment sizes in bp). **Lane 1:** Blank **Lane 2:** Lymphoblastoid cell line (LCL) **Lane 3:** Sterile water **Lanes 4-12:** Lymph nodes. The 110bp β-globin product is indicated.

3.6 Analysis of the structure and expression of the p53 gene family in PGL

In the immunosuppressed host, particularly in AIDS-NHL mutations in p53 occur at a frequency of around 38%, with a high percentage (60%) clustering in the AIDS-BL sub-type (Ballerini *et al.*, 1993).

The role of the p53 family members, p63 and p73 in AIDS-NHL is unknown. Somatic mutations in both genes are rare in human cancer (Ichimiya *et al.*, 1999; Ikawa *et al.*, 1999). However, transcriptional silencing of p73 by intragenic hypermethylation in a subset of haematological malignancies is consistent with a tumour suppressor role for this gene (Corn *et al.*, 1999). N-terminal variants of p63 (ΔN p63) are overexpressed in some squamous cancers indicating a potential oncogenic function for this gene (Yamaguchi *et al.*, 2000; Crook *et al.*, 2000).

Unlike p53, p63 and p73 are spliced at their C-termini, and expression shows tissue specificity. Similar to ΔN p63, N-terminal deleted variants of p73 lacking exon 2 (Δ2 p73) have recently been described in ovarian and breast cancer (Yang *et al.*, 1998; De Laurenzi *et al.*, 1998, Ng *et al.*, 2000; reviewed in section 1.4).

The objectives of the studies described in this chapter were as follows:

(i) To determine whether somatic mutations in p53 occur in PGL.

(ii) To define patterns of expression of p63 and p73 in normal lymphoid tissue and PGL.

(iii) To seek experimental evidence in support of a tumour suppressor role for p73 in PGL.

3.6.1 PCR without radioactive ^{33}P using primers for p53 exons 2-11

DNA from PGL and control tissue was initially amplified without any radioactivity using primers for p53 exons 2-11, to assess the specificity of the PCR, using the primers shown in Table 17, page 91. 500ng of DNA from each of the samples were amplified using the conditions specified in section 2.16.3. A nasopharyngeal carcinoma (NPC) cell line, C18, was used as a positive control for amplification and sterile distilled water as a control for PCR contamination.

Figures 29A to D are representative results of PCRs with primer pairs for exons 5,6,7, and 8 of p53. These experiments clearly demonstrated that the PCR is specific,

Figure 29 A PCR amplification of exon 5 of p53

500ng of DNA was subjected to amplification in a 35-cycle PCR reaction using the p53 exon 5 primer pair. 20μl of the PCR product was resolved on a 2% w/v agarose gel and the bands were visualised under UV light. **M:** 1kb DNA size marker (fragment sizes in bp) **Lanes 1-2:** Blank **Lane 3:** SDW **Lanes 4-12:** PGL samples **Lane 13:** C18. The exon 5 amplified fragment (211bp) is indicated.

Figure 29 B PCR amplification of exon 6 of p53

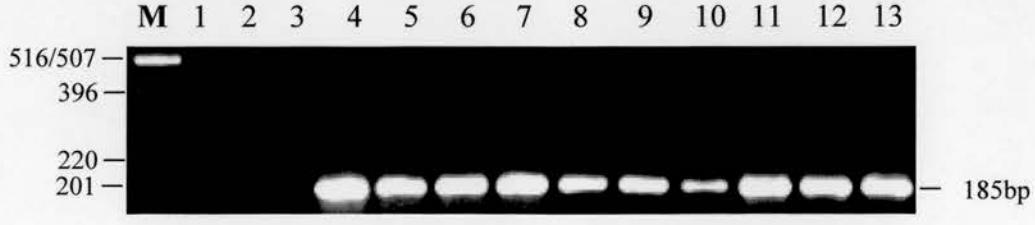

500ng of DNA was subjected to amplification in a 35-cycle PCR reaction using the p53 exon 6 primer pair. 20μl of the PCR product was resolved on a 2% w/v agarose gel and the bands were visualised under UV light. **M:** 1kb DNA size marker (fragment sizes in bp). **Lanes 1-2:** Blank **Lane 3:** SDW **Lanes 4-12:** PGL samples **Lane 13:** C18. The exon 6 amplified fragment (185bp) is indicated.

Figure 29 C **PCR amplification of exon 7 of p53**

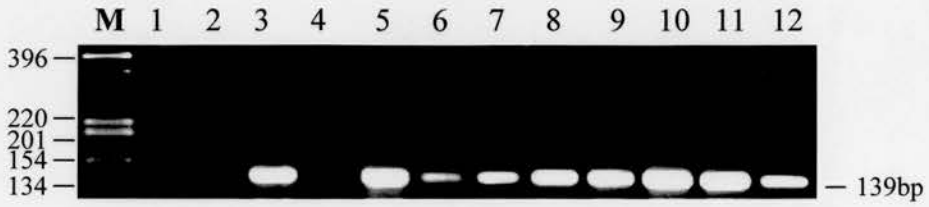

500ng of DNA was subjected to amplification in a 35-cycle PCR reaction using the p53 exon 7 primer pair. 20μl of the PCR product was resolved on a 2% w/v agarose gel and the bands were visualised under UV light. **M:** 1kb DNA size marker (fragment sizes in bp). **Lanes 1:** Blank **Lane 2:** SDW **Lane 3:** C18 **Lane 4:** Blank **Lane 5-12:** PGL samples. The exon 7 amplified fragment (139bp) is indicated.

Figure 29 D **PCR amplification of exon 8 of p53**

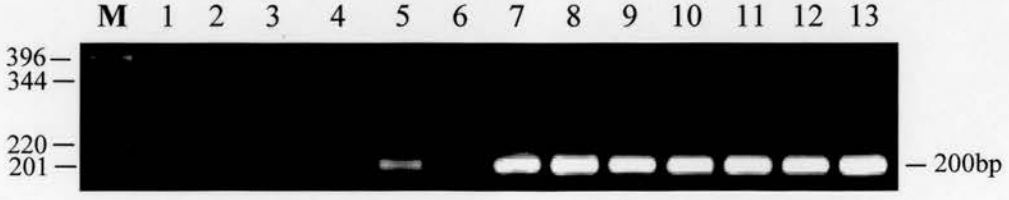

500ng of DNA was subjected to amplification in a 35-cycle PCR reaction using the p53 exon 8 primer pair. 20μl of the PCR product was resolved on a 2% w/v agarose gel and the bands were visualised under UV light. **M:** 1kb DNA size marker (fragment sizes in bp). **Lanes 1-2:** Blank **Lane 3:** SDW **Lanes 4-12:** PGL samples **Lane 13:** C18. The exon 8 amplified fragment (200bp) is indicated.

since only a single band was amplified with each primer pair (the sizes of the PCR products 211bp (exon 5), 185bp (exon 6), 139bp (exon 7) and 200bp (exon 8) are indicated in figures 29A to D respectively).

3.6.2 Comparison of radio-isotopes ^{32}P with ^{33}P for SSCP analysis

^{33}P is a low-energy beta emitter, and hence is safer to work with, when compared to ^{32}P. To assess whether the ^{33}P isotope was comparable to the ^{32}P isotope in detecting SSCP mobility shifts, the following experiment was carried out.

SSCP-PCR was performed with primers to amplify exon 5 of p53, on PGL samples, a positive control (C18) and a negative control (LCL), using both [$\alpha^{33}P$] dCTP and [$\alpha^{32}P$] dCTP.

Figures 30A and 30B are representative SSCP-PCR amplifications of exon 5 of p53 using ^{32}P and ^{33}P isotopes respectively. A positive SSCP shift observed with the positive control, C18, in figure 30A was similarly observed in figure 30B.

It was concluded from the above experiment that SSCP-PCR using ^{33}P as the radioisotope was as sensitive as ^{32}P in detecting mobility shifts.

Figure 30. SSCP analysis of exon 5 with radioactive phosphorus isotopes ^{32}P and ^{33}P

Figure 30 A SSCP analysis of exon 5 using [$\alpha^{32}P$] dCTP

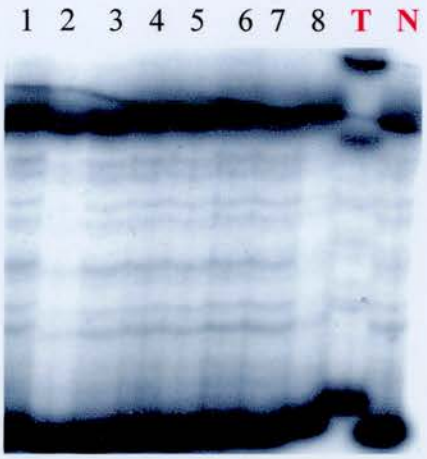

500ng of DNA was subjected to amplification in a 35-cycle PCR using primers PU5 and PD5 and 2μCi of [$\alpha^{32}P$] dCTP per reaction. Following amplification, 3μl of radiolabelled PCR product was mixed with 3μl of loading dye. The samples were heat-denatured at 94°C for 5 minutes and resolved on a 6% polyacrylamide (PAGE) gel with 10% glycerol. After being dried the gel was exposed to Kodak XR film at room temperature for 24 hours with intensifying screens. **Lanes 1-8:** PGL samples **T:** C18 (duplication of codons 149-153, codon 154 deleted) **N:** LCL.

Figure 30 B SSCP analysis of exon 5 using [$\alpha^{33}P$] dCTP

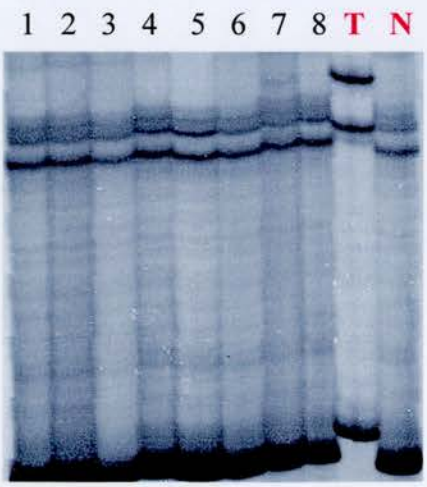

500ng of DNA was subjected to amplification in a 35-cycle PCR using primers PU5 and PD5 and 10μCi of [$\alpha^{33}P$] dCTP per reaction. Following amplification 3μl of radiolabelled PCR product was mixed with 3μl of loading dye. The samples were heat-denatured at 94°C for 5 minutes and resolved on a 6% polyacrylamide (PAGE) gel with 10% glycerol. After being dried the gel was exposed to Kodak XR film at -70°C for 24 hours with intensifying screens. **Lanes 1-8:** PGL samples **T:** C18 (duplication of codons 149-153, codon 154 deleted) **N:** LCL.

3.6.3 SSCP mobility shifts are detected in PGL tissue

The presence of p53 mutations in the current series of PGL was sought using SSCP analysis of each coding exon of the gene (exons 2-11) and genomic DNA as a substrate. The amplification reactions included 10μCi of [α^{33}P] dCTP. The sequences of the primer pairs are given in Table 17, page 91. Positive and negative controls are shown in Table 20, page 93. Representative SSCP autoradiographs for each analysed exon are presented in Figures 31 to 39. Samples with altered migration are indicated in blue. Positive and negative controls are indicated in red.

Mobility shifts suggestive of sequence changes were detected in 6/23 (26%) analysed DNA samples from HIV-infected individuals with PGL. These comprised 5 PGL samples in exon 7 (figure 35 lanes 1,9,11,12 and 21), and 1 PGL sample in exon 10 (figure 38 lane 4). Abnormal migration was also detected in one tonsil (6.3%) from an HIV-uninfected individual in exon 6 (figure 34 lane 13). In the case of exon 2/3 (figure 31), two distinct patterns of migration were observed, suggestive of a polymorphism, which occurs in exon 2 (GAC>GAT) (Ahuja *et al.*, 1990). Samples in lanes 2,5,7,8,10,11, and 12 showed a pattern of migration that differed from those samples in lanes 1,3,4, and 6. Normal migration patterns in all the other exons were observed in the remaining PGL samples and controls.

3.6.4 Amplification of DNA using a high-fidelity polymerase- *Pfx*

Each DNA sample exhibiting a mobility shift was subjected to re-amplification of the exon containing the suggested mutation, with a high fidelity thermostable DNA polymerase, *Pfx*, since it has an error rate ~26 times lower than *Taq* (Lackovich *et al.*, 2001). The error rate of *Taq*, *Pfu* and *Pfx* polymerases is shown in Table 27.

Table 27

Error-rates of *Taq*, *Pfu* and *Pfx* polymerase

Polymerase	Error-rate (x 10^{-6})	Relative fidelity
Taq	42 ± 19	1
Pfu	3 ± 1	14
Pfx	1.6 ± 0.5	26

Adapted from Lackovich *et al.*, 2001 and Takagi *et al.*, 1997

Figure 31. SSCP analysis of exon 2/3 of p53

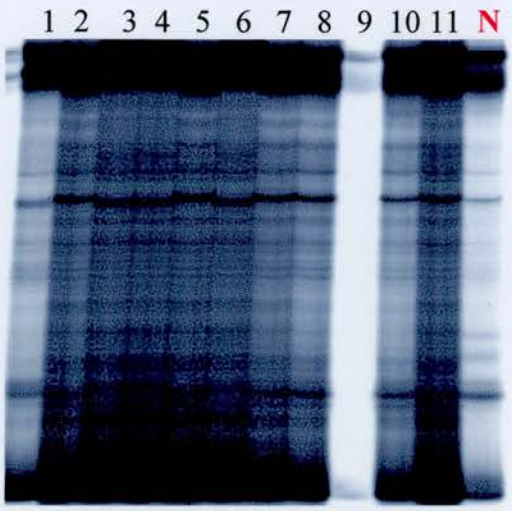

500ng of DNA was subjected to amplification using primers PU2 and PD3. 3μl of radiolabelled PCR product was mixed with 3μl of loading dye. The samples were heat-denatured and resolved on a 6% polyacrylamide (PAGE) gel with 10% glycerol. The dried gel was exposed to Kodak XR film at -70°C for 2-3 days. **Lanes 1-8:** PGL samples **Lane 9:** Blank **Lanes 10-11:** PGL samples **N:** Negative control.

Figure 32. SSCP analysis of exon 4 of p53

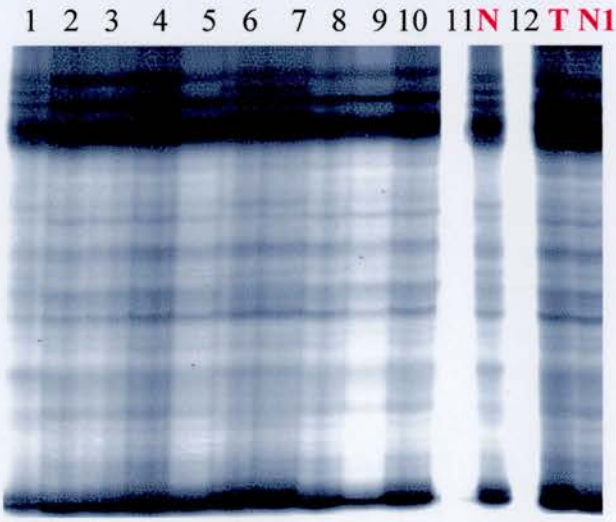

500ng of DNA was subjected to amplification using primers PU4 and PD4. 3μl of radiolabelled PCR product was mixed with 3μl of loading dye. The samples were heat-denatured and resolved on a 6% polyacrylamide (PAGE) gel with 10% glycerol. The dried gel was exposed to Kodak XR film at -70°C for 2-3 days. **Lanes 1-10:** PGL samples **Lanes 11&12:** Blank **T:** Tumour control (arginine at codon 72) **N:** Normal control (arginine at codon 72) **N1:** Normal control (proline at codon 72).

Figure 33. SSCP analysis of exon 5 of p53

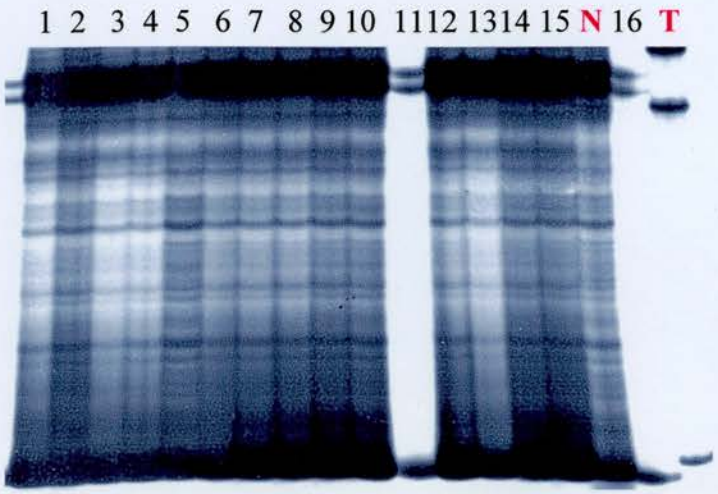

500ng of DNA was subjected to amplification using primers PU5 and PD5. 3µl of radiolabelled PCR product was mixed with 3µl of loading dye. The samples were heat-denatured and resolved on a 6% polyacrylamide (PAGE) gel with 10% glycerol. The dried gel was exposed to Kodak XR film at -70°C for 2-3 days. **Lanes 1-6:** Tonsil controls. **Lane 7-15:** Lymph node controls **Lane 16:** Blank **T:** Tumour control C18 (duplication of codons 149-153, codon 154 deleted); **N:** Normal control 28697N.

Figure 34. SSCP analysis of exon 6 of p53

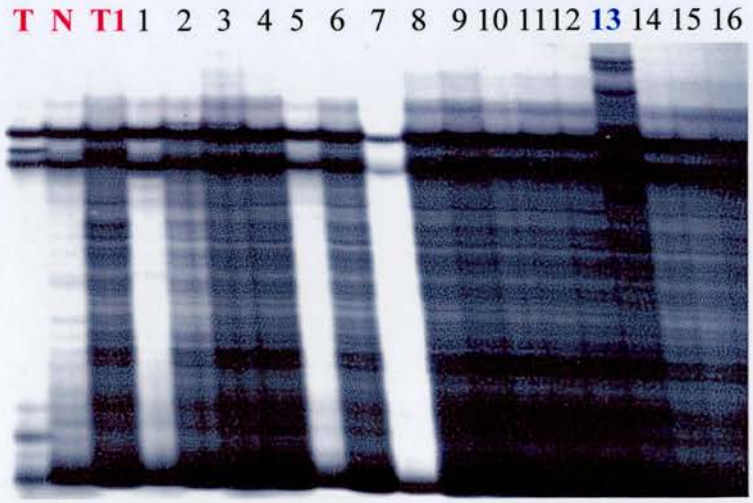

500ng of DNA was subjected to amplification using primers PU6 and PD6. 3µl of radiolabelled PCR product was mixed with 3µl of loading dye. The samples were heat-denatured and resolved on a 6% polyacrylamide (PAGE) gel with 10% glycerol. The dried gel was exposed to Kodak XR film at -70°C for 2-3 days. **Lanes 1-9:** Lymph node controls **Lanes 10-16:** Tonsil controls **Lane 13:** Abnormally migrating sample (T6) **T:** Tumour control 03157T (codon 213, CGA-TGA); **T1:** Tumour control 13758T (codon 202, CGT-CAT) **N:** Normal control 03157N.

Figure 35. **SSCP analysis of exon 7 of p53**

500ng of DNA was subjected to amplification using primers PU7 and PD7. 3μl of radiolabelled PCR product was mixed with 3μl of loading dye. The samples were heat-denatured and resolved on a 6% polyacrylamide (PAGE) gel with 10% glycerol. The dried gel was exposed to Kodak XR film at -70°C for 2-3 days. **Lanes 1-21:** PGL samples **Lanes 1,9,11,12 and 21:** Abnormally migrating samples (LN1,9,15,16 and 20 respectively) **Lane 22:** Blank **T:** Tumour control 00997T (codon 248, CGG-TGG); **N:** Normal control 00997N.

Figure 36. **SSCP analysis of exon 8 of p53**

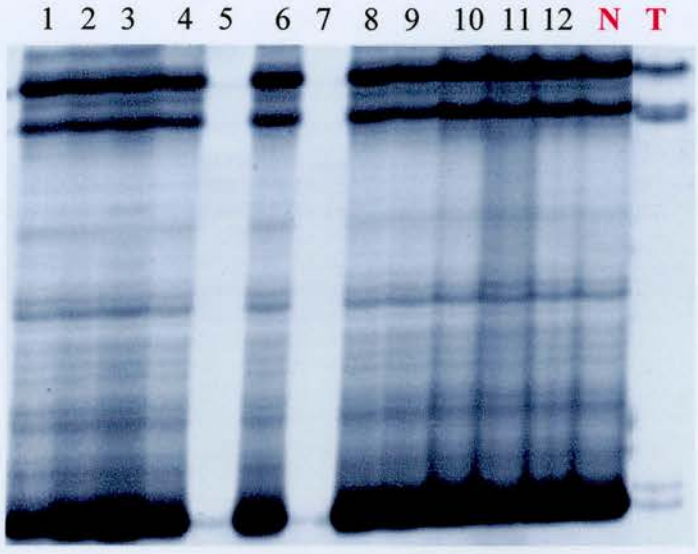

500ng of DNA was subjected to amplification using primers PU8 and PD8. 3μl of radiolabelled PCR product was mixed with 3μl of loading dye. The samples were heat-denatured and resolved on a 6% polyacrylamide (PAGE) gel with 10% glycerol. The dried gel was exposed to Kodak XR film at -70°C for 2-3 days. **Lanes 1-4,6 & 8-12:** PGL samples **Lanes 5& 7:** Blank **T:** Tumour control 05747T (codon 281, GAC-AAC); **N:** Normal control 05747N.

Figure 37. **SSCP analysis of exon 9 of p53**

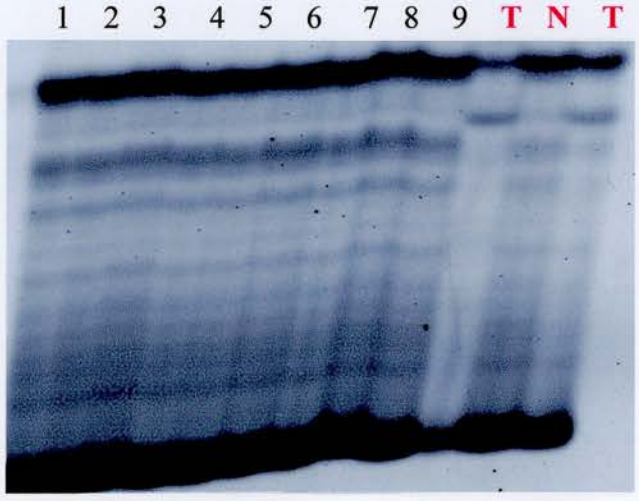

500ng of DNA was subjected to amplification using primers PU9 and PD9. 3μl of radiolabelled PCR product was mixed with 3μl of loading dye. The samples were heat-denatured and resolved on a 6% polyacrylamide (PAGE) gel with 10% glycerol. The dried gel was exposed to Kodak XR film at -70°C for 2-3 days. **Lanes 1-9:** PGL samples **T:** Tumour controls C17 and C18; **N:** Normal control, DNA from fibroblasts.

Figure 38. **SSCP analysis of exon 10 of p53**

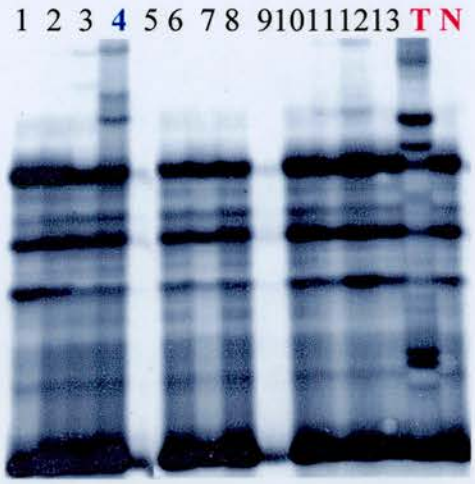

500ng of DNA was subjected to amplification using primers PU10 and PD10. 3μl of radiolabelled PCR product was mixed with 3μl of loading dye. The samples were heat-denatured and resolved on a 6% polyacrylamide (PAGE) gel with 10% glycerol. The dried gel was exposed to Kodak XR film at -70°C for 2-3 days. **Lanes 1-3,4,6-8,10-13:** PGL samples **Lanes 5 and 9:** Blank **Lane 4:** Abnormally migrating sample (LN5) **T:** Tumour control, C17; **N:** Normal control, DNA from fibroblasts.

Figure 39. **SSCP analysis of exon 11 of p53**

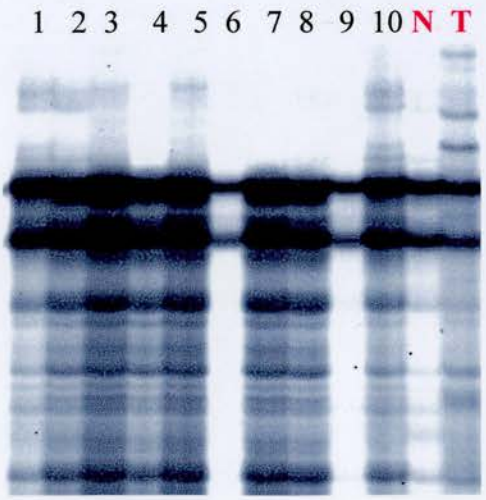

500ng of DNA was subjected to amplification using primers PU11 and PD11. 3μl of radiolabelled PCR product was mixed with 3μl of loading dye. The samples were heat-denatured and resolved on a 6% polyacrylamide (PAGE) gel with 10% glycerol. The dried gel was exposed to Kodak XR film at -70°C for 2-3 days. **Lanes 1-10:** PGL samples **T:** Tumour control, C17; **N:** Normal control, DNA from fibroblasts.

3.6.4.1 Optimisation of annealing temperature using *Pfx* polymerase

These studies were carried out to establish the optimal annealing temperature for the re-amplification of DNA, using *Pfx* polymerase, which was to be subsequently cloned and sequenced. 300ng of DNA was amplified in a 35-cycle PCR reaction containing $MgSO_4$, *Pfx* and primer at concentrations recommended by the manufacturer (Life Technologies, see section 2.8.6). The minimum recommended temperature was 55°C. PCR was carried out using primers for exon 7, at annealing temperatures of 55-63°C, in one-degree increments, as shown in figure 40 (lanes 2 to 10 respectively). The efficiency of amplification and quantity of the product (as judged by the intensity of the bands on the gel) was similar at temperatures between 61-63°C, whereas at temperatures below 61°C, amplification specificity was compromised and non-specific bands were observed. The optimum annealing temperature was determined to be 63°C (figure 40, lane 10). The optimum annealing temperature for the other primer pairs was established in a similar fashion, and was found to be 66°C for exon 2/3 and exon 10 primer pairs.

Figure 41 is a representative result of PGL samples amplified using primers for exon 7 of p53 and *Pfx* polymerase.

3.6.5 p53 mutations are detected in PGL

Pfx-amplified PCR fragments were either gel-purified or ligated directly into pCR®-BLUNT (2.17.1.3). Following restriction enzyme digest of individual clones, 20-30 clones that contained an insert of the right size were sequenced using the LICOR 4000L automated sequencer (MWG Biotech, Milton Keynes, UK), and the Sequitherm Excel™ II kit (Cambio, Cambridge, UK) using M13 forward and reverse primers. Proposed mutations were confirmed by sequencing both DNA strands as well as re-amplification of the DNA in an independent PCR reaction, followed by cloning and sequencing (Table 28, page 138, and figure 42). No sequence changes were observed in the exon 2/3 fragments with altered mobility shifts. It was thus concluded that these shifts were an artefact of SSCP analysis. Mutations were however identified in each of the 6 PGL DNA samples and 1 HIV-uninfected tonsil that had mobility shifts by SSCP, which are represented in Figures 42 A to G, pages 139-140 and Table 28, page 138. Nucleotide changes are indicated in red.

Figure 40. Optimisation of annealing temperature using *Pfx* polymerase

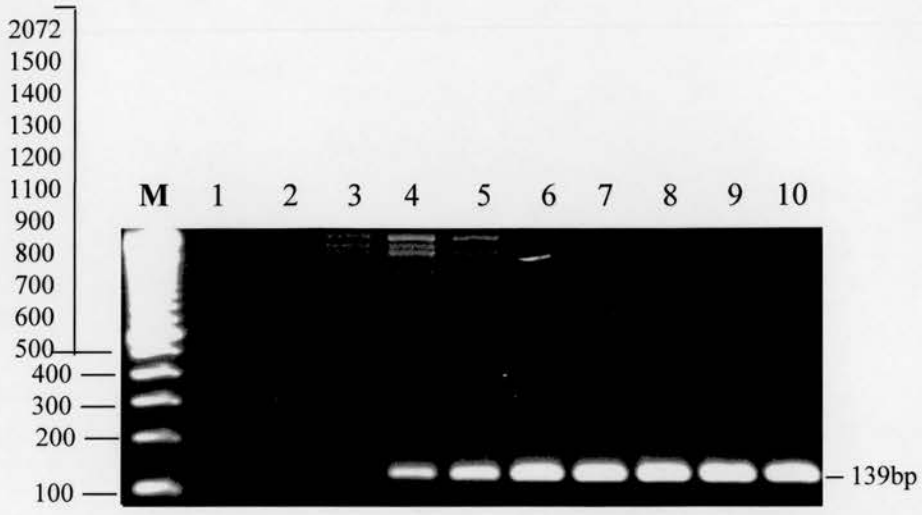

300ng of DNA was subjected to amplification in a 35-cycle PCR using exon 7 primers and *Pfx* polymerase. The DNA was subjected to amplification using annealing temperatures between 55°C and 63°C, in one-degree increments. 20µl of PCR product was resolved on a 2% w/v agarose gel and the bands were visualised under UV light. **M:** 100bp DNA size marker (fragment sizes in bp). **Lane 1:** SDW **Lanes 2-10:** 55°C - 63°C respectively. The exon 7 amplified product (139bp) is indicated.

Figure 41. PCR amplification of exon 7 using *Pfx* polymerase

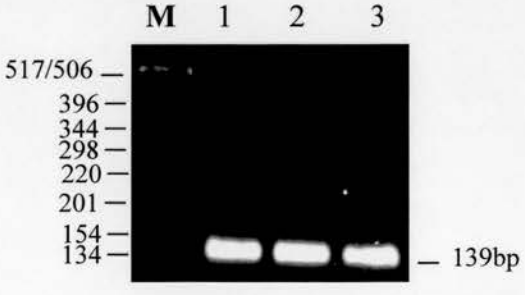

300ng of DNA was subjected to amplification in a 35-cycle PCR using primers for exon 7 and *Pfx* polymerase. 20µl of PCR product was resolved on a 2% w/v agarose gel and the bands were visualised under UV light. **M:** 1kb DNA size marker (fragment sizes in bp). **Lanes 1-3:** PGL samples (LN1, LN9 and LN15 respectively). The exon 7 amplified product (139bp) is indicated.

Missense mutations were detected in cases LN 1 (codon 229), LN 9 (codon 242), LN 15 (codon 238) and LN 16 (codon 249) in exon 7. A silent mutation was observed in codon 245 (exon 7) in case LN 24. In case LN 5, deletion of a guanine residue in codon 361 (exon 10) was observed, resulting in a shift in the reading frame by -1. Although the nucleotide deletion resulted in no change in the amino acid at codon 361, a termination codon (TGA) observed in codon 369 could result in premature termination of translation. In the HIV-uninfected tonsil (T6) a silent mutation was detected in exon 6, codon 222. The nucleotide substitutions and amino acid changes are shown in Table 28. Although the p53 mutants described in this study have not been functionally characterised, the phenotype of mutants involving the same codon but different amino acid substitutions have also been indicated. The nature of nucleotide substitutions was a transversion in case numbers 15, 16, and T6 and transition in case numbers 1,9 and 24. All the mutations occur within evolutionarily conserved codons and codon 249 (LN 16) is considered to be a mutational hot spot.

Table 28
Summary of sequence analysis of *p53*

Case No.	Exon	Codon	Nucleotide substitution	Type of mutation	Amino acid change	Phenotype**	
						Transdom.	Transact.
LN 1	7	229	TGT → CGT	Missense (Transition)	C → R	nk	nk
LN 9	7	242	TGC → CGC	Missense (Transition)	C → R	242Y[1] nk	242Y[1] No
LN 15	7	238	TGT → GGT	Missense (Transversion)	C → G	Δ238-239[2] Yes	238R/238W[1] No
LN 16	7	249	AGG → ATG	Missense (Transversion)	R → M	249S Yes[2, 3]	249S No[3]
LN 24	7	245	GGC → GGT	Silent (Transition)	G → G	NA	NA
LN 5	10	361	GGG→ GGΔG	Nonsense*		nk	nk
T6	6	222	CCG → CCT	Silent (Transversion)	P → P	NA	NA

T= normal tonsil; LN = lymph node from PGL; *, Termination (TGA) codon 369, exon 11; C, Cysteine; R, Arginine; G, Glycine; M, Methionine; P, Proline; Y, Tyrosine; S, serine; W, Tryptophan; **, Transdominance tested in yeast, and transactivation of the *waf1* or h*mdm2* promoter; Transdom., transdominant; Transact., transactivation; nk, not known; NA, not applicable; [1], Campomenosi *et al.*, 2001; [2], Marutani *et al.*, 1999; [3], Crook *et al.*, 1994

Figure 42. Sequence analysis of p53

Figure 42 A

Sequence of LN 1

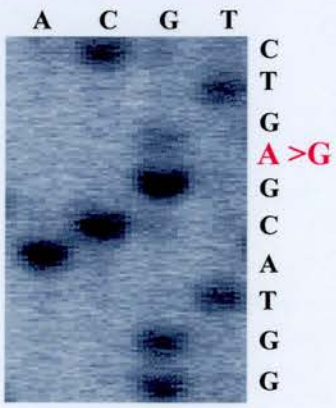

TGT → CGT

(anti-sense shown)

Figure 42 B

Sequence of LN 9

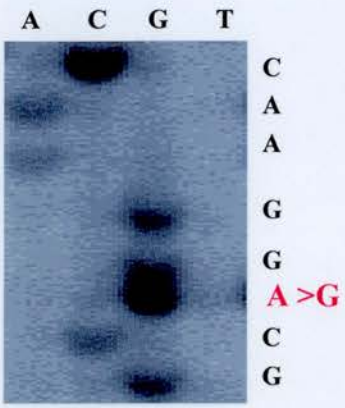

TGC → CGC

(anti-sense shown)

Figure 42 C

Sequence of LN 15

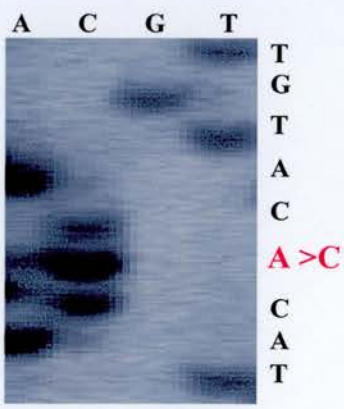

TGT → GGT

(anti-sense shown)

Figure 42 D

Sequence of LN 16

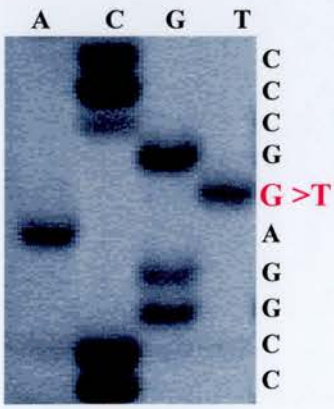

AGG → ATG

(sense shown)

Figure 42 E

Sequence of LN 5

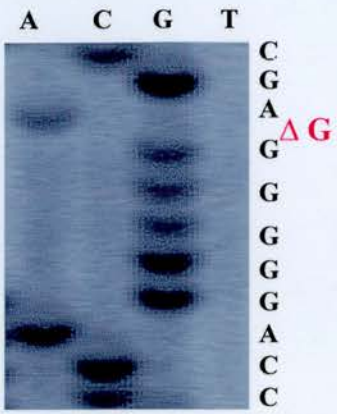

GGG→ GGΔG

(sense shown)

Figure 42 F

Sequence of LN 24

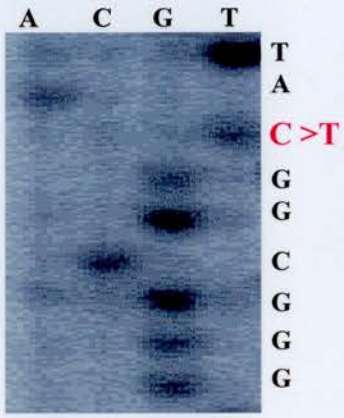

GGC→ GGT

(sense shown)

Figure 42 G

Sequence of T6

CCG→ CCT

(anti-sense shown)

Figure 42. Sequence analysis of *p53*. Samples that showed a positive shift on SSCP analysis were re-amplified with *Pfx* polymerase, cloned into plasmid vectors and sequenced using LICOR 4000L automated sequencer (MWG Biotech, Milton Keynes, UK), and the Sequitherm Excel™ II kit (Cambio, Cambridge, UK). Labelled M13 forward and reverse primers were used. Nucleotide substitutions are indicated in red.

Figure 42 A: Sequence of LN 1 (lane 1, figure 35, exon 7)

Figure 42 B: Sequence of LN 9 (lane 9, figure 35, exon 7)

Figure 42 C: Sequence of LN 15 (lane 11, figure 35, exon 7)

Figure 42 D: Sequence of LN 16 (lane 12, figure 35, exon 7)

Figure 42 E: Sequence of LN 5 (lane 4, figure 38, exon 10)

Figure 42 F: Sequence of LN 24 (lane 21, figure 35, exon 7)

Figure 42 G: Sequence of T6 (lane 16, figure 34, exon 6)

3.6.6 Analysis of p73 expression in HIV-PGL and HIV-uninfected tissue

3.6.6.1 Multiple C-terminal isoforms of p73 are expressed in PGL

RT-PCR was used to analyse expression of the p73 gene using primers located in exon 10 (sense) and exon 14 (antisense) of the gene (Table 11, page 80). The location of the primers allowed for the detection of the multiple C-terminal isoforms, of which 6 have been reported to date (De Laurenzi *et al.*, 1998, 1999). Following amplification, RT-PCR products were hybridised to a [γ^{32}P] ATP-labelled p73 oligonucleotide located in exon 10.

Expression of p73 was detected in 19/19 HIV-infected PGL tissue and in 9 of 15 HIV uninfected tonsils and lymph nodes (figure 43A, lanes 3,4,6,7,8,9,10,13 and 14). 8 individual bands were detected in the PGL samples, whereas only 4 bands were detected in the normal lymph nodes and tonsils (figure 43B). Note that the pattern of expression in the vulval cancers (positive controls) is different to that observed in the HIV-infected and uninfected lymphoid tissue (figure 43C).

3.6.6.2 Detection of the alpha and beta isoforms of p73 using colony hybridisation and sequencing

To identify the RT-PCR amplified products (see above) and determine whether the transcripts were p73-specific, colony hybridisation using a [γ^{32}P] ATP-labelled p73 oligonucleotide (Table 11, page 80) was carried out (see section 2.17.2). DNA from the clones that hybridised with the probe was purified (see section 2.17.3) and sequenced (see section 2.18).

Of the 50 clones screened, 6 hybridised to the p73 probe (figure 44, A-F). The remaining 44 clones did not hybridise to the probe indicating absence of a p73-specific product. On subsequent sequencing of these 6 clones, 5 were identified as the alpha transcript (535bp) of the p73 gene (figure 45, lanes 2,4,6,8 and 10), and 1 as the beta transcript (440bp) (figure 45, lane 12).

Figure 43. Detection of p73 transcripts in HIV-PGL and HIV-uninfected tissue

43 A

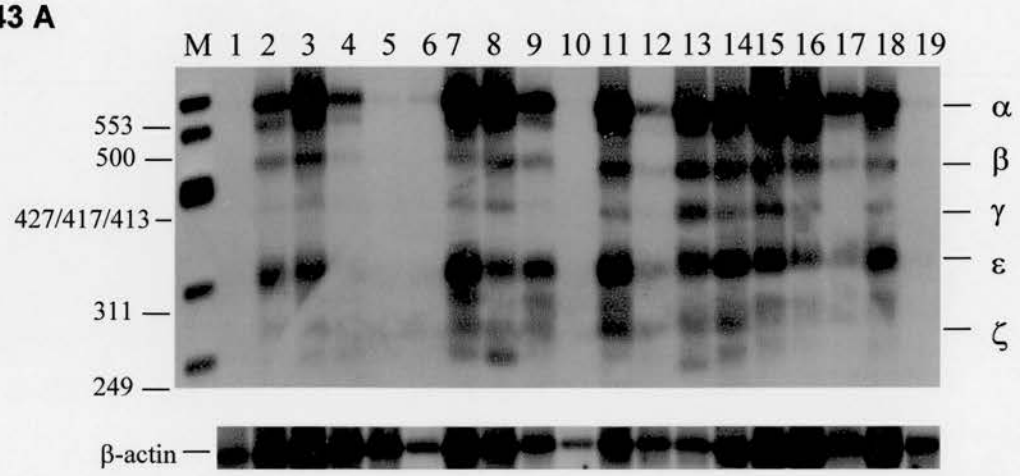

43 B

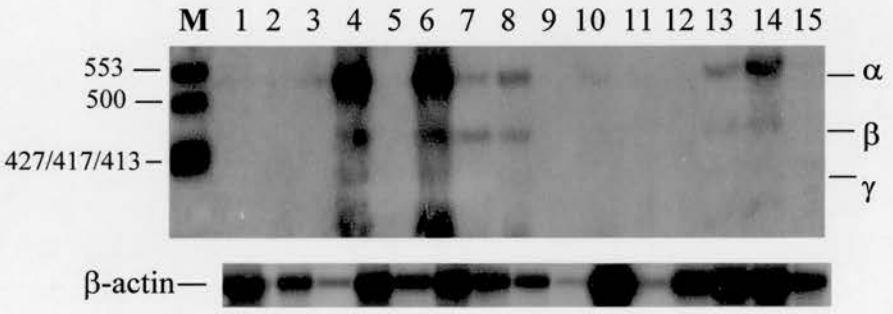

43 C

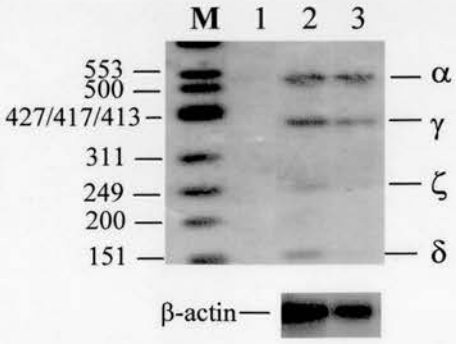

A 535bp region of p73 was amplified from cDNA in a 35-cycle RT-PCR reaction using p73 primers. 20μl of PCR product was resolved on a 3% w/v agarose gel run slowly for 6 hours at 30mA. PCR products were transferred to Hybond N^+ membrane and probed with a ^{32}P-labelled oligonucleotide located in exon 10. **M:** *Hinf1* digested ϕX-174 DNA size marker (fragment sizes in bp). The presence of amplifiable cDNA is indicated by amplification of β-actin. **Figure 43A Lanes 1-19:** PGL samples. **Figure 43B Lanes 1-7:** HIV-uninfected tonsils. **Lanes 8-15:** HIV-uninfected lymph nodes. **Figure 43C Lane 1:** Sterile distilled water. **Lanes 2 and 3:** cDNA from vulval cancers (T1 and T2 respectively).

Figure 44. Colony hybridisation to identify p73 transcripts

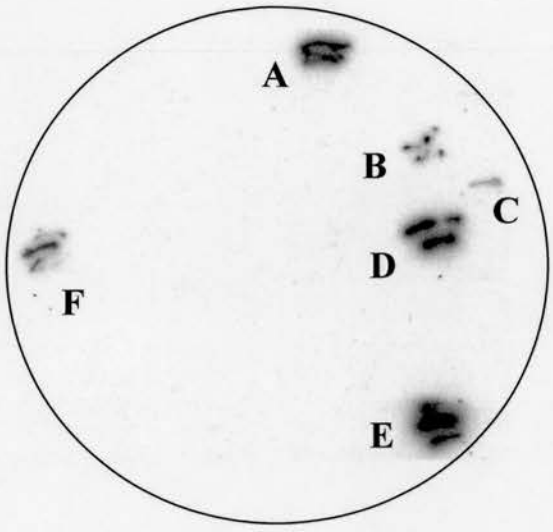

The p73 RT-PCR product was cloned using the TOPO TA® Cloning Kit and the colonies recovered were screened using a [γ^{32}P] ATP-labelled p73 oligonucleotide located in exon 10. **A-F:** Colonies that hybridised with the [γ^{32}P] ATP-labelled p73 oligonucleotide.

Figure 45. Restriction enzyme digest of clones that hybridised with the [γ^{32}P] ATP-labelled p73 oligonucleotide

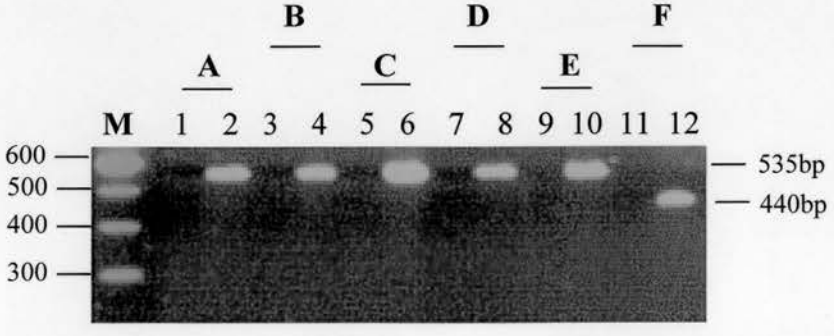

Plasmid DNA extracted from the colonies that hybridised with the ^{32}P-labelled p73 oligonucleotide were digested with the restriction enzyme *EcoRI* for 3 hours at 37°C. 20μl of the digested DNA was resolved on a 2% w/v agarose gel and the bands visualised under UV light. **M:** A 100bp DNA size marker (fragment sizes in bp). **Lanes 1,3,5,7,9 and 11:** Undigested DNA. **Lanes 2,4,6,8,10 and 12:** DNA digested with *EcoR1*. The clones that hybridised with the ^{32}P-labelled p73 oligonucleotide (**A-F**) are indicated. The α fragment (535bp) and the β fragment (440bp) are indicated. Plasmid vector not shown.

3.6.6.3 Detection of p73 isoforms using radioactive PCR and sequencing

Radioactive PCR, using [α^{32}P] dCTP (2.18.2) and primers specified in Table 11 (page 80) was performed to further identify those transcripts that could not be detected by the colony hybridisation technique. Individual DNA fragments excised from the gel, were re-amplified in a 40-cycle RT-PCR reaction and ligated into a TOPO TA vector (see section 2.17.1.2). Clones representing each DNA fragment were sequenced and 5 transcripts were identified, which were the α (535bp), β (440bp), γ (386bp), ε (291bp) and ζ (249bp) transcripts (figure 46). Sequencing of the other cloned fragments revealed that they did not derive from the p73 gene.

3.6.6.4 Δ2 isoforms of p73 are expressed in both HIV-PGL and normal lymph nodes and tonsils

RT-PCR to detect p73 variants that lack exon 2 was performed using primers that amplify a 344bp region of p73 (Ng *et al.*, 2000). The sense primer was located in exon 1 and the antisense primer in exon 4 (Table 11, page 80). Following amplification RT-PCR products were hybridised to a [γ^{32}P] ATP-labelled p73 oligonucleotide (Table 11, page 80) located in exon 3.

The full-length transcript was not detectable in any of the samples analysed. A smaller fragment (242bp), representing the Δ2 p73 variant was detected in 16/16 HIV-PGL tissue (figure 47A) and in 8/15 HIV-uninfected samples (figure 47B). RT-PCR products were re-hybridised to a probe in exon 2 (Table 11, page 80). The absence of detectable product confirmed that only the Δ2 p73 variant was expressed in all samples analysed.

3.6.6.5 Hypermethylation of p73 is not detectable in PGL

To assess whether p73 is silenced by hypermethylation in HIV-infected individuals with PGL, which might suggest a tumour suppressor role for this gene, methylation-specific PCR (MSP) was performed using primers specific for the methylated and unmethylated reactions (Table 23, page 104). Methylated and unmethylated human genomic DNA (Intergen, U.S.A) was used as positive and negative controls respectively. In addition, Burkitt's lymphoma (BL) cell lines, Raji and Namalwa were also analysed, which have documented hypermethylation in the p16^{INK4a} and

Figure 46. Radioactive RT-PCR to detect splice variants of p73

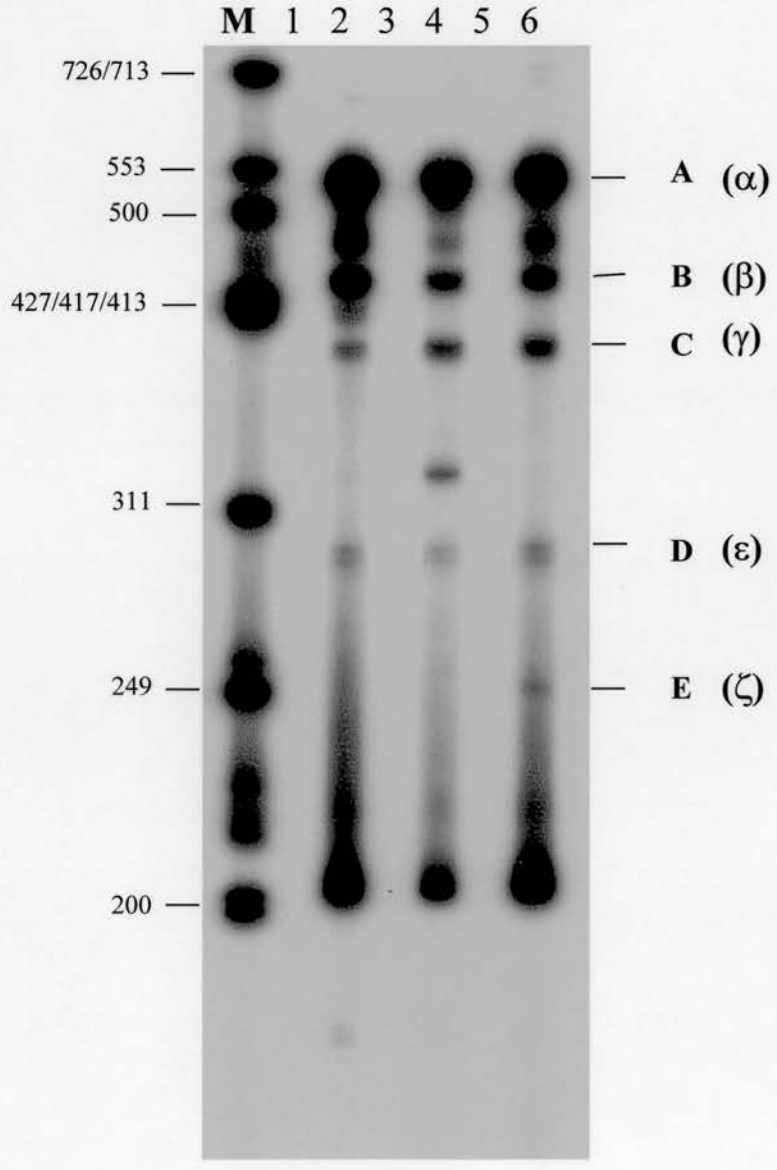

cDNA synthesised from 40ng of RNA from HIV-infected PGL tissue was subjected to amplification in a 40-cycle p73 RT-PCR, and 10μCi of [α^{32}P] dCTP was included in each reaction. 3μl of radiolabelled PCR product was mixed with 3μl of loading dye, containing formamide, heat-denatured and resolved on a 6% denaturing polyacrylamide gel. **M:** *Hinf1* digested ϕX-174 DNA size marker (fragment sizes in bp). **Lanes 1,3 and 5:** Blank. **Lanes 2,4 and 6:** HIV-infected PGL tissue.

Upon sequencing, bands A-E were identified as **A:** α transcript (535bp), **B:** β transcript (440bp), **C:** γ transcript (386bp), **D:** ε transcript (291bp), **F:** ζ transcript (249bp) respectively.

Figure 47. Detection of the Δ2 p73 variant in HIV-PGL and HIV-uninfected tissue

47 A

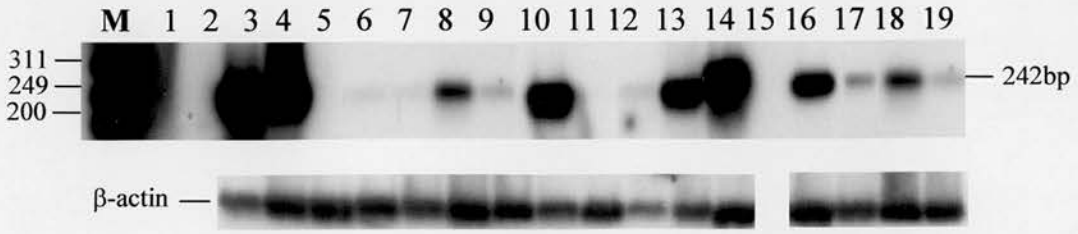

47 B

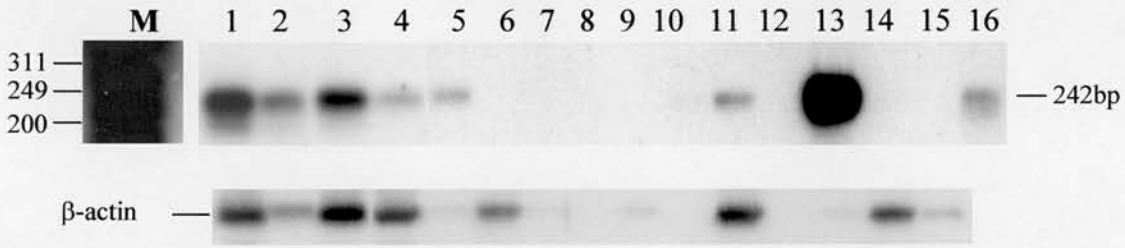

cDNA synthesised from 40ng of RNA was subjected to amplification in a 35-cycle RT-PCR reaction using primers for the detection of the Δ2 p73. 20μl of the RT-PCR product was resolved on a 2% w/v agarose gel, Southern transferred to a Hybond N^+ membrane and hybridised with a ^{32}P-labelled p73 oligonucleotide located in exon 3. **M:** *Hinf1* digested ϕX-174 DNA size marker (fragment sizes in bp). The presence of amplifiable cDNA is indicated by amplification of β-actin. **Figure 47A Lane 1:** SDW **Lane 2&15:** Blank **Lanes 3-18:** PGL samples.
Figure 47B Top panel (96 hour exposure) Lanes 1-7: HIV-uninfected tonsils **Lanes 8-15:** HIV-uninfected lymph nodes **Lane 16:** Vulval squamous carcinoma (5T). The Δ2 variant of p73 (242bp) is indicated.

$p15^{INK4b}$ genes (Klangby *et al.*, 1998 and see Table 29). The methylation status of the p73 gene in these cell lines was assessed in this study.

Methylation of the p73 gene was not found in any of the HIV-infected PGL samples. Methylation analysis of the BL cell lines indicated complete methylation of the Namalwa cell line (figure 48, lane 23). The Raji cell line contained both methylated as well as unmethylated copies of the gene (Table 29), but this cell line was not included for MSP analysis in this experiment. Amplification of the positive control methylated DNA (figure 48, lane 22) with only the methylated primer set, and the unmethylated control DNA with the unmethylated primer set (figure 48, lane 21), confirmed the specificity of the PCR. These results suggest that hypermethylation of p73 is not characteristic of HIV-infected PGL.

Table 29

Methylation status of $p16^{INK4a}$, $p15^{INK4b}$ and p73 in BL cell lines Raji and Namalwa

BL cell line	$p16^{INK4a}$	$p15^{INK4b}$	p73[1]
Raji	+	(+)	(+)
Namalwa	+	(+)	+

BL, Burkitt's lymphoma; +, complete methylation; (+), partial methylation; [1], methylation status assessed in this study

3.6.7 Analysis of p63 expression in HIV-PGL and HIV-uninfected tissue

3.6.7.1 TA is the predominant isoform of p63 expressed in lymphoid tissue

RT-PCR was performed to assess expression of TA p63 in lymph node and tonsil tissue. These primers amplify a 629bp fragment, with the sense primer located in exon 2 and the antisense primer in exon 5 (Table 11). Following amplification, RT-PCR products were hybridised to a $[\gamma^{32}P]$ ATP-labelled p63 oligonucleotide (Table 10) located in exon 3.

Expression of TA p63 was observed in 14 of 19 (73%) PGL samples (figure 49A, lanes 2-6,8,9, and 12-17 and figure 49B, lane 2). The transcript was also detected in 1 tonsil (figure 49B lane 10) and in 5 of 9 (55%) HIV-uninfected lymph nodes (figure 49B lanes 12,14 and 16-18).

Figure 48. Methylation status of the p73 gene in HIV-PGL

40 ng of genomic DNA modified by sodium bisulphite was used in a 35-cycle MSP reaction to amplify 60bp and 69bp fragments of the p73 gene, using primers specific for the methylated and unmethylated reactions respectively. 20μl of the PCR product was resolved on a 3% w/v agarose gel and the bands were visualised under UV light. **L:** A 100bp DNA size marker (fragment sizes in bp). **U:** Unmethylated DNA. **M:** Methylated DNA.
Lanes 1 to 20: PGL samples. **Lane 21:** Unmethylated control DNA. **Lane 22:** Methylated control DNA. **Lane 23:** Namalwa cell line. The unmethylated (69bp) and methylated (60bp) products are indicated.

Figure 49. Detection of TA p63 transcripts in HIV-PGL and HIV-uninfected tissue

49 A

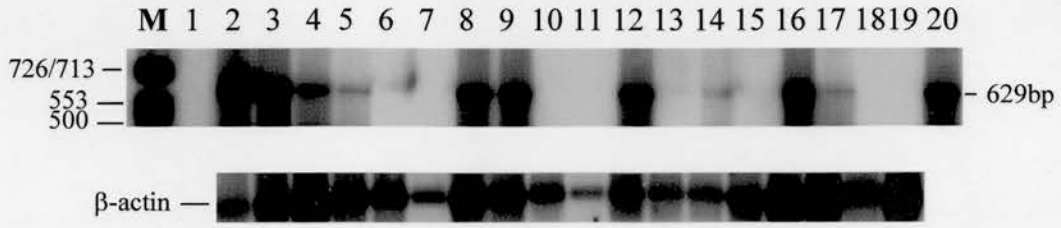

49 B

A 629bp region of p63, specific for the TA isoform, was amplified from cDNA in a 30-cycle RT-PCR reaction. 20μl of PCR product was resolved on a 2% w/v agarose gel. PCR products were transferred to Hybond N^+ membrane and probed with a ^{32}P-labelled oligonucleotide located in exon 3. **M:** *Hinf1* digested ϕX-174 DNA size marker (fragment sizes in bp). The presence of amplifiable cDNA is indicated by the amplification of β-actin. The TA p63 RT-PCR product (629bp) is indicated.

Figure 49 A

Lane 1: Blank **Lanes 2-19:** PGL samples **Lane 20:** cDNA from lymphoblastoid cell line (PD-LCL).

Figure 49 B

Lane 1: Blank **Lane 2:** PGL sample **Lane 3:** Sterile distilled water **Lanes 4-10:** HIV-uninfected tonsils **Lanes 11-19:** HIV-uninfected lymph nodes.

3.6.7.2 The ΔN isoform of p63 is expressed only in HIV-uninfected tonsils

RT-PCR was performed to analyse the expression of ΔN p63. Primers were designed to amplify a 440bp region, with the sense primer located in exon 3' and the antisense primer located in exon 5 (Table 11, page 80). Following amplification, RT-PCR products were hybridised to a [γ^{32}P] ATP-labelled p63 oligonucleotide (Table 11, page 80) located in exon 4.

Expression of ΔN p63 was only observed in the HIV-uninfected tonsils, with a 440bp fragment being detected in 6 of 7 tonsils (85%) (figure 50B, lanes 4-8 and 10). There was complete absence of expression in the PGL samples and HIV-uninfected lymph nodes (figure 50A, lanes 2 to 19 and figure 50B, lanes 11-19).

3.7 Genetic, epigenetic and expression analysis of the *INK4* locus in PGL

Tumour suppressor roles for the cyclin-dependent kinase inhibitors, $p16^{INK4a}$ and $p15^{INK4b}$ in human cancer have been well established (see section 1.5.5). A putative tumour-suppressor role has been suggested for the alternate protein product of the *INK4A* locus, designated $p14^{ARF}$ in humans and $p19^{ARF}$ (*ARF* for **a**lternate **r**eading **f**rame) in the mouse, based on gene targeting studies in mice. Although exon 1β mutations are rare, exon 2 mutations affecting both $p16^{INK4a}$ and $p14^{ARF}$ have been reported (Sanchez-Cespedes *et al.*, 1999; Rizos *et al.*, 2000). Deletion of exon 1β of $p14^{ARF}$ has been reported in hepatocellular and gastric carcinomas (Jin *et al.*, 2000; Iida *et al.*, 2000). In addition, hypermethylation of the promoter region of *ARF* has been described in some human colorectal and gastric tumours (Esteller *et al.*, 2000; Iida *et al.*, 2000).

In NHLs that arise in immunocompetent hosts, deletions and transcriptional silencing via aberrant promoter hypermethylation are the most common mechanisms of *INK4a* and *INK4b* inactivation. Both genes are subject to hypermethylation in high-grade B-cell lymphomas (Herman *et al.*, 1997). Inactivating mutations in $p15^{INK4b}$ and those that target exon 1α and exon 2 of $p16^{INK4a}$ are rarely observed (<1%) in these malignancies.

Figure 50. Detection of ΔN p63 transcripts in HIV-PGL and HIV-uninfected tissue

50 A

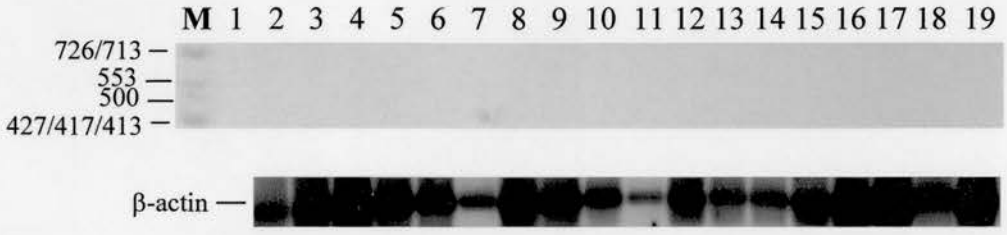

50 B

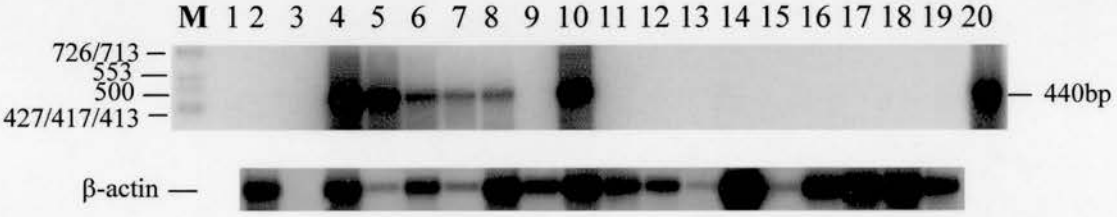

A 440p region of p63 was amplified from cDNA in a 30-cycle RT-PCR reaction. 20μl of PCR product was resolved on a 2% w/v agarose gel. PCR products were transferred to Hybond N^+ membrane and probed with a ^{32}P-labelled oligonucleotide located in exon 4. **M:** *Hinf1* digested ϕX-174 DNA size marker (fragment sizes in bp). The presence of amplifiable cDNA is indicated by the amplification of β-actin. The ΔN p63 RT-PCR product (440bp) is indicated.

Figure 50 A

Lane 1: Blank **Lanes 2-19:** PGL samples.

Figure 50 B

Lane 1: Blank **Lane 2:** PGL sample **Lane 3:** Sterile distilled water **Lanes 4-10:** HIV-uninfected tonsils **Lanes 11-19:** HIV-uninfected lymph nodes **Lane 20:** cDNA from squamous cell cancer (S1).

Given the importance of these genes in neoplasia, the studies described in this chapter were carried out to assess whether changes in structure, expression and/or gene hypermethylation of members of the *INK4* locus occur in HIV-related PGL.

3.7.1 SSCP analysis of the *INK4a/ARF* locus

To determine whether the *INK4a/ARF* locus is structurally altered in HIV-infected PGL, SSCP-PCR was performed on genomic DNA, using primers that amplify a 278bp fragment in exon 1α and 243bp and 241bp fragments in exon 2 (fragments 2a and 2b respectively). Exon 1β was analysed from cDNA (Table 18, page 92). Since it was not possible to obtain positive controls, it was decided that any sample with a migration pattern different from that observed in the negative (normal) control would be cloned and sequenced. Mobility shifts indicative of sequence changes were not observed in exons 1α, 1β or 2 (figures 51 to 53 respectively) by SSCP analysis of the corresponding exons.

3.7.2 Analysis of expression of $p16^{INK4a}$, $p14^{ARF}$ and $p15^{INK4b}$ in HIV-infected and uninfected tissue

(i) Expression of $p16^{INK4a}$

The $p16^{INK4a}$ tumour suppressor gene product acts as a negative regulator of proliferation by inhibiting the activity of CDK4, thus preventing the phosphorylation of pRb and subsequent G1/S progression (see section 1.5). Expression of $p16^{INK4a}$ was analysed in HIV-infected lymphoid tissue by RT-PCR, using a sense primer in exon 1α and an antisense primer in exon 2, followed by hybridisation of the amplified products to a ^{32}P-labelled $p16^{INK4a}$ cDNA.

$p16^{INK4a}$ mRNA was detected in 16 of 16 (100%) HIV-infected PGL samples tested (figure 54A, lanes 2 to 19). 3 PGL samples were unavailable for analysis due to insufficient material. In addition, the gene was expressed in all (16/16) of the HIV-uninfected lymph nodes and tonsils (figure 54B, lanes 2 to 17).

Figure 51. **SSCP analysis of exon 1α in PGL**

Figure 52. **SSCP analysis of exon 1β in PGL**

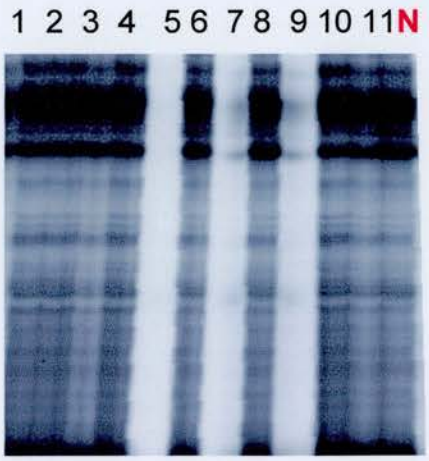

Figure 53. **SSCP analysis of exon 2a in PGL**

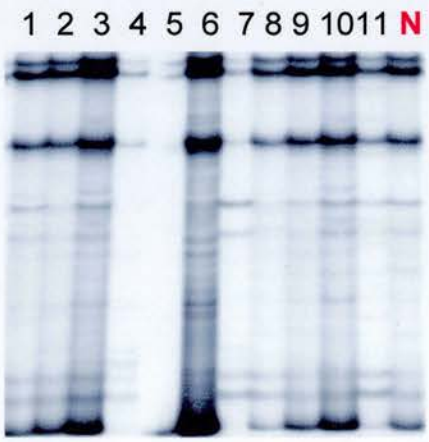

Figure 51. SSCP analysis of exon 1α of $p16^{INK4a}$. 500ng of DNA was subjected to amplification using the appropriate primers (Table 18). 3μl of radiolabelled PCR product was mixed with 3μl of loading dye. Samples were heat-denatured at 94°C for 5 minutes, then resolved on a 6% polyacrylamide (PAGE) gel with 10% glycerol. Dried gels were exposed to Kodak XR film at -70°C for 2-3 days with intensifying screens. **Lanes 1-10:** PGL samples **N:** Normal control (DNA from fibroblasts).

Figure 52. SSCP analysis of exon 1β of $p14^{ARF}$. 500ng of DNA was subjected to amplification using the appropriate primers (Table 18). 3μl of radiolabelled PCR product was mixed with 3μl of loading dye. The samples were heat-denatured at 94°C for 5 minutes, then resolved on a 6% polyacrylamide (PAGE) gel with 10% glycerol. Dried gels were exposed to Kodak XR film at -70°C for 2-3 days with intensifying screens. **Lanes 1-4, 6,8,10,11:** PGL samples **Lanes 5,7 & 9:** Blank **N:** Normal control (DNA from fibroblasts).

Figure 53. SSCP analysis of exon 2a of $p16^{INK4a}$. SSCP of the 5' half of exon 2 (2a) of $p16^{INK4a}$. 500ng of DNA was subjected to amplification using the appropriate primers (Table 18). 3μl of radiolabelled PCR product was mixed with 3μl of loading dye. The samples were heat-denatured at 94°C for 5 minutes, then resolved on a 6% polyacrylamide (PAGE) gel with 10% glycerol. Dried gels were exposed to Kodak XR film at -70°C for 2-3 days. **Lanes 1-11:** PGL samples **N:** Normal control (DNA from fibroblasts).

Figure 54. Analysis of $p16^{INK4a}$ mRNA expression in HIV-PGL and HIV-uninfected tissue

54 A

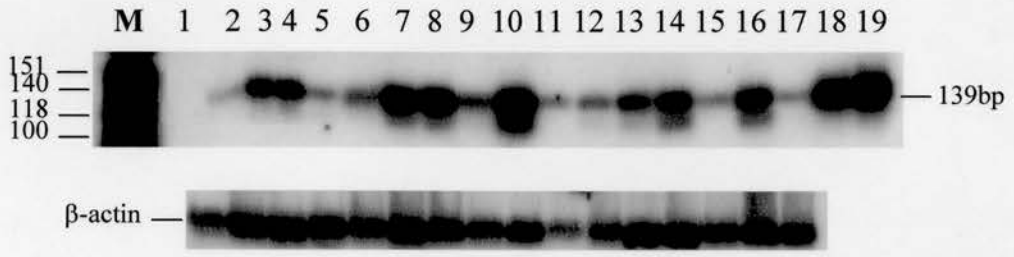

54 B

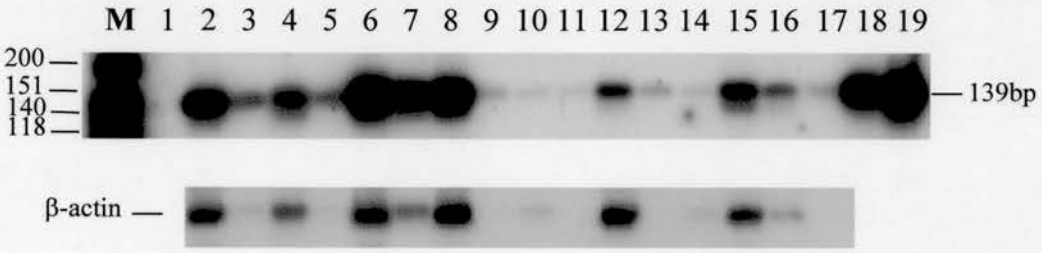

A 139bp region of $p16^{INK4a}$ was amplified from cDNA in a 22-cycle RT-PCR reaction. 20μl of the product was resolved on a 2% w/v agarose gel, then transferred to a Hybond N^+ membrane and probed with a ^{32}P-labelled $p16^{INK4a}$ cDNA. **M:** *Hinf1* digested ϕX-174 DNA size marker (fragment sizes in bp). The $p16^{INK4a}$ RT-PCR product (139bp) is indicated. The presence of amplifiable cDNA is indicated by the amplification of β-actin.

Figure 54 A

Lane 1: Sterile distilled water **Lanes 2-17:** HIV-infected PGL samples **Lane 18:** cDNA from breast tumour **Lane 19:** Lymphoblastoid cell line (PD-LCL).

Figure 54 B

Lane 1: Blank **Lanes 2-8:** HIV-uninfected tonsils **Lanes 9-17:** HIV-uninfected lymph nodes **Lane 18:** cDNA from breast tumour **Lane 19:** Lymphoblastoid cell line (OTIS).

(ii) Expression of $p14^{ARF}$

Deregulation of $p14^{ARF}$ occurs in cells that are functionally null for p53. $p14^{ARF}$ can suppress oncogenic transformation in primary fibroblasts via p53-dependent as well independent mechanisms (Pomerantz *et al.*, 1998; Weber *et al.*, 2000). Hence it was decided to investigate whether the PGL samples with p53 mutations expressed the $p14^{ARF}$ transcript at higher levels than those samples, which lacked p53 mutation.

Initial experiments were designed to determine appropriate conditions for semi-quantitative assessment of relative expression levels of $p14^{ARF}$, by optimising the cycle number for RT-PCR amplification of the gene (figure 55A and 55B). cDNA from a vulval squamous cell cancer that was known to be positive for $p14^{ARF}$ expression was subjected to 15-30 cycles of amplification, to amplify a 188bp fragment using a sense primer in exon 1β and an antisense primer in exon 2 of *INK4a/ARF* (see Table 11, page 80), followed by hybridisation of the amplified products to a ^{32}P-labelled $p14^{ARF}$ cDNA as described in sections 2.12 and 2.13 (figure 55A, lanes 1 to 4 respectively). Band intensity was measured using scanning densitometry (UVP Gel Works). The optimum cycle number was determined to be 22 cycles, between 20 and 25 cycles (exponential phase of the amplification curve) (figure 55B).

RT-PCR of the HIV-infected and uninfected samples was performed at 22 cycles. $p14^{ARF}$ mRNA was detected in 19/19 of the PGL samples (figure 56A, lanes 1-19) and in all (14/15) the HIV-uninfected samples, except in one lymph node (figure 56B lane 12). Elevated steady-state levels of $p14^{ARF}$ mRNA, indicative of possible deregulation, was not observed in those samples with missense mutations in p53 (figure 56A, lanes 4, 7, 11, 12).

(iii) Expression of $p15^{INK4b}$

$p15^{INK4b}$ is another member of the INK4 family of proteins that can specifically bind to CDK4/6 and impose a G1 phase cell cycle arrest, provided the cell contains functional pRb. RT-PCR to analyse expression of this gene was performed using a sense primer that was common to both $p16^{INK4a}$ and $p15^{INK4b}$ and an antisense primer located in exon 2 of the $p15^{INK4b}$ gene, followed by hybridisation of the amplified products to a ^{32}P-labelled oligonucleotide located in exon 2 of the $p15^{INK4b}$ gene.

Figure 55. Determination of optimal cycle number for semi-quantitative analysis of $p14^{ARF}$ expression

55 A

55 B

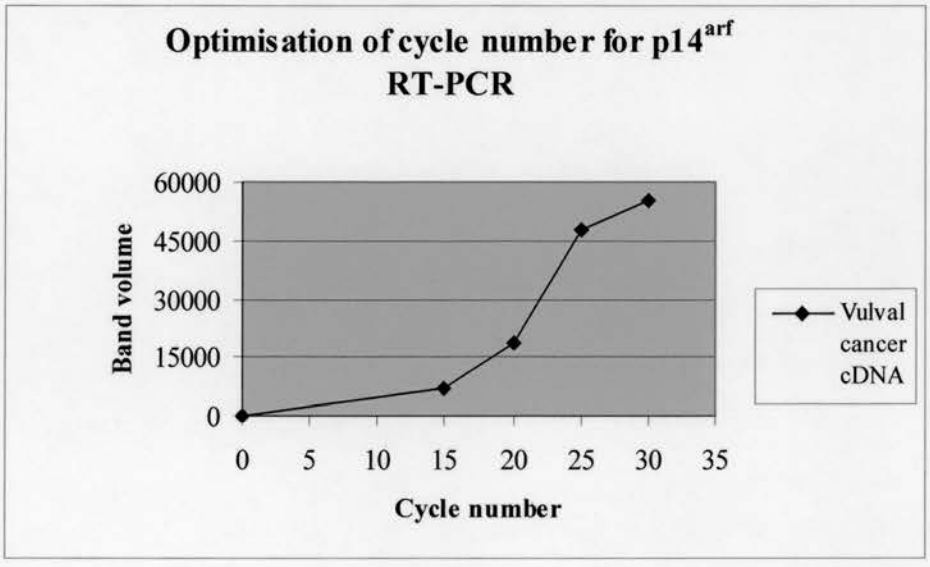

A 188bp region of $p14^{ARF}$ was amplified at 15, 20, 25 and 30 cycles, using cDNA from a vulval squamous cancer cell line. 20µl of the PCR product was resolved on a 2% w/v agarose gel, then transferred to a Hybond N^+ membrane and probed with a ^{32}P-labelled $p14^{ARF}$ cDNA. **M:** *Hinf1* digested ϕX-174 DNA was used as a DNA size marker (fragment sizes in bp).

Figure 55 A: Lanes 1 to 4: 15, 20, 25 and 30 cycles of amplification respectively.

Figure 55 B: The intensity of the bands, obtained after hybridization of the $p14^{ARF}$ RT-PCR product with a ^{32}P-labelled cDNA, was measured using scanning densitometry (UVP Gel Works). A graph was then plotted with the cycle number on the X-axis and the band volume on the Y-axis. The optimal cycle number for the $p14^{ARF}$ RT-PCR was determined to be 22 cycles, which is on the exponential portion of the amplification curve.

Figure 56. Analysis of p14^{ARF} mRNA expression in HIV-PGL and HIV-uninfected tissue

56 A

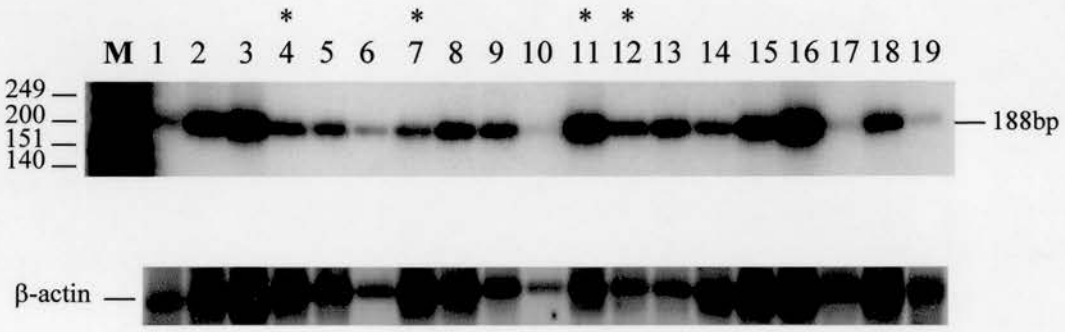

56 B

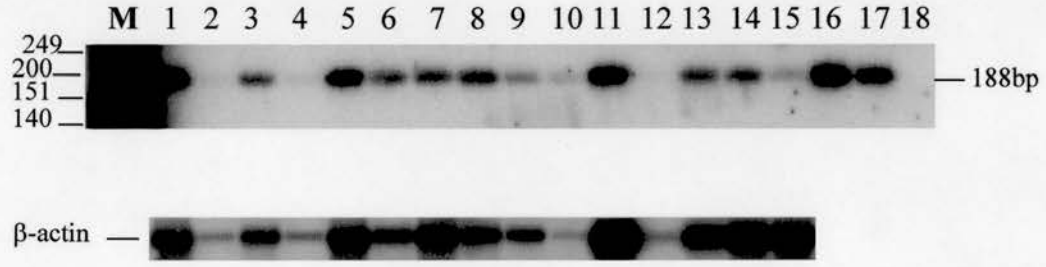

A 188bp region of p14^{ARF} was amplified from cDNA in a 22-cycle RT-PCR reaction. 20μl of the PCR product was resolved on a 2% w/v agarose gel, then transferred to a Hybond N$^+$ membrane and probed with a ^{32}P-labelled p14^{ARF} plasmid. **M:** *Hinf1* digested ϕX-174 DNA size marker (fragment sizes in bp). The p14^{ARF} RT-PCR product (188bp) is indicated. The presence of amplifiable cDNA is indicated by the amplification of β-actin.

Figure 56 A: Lanes 1-19: HIV-infected PGL samples. The * indicates PGL samples with p53 mutation.

Figure 56 B: Lanes 1-7: HIV-uninfected tonsils. **Lanes 8-15:** HIV-uninfected lymph nodes. **Lanes 16 and 17:** cDNA from vulval cancers (T1 and T2). **Lane 18:** Sterile distilled water.

$p15^{INK4b}$ mRNA was detected in 16/16 HIV-infected lymph nodes tested (figure 57A, lanes 2 to 17). 3 PGL samples were unavailable for analysis due to insufficient material. The gene was expressed in all the HIV-uninfected tonsils (figure 57B, lanes 1 to 7), in contrast to expression in only 1 HIV-uninfected lymph node (figure 57B, lane 11).

3.7.3 Methylation analysis of $p16^{INK4a}$ and $p15^{INK4b}$

Although expression of $p16^{INK4a}$ and $p15^{INK4b}$ could be detected in all HIV-PGL samples analysed, it is possible that partial methylation could have contributed to the low or null expression that was observed in some of the samples (see figures 54A and 57A). Therefore, to assess the methylation status of the *INK4a* and *INK4b* genes in HIV-PGL, DNA from 22 of 24 HIV-infected PGL samples was chemically modified using sodium bisulfite (see section 2.19.1), and subjected to MSP analysis (see section 2.19.2) using primers specific for the unmethylated and methylated reactions (Table 23, page 104).

Methylation of the $p16^{INK4a}$ and $p15^{INK4b}$ genes was not detected in any of the PGL samples (figures 58 and 59). However methylation was observed in the BL cell lines Namalwa and Raji (positive controls). Both cell lines contained methylated copies of the $p16^{INK4a}$ gene (figure 58, lanes 22 and 23 respectively), whereas the $p15^{INK4b}$ gene was found to be partially methylated (containing both methylated and unmethylated alleles) in both these BL cell lines (figure 59, lanes 23 and 24). These results are in agreement with previous studies (Klangby *et al.*, 1998).

The data indicates that methylation of $p16^{INK4a}$ and $p15^{INK4b}$ is not a common event in PGL.

3.8 Analysis of structural alterations in c-*myc*, *bcl-2* and *bcl-6* in PGL

3.8.1 Analysis of the t(8:14) translocation

The t(8;14) (q24;q32) translocation between the c-*myc* gene (8q24) and the immunoglobulin heavy chain (*IgH*) locus (14q32) is the most frequent genetic alteration described in endemic Burkitt's lymphoma (eBL), sporadic BL (sBL) and AIDS-BL (Dalla-Favera *et al.*, 1982b, Gaidano *et al.*, 1997b). The breakpoint in AIDS-BL and sBL is preferentially located within intron 1 or exon 1 of c-*myc* and in

Figure 57. Analysis of p15^{INK4b} mRNA expression in HIV-PGL and HIV-uninfected tissue

57 A

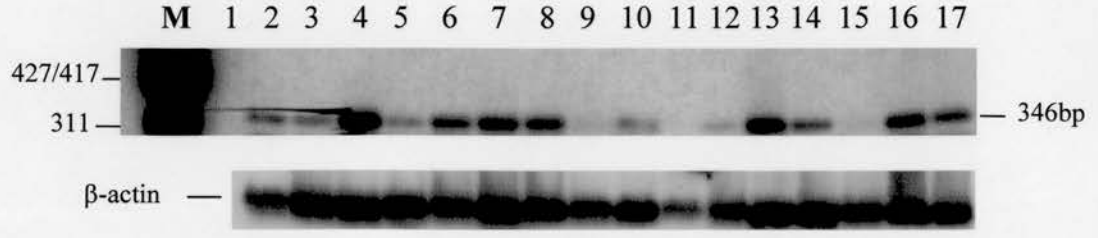

57 B

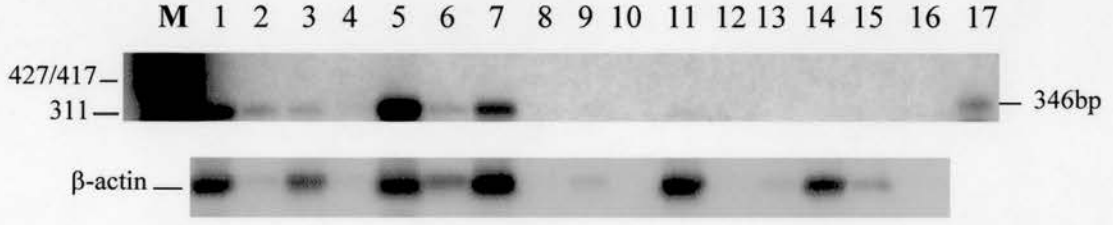

A 346bp region of p15^{INK4b} was subjected to amplification in a 28-cycle RT-PCR reaction. 20μl of the PCR product was resolved on a 2% w/v agarose gel, then transferred to a Hybond N$^+$ membrane and probed with a ^{32}P-labelled p15^{INK4b} oligonucleotide located in exon 2. **M:** *Hinf1* digested ϕX-174 DNA size marker (fragment sizes in bp). The p15^{INK4b} RT-PCR product (346bp) is indicated. The presence of amplifiable cDNA is indicated by the amplification of β-actin.

Figure 58 A: Lane 1: Sterile distilled water **Lanes 2-17:** HIV-infected PGL samples.

Figure 58 B: Lanes 1-7: HIV-uninfected tonsils **Lanes 8-16:** HIV-uninfected lymph nodes **Lane 17:** BL-41 cell line.

Figure 58. Methylation status of the p16^{INK4a} gene in HIV-PGL tissue

40 ng of DNA modified by sodium bisulphite was used in a 35-cycle MSP reaction to amplify a 145bp and 154bp region of the p16^{INK4a} gene, using primers specific for the methylated and unmethylated reactions respectively. 20μl of the PCR product was resolved on a 3% w/v agarose gel and the bands were visualised under UV light.
L: A 100bp DNA size marker (fragment sizes in bp).
U: Unmethylated DNA. **M:** Methylated DNA.
Lanes 1 to 20: HIV-infected PGL samples. **Lane 21:** Unmethylated control DNA. **Lane 22:** Namalwa cell line. **Lane 23:** Raji cell line. **Lane 24:** Methylated control DNA.

Figure 59. Methylation status of the $p15^{INK4b}$ gene in HIV-PGL tissue

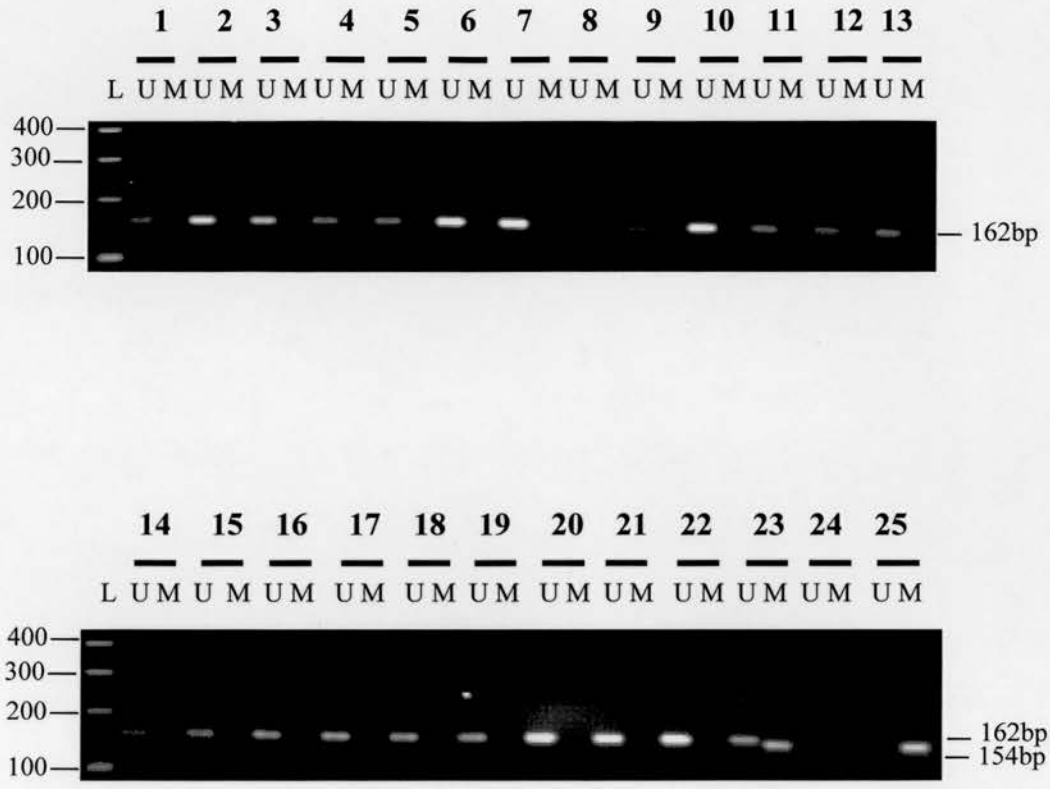

40 ng of DNA modified by sodium bisulphite was used in a 35-cycle MSP reaction to amplify a 154bp and 162bp region of the $p15^{INK4b}$ gene, using primers specific for the methylated and unmethylated reactions respectively. 20μl of the PCR product was resolved on a 3% w/v agarose gel and the bands were visualised under UV light.

L: A 100bp DNA size marker (fragment sizes in bp). **U:** unmethylated DNA. **M:** Methylated DNA.

Lanes 1 to 21: HIV-infected PGL samples. **Lane 22:** Unmethylated control DNA. **Lane 23:** Namalwa cell line. **Lane 24:** Raji cell line. **Lane 25:** Methylated control DNA.

the switch region (s) of the *IgH* locus (Neri *et al.*, 1991).

Thus, to analyse whether rearrangement of c-*myc* is a characteristic feature of HIV-associated PGL syndrome, LD-PCR amplification of the c-*myc*/*IgH* switch junctions was carried out, using primers specified in Table 14, page 85.

LD-PCR of the HIV-infected PGL tissue did not reveal any translocations, although the positive control for each primer pair was successfully amplified: Raji cell line using the c-*myc*/Cγ primer pair (figure 60A, lane 1), Ramos cell line using the c-*myc*/Cμ primer pair (figure 60B, lane 1) and the BL-41 cell line using the c-*myc*/Cα primer pair (figure 60C, lane 1).

However, LD-PCR analysis for the t(8:14) translocation in HIV-uninfected lymph nodes and tonsils revealed positive amplification in a single lymph node tissue, case number 2435, using the c-*myc*/Cγ primer set (figure 60A, lane 9). The breakpoint region in this material was identified by cloning and sequencing of the PCR product. In 6/6 clones that were examined the breakpoint was identified in the 5' flanking region of c-*myc*, 424bp upstream of the 1st exon (nucleotide position 1904, antisense strand, Genbank accession X00364), and in the Sγ4 region of the *IgH* locus (nucleotide position 3431, sense strand, Genbank accession X56796) (figures 61A and 61B, page 167). Fusion of the chromosomal segments was imprecise, with an insertion of 6 nucleotide residues, mapping neither to the c-*myc* nor Sγ4 regions at the interchromosomal junction (figures 61B and 61C, page 167).

Figure 60. Analysis of c-*myc* translocations by LD-PCR

60 A c-*myc*/Cγ LD-PCR

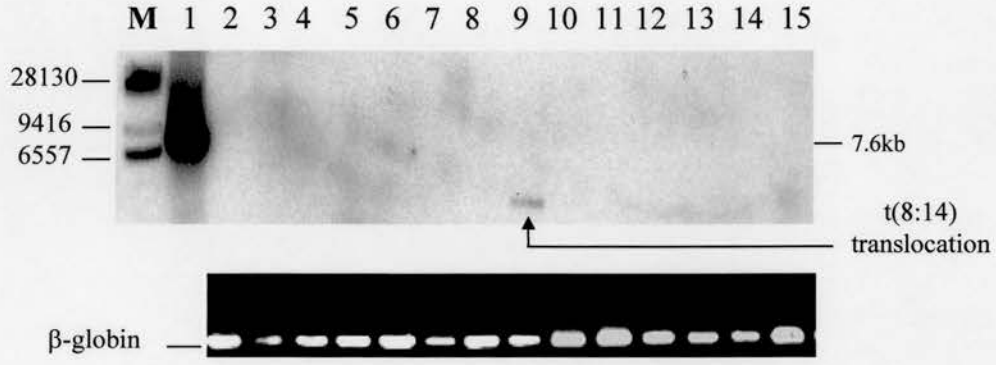

60 B c-*myc*/Cμ LD-PCR

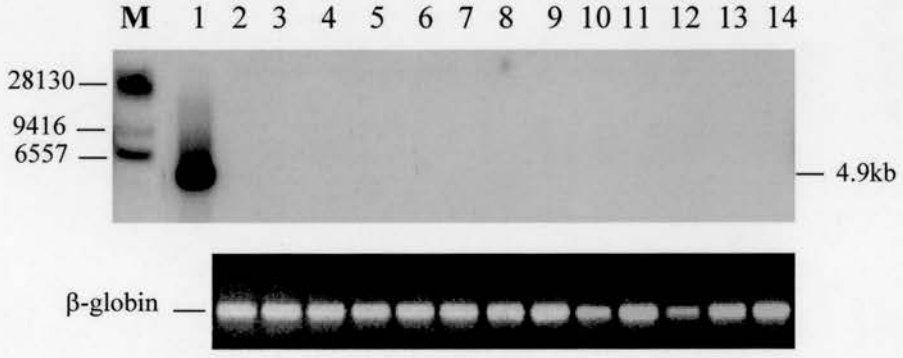

60 C c-*myc*/Cα LD-PCR

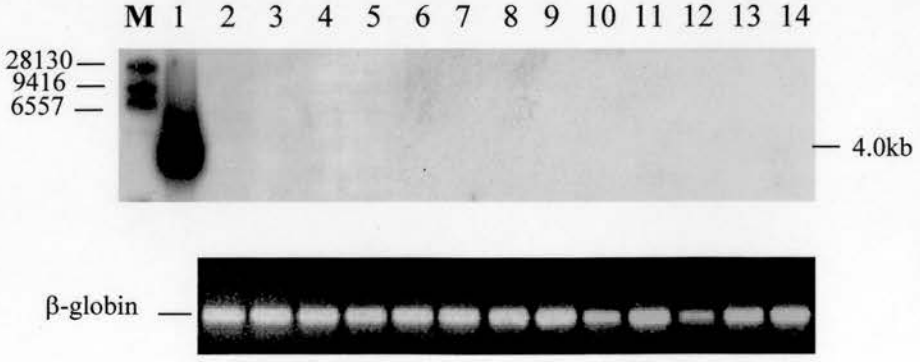

Figure 60. Analysis of c-*myc* translocations by LD-PCR. 100ng of genomic DNA from HIV-infected PGL tissue and HIV-uninfected lymph nodes and tonsils was subjected to amplification in a 35-cycle LD-PCR reaction using the c-*myc*/Cγ, c-*myc*/Cμ, and c-*myc*/Cα primer pairs. 20μl of the PCR products were resolved on a 0.8% w/v agarose gel, transferred to a Hybond N^+ membrane and hybridised with a [γ^{32}P] ATP-labelled oligonucleotide probe specific to exon 2 of the c-*myc* gene. **M:** Lambda (λ) DNA digested with Hind III DNA size marker (fragment sizes in bp). The presence of amplifiable DNA is indicated by amplification of β-globin.

Figure 60 A. c-*myc*/Cγ LD-PCR
Lane 1: Raji cell line (7.6kb band is indicated) **Lanes 2 to 8:** HIV-uninfected tonsils **Lane 9:** HIV-uninfected lymph node with a t(8:14) translocation **Lanes 10 to 14:** HIV-uninfected lymph nodes **Lane 15:** P3HR1 cell line (negative control).

Figure 60 B. c-*myc*/Cμ LD-PCR
Lane 1: Ramos cell line (4.9kb band is indicated) **Lanes 2 to 13:** HIV-PGL samples **Lane 14:** P3HR1 cell line (negative control).

Figure 60 C. c-*myc*/Cα LD-PCR
Lane 1: BL-41 cell line (4.0kb band is indicated) **Lanes 2 to 13:** HIV-PGL samples **Lane 14:** P3HR1 cell line (negative control).

Figure 61. **t(8:14) chromosomal breakpoint in an HIV-uninfected lymph node (case no. 2435)**

61 A

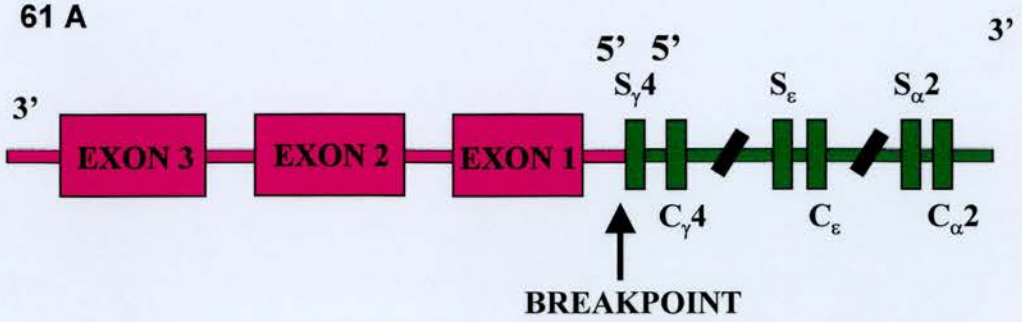

61 B

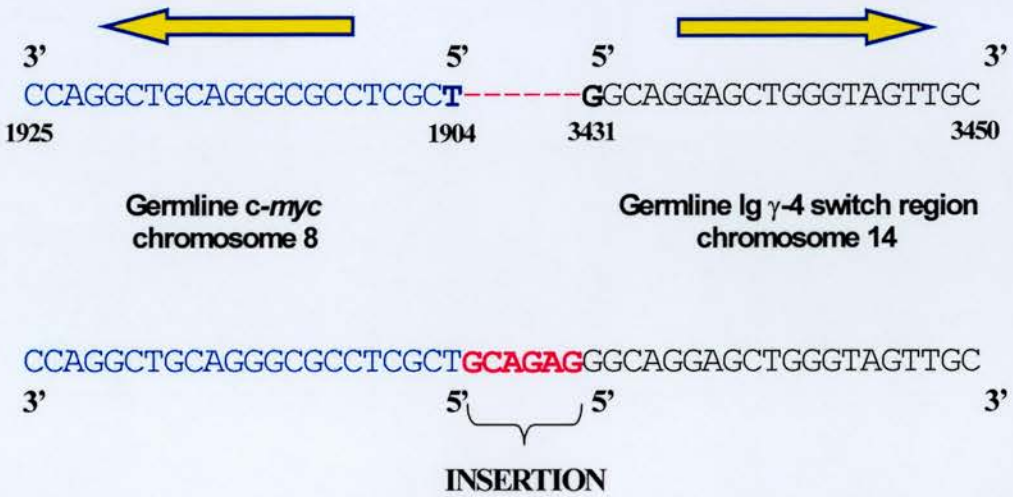

61 C

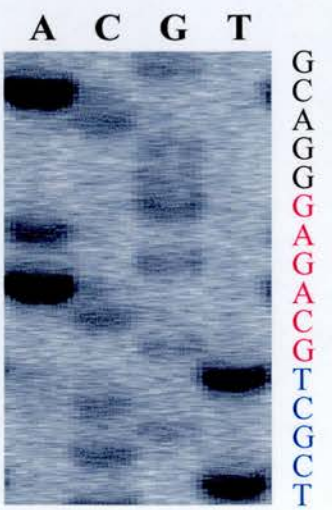

Figure 61. t(8:14) chromosomal breakpoint in an HIV-uninfected lymph node (case no. 2435). Genomic DNA from case 2435 was subjected to amplification using the c-*myc*/Cγ primer pair and the product was ligated directly into the pCR®4-TOPO® vector. Cloned DNA was then sequenced using the LICOR 4000L automated sequencer (MWG Biotech, Milton Keynes, UK), and the Sequitherm Excel™ II kit (Cambio, Cambridge, UK).

Figure 61 A. Schematic representation of the t(8:14) breakpoint observed in case 2435. A black arrow indicates the position of the breakpoint, between the 5' flanking region of c-*myc* and the Sγ4 region of the *IgH* locus.

Figure 61 B. Sequence of the t(8:14) chromosomal breakpoint junction. The c-*myc* gene is indicated in blue and the Sγ4 gene in black. The two genes are placed in a head-to-head orientation. The positions of the breakpoint in the 5' flanking region of c-*myc* (nucleotide position 1904, antisense strand, Genbank accession X00364), and in the Sγ4 region of the *IgH* locus (nucleotide position 3431, sense strand, Genbank accession X56796) are indicated. An insertion of 6 nucleotide residues at the interchromosomal junction is indicated in red.

Figure 61 C. Pictorial representation of the c-*myc*/Sγ4 breakpoint sequence. The c-*myc* gene is indicated in blue. The Sγ4 gene is indicated in black. The insertion of 6 residues at the breakpoint junction is indicated in red.

3.8.2 Analysis of the t(14:18) translocation

The t(14;18) (q32;q21) translocation involving the immunoglobulin heavy chain gene (*IgH*) and the *bcl-2* gene respectively, is the most common chromosomal translocation in follicular lymphoma (85%) and diffuse large-cell lymphomas (30%) (Yunis *et al.*, 1987). More than 70% of the translocations in the *bcl-2* gene are clustered in a 150bp segment at the 3' untranslated region, designated the major breakpoint region (MBR) and a small number of translocations have been identified at a site 30kb 3' to the MBR called the minor cluster region (mcr) (Tsujimoto *et al.*, 1985; Cleary *et al.*, 1986). The corresponding breakpoints on chromosome 14 occur predominantly at or close to the members of the joining region genes (JH) (Bakhshi *et al.*, 1987). To investigate whether *bcl-2* translocations occur in HIV-associated PGL syndrome, LD-PCR of both the MBR and mcr regions and upstream of these regions on the *bcl-2* locus was carried out.

Figures 62A and 62B are representative autoradiographs of LD-PCR amplification of the t(14:18) translocation using MBR-1/Eμ and mcr-2/Eμ primer sets respectively. Although the sensitivity of the primers were confirmed for the *bcl-2* LD-PCR analysis (see section 3.4.1.4) and the primers could detect translocations known to be present in lymph node positive controls 1119 and 1143 (figure 62A, lane 15 and figure 62B, lane 1 respectively), translocations were not detected in the present series of PGL samples or HIV-uninfected individuals.

It was thus concluded that chromosomal aberration involving the *bcl-2* gene is not an early characteristic feature of HIV-associated lymphomas. This observation is consistent with previous studies that have reported lack of involvement of the *bcl-2* gene in AIDS-NHL (Subar *et al.*, 1988; Gaidano *et al.*, 1997b; Davi *et al.*, 1998).

3.8.3 Analysis of *bcl-6* mutations in HIV-PGL

In contrast to the coding region of *bcl-6*, its 5' non-coding region displays extensive structural instability (Ye *et al.*, 1993; Capello *et al.*, 2000). Rearrangements of *bcl-6* with heterogeneous promoters occur in approximately 40% of diffuse large-cell lymphomas and 6-14% of follicular lymphomas in the immunocompetent host (Lo Coco *et al.*, 1994). In HIV-infected individuals alterations are detectable in 20% of AIDS-DLCL (Gaidano *et al.*, 1994).

Figure 62. Analysis of *bcl-2* translocations by LD-PCR

62 A

62 B

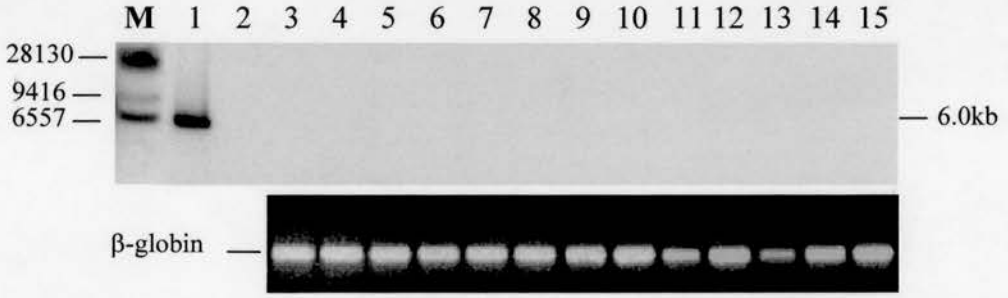

100ng of genomic DNA from HIV-PGL tissue and HIV-uninfected lymph nodes and tonsils was subjected to amplification in a 35-cycle LD-PCR reaction using the MBR-1/Eμ, mcr-2/Eμ primer pairs. 20μl of the PCR product was resolved on a 0.8% w/v agarose gel, transferred to a Hybond N^+ membrane and hybridised with a [γ^{32}P] ATP-labelled oligonucleotide probe in the Eμ region of the IgH locus. The presence of amplifiable DNA is indicated by amplification of β-globin. **M:** Lambda (λ) DNA digested with Hind III DNA size marker (fragement sizes in bp).

Figure 63 A: Lane 1: Sterile distilled water **Lane 2:** Lymph node 761 (negative control) **Lanes 3 to 14:** HIV-PGL samples **Lane 15:** Lymph node 1119 (4.2kb band is indicated).

Figure 63 B: Lane 1: Lymph node 1143 (6.0kb band is indicated) **Lane 2:** Sterile distilled water **Lane 3:** Lymph node 761(negative control) **Lanes 4 to 15:** HIV-PGL samples.

In addition to translocations and small intragenic deletions, which can deregulate *bcl-6* expression (Ye *et al.*, 1995a; Nakamura *et al.*, 1999), this region is targeted by somatic mutations, both in GC-derived tumours and in normal B cells (Migliazza *et al.*, 1995; Shen *et al.*, 1998). These 5' *bcl-6* mutations are detectable in about 70% of DLCL and 45% of FL, are bi-allelic and present in both germline and translocated *bcl-6* alleles. Furthermore, they also occur independently of translocation, as seen in 70% of AIDS-NHL (excluding DLCL), certain B-NHL without a 3q27 abnormality, and 28 to 50% of non-AIDS BL (Gaidano *et al.*, 1997d; Capello *et al.*, 1997).
To determine the frequency of mutations in *bcl-6* in both HIV-infected and uninfected tissue, SSCP analysis of a 735bp region was performed, which represents a mutational hot-spot, harbouring more than 90% of *bcl-6* mutations reported in diffuse large-cell and follicular lymphoma (Migliazza *et al.*, 1995).

3.8.3.1 SSCP variants in *bcl-6* are detected in HIV-infected and uninfected tissue
Mutations in *bcl-6* were sought in PGL samples and in uninfected lymph nodes and tonsil controls using SSCP. Three partially overlapping PCR fragments (E1.10, E1.11 and E1.12) spanning a 735bp region, located 100bp downstream of the first *bcl-6* non-coding exon (Migliazza *et al.*, 1995) were amplified in separate reactions using primers specified in Table 19, page 92. The first nucleotide of *bcl-6* cDNA from the reported germline database sequence (Genbank accession number Z79581) was arbitrarily chosen as position +1 (Migliazza *et al.*, 1995), and the amplified *bcl-6* 5' intronic region spanned +406 to +1140.
All samples with a mobility pattern different from that of the normal (negative) control were scored as positive. Abnormally migrating samples are indicated in blue. SSCP variants were detected in 3/23 PGL samples in E1.10 (figure 63B, lanes 3,11 and 20), 7/23 PGL samples in E1.11 (figure 64B, lanes 4,8,11,12,16,18,19) and in 10/23 PGL samples in E1.12 (figure 65B, lanes 1,2,5,6,9,12,13,15,16,19; see Table 32, page 181). In the HIV-uninfected tissue, variants were observed in 4/16 samples in E1.11 (figure 64A, lanes 2,8,9,10) and in 7/16 samples in E1.12 (figure 65A, lanes 1,2,3,8,10,11,14) (see Table 32, page 181). All those samples with a mobility shift were re-amplified using a high-fidelity enzyme, *Pfx* polymerase, and subsequently cloned (see section 2.17.1.3) and sequenced (see section 2.18.1).

Figure 63. SSCP analysis of fragment E1.10 of *bcl-6*

63 A

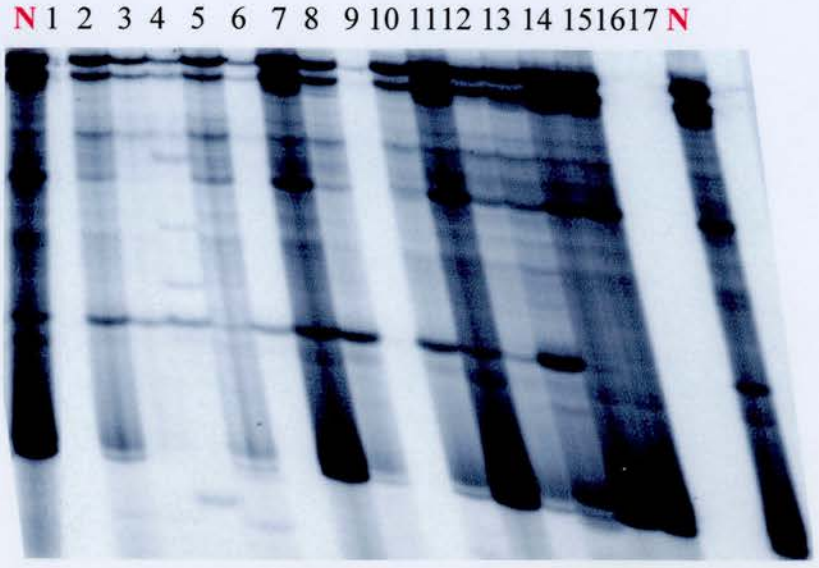

63 B

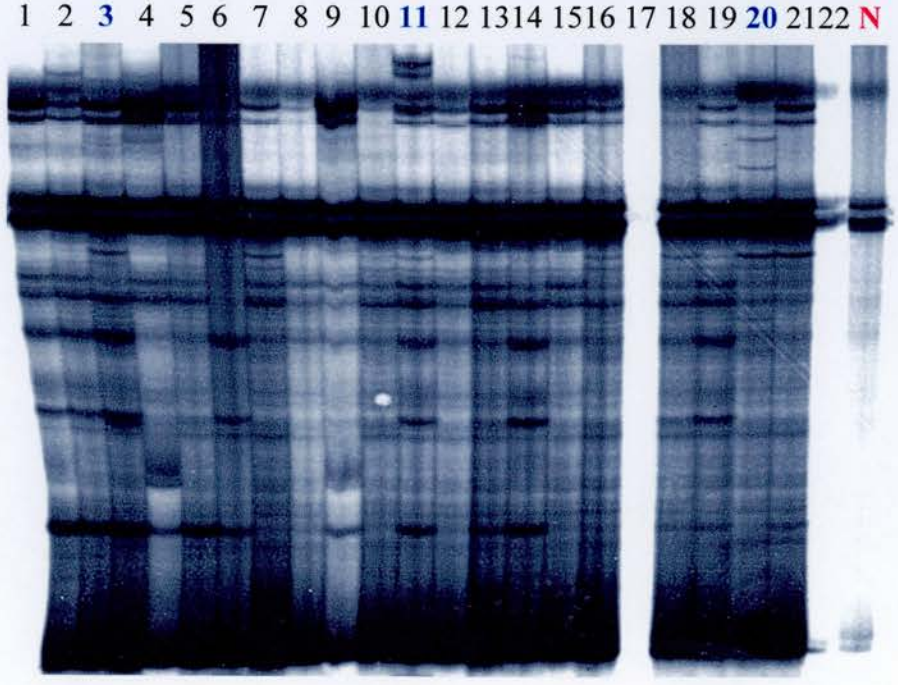

Figure 63. SSCP analysis of fragment E1.10 of *bcl-6.* 500ng of DNA was subjected to amplification using primers E1.10 5' and E1.10 3'. 3μl of radiolabelled PCR product was mixed with 3μl of loading dye. The samples were heat-denatured at 94°C for 5 minutes and resolved on a 6% polyacrylamide (PAGE) gel with 10% glycerol. After being dried the gel was exposed to Kodak XR film at -70°C for 2-3 days with intensifying screens. Abnormally migrating samples are indicated in blue.

Figure 63 A. Lane 1: Blank **Lanes 2-8:** HIV-uninfected tonsils **Lanes 9-17:** HIV-uninfected lymph nodes **N:** Negative control (Raji cell line).

Figure 63 B. Lanes 1-22: HIV-PGL samples **Lanes 3,11 and 20:** Abnormally migrating samples (LN 5, 15 and 24 respectively) **N:** Negative control (Raji cell line).

Figure 64. SSCP analysis of fragment E1.11 of *bcl-6*

64 A

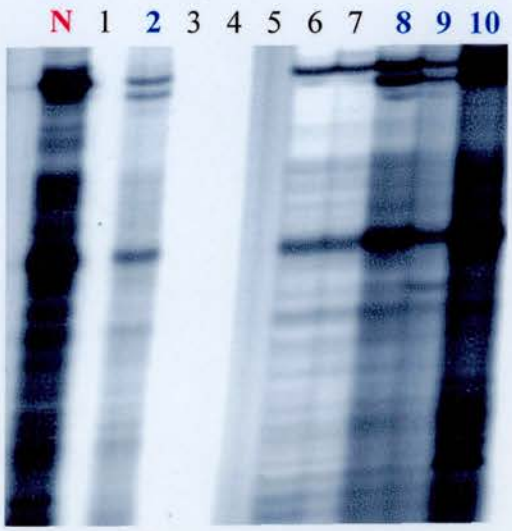

64 B

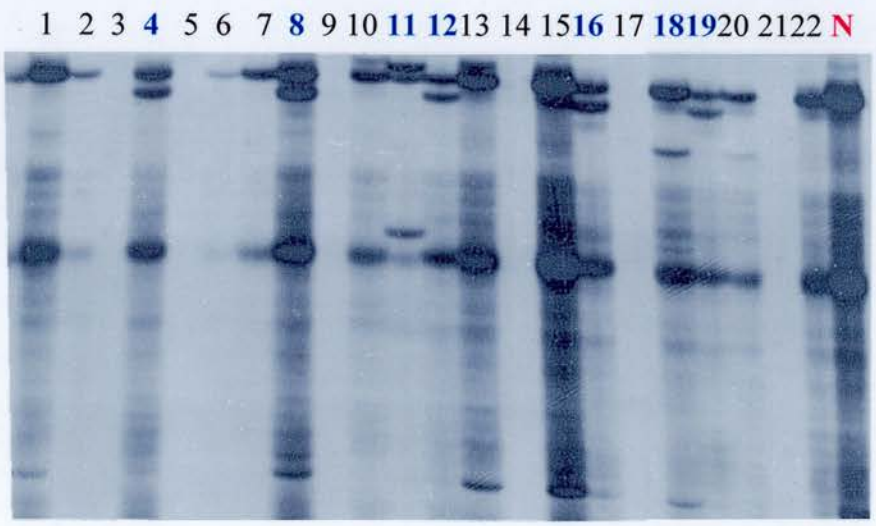

Figure 64. SSCP analysis of fragment E1.11 of *bcl-6.* 500ng of DNA was subjected to amplification using primers E1.11 5' and E1.11 3'. 3μl of radiolabelled PCR product was mixed with 3μl of loading dye. The samples were heat-denatured at 94°C for 5 minutes and resolved on a 6% polyacrylamide (PAGE) gel with 10% glycerol. After being dried the gel was exposed to Kodak XR film at -70°C for 2-3 days with intensifying screens. Abnormally migrating samples are indicated in blue.

Figure 64 A. Lanes 1-5: HIV-uninfected tonsils **Lanes 6-10:** HIV-uninfected lymph nodes **Lanes 2,8,9 and 10:** Abnormally migrating samples (T2, 2478, 2495 and 2499 respectively) **N:** Negative control (Namalwa cell line).

Figure 64 B. Lanes 1-22: HIV-PGL samples **Lanes 4,8,11,12,16,18,19:** Abnormally migrating samples (LN 9,12,1,15,17, 14 and 20 respectively) **N:** Negative control (Namalwa cell line).

Figure 65. SSCP analysis of fragment E1.12 of *bcl-6*

65 A

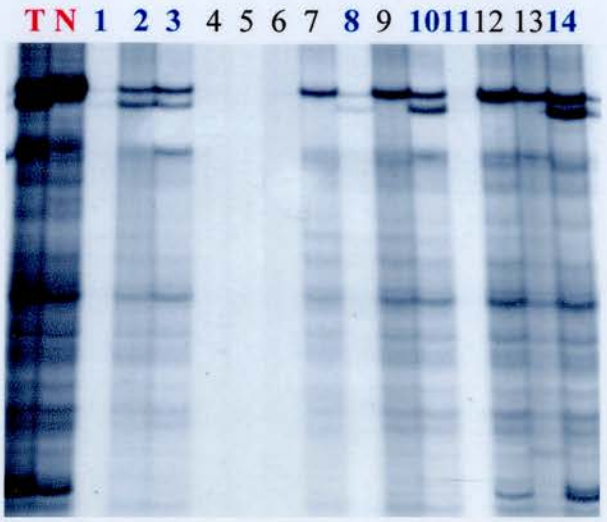

65 B

Figure 65. SSCP analysis of fragment E1.12 of *bcl-6.* 500ng of DNA was subjected to amplification using primers E1.12 5' and E1.12 3'. 3μl of radiolabelled PCR product was mixed with 3μl of loading dye. The samples were heat-denatured at 94°C for 5 minutes and resolved on a 6% polyacrylamide (PAGE) gel with 10% glycerol. After being dried the gel was exposed to Kodak XR film at -70°C for 2-3 days with intensifying screens. Abnormally migrating samples are indicated in blue.

Figure 65 A. Lanes 1-6: HIV-uninfected tonsils **Lanes 7-14**: HIV-uninfected lymph nodes Lanes 1,2,3,8,10,11 and 14: Abnormally migrating samples (T1, T2, T3, 2435, 2462, 2478 and 2499 respectively) **T:** Positive control (Raji cell line) **N:** Negative control (Namalwa cell line).

Figure 65 B. Lanes 1-22: HIV-PGL samples **Lanes 1,2,5,6,9,12,13,15,16 and 19:** Abnormally migrating samples (LN1,3,6,8,12,16,17,20,19 and 23 respectively) **T:** Positive control (Raji cell line) **N:** Negative control (Namalwa cell line).

3.8.3.2 Mutations in *bcl-6* are present at a higher frequency in HIV-PGL than in uninfected control tissue

bcl-6 mutations were detected in 11/23 HIV-infected individuals and in 2/16 HIV-uninfected controls (48% vs. 12.5% respectively, $p<0.05$, Fisher's exact test). A total of 24 mutations were detected in the 735bp region analysed, with 19/24 (79%) occurring in the PGL samples and 5/24 in the control samples (21%) ($p<0.001$, Fisher's exact test) (Tables 30A to C and Table 32, page 181). The 3 mutations detected in fragment E1.10 were within a negative regulatory sequence in the first intron of *bcl-6*.

The mutation frequency in both the HIV-infected and uninfected population was calculated using the formula:

Number of mutations/ (Number of clones analysed × Sequence length of region tested)

The mutation frequency was estimated to be between $9.8x10^{-4}$ to $1.3x10^{-3}$ per bp in the HIV-infected group and $8.2x10^{-5}$ to $5x10^{-4}$ per bp in the uninfected group.

Table 30 A
Nucleotide substitutions in the *bcl-6* intronic region +406 to +670 (E1.10)

HIV status	Case no.	*bcl-6* mutation*	Polymorphic (nucleotide) substitution	Allele
+	5	T→C (575)	None	nk
+	15	A→G (609)	None	nk
+	24	T→C (556)	None	nk

*, intronic region amplified is +406 to +670 (+1 corresponds to the first nucleotide of *bcl-6* cDNA, Genbank accession number Z79581); +, positive; nk, not known

Table 30 B

Nucleotide substitutions in the *bcl-6* intronic region +654 to +867 (E1.11)

HIV status	Case no.	*bcl-6* mutation*	Polymorphic (nucleotide) substitution	Allele**
+	1	C→G (787)	None	C
		C→A (790)		C
		T→C (799)		C
+	9	G→A (820)	G→C (753)	A
		T→C (726)		B
+	14	G→A (684)	None	nk
+	15	G→T (680)	G→C (753)	A
+	20	T→C (714)	G→C (753)	A
+		T→C (729)	G→C (753)	A
-	2499	T→C (795)	G→C (753)	A
		T→C (788)	G→C (753)	A
		T→G (788)		B

*, intronic region amplified is +654 to +867 (+1 corresponds to the first nucleotide of *bcl-6* cDNA, Genbank accession number Z79581); **, polymorphic substitutions are arbitrarily designated on allele A and are indicated in blue, C indicates mutations that exist on the same allele; -, negative; +, positive; nk, not known

Table 30 C

Nucleotide substitutions in the *bcl-6* intronic region +848 to +1140 (E1.12)

HIV status	Case no.	bcl-6 mutation*	Polymorphic (nucleotide) substitution	Allele**
+	6	C→A (997)		B
+	12	A→G (1068)		B
		A→G (1117)		B
		T→G (901)	ΔT (875)	A
		A→G (969)	ΔT (875)	A
+	19	A→T (1027)	None	nk
+	23	T→A (1094)		B
-	2499	C→A (903)		B
-	2495	G→A (878)	None	nk

*, intronic region amplified is +848 to +1140 (+1 corresponds to the first nucleotide of *bcl-6* cDNA, Genbank accession number Z79581);**, polymorphic substitutions are arbitrarily designated on allele A and are indicated in blue; -, negative; +, positive; nk, not known

Single nucleotide substitutions were the only type of mutation that was detected in this study. Transitions were favoured over transversions accounting for approximately 63% of mutations observed. Furthermore, preferential bias for T:N over A:N target bases (see Table 31) was observed. Mutations were bi-allelic and multiple within the same allele (LN 1 and LN 12). In cases LN 15 and 2499, mutations were detected in more than one fragment (Tables 30A to C).

Table 31

Nature of *bcl-6* mutations

	A	C	G	T	Total
A →	-	-	4	1	5
C →	3	-	1	-	4
G →	3	-	-	1	4
T →	1	8	2	-	11
Total	7	8	7	2	**24**

3.8.3.3 Polymorphic variants in *bcl-6*

Nucleotide substitutions likely to represent population polymorphisms were observed, a G to C change at position +753 in fragment E1.11 and a single base thymidine deletion (ΔT) at position +875 in fragment E1.12. The polymorphism at +753 was observed in 5/7 PGL samples and 4/4 HIV-uninfected samples with abnormal mobility shifts by PCR-SSCP, and the polymorphism at +875 in 8/10 PGL samples and 7/7 HIV-uninfected samples with abnormal PCR-SSCP shifts (see Table 32).

The polymorphic variants identified in this study, which have been described previously (Migliazza *et al.*, 1995), also permitted the identification of bi-allelic mutations in *bcl-6*. Polymorphic substitutions in Tables 30B and 30C are indicated in blue and are arbitrarily designated on allele A and those designated on allele B are indicated in red. Mutations were detected in 4/9 individuals with a polymorphic substitution at position +753 (LN 9,15,20 and 2499) (see Table 30B), and in 4/15 individuals with a substitution at +875 (LN 6, 12, 23 and 2499) (see Table 30C).

8 of the total 12 mutations found in fragment E1.11 were associated with the polymorphism at +753. Interestingly, of these mutations 6/8 (75%) was found on the allele that had a cytosine substitution at position +753 (Table 30A). 7 of the total 9 mutations found in fragment E1.12 were associated with the polymorphism at +875. 5/7 (71%) of these mutations was on the allele that had a thymidine residue present at position +875 (Table 30B). Polymorphic substitutions were not observed at position +753 in LN 1 and LN 14 (Table 30B) and at position +875 in LN 19 and 2495 (Table 30C).

Table 32

Summary of structural changes in *bcl-6* fragments E1.10, E1.11 and E1.12

***bcl-6* fragment**	**SSCP variants**		**Nucleotide substitutions**			
			Polymorphism		**Mutation**	
	HIV^+ (23)	**HIV^- (16)**	**HIV^+**	**HIV^-**	**HIV^+**	**HIV^-**
E1.10	3	-	-	-	3	-
E1.11	7	4	5/7	4/4	9	3
E1.12	10	7	8/10	7/7	7	2

3.9 Analysis of EBV and KSHV infection in HIV-PGL

Neoplasms arising in HIV-infected individuals are frequently associated with DNA tumour viruses such as EBV, KSHV and HPV (Mueller, 1999; Feigal, 1999). Approximately 30% of AIDS-NHL harbour EBV, although the frequency of association rises to nearly 100% in HIV-related primary central nervous system lymphoma and diffuse large-cell lymphomas of the immunoblastic subtype (Knowles, 1997). KSHV is invariably associated with a distinct set of malignancies in both HIV-infected and uninfected individuals, particularly, Kaposi's sarcoma, multicentric Castleman's disease and primary effusion lymphomas (Boshoff and Weiss, 1998; Cannon and Cesarman, 2000).

To address the presence and expression of EBV and KSHV in HIV-associated PGL

and in uninfected lymph nodes and tonsils, PCR-based analysis of both genomic DNA and mRNA was performed.

3.9.1 Detection of EBV in HIV-PGL using primers for the BamH1 W repeat sequence

The EBV W-repeat PCR, which detects the BamH1 W repeat sequence of the EBV genome, was used to determine the EBV status of PGL and of control tissues. The sensitivity of the BamH1 W primers was established in initial studies. Ten-fold dilutions of the BL cell line Namalwa (which contains 1-2 copies of the EBV genome per cell) in a background of 10^6 cells from an EBV negative cell line BJAB were prepared (see section 2.8.3) and subjected to PCR analysis as described in section 2.8.2.3 and Table 10, page 78. Under these assay conditions, the BamH1 W primers allowed detection of 10 copies of the EBV genome, as indicated by a 298bp fragment (figure 66A, lane 7). The sensitivity of detection was increased by one order of magnitude after hybridisation with a ^{32}P-labelled oligonucleotide probe (figure 66B, lane 8).

EBV was detectable in 12/14 (86%) HIV-uninfected lymph nodes and tonsils (figure 67, lanes 7 to 21). The EBV copy number was between 1 and 10 genomes per million cells for all the samples that tested positive, except for one HIV-uninfected lymph node, 2478 (figure 67, lane 16), which had an EBV load of $>10^5$ genomes per million cells. EBV could not be detected in cases 2435 and 2512 (figure 67, lanes 13 and 21) even after repeat amplification in an independent PCR. Samples T3 and 2425 could not be analysed due to insufficient DNA.

EBV was detected in 23 of 23 (100%) PGL samples analysed (figures 68A and 68B). The EBV genome copy number was greater than 10,000 copies per million cells in 74% (17/23) of the PGL samples, as determined by analysis of band intensity by scanning densitometry (UVP Gel Works). The EBV genome copy number in 4/23 samples was between 1 and 100 genomes (figure 68A, lane 12; 68B, lanes 20,21 and 25). Samples LN18 and LN19 (figure 68A, lanes 6 and 7) that were initially negative for the EB viral genome were found to harbour between 1-10 copies of the genome through repeat amplification in an independent PCR and hybridisation of the PCR product with a ^{32}P-labelled oligonucleotide.

Figure 66. Sensitivity of the EBV BamH1 W primers

66 A

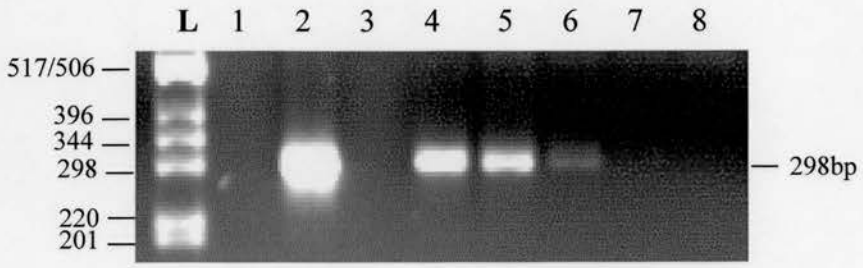

66 B

Figure 67. Detection of EBV DNA in HIV-uninfected tissue

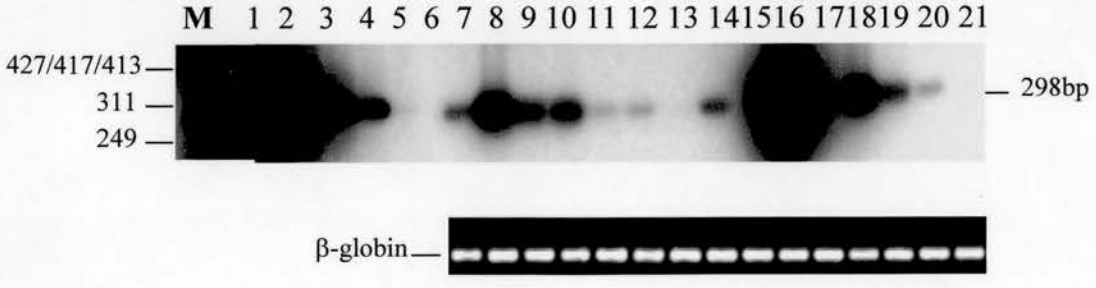

Figure 66. Sensitivity of the EBV BamH1 W primers. The Burkitt's lymphoma cell line Namalwa which contains 1-2 EBV genomes per cell was diluted ten-fold (10^6 cells to 1 cell per reaction) in 10^6 cells from an EBV negative cell line BJAB. 28 cycles of PCR were performed using BamH1 W primers. 20μl of the PCR product was resolved on a 2% w/v agarose gel, visualised under UV light (Figure 66A), transferred to Hybond N^+ membrane and hybridised with a ^{32}P-labelled oligonucleotide probe (Figure 66B).

Figure 66 A and 66 B. M: *Hinf1* digested ϕX-174 DNA size marker (fragment sizes in bp). **L:** 1kb DNA size marker (fragment sizes in bp). **Lane 1:** 10^6 BJAB cells **Lane 2:** 10^5 Namalwa cells **Lane 3:** Sterile distilled water **Lanes 4-8:** 10^4, 10^3, 10^2, 10 and 1 Namalwa cell (s) respectively.

Figure 67. Detection of EBV DNA in HIV-uninfected tissue. 28 cycles of PCR were carried out using BamH1 W primers. 20μl of the PCR product was resolved on a 2% w/v agarose gel and the bands were visualised under UV light. The PCR products were then transferred to Hybond N^+ membrane and hybridised with a ^{32}P-labelled oligonucleotide probe. The presence of amplifiable DNA is indicated by the amplification of β-globin. The BamH1 W fragment (298bp) is indicated. **M:** *Hinf1* digested ϕX-174 DNA size marker (fragment sizes in bp). **Lanes 1-6:** 10^5, 10^4, 10^3, 10^2, 10 and 1 Namalwa cell (s) in a background of 10^6 BJAB cells respectively **Lanes 7-21:** HIV-uninfected tonsils and lymph nodes.

Figure 68. Detection of EBV DNA in HIV-PGL tissue

68 A

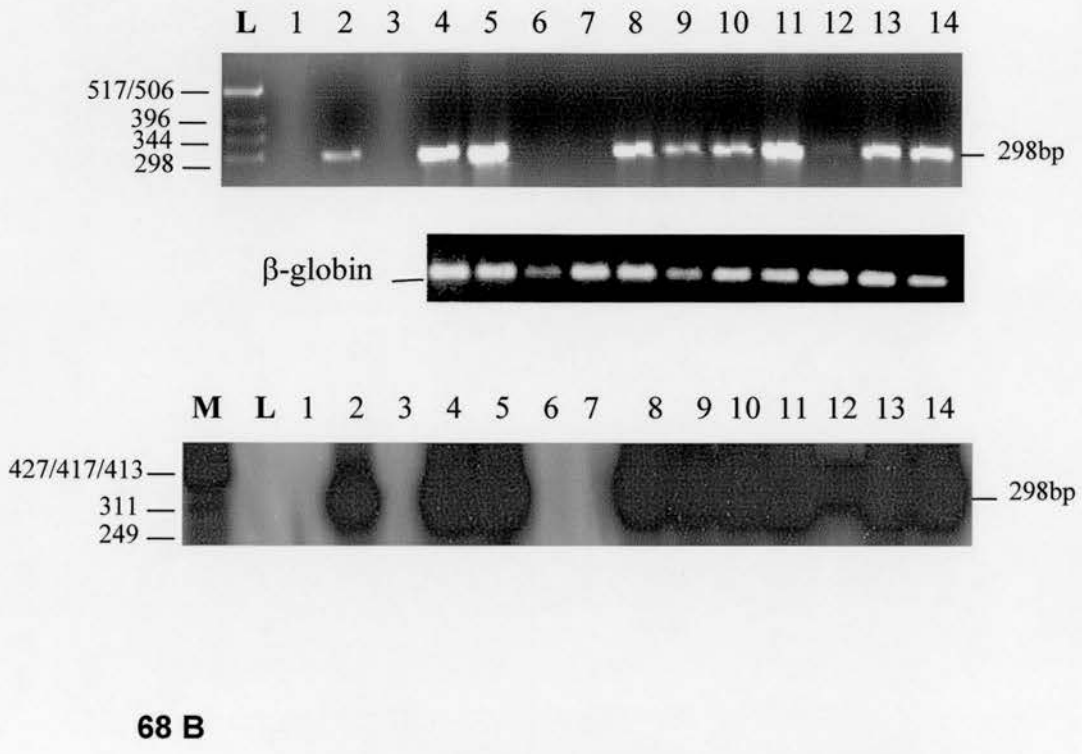

68 B

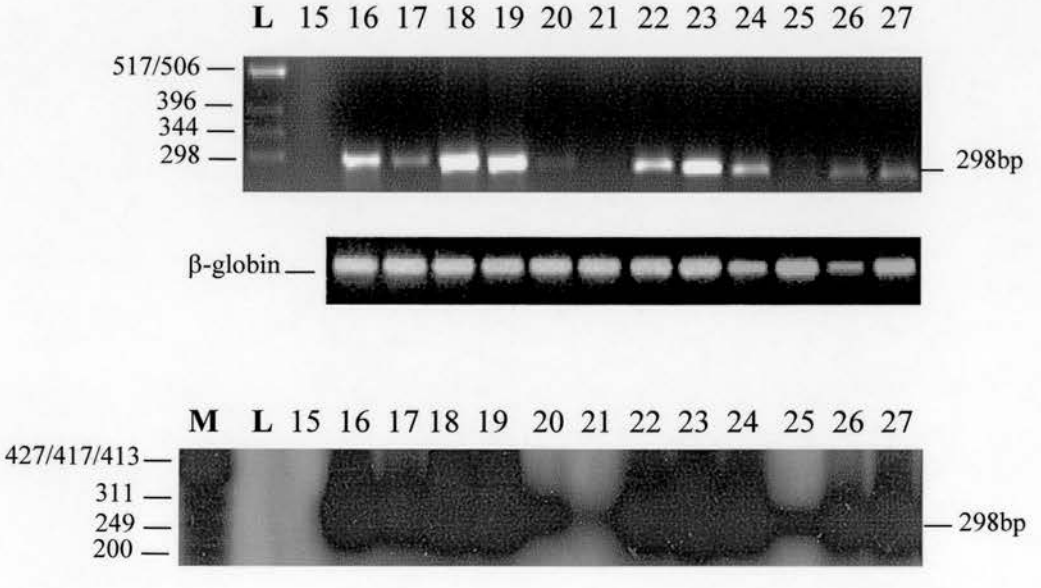

Figure 68. Detection of EBV DNA in HIV-PGL tissue. 28 cycles of PCR were carried out using BamH1 W primers. 20μl of the PCR product was resolved on a 2% w/v agarose gel and the bands were visualised under UV light. The PCR products were then transferred to Hybond N^+ membrane and hybridised with a ^{32}P-labelled oligonucleotide probe, specific to the amplified fragment.

DNA size markers: M: *Hinf1* digested ϕX-174 DNA size marker (fragment sizes in bp).
L: Unlabelled 1kb DNA size marker (fragment sizes in bp).

Figure 68 A. Lane 1: Blank **Lane 2:** 10^3 Namalwa cells **Lane 3:** Sterile distilled water **Lanes 4-14:** HIV-infected PGL samples. The BamH1 W fragment (298bp) is indicated.

Figure 68 B. Lane 15: Blank **Lanes 16 to 27:** HIV-infected PGL samples. The BamH1 W fragment (298bp) is indicated.

3.9.2 Detection of the presence and expression of KSHV

3.9.2.1 Analysis for the presence of the KSHV genome

The KSHV LNA PCR, which amplifies a 376bp fragment, was used to determine the KSHV status of the PGL and of control tissue.

To establish the sensitivity of the KSHV PCR using the LNA primers (Table 9, page 78), a ten-fold dilution series of the body cavity-based lymphoma cell line BCP-1 (which contains 30-50 copies of the KSHV genome per cell) was prepared in a background of 10^6 cells from a KSHV negative cell line, BJAB (see section 2.8.4). A 376bp fragment was detected at a dilution of 1 BCP-1 cell in a background of 10^6 BJAB cells (figure 69, lane 7), confirming the sensitivity of the LNA primers.

KSHV LNA was detected in 2 of 23 (8.7%) PGL samples (figure 69, lanes 12 and 18) and in none of the HIV-uninfected lymph nodes and tonsils (figure 70), despite the presence of amplifiable DNA as shown by amplification of β-globin from the same DNA samples.

Figure 69. Detection of KSHV DNA in HIV-PGL using LNA primers

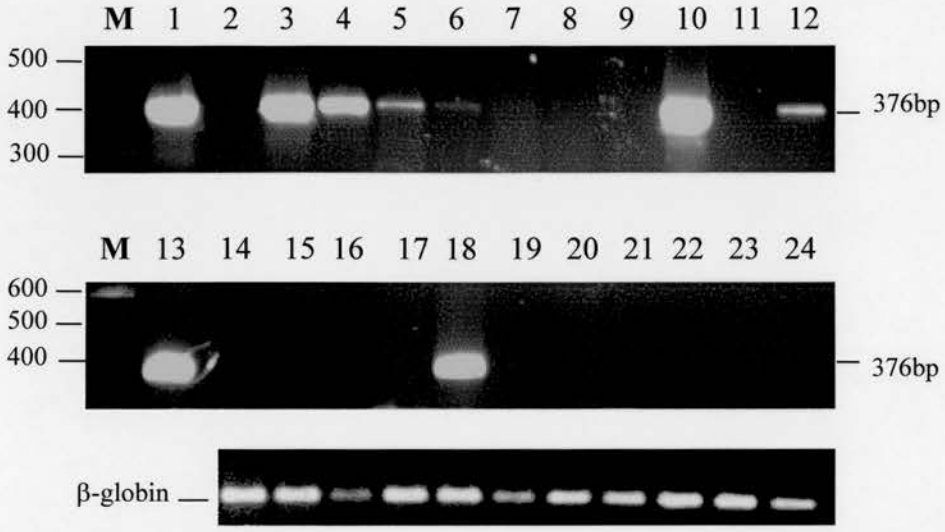

Figure 70. Detection of KSHV DNA in HIV-uninfected tissue using LNA primers

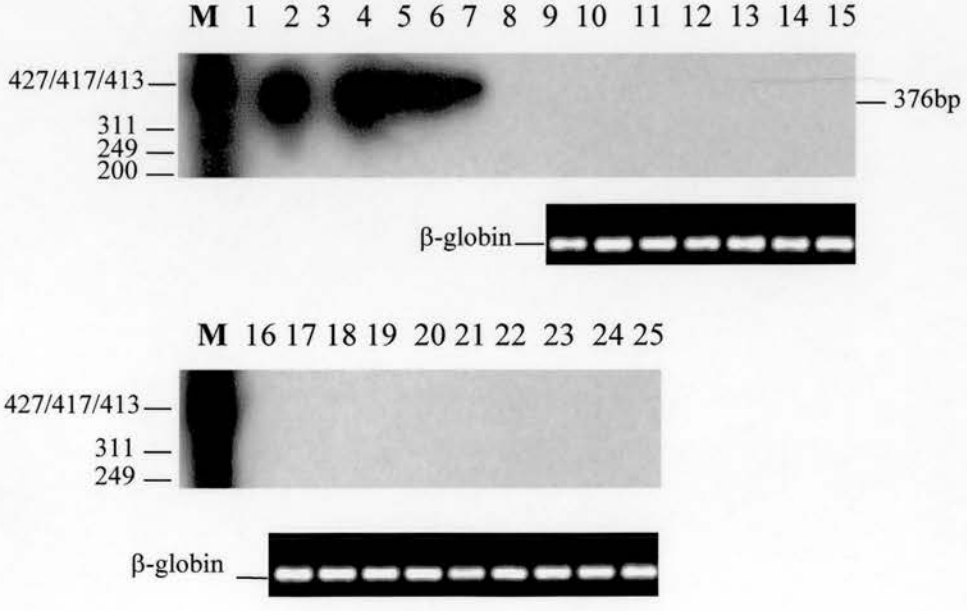

Figure 69. Detection of KSHV DNA in HIV-PGL using LNA primers. A ten-fold dilution series of the body cavity-based lymphoma cell line BCP-1 (which contains 30-50 copies of the KSHV gene per cell) was prepared in a background of 10^6 cells from the BJAB cell line, which lacks KSHV sequences. 35 cycles of PCR were performed on the dilution series and HIV-infected PGL tissue using LNA primers, after which 20μl of the PCR product was resolved on a 2% w/v agarose gel and visualised under UV light. **M:** 100bp DNA size marker (fragment sizes in bp). **Lane 1:** 10^5 BCP-1 cells **Lane 2:** Blank **Lanes 3-7:** 10^4, 10^3 10^2, 10 and 1 BCP-1 cell (s) respectively **Lane 8:** 10^6 BJAB cells **Lane 9:** Sterile distilled water **Lane 10:** 10^6 BCP-1 cells **Lane 11:** Blank **Lane 12:** PGL sample (LN 1) **Lane 13:** 10^4 BCP-1 cells **Lanes 14-24:** PGL samples. The LNA fragment (376bp) is indicated.

Figure 70. Detection of KSHV DNA in HIV-uninfected tissue using LNA primers. A ten-fold dilution series of the body cavity-based lymphoma cell line BCP-1 (which contains 30-50 copies of the KSHV gene per cell) was prepared in a background of 10^6 cells from the BJAB cell line, which lacks KSHV sequences. 35 cycles of PCR were performed on the dilution series and the HIV-uninfected tissue using LNA primers, after which 20μl of the PCR product was resolved on a 2% w/v agarose gel and visualised under UV light. The PCR products were then transferred to Hybond N^+ membrane and hybridised with a ^{32}P-labelled oligonucleotide probe. **M:** *Hinf1* digested ϕX-174 DNA size marker (fragment sizes in bp). **Lane 1:** Blank **Lane 2:** 10^5 BCP-1 cells **Lane 3:** 10^6 BJAB cells **Lanes 4-8:** 10^4, 10^3 10^2, 10 and 1 BCP-1 cell (s) respectively **Lanes 9-15:** HIV-uninfected tonsils **Lane 16:** Sterile distilled water **Lanes 17-25:** HIV-uninfected lymph nodes. The LNA fragment (376bp) is indicated.

3.9.2.2 Expression of a KSHV transcript encoding ORF 72

3 genes encoding KSHV v-FLIP (ORF 71), v-cyclin (ORF 72) and LNA (ORF 73) are transcribed from a single promoter as a polycistronic transcript and expressed during both the lytic and latent phases of the viral life cycle. A ~6kb transcript arises from the splicing of a small intron (499bp) in the 5' untranslated region, and further splicing of this transcript, yields a 1.7kb bicistronic message encoding v-cyclin and v-FLIP (Talbot *et al.*, 1999).

To analyse expression from this promoter and to further confirm the presence of KSHV detected by the LNA genomic PCR, a 35-cycle RT-PCR reaction was performed using a sense primer located in the 5' untranslated region of LNA and the antisense primer within the v-cyclin ORF. Primers and thermal cycling conditions are shown in Table 11, page 80 and Table 13, page 83). RT-PCR analysis revealed the presence of a >700bp transcript in one (LN 15) of the 23 PGL samples (figure 71A, lane 12). This sample also harboured KSHV DNA (figure 69, lane 18). Cloning (see section 2.17.1.3) and sequencing (see section 2.18.1) of the PCR product identified a 956bp transcript encoding a part of ORF72 and splicing out of LNA, using the LNA/v-cyclin splice donor site at position 127812 and the v-cyclin splice acceptor site at position 123777 (figure 71B). RNA was unavailable for the other PGL sample (LN1) that was positive for KSHV DNA (figure 69, lane 12). Therefore, KSHV gene expression could not be tested in this sample.

Figure 71. Expression of a KSHV transcript encoding ORF 72

71 A

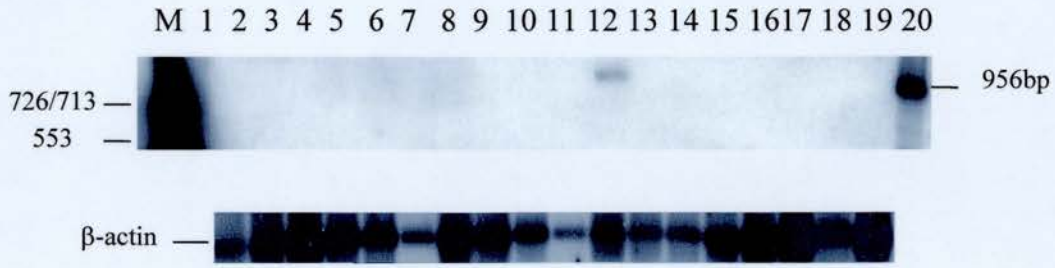

71 B

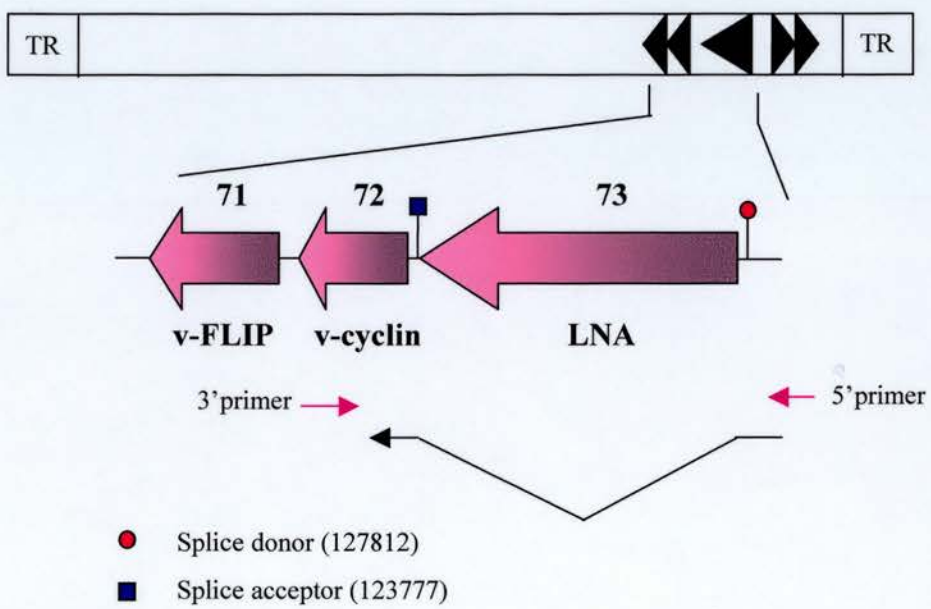

cDNA synthesised from 40ng of total RNA was subjected to amplification in a 35-cycle PCR reaction, using a sense primer located in the 5' untranslated region of LNA and the antisense primer within the v-cyclin ORF. 20μl of the product was resolved on a 1.5% w/v agarose gel, then transferred to a Hybond N^+ membrane and hybridised with a ^{32}P-labelled oligonucleotide probe, 23bp internal to the sense primer. **M:** *Hinf1* digested ϕX-174 DNA size marker (fragment sizes in bp). **Lane 1:** Sterile distilled water **Lanes 2 to 19:** PGL samples **Lane 20:** BCP-1 cell line. The v-cyclin/v-FLIP RT-PCR product (956bp) is indicated.

CHAPTER FOUR

DISCUSSION

AIDS-associated lymphomas represent a heterogeneous entity that is part of a continuum, ranging from benign polyclonal lymphoid hyperplasia, to aggressive high-grade malignancies most commonly of B cell origin (Meyer *et al.*, 1984). PGL is an early manifestation of HIV infection that is suggested to predispose to AIDS-related B-NHL (Abrams *et al.*, 1986; Pelicci *et al.*, 1986b; Alonso *et al.*, 1987). It is now recognised that the majority of individuals with PGL do not, however, progress to lymphoma, implying that additional molecular genetic events are required to facilitate lymphomagenesis. Identification of these events would not only provide insights into mechanisms that promote neoplastic transformation in the setting of altered immunity, but also help define molecular markers with potential utility in diagnosis and prognosis.

Molecular genetic changes in AIDS-related lymphomas have been described by a number of authors (Ballerini *et al.*, 1993; Gaidano *et al.*, 1997b, Gaidano *et al.*, 1997d, Lo Coco *et al.*, 1994). However, only a few studies have performed molecular genetic analyses in AIDS-associated lymphadenopathy (Alonso *et al.*, 1987; Pelicci *et al.*, 1986b). Therefore, in this thesis, a molecular genetic and virological study of PGL was performed. Structural, epigenetic and expression changes were analysed in genomic DNA and RNA from lymph nodes of HIV-infected individuals with PGL syndrome and in a control group of reactive lymph nodes and tonsils from HIV-uninfected individuals. The changes identified are discussed in the context of a model of multi-step carcinogenesis occurring in the chronically immunocompromised host.

Analysis of tumour suppressor genes

4.1 p53 mutations are detectable in some cases of PGL

p53 mutations have been identified in approximately 50% of human cancers (reviewed in section 1.3.4 and Levine, 1997). In AIDS-NHL, mutations in p53 occur at a frequency of around 30-40%, clustering predominantly in the small non-cleaved cell lymphoma sub-type (60%), and to a lesser extent in immunoblastic lymphomas

(14%) (Ballerini *et al.*, 1993; Nakamura *et al.*, 1993). These findings prompted a structural analysis of p53 in PGL. Using established SSCP and DNA sequencing methodology, p53 mutations were detected in 6/23 PGL samples. Of these, one was a non-coding sequence change, whilst a second mutation was deletion of a single 'G' residue in codon 361 causing a frame-shift of -1 and termination in codon 369. The remaining 4 were point mutations, all occurring in exon 7 and each resulting in amino acid substitutions (Table 28, page 138). Searching of the International Agency for Research on Cancer (IARC) *TP53* mutation database revealed that each of the missense mutations detected in this study has been previously described (http://www.iarc.fr/p53/Index.html). Moreover, each mutation affects conserved amino acids important to p53 function, suggesting that wild-type p53 function will be compromised as a result of the mutation. Taken together, these considerations support the hypothesis that mutation in p53 may be an early molecular genetic change in HIV-associated lymphomagenesis, at least in a subset of cases.

It is interesting and instructive to consider the selective advantage imparted to cells containing p53 mutations in the context of HIV infection. One possibility is that loss of wild-type p53 function confers a replicative advantage to HIV, and that this, rather than selective pressure for growth advantage to the host cell is the mechanism for the outgrowth of clones containing p53 mutations. This hypothesis is supported by the ability of p53 mutants to transactivate the LTR of HIV-1 (Subler *et al.*, 1994). Furthermore, wild-type p53 is a potent suppressor of Tat-dependent HIV LTR transcription, whereas, in turn, Tat can inhibit p53-mediated transactivation (Li *et al.*, 1995). In this model, it is proposed that mutations in p53 would abrogate the repressive effects of the protein on HIV replication, resulting in increased levels of Tat. A second model envisages that mutations are selected as a result of the growth advantage, due to loss of one or more of the wild-type functions of p53, conferred to the host cell, rather than HIV. Such a hypothesis has been proposed in many models of multi-step carcinogenesis (Fearon and Vogelstein, 1990). The properties of the p53 mutants detected in the PGL samples have not been formally investigated in the present study. However, based on previous studies, it is highly likely that such mutants will be functionally compromised (Raycroft *et al.*, 1990; Rowan *et al.*,

1996). A third possibility which merits consideration is suggested by the observation that apoptosis of HIV-infected B and T cells may occur through a p53-dependent pathway (Genini *et al.*, 2001). In this study, it was demonstrated that HIV activates a p53-dependent apoptotic program in $CD4^+$ T cells, through the release of cytochrome c and subsequent caspase induction. It is possible therefore, that HIV may induce a similar p53-regulated death program in B cells and that functional inactivation of the gene by mutation would inhibit such a pathway. Whichever of these possibilities is the underlying mechanism, it is likely that cells expressing mutant p53 will possess a selective growth advantage over those with wild-type p53.

It is intriguing that p53 mutations are detectable in PGL, at a stage significantly preceding clinical presentation of lymphoma. As such, it is clearly of interest to question (i) whether such mutations function as initiating genetic events in lymphomagenesis, and /or (ii) whether the detection of such mutations is predictive of future development of lymphoma. When considering the possibility that p53 mutation may initiate lymphomagenesis, it is pertinent to note that mutations are consistently absent in most AIDS-DLCLs and AIDS-PELs, although present in 60% of AIDS-SNCCL (Ballerini *et al.*, 1993; Carbone *et al.*, 1996b). This clearly demonstrates that mutation in p53 is not an obligatory genetic change during AIDS-associated lymphomagenesis. However, it is particularly attractive to hypothesise that the cases of PGL with detectable p53 mutations are those which may subsequently progress to p53 mutant lymphomas. This hypothesis is certainly viable in the context of AIDS-SNCCL sub-type in which p53 mutation occurs commonly (see above, Ballerini *et al.*, 1993; Gaidano *et al.*, 1997b). It is therefore entirely possible that p53 mutation may represent an initiating or at least early molecular event in this subset of lymphomas. Such lymphomas typically harbour chromosomal translocations involving the c-*myc* gene. Analysis of PGL for such translocations, was however, uniformly negative (see later). A study of additional samples will be required to further define the role of p53 mutation in AIDS-associated lymphomagenesis.

The presence of p53 mutations in PGL also raises the possibility that they may have

use as molecular markers predictive of future lymphoma development. This can only be definitively tested in cases where both PGL and lymphoma are available from the same individual(s) for p53 analysis. Unfortunately, it is unknown which individuals with PGL in the present series subsequently developed lymphoma and therefore this issue cannot be addressed, but would clearly merit such an approach when suitable tissue becomes available.

An interesting finding in the present study was the detection of a silent p53 mutation in genomic DNA from the tonsil of an HIV-uninfected, healthy individual. It was first important to exclude the possibility that this is due to experimental artefact. This is unlikely to be the case since SSCP analysis of this DNA revealed a distinct mobility shift consistent with the presence of a mutation (figure 34, page 132). Moreover, the DNA was re-amplified using a thermostable DNA polymerase, *Pfx*, which has an extremely high degree of replication fidelity (see Table 27, page 130), before subsequent cloning and sequencing. The presence of the same mutation in multiple independent plasmid clones further argues strongly against the possibility that errors arising in cloning or amplification account for the presence of this mutation. Experimental studies of p53 mutations in healthy individuals are limited (Mao *et al.*, 1996; Lazarus *et al.*, 1995). However, in a recent analysis of base substitution mutations, Wilson and co-workers reported that p53 mutations in codon 248 were detectable in the circulating peripheral blood lymphocytes of 22% of normal individuals. This remarkably high frequency of mutations was thought to be due to the presence of a highly mutable CpG site (Wilson *et al.*, 2000). In the present study, such a high frequency of mutations was not observed, although this may be attributable to the different methodologies employed. The SSCP technique used here is able to detect mutations at a frequency of 5% mutant alleles (T. Crook, personal communication), whereas the Needle-in-a-haystack mutation assay employed by Wilson *et al* had a detection sensitivity of one cell in a million. Silent mutations have been reported at variable frequencies in several tumour types. Such mutations play no role in tumour development, but, according to some authorities are sensitive indicators of genomic instability and hence of random mutation within a tissue or cell type (Strauss, 2000).

4.2 Exon 2 deleted isoforms of p73 (Δ2 p73) are over-expressed in PGL

The discovery of 2 novel members of the p53 family, p63 and p73, during the course of this study, prompted an investigation into their possible role(s) in PGL and predictive value, if any, in the development of AIDS-NHL. The extreme infrequency of somatic mutations in p63 and p73 in human cancer (Osada *et al.*, 1998; Ichimiya *et al.*, 1999) has raised doubts as to the tumour suppressor function of the two proteins. However, it is now clear that mechanisms of inactivation independent of mutation occur in human cancer. For example, specific p53 mutants are able to abrogate p63 and p73 function via formation of heterotypic protein-protein complexes (Di Como *et al.*, 1999; Marin *et al.*, 2000). Furthermore, p73 has been shown to be subject to methylation-dependent transcriptional silencing in some haematological malignancies (Corn *et al.*, 1999).
Alternative splicing of both p63 and p73 generates multiple isoforms, differing at both N- and C-termini (Yang *et al.*, 1998; De Laurenzi *et al.*, 1998, 1999 and see section 1.4.1). The N-terminal variants of p73 (Δ2 p73) and p63 (ΔN p63) can behave in a dominant negative manner with respect to their full-length counterparts and wild-type p53. The Δ2 form of p73 inhibits full-length p73 and p53, whereas ΔN p63 inhibits wild-type p53 (Pozniak *et al.*, 2000; Yang *et al.*, 1998).

Little is known, however, of the patterns of expression of p63 and p73 in normal and neoplastic lymphoid tissues. Neither is it known by which mechanism (if any) p63 and p73 are inactivated in AIDS-NHL. These questions were addressed in the present study by RT-PCR expression analysis of full-length and deleted variants of p63 and p73 and also by analysis of CpG methylation in the p73 promoter by methylation-specific PCR (MSP).

In initial work, expression of C-terminal splice variants of p73 was investigated and these analyses revealed that p73 mRNA was expressed in all cases of PGL. In contrast, p73 expression was detected in approximately 50% of control, reactive tonsil and lymph node tissues. Importantly, the steady-state level of p73 mRNA was markedly higher in the majority of cases of PGL than in controls (figures 43A and B,

page 143). These observations reveal that p73 over-expression is common in PGL. A further significant finding was afforded by the observation of qualitative differences in expression of p73 isoforms between PGL and controls. Whereas only 3 variants (α, β and γ) were identified in the HIV-uninfected tissue, at least 5 isoforms (α, β, γ, ε and ζ) were detected in PGL. The predominance of the p73 α and β variants in both PGL and control tissues is consistent with previous analyses of other tissues (Yang *et al.*, 1998; Ozaki *et al.*, 1999). Although the γ isoform was expressed to a similar extent as the α and β variants in PGL tissue, this isoform was detected in only 3/16 (18%) HIV-uninfected normal tissue. Two recently described splice variants, ε and ζ, were weakly expressed in the PGL tissue but were consistently absent in the uninfected tissue. Taken together, these experiments clearly indicate both quantitative and qualitative differences in expression of p73 between HIV-infected and uninfected lymphoid tissue. Interestingly, the expression pattern of p73 isoforms in control vulval (epithelial) tissue was different to that observed in lymphoid tissue, with expression of the α, γ, ζ and δ but not the β isoforms in normal vulval epithelium. In contrast, whereas the β form was readily detectable in lymphoid tissue in the present study, the δ form could not be detected. These results suggest that different C-terminal variants have distinct roles in different tissues *in vivo*.

Over-expression of p73 relative to surrounding normal tissue has been observed in several cancers, including prostate, breast, lung, colorectal and bladder carcinomas (reviewed in Ikawa *et al.*, 1999). The high frequency of p73 over-expression in PGL is, therefore an intriguing observation as it reveals clear similarity between PGL and common carcinomas. Having demonstrated over-expression of p73 mRNA in PGL, it was important to determine whether this was the full-length form or the more recently described Δ2 variant which lacks exon 2. RT-PCR analysis revealed that Δ2 variant was the only form expressed in both PGL and in p73-expressing control lymphoid tissue. Interestingly, expression of the Δ2 form of p73 was accompanied by the absence of full-length p73 in all the samples tested. Previous studies of Δ2 p73 have been limited, but expression has been described in malignant but not normal ovarian epithelium (Ng *et al.*, 2000), in breast cancer cell lines (Fillippovich *et al.*, 2001) and also in the developing neurons of mice (Pozniak *et al.*, 2000).

What then are the mechanistic and biological implications of the over-expression of various forms of p73 in PGL? One possibility is that over-expressed full-length p73 competitively inhibits p53-dependent transactivation of p53-responsive promoters (Ueda *et al.*, 1999). If this mechanism operates in PGL, attenuation of p53-dependent transactivation would result from over-expression of p73. In view of the predominant detection of Δ2 forms of p73, the most likely effect of p73 over-expression is trans-dominant inhibition of wild-type p53 and of full-length p73, since both activities have been clearly attributed to Δ2 p73 (Fillippovich *et al.*, 2001; Pozniak *et al.*, 2000).

4.3 Aberrant hypermethylation of p73 is not a feature of PGL

Hypermethylation of the promoter region of p73 was examined by methylation-specific PCR (MSP), given that silencing of p73 by this mechanism is operative in specific haematological malignancies, but not in normal lymphocytes (Kawano *et al.*, 1999; Corn *et al.*, 1999). The absence of aberrant hypermethylation of p73 in this study was well supported by the observation of mRNA expression in all the PGL samples analysed, indicating that epigenetic silencing of p73 is not a feature of HIV-infected PGL. The detection of 1/1000 methylated alleles, established in preliminary studies of the sensitivity of MSP, in a background of unmethylated DNA, excluded possible lack of sensitivity of the MSP analysis used in this study as the reason. A point to note is that p73 may be functionally compromised by mechanisms other than epigenetic silencing of the promoter region. This hypothesis is supported by the observation that a subset of p53 mutants can bind and inhibit the transcriptional activity of various isoforms of p73 (Marin *et al.*, 2000; (Gaiddon *et al.*, 2001). Although yet to be formally demonstrated, it is conceivable that the p53 mutants detected in this study have similar trans-dominant properties with regards p73.

4.4 Over-expression of the TA, but not the ΔN isoform of p63 occurs in PGL

RT-PCR analysis of PGL and control lymphoid tissues revealed a difference in patterns of expression. The TA isoform was predominantly expressed in HIV-

infected and uninfected lymph nodes and in one tonsil. In contrast, expression of the ΔN isoform was strictly limited to the HIV-uninfected tonsils, with expression of this isoform being undetectable in the PGL cases. The most likely explanation for the expression of the ΔN isoform in non-PGL lymphoid tissue is that this expression is in the epithelial tissue within the tonsils. This hypothesis is favoured by data from other studies which indicate an epithelial-specific expression of ΔN p63 in both normal and malignant tissue (Yang *et al.*, 1998; Crook *et al.*, 2000), but clearly requires immunocytochemical analysis for verification. It is unclear, however, why the ΔN isoform is expressed in reactive nodes and tonsils, but not, apparently, in PGL. Again, immunocytochemistry might provide insight as to whether this is a reflection of the absence of epithelial tissue in PGL nodes or whether isoform switching has occurred. In any case, the biological significance of expression of TA p63 in PGL and in other lymphoid tissues awaits clarification.

The absence of somatic mutations in p63 has led some authors to question the putative tumour suppressor role of this gene. Similar to p73, there is now evidence that specific mutant forms of p53 can exert trans-dominant inhibitory effects on the function of p63 (Gaiddon *et al.*, 2001), suggesting that alternative mechanisms of inactivation may occur in some cancers. The presence of p53 mutations within some PGL cases expressing TA p63, suggests that inhibition of p63 function by these mutants might be operative at least in these cases.

Over-expression of ΔN p63 occurs in some squamous carcinomas. For example, Yamaguchi *et al* (2000) reported amplification and over-expression of ΔN p63 in head and neck cancer, consistent with a potential oncogenic function (Yamaguchi *et al.*, 2000). Similarly, over-expression of ΔN p63 was observed invariably in undifferentiated NPC, wherein it was proposed that over-expression of ΔN p63 might function via trans-dominant inhibition to counteract the negative growth regulatory effects of over-expressed wild-type p53 protein, which characterises this cancer (Crook *et al.*, 2000). In any case, data from this study do not support a role, either tumour suppressor or oncogenic, for this gene in the pathogenesis of PGL.

4.5 Lack of involvement of the INK4 locus in the pathogenesis of PGL

The *INK4* locus contains 3 genes, $p16^{INK4a}$, $p15^{INK4b}$ and $p14^{ARF}$ that function in pRb- and p53-dependent pathways of tumour suppression (see section 1.5). In cases of PGL which lack mutations in p53, it was of interest to determine whether alterations occur in $p14^{ARF}$ which might functionally substitute for such mutations. In the case of *RB*, no mutations have been reported in AIDS-NHL. As such, it was important to determine whether the $p16^{INK4a}$ and $p15^{INK4b}$ genes are subject to genetic or epigenetic changes, which might themselves compromise pRb function.

A *bona fide* tumour suppressor role for $p16^{INK4a}$ has been firmly established (Kamb *et al.*, 1994; Hussussian *et al.*, 1994). Inactivation of the gene by homozygous deletion, mutation, and/or methylation has been observed in a diverse range of human cancers (reviewed in Ruas and Peters, 1998 and see section 1.5). Abnormalities in $p15^{INK4b}$ and $p16^{INK4a}$ occur commonly in B cell lymphomas, with aberrant hypermethylation being the most common mechanism of inactivation (Klangby *et al.*, 1998; Baur *et al.*, 1999). The status of the gene in lymphomas affecting HIV-infected individuals is, however, unknown. Therefore, a detailed analysis of the mutation status, methylation and expression pattern of the *INK4* locus was performed in HIV-PGL.

4.5.1 No evidence for mutation or hypermethylation in *INK4a*

SSCP analysis of exon 1α and 2 of *INK4a* did not reveal any abnormally migrating bands indicative of mutations. This result is consistent with studies of B cell lymphomas in which inactivation of the gene by point mutation was shown to be a relatively uncommon event (Ruas and Peters, 1998; Uchida *et al.*, 1995). No attempt was made to examine the *INK4* locus for genomic deletion in the present study. Not all germinal centre (GC) B cells in PGL lymph nodes are maintained in an equivalent hyperproliferative state, and as such the proportion of "normal" B cells in each sample cannot be assessed, making interpretation of deletion analysis unreliable. In the absence of point mutations in the coding sequence of the gene, a study of gene deletion would be of obvious value and interest, but would require the availability of

micro-dissected malignant and matched normal tissue for each case.

Aberrant hypermethylation is a common mechanism of inactivation of $p16^{INK4a}$ in NHL occurring in immunocompetent individuals (Baur *et al.*, 1999; Klangby *et al.*, 1998). MSP was therefore utilised to seek evidence of aberrant CpG hypermethylation in the $p16^{INK4a}$ gene in the series of PGL. However, no evidence of CpG methylation in exon 1α was observed in this study. It should be noted that the sensitivity of the MSP technique to detect hypermethylated alleles of $p16^{INK4a}$ had been carefully titrated in initial experiments using genomic DNA from the Raji cell line, in which both $p16^{INK4a}$ alleles are methylated. Methylated $p16^{INK4a}$ DNA was readily detectable at a dilution of 1:1000, suggesting that the inability to detect CpG methylation in the PGL samples is unlikely to be attributable to sensitivity limitations. Moreover, RT-PCR analysis revealed that $p16^{INK4a}$ mRNA was detectable in all samples analysed. Although the presence of some normal tissue in the PGL samples is a potential complicating factor in interpretation of these RT-PCR studies, expression of $p16^{INK4a}$ RNA is, nonetheless, consistent with the absence of gene methylation. Immunocytochemical analysis would provide definitive evidence of $p16^{INK4a}$ expression in PGL, but suitable tissue sections were not available in the present study.

4.5.2 No evidence for abnormalities of $p15^{INK4b}$ in PGL

$p15^{INK4b}$ is a tumour suppressor gene located adjacent to the $p16^{INK4a}$ gene on chromosome 9p21. Inactivation of $p15^{INK4b}$ in human cancers may occur by deletion, which is often, but not invariably, accompanied by simultaneous loss of $p16^{INK4a}$ (Drexler, 1998). Mutations in $p15^{INK4b}$ are extremely rare in human cancers in general and are virtually absent in NHLs (Gombart *et al.*, 1995; Koduru *et al.*, 1995). The gene is, however, frequently inactivated (>70%) by methylation in acute leukaemias of the myeloid and lymphoblastic subtypes, and to a lesser extent in B-NHL (11%). A distinct role for this gene has been indicated in murine T-cell lymphomas, wherein gene inactivation was found to be independent of $p16^{INK4a}$ alterations (Malumbres *et al.*, 1997). Again, because of the lack of micro-dissected PGL biopsy material available for analysis, examination of gene deletion was not

attempted and work in the present study was focused on examination of the methylation status and mRNA expression pattern of the gene. No evidence was obtained for methylation of $p15^{INK4b}$ in any of the PGL samples analysed, despite preliminary studies showing the adequate sensitivity of the MSP conditions employed. Consistent with the lack of methylation, RT-PCR analysis revealed abundant expression of $p15^{INK4b}$ mRNA in all the PGL lymph nodes analysed, although expression was absent in 8/16 uninfected controls (7 lymph nodes and one tonsil). It is likely therefore, that $p15^{INK4b}$ is expressed in the hyperproliferating GC B cells of PGL tissue, although definitive conclusions can be drawn only after immunocytochemical examination of tissue sections or genetic analysis of micro-dissected material.

In conclusion, no evidence was obtained in the present study to support genetic or epigenetic inactivation of the $p16^{INK4a}$ and $p15^{INK4b}$ genes in PGL and the results, as such, do not support a contributory role for these genes in the pathogenesis of PGL. Structural and epigenetic alterations affecting the *INK4* locus have previously been reported to correlate with aggressive high-grade tumours and with the histological transformation/progression of indolent lymphomas (Garcia-Sanz *et al.*, 1997; Pinyol *et al.*, 1998; Villuendas *et al.*, 1998). With regards to the findings in this study, it is hypothesised that the absence of detectable mutations and aberrant hypermethylation in the *INK4* genes analysed may reflect the fact that such abnormalities occur late in HIV-associated lymphomagenesis, probably as secondary genetic events contributing to the more aggressive biological nature of lymphomas.

4.5.3 Analysis of $p14^{ARF}$ in PGL

Inactivation of the p53 pathway can occur by a number of mechanisms in cancer. These include, loss of function of p53, alteration of *ARF*, or alternatively over-expression of hMDM2 (Eischen *et al.*, 1999; Sanchez-Cespedes *et al.*, 1999). Functional inactivation of *ARF* by deletion and less frequently by mutation, often but not always, occurs concurrently with alterations in *INK4a* (Ruas and Peters, 1998). Their concomitant disruption has been associated with progression and a poor prognosis in up to 40% of aggressive NHLs (Pinyol *et al.*, 2000; Gronbaek *et al.*,

2000). These observations suggested the possibility of $p14^{ARF}$ abnormalities in PGL. SSCP analysis of exon 1β however, revealed no abnormally migrating conformers suggestive of mutation in any of the PGL cases. This is consistent with reports from previous studies (Pinyol *et al.*, 2000; Tanaka *et al.*, 1997).

Deletions targeting the *INK4a/ARF* locus commonly inactivate both $p16^{INK4a}$ and ARF, whereas cancer-associated mutations within exon 2 of the mouse *INK4a* gene have been shown to specifically target $p16^{INK4a}$, and not $p19^{ARF}$, for inactivation (Quelle *et al.*, 1997). Conversely, mutations in human *ARF* exon 2 have been shown to disrupt its nucleolar localisation and impair its ability to block nuclear export of hMDM2 and p53 and subsequent p53 stabilisation (Zhang and Xiong, 1999). Furthermore, Rizos *et al* have shown that in the human *ARF* gene the carboxy-terminal nucleolar localisation domain lies within the shared *INK4a/ARF* exon 2 and is mutated in some melanoma-prone kindreds (Rizos *et al.*, 2000). However, mutations in exon 2 were not observed in the present study, and therefore it is reasonable to conclude that ARF inactivation by point mutations is not a characteristic feature of HIV-associated PGL.

An inverse correlation between p53 and ARF expression/inactivation in human tumours has been suggested by some investigators, consistent with the theory that they are functionally linked in the same pathway (Stott *et al.*, 1998; Vonlanthen *et al.*, 1998). The expression of $p14^{ARF}$ was, therefore, examined by RT-PCR using cycling conditions determined in preliminary experiments to be in the exponential phase of amplification. Despite the evidence that p53 negatively regulates the expression of ARF and generally increased levels of endogenous ARF mRNA and protein are observed in cells that lack functional p53 (Stott *et al.*, 1998), such findings were not validated in this study. Of note, $p14^{ARF}$ protein expression was not examined in this study, due to lack of suitable tissue sections for immunocytochemical analysis. Expression of ARF mRNA was observed in both the HIV-infected and uninfected samples investigated, independent of their p53 mutational status. There are several explanations that may account for the apparent lack of reciprocity between expression of ARF and p53. One is that the p53

mutations documented in this study do not abrogate its function and hence ARF expression would be under the normal regulatory control of p53. Although unlikely, without formal testing of each mutant, this hypothesis cannot be disproved. Secondly, in cases in which p53 is functionally compromised by such mutations, it is possible that ARF expression is regulated by a p53-independent mechanism. Recently, ARF has been shown to act independently of the hMDM2-p53 pathway, by arresting cell growth in mice that were lacking in p53 alone or both p53 and hMDM2 (Weber *et al.*, 2000). Finally, contrary to evidence that p53 and ARF are inversely correlated, in lung cancer it has been demonstrated that inactivation of ARF and mutation of p53 are not mutually exclusive events (Gazzeri *et al.*, 1998; Sanchez-Cespedes *et al.*, 1999). Additionally, post-transcriptional modification was suggested to account for the discrepancy observed between ARF mRNA and protein expression (absence of protein in tumours with detectable mRNA) in these tumours (Gazzeri *et al.*, 1998). A plausible theory in the present context would be that in cells with mutant p53, post-transcriptional modification of ARF mRNA occurs, despite apparently normal levels of the β transcript. However, this hypothesis can be confirmed only by immunocytochemical staining of the lymph node tissue for ARF protein expression. It should be re-emphasised here that the complicating effects of "normal" B cells in PGL nodes on the analysis of mRNA levels are not known, and again micro-dissected tissue would prove invaluable in validating the above findings.

Epigenetic silencing of ARF by promoter hypermethylation has been demonstrated in gastric and colorectal cancer (Iida *et al.*, 2000; Esteller *et al.*, 2000), and infrequently in murine lymphomas. Future studies of methylation of $p14^{ARF}$, combined with immunocytochemical analysis of protein expression would be of obvious interest in NHL and PGL.

Analysis of oncogenes

Given the importance of deregulated oncogene expression in the pathogenesis of certain B cell lymphomas in both the immune-competent and -compromised host, alterations including chromosomal translocations and mutations in relevant genes

such as c-*myc*, *bcl-2* and *bcl-6* were investigated in the present study.

4.6 Absence of c-*myc*/*IgH* translocations in PGL

Chromosomal translocations juxtaposing the c-*myc* and immunoglobulin genes are an invariant feature of Burkitt's lymphoma (BL) in the immunocompetent host (Dalla-Favera *et al.*, 1982b). Although, this translocation is also invariably present in AIDS-BL, it is detected in only 20-50% of AIDS large-cell lymphomas (Ballerini *et al.*, 1993; Delecluse *et al.*, 1993b). Recombination in AIDS-BL, commonly involves the first exon or first intron of the c-*myc* gene and the switch regions of the *IgH* locus, similar to sBL (Pelicci *et al.*, 1986a; Ballerini *et al.*, 1993). Taken together, these observations suggested that c-*myc* translocation might occur in HIV-PGL. This was addressed in the present study by use of a LD-PCR assay to amplify the t(8:14) translocation breakpoint.

The translocation was however, not detected in any of the PGL samples. One possibility is that the LD-PCR assay used is insufficiently sensitive to detect a low frequency of translocations occurring in a background of normal lymphocytes. However, the assay used in this study is able to detect 1 translocation-positive cell in a background of 10^3 normal lymphoblastoid cells and this sensitivity is comparable to that used in previous studies to detect c-*myc* translocations in BL (Akasaka *et al.*, 1996; Basso *et al.*, 1999). Nevertheless it is worth considering the possibility that a minor population of translocation-bearing cells characteristic of an initiating event in a single clone of cells will escape detection, whereas the greater number of translocations present in BL tumours will be readily detected. Arguing against this was the surprising discovery of a translocation event in an HIV-uninfected lymph node (case no. 2435). It is highly likely that this translocation is present in only a minority of cells within the normal lymph node. For this reason it is highly improbable that the failure to detect similar translocations in PGL is attributable to lack of sensitivity.

The second possibility is that PGL is not *per se* a precursor of HIV-associated BL. A

third interpretation is that such translocations occur as later events in lymphomagenesis. Polack *et al* (1996) made the intriguing observation that activation of c-*myc* in EBV-immortalised, B lymphocytes rendered growth of the cells independent of EBV-encoded proteins. These studies suggested a model of lymphomagenesis in which c-*myc* activation occurs subsequent to an initial immortalisation step effected by EBV (Polack *et al.*, 1996). This model is particularly interesting in the light of the observation that EBV was present at a high copy-number in 23/23 lymph nodes of HIV-infected individuals with PGL (see later).

Cloning and sequencing of the PCR product from case 2435, identified a reciprocal exchange of chromosomal segments involving the 5' flanking region, 424bp upstream of the ATG in the first exon of c-*myc*, and the switch gamma 4 (*Sγ*) region of the *Ig* locus. Surprisingly, the breakpoint was detected in 5/5 translocation-bearing clones, indicating possible clonal outgrowth of a cell that may have a distinct survival advantage as a result of the translocation event. This hypothesis is currently under investigation. Of further interest, was the identification of a run of 5 nucleotides, mapping to neither the c-*myc* gene nor the *Sγ* region at the inter-chromosomal junction of the breakpoint. In a study of c-*myc* translocations in murine plasmacytomas, Gerondakis and colleagues have observed deletions, duplications and/or small insertions at most of the breakpoint junctions sequenced (Gerondakis *et al.*, 1984). The authors believe that the insertion of residues is a result of competing polymerase (repair) and exonuclease activities following single-stranded breaks in either chromosome.

The observation of a c-*myc* translocation in an apparently healthy individual is not unique. In a study of t(8:14) recombinations in the blood lymphocytes of HIV-infected and uninfected homosexual men, c-*myc* translocation-bearing clones have been detected at a frequency of 10.5% and 2% respectively (Muller *et al.*, 1995). In addition, c-*myc* deregulation by chromosomal recombination is believed to be associated with the normal physiological process of B cell differentiation, increasing in frequency with antigenic stimulation (Roschke *et al.*, 1997). It may be pertinent in this respect that the lymph node in which the translocation was identified was

"reactive", implying that an active immune response was in progress at the time of biopsy. The clinical history and follow-up of the individual in whom the translocation was detected is not available. Nevertheless, it is known that the individual had no evidence of a lymphoma at the time of biopsy. The presence of a c-*myc* translocation event in the absence of detectable lymphoma in case 2435 can readily be explained by the fact that secondary "hits" by co-operating oncogenes are required for tumourigenesis to occur (Land *et al.*, 1983). This hypothesis is supported by the fact that, in this individual, no abnormalities were detected in any of the genes analysed in this study. Furthermore, EBV, which is believed to have a contributory role in the development of BL, was below the detectable level (sensitivity of PCR assay was <10 genomes). Therefore, it is possible that in this case subsequent aberrant alterations in oncogenes and/or tumour suppressor genes, not analysed in this study, maybe required for malignant transformation to occur.

Although the finding of a c-*myc* translocation in a healthy individual is of interest, the most important conclusion to be drawn from the above observations is that such translocations were not detectable in PGL. It will be of interest to determine whether the deregulation or stability of c-*myc* in PGL is affected by mechanisms other than translocation. This would involve mutations, which have been shown to occur in the exon1/intron1 regions (Cesarman *et al.*, 1987; Bhatia *et al.*, 1994) or within the transactivation domains of c-*myc* (Salghetti *et al.*, 1999; Gu *et al.*, 1994).

4.7 *bcl-2/IgH* translocations are not detected in PGL

Another translocation involving the Ig loci, and observed in more than 70% of follicular lymphomas and 20% of diffuse B cell lymphomas in the immunocompetent host, is the t(14:18), which involves the *bcl-2* gene on chromosome 18 resulting in its deregulated expression (Yunis *et al.*, 1987; Weiss *et al.*, 1987). The relatively few studies that have looked for *bcl-2* alterations in AIDS-associated lymphomas have found no evidence of *bcl-2/IgH* rearrangements (Subar *et al.*, 1988; Gaidano *et al.*, 1997b; Davi *et al.*, 1998). Furthermore, t(14:18) rearrangements have also been detected in the peripheral blood B cells of up to 60% of healthy individuals (Limpens *et al.*, 1991, 1995; Aster *et al.*, 1992; Liu *et al.*, 1997). These studies, however, have

only examined breakpoints within defined regions, the MBR and mcr, which harbour roughly 70% of translocations. In the present study, utilisation of the primers designed by Akasaka *et al* (1998), allowed for the detection of breakpoints 5' of the mcr and 3' of the MBR, including >20kb of intervening sequence (Akasaka *et al.*, 1998). This region has been shown to harbour approximately 30% of translocations (Akasaka *et al.*, 1998). Despite the comprehensive methodology employed, no rearrangements were detected in the present study in either the HIV-infected or uninfected population. The most likely explanation for the lack of detection of translocation events in PGL is that the sensitivity of the LD-PCR assay used in this study is one translocation-positive cell in a background of 10^4 normal lymphoblastoid cells (see section 3.4.1.4). The prevalence of translocation-bearing clones in "normal" individuals, however, as assessed by previous studies, is 10-fold lower (Limpens *et al.*, 1991; Aster *et al.*, 1992). In conclusion, there was no evidence from the present studies that constitutive expression of *bcl-2*, secondary to deregulation due to chromosomal translocation, has a role in PGL.

4.8 Mutations in *bcl-6* are frequently detected in PGL

The *bcl-6* gene is characteristically altered by translocations and mutations in B cell NHL (Lo Coco *et al.*, 1994; Migliazza *et al.*, 1995). Greater than 90% of the mutations cluster within the 5' non-coding region of the gene, are often multiple in the same allele, frequently bi-allelic and have been reported in lymphomas displaying both normal and rearranged *bcl-6* genes (Migliazza *et al.*, 1995). Importantly, mutations in *bcl-6* are observed at a similar frequency (70%) throughout the clinico-pathologic spectrum of AIDS-NHL and they represent the most commonly observed genetic alteration in these lymphomas (Gaidano *et al.*, 1997d).

Interestingly, the gene is mutated both in lymphoma tissue and in normal B cells (Migliazza *et al.*, 1995; Shen *et al.*, 1998). The frequency of mutation in *bcl-6* is estimated to be $1.4x10^{-3}$ to $1.6x10^{-2}$ per bp in B-NHL and $6.8x10^{-4}$ to $1.9x10^{-3}$ per bp in normal memory B cells (Pasqualucci *et al.*, 1998; Shen *et al.*, 1998). Consistent with this marked difference in mutation frequency, *bcl-6* mutations in the present

study were observed at an increased incidence, by SSCP and sequencing analysis of a 735bp region within the first intron that represents a mutational hot-spot (Migliazza *et al.*, 1995). The frequency of mutations was found to be 5-10 times higher ($9.8x10^{-4}$ to $1.3x10^{-3}$ per bp) in the HIV-PGL samples than in the healthy controls ($8.2x10^{-5}$ to $5x10^{-4}$ per bp). Intriguingly, this observation lends indirect support to the hypothesis that PGL lesions may serve as precursors of AIDS-NHL, as the mutation rate is similar in the two pathological entities and is significantly higher than that observed in normal B cells. Identifying identical mutations in the corresponding tumour tissue would help clarify whether these mutations are enriched and selected for in the GC, and highlight their usefulness as possible predictive markers of lymphoma outgrowth. These results should however be interpreted with caution, as one cannot definitively exclude the fact that contamination with normal B cells in the PGL tissue accounts for this difference.

It is currently unclear why *bcl-6* is mutated more frequently in tumour cells than in normal B cells. *bcl-6* mutations are regarded as a marker of a transition of a given B cell through the GC. Mutations arise only in tumours and normal B cells of GC or post-GC origin, whereas they are absent in precursor and virgin B cells (Gaidano *et al.*, 1997d; Pasqualucci *et al.*, 1998; Shen *et al.*, 1998). One possible explanation to account for the increased frequency of mutations observed in the HIV-infected tissue in this study, is that the "explosive" nature of follicular hyperplasia seen in PGL maybe characterised by a greater number of follicular germinal centres than reactive lymph nodes and tonsils (Metroka *et al.*, 1983). However, this hypothesis can be ascertained unequivocally only through histopathological examination of the tissues, but no such material was available during the period of study. Further substantiation of the origin of the mutations in this study would require micro-dissection of the PGL and control tissue, to verify whether these mutations, do in fact, arise from the GC B cells of these nodes.

So why then do mutations occur both in tumour and normal B cells? Some researchers postulate that such mutations are a consequence of the same hypermutation mechanism that generates antibody diversity in germinal centre (GC)

B cells, during the process of affinity maturation (Chang and Casali, 1994; Capello *et al.*, 1997; Migliazza *et al.*, 1995). The characteristics of the *bcl-6* mutations observed in this study lend further credibility to this hypothesis, and are consistent with reports from other studies (Migliazza *et al.*, 1995; Gaidano *et al.*, 1997d; Betz *et al.*, 1993). Observed mutations were single nucleotide substitutions, with absence of deletions and insertions, somatic in nature, bi-allelic and multiple within the same allele. Transitions were favoured over transversions, with the 'T' residue being more frequently targeted than the 'A' residue. Although consistent with previous studies (Capello *et al.*, 2000; Sahota *et al.*, 2000), the T>A bias was at variance with that associated with somatic *Ig* hypermutation, which preferentially targets 'A' over 'T'. Studies of the *cis*-acting regulatory sequences on *bcl-6* and *Ig* gene mutations might aid in the understanding of why this gene is targeted.

In contrast to mutations in p53, *bcl-6* mutations target the non-coding region of the gene. The high frequency of mutation and the clustering of breakpoints in the 5' non-coding region of *bcl-6* may reflect the importance of this region in the normal regulation of the gene (Ye *et al.*, 1993; Lo Coco *et al.*, 1994). Recently, Kikuchi and co-workers have provided provocative evidence of 2 *cis*-acting regulatory elements within the first exon (ES) and intron (IS) of *bcl-6*, which negatively regulate Bcl-6 expression. Interestingly, the IS region is entirely included within the 735bp region analysed in this study (Kikuchi *et al.*, 2000). Thus, a functional consequence of the mutations that occur within these regions, as seen in this study, might be the de-repression of negative inhibitory effects on Bcl-6 expression, leading to inappropriate expression and subsequent lymphomagenesis. However, the presence of mutations outside this region, and also within healthy individuals, questions the "oncogenicity" of all *bcl-6* mutations, and suggests that these might simply reflect a GC-associated physiological process (see above).

Of further interest, 2 nucleotide substitutions likely to represent polymorphic variants were detected in this study. These variants, a G to C transversion at position +753, and a single base deletion (ΔT) at position +875, have been previously described (Migliazza *et al.*, 1995; Sahota *et al.*, 2000) and permitted the identification of bi-

allelic mutations in *bcl-6*. Interestingly, of all the mutations found to be associated with the individual polymorphic variants in both the study and control groups, 6/8 (75%) were found on the allele that had the 'C' residue at position +753, and 5/7 (71%) on the allele that had the 'T' residue at position +875, (see Tables 30 B and C, page 179). Of great interest is the fact that such an association of *bcl-6* mutations with polymorphic variants has not been previously reported. These results however, need to be interpreted with caution due to the relatively limited number of samples analysed. Furthermore, it remains to be determined whether polymorphic association with *bcl-6* mutant alleles has any biological relevance in the context of deregulation of *bcl-6*. Both questions represent issues that warrant further research.

To establish functional significance for the observed *bcl-6* mutations it needs to be determined whether mutated alleles in HIV-PGL have altered transcriptional activity and consequently deregulate Bcl-6 expression. It would then be interesting to observe whether those mutants with altered transcriptional activity cluster with specific polymorphic alleles. In addition, analysis of *bcl-6* translocations would also help ascertain whether this gene has any role in the pathogenesis of PGL.

The predictive value of *bcl-6* mutations has been demonstrated in post-transplant lymphoproliferative disorders, arising in organ transplant recipients. Cesarman *et al* (1998) have shown that the presence of *bcl-6* mutations predicted shorter survival and the need for aggressive therapeutic intervention (Cesarman *et al.*, 1998). Therefore, the analyses of bcl-6 mutations in this study may be clinically relevant in the context of predictiveness of lymphoma outgrowth, although further investigations are clearly required to verify such a possibility.

Virological analysis of PGL

On account of their association with lymphoid malignancies in the immunocompromised host, the presence of DNA viruses, EBV and KSHV was analysed in the current study.

4.9 EBV is uniformly detectable in PGL

EBV is associated with approximately 30-90% of AIDS-NHL, unlike its invariable association with other malignancies of immunosuppressed hosts (Hamilton-Dutoit *et al.*, 1991). However, the presence of EBV genomes in the lymph nodes of HIV-infected individuals has been considered as a predictive marker of subsequent lymphoma outgrowth (Shibata *et al.*, 1991). Therefore, to address the presence of EBV in the lymph nodes of HIV-infected individuals, the BamH1 W fragment of the EBV genome was amplified in a semi-quantitative PCR. EBV was detectable in 23/23 (100%) cases in the HIV-infected group and in 12/14 (86%) tissues in the control group. In comparison to the HIV-uninfected group (median viral load: <10 genomes/10^6 EBV negative cells), a greatly increased viral load (median viral load: 10^4 genomes/10^6 EBV negative cells) was observed in the HIV-infected individuals ($p<0.005$, Mann-Whitney test). These findings are in agreement with previous studies carried out in HIV-infected (Birx *et al.*, 1986) and healthy individuals (Miyashita *et al.*, 1995), and can be explained as a loss of immune control of EBV consequent to the immunodeficiency induced by HIV. However, whether the increased levels of virus detected contributes directly to the pathogenesis of PGL or indirectly contributes to the polyclonal activation of B cells is not known. Interestingly, one HIV-uninfected individual (2478) was found to harbour 10^5 EBV copies/10^6 cells. The significance of this high viral load is unknown, as the case histories of these individuals were not available.

4.10 Analysis of the presence of KSHV

Apart from its etiological association with KS and primary effusion lymphoma (PEL), KSHV has also been found to be present in lymphoproliferative disorders such as multicentric Castleman's disease (MCD) (Cesarman and Knowles, 1999). Hence, the extent of its involvement in HIV-PGL was considered a relevant investigation. In a recent study by O'Leary *et al* KSHV was detected by PCR in 14.2% of AIDS-related lymphadenopathy cases, and all the positive cases either subsequently developed KS or had KS at the time of diagnosis (O'Leary *et al.*, 2000).

Similarly, in the present study, 2/23 (8.7%) HIV-PGL cases was found to be positive by PCR amplification of KSHV-LNA. Since the presence of KSHV in AIDS related lymphadenopathy is predictive of KS development (O'Leary *et al.*, 2000), it will be interesting to determine the clinical outcome of those individuals with detectable virus.

KSHV is also known to target non-neoplastic and reactive lymph nodes in immunocompetent individuals, albeit rarely (Chadburn *et al.*, 1997, Trovato *et al.*, 1999). The absence of KSHV in the HIV-uninfected lymph nodes and tonsils investigated in this study is thus not remarkable. Moreover, the PCR conditions used were sensitive enough to detect between 30 and 50 viral copies. Serological analysis using antibodies to KSHV LNA would help verify the absence of KSHV DNA, provided stored serum from these individuals is available for analysis.

4.11 Conclusions

The studies described in this thesis are an initial attempt to identify virological, genetic and epigenetic characteristics of HIV-associated PGL. The starting point of the work was to examine in PGL genes and viruses known from previous work to be implicated in lymphomagenesis in either the immunocompetent or the immunocompromised host. The principal results from the work are: i) the finding of p53 missense mutations in 5/23 cases studied; ii) a potentially interesting spectrum of polymorphisms and mutations in *bcl-6*; iii) over-expression of the trans-dominant p73 isoform, Δ2 p73, in a majority of cases; iv) the absence of genetic or epigenetic changes in any other tumour suppressor genes studied; v) the lack of detectable chromosomal translocations implicated in non-Hodgkin's lymphomas. A comprehensive overview of the results of this study is presented in Appendices 1 and 2.

The results suggest that loss of p53 function, mediated by mutation within the gene or perhaps by over-expression of trans-dominant members of the p53 family, may be an early event in the pathogenesis of PGL and perhaps in HIV-associated

lymphomagenesis. In contrast, inactivation of the *INK4* gene locus, which occurs commonly in NHL, predominantly by methylation of CpG sequences in the gene promoters, does not appear to occur in PGL, implying that such changes are later events. Whereas the identification of p53 mutation can be regarded with confidence as a *bona fide* result, other findings need to be interpreted within the limitations imposed by the lack of immunocytochemical analysis and micro-dissected tissue, enriched for hyperproliferating germinal centre B cells, for direct comparison with matched normal (see later). For example, it was not possible to definitely analyse $p16^{INK4a}$ expression in the presence of unknown amounts of normal tissue. Nevertheless, the sensitivity of the methylation analyses established in preliminary experiments does suggest that sensitivity was adequate to exclude methylation-dependent transcriptional silencing of the *INK4* locus and the *p73* genes in PGL. Whether such changes occur later in the natural history of the disease awaits further study, ideally by *in situ* methylation analysis.

Throughout the course of this work, a major limiting factor was the unavailability of tissue sections from the lymph nodes analysed. It is highly likely that many of the candidate genetic and epigenetic changes sought are restricted to sub-populations of cells within the lymph node and therefore in a minority of cells within the population analysed. As a result, detection of these changes in nucleic acid preparations from whole lymph nodes will suffer from reduced sensitivity due to the dilutional effect of the normal tissue within the biopsy material. Future studies would undoubtedly benefit from the availability of tissue sections. For example, it would be of interest to determine what proportion of cells have detectable p53 protein, since the mutants detected in the present work would be predicted to be readily detectable by immunocytochemistry. The question could then be addressed of whether discrete clones of mutant p53 cells are present within the node.

Immunocytochemistry would also enable a more accurate assessment of the expression of other tumour suppressor genes such as $p16^{INK4a}$ and $p15^{INK4b}$. Analysis of expression by RT-PCR of whole lymph node RNA preparations is clearly significantly affected by the presence of normal tissue and immunocytochemical

analysis would provide a definitive answer to the question of whether loss of expression occurs during HIV-associated lymphomagenesis. Furthermore, the availability of paraffin sections would enable micro-dissection of abnormal and normal tissue from the same node, allowing analysis of LOH and gene sequence in the PGL tissue and tumour, free from the masking effects of normal tissue contamination. Moreover, it would also permit conclusive analysis of the cell of origin of the *bcl-6* mutations.

It would also have been extremely informative to have obtained clinico-pathological follow up data from the individual patients in this series of PGL. Since it was known that some of the individuals subsequently developed lymphoma, such data would have allowed several pertinent questions to be addressed. Primarily, whether p53 and *bcl-6* mutations predict future lymphoma outgrowth, and also whether genetic and epigenetic changes not observed in PGL truly occur as later events in AIDS-lymphomagenesis.

4.12 A speculative model for AIDS-lymphomagenesis

AIDS-NHL is a strikingly heterogeneous disease. Based on the data summarised from several studies 3 major pathogenetic pathways can be identified. The first of these pathways associates with AIDS-SNCCL, which is characterised by relatively mild immunosuppression (Beral *et al.*, 1991; Boyle *et al.*, 1990) and more frequently than other AIDS-NHL, is preceded by a PGL phase (Kalter *et al.*, 1985). These tumours harbour multiple genetic lesions including deregulation of c-*myc* (100%), deletions of 6q (15%), mutations in *p53*, *bcl-6* and *ras* in 60, 70 and 15% of cases respectively and less frequently infection with EBV (30-60%) (Ballerini *et al.*, 1993; Gaidano *et al.*, 1993, 1994).

A second major pathway generally characterised by a marked disruption of immune function is associated with variants of AIDS-DLCL- AIDS-LNCCL and AIDS-IBL, as well as AIDS-PCNSL (Beral *et al.*, 1991). These tumours are thought to be EBV-driven lymphoproliferations, a view supported by the presence of EBV in >90% of AIDS-IBL and 40% of AIDS-LNCCL, and the lack of molecular lesions in the

majority of these cases (Hamilton-Dutoit *et al.*, 1993). Genetic lesions when present, include *bcl-6* rearrangement and mutations (20% and 70%) and c-*myc* translocations (20%) (Ballerini *et al.*, 1993; Gaidano *et al.*, 1994).

A third and final pathway associates with AIDS-PEL. This rare lymphoma type consistently harbors KSHV and frequently also EBV (Nador *et al.*, 1996). Apart from mutations in *bcl-6* in 20% of cases, all other genetic lesions commonly detected among AIDS-NHL are consistently absent in AIDS-PEL (Nador *et al.*, 1996; Carbone *et al.*, 1996a).

Taken together the genetic and virological findings of this study permit construction of a speculative model for the evolution of AIDS-NHL in the context of the heterogeneous and multi-factorial nature of this disease (see above and figure 72). It is proposed that AIDS-lymphomagenesis begins with a complex interplay of one or more factors (outlined below) leading to the florid B cell hyperplasia within enlarged, reactive PGL lymph nodes. These factors include:

a) Chronic antigenic stimulation (Riboldi *et al.*, 1994).

b) Viral infection: direct or indirect role for EBV and/or HIV (Kundu *et al.*, 1999; Birx *et al.*, 1986; Pelicci *et al.*, 1986b).

c) Disturbance of cytokine (IL-6 and IL-10) and co-stimulatory (CD40/CD40L) networks that are critical to the growth and differentiation of B cells (Kundu *et al.*, 1999; Moses *et al.*, 1997).

Identification of EBV DNA in the lymph nodes of PGL patients in this study, does not solely justify a role for this virus in the pathogenesis of PGL. However, the virus may perhaps indirectly contribute to and maintain the characteristic B cell hyperproliferation by inducing IL-6 secretion (Liebowitz 1998) and/or inhibiting EBV-specific memory CTL response via upregulation of viral and cellular IL-10 (Bejarano and Masucci, 1998). In addition, the HIV-Tat gene product may similarly induce cellular IL-6 and IL-10 expression (Kundu *et al.*, 1999) and possibly contribute to the B cell hyperplasia in PGL.

Figure 72. A speculative model for AIDS-lymphomagenesis

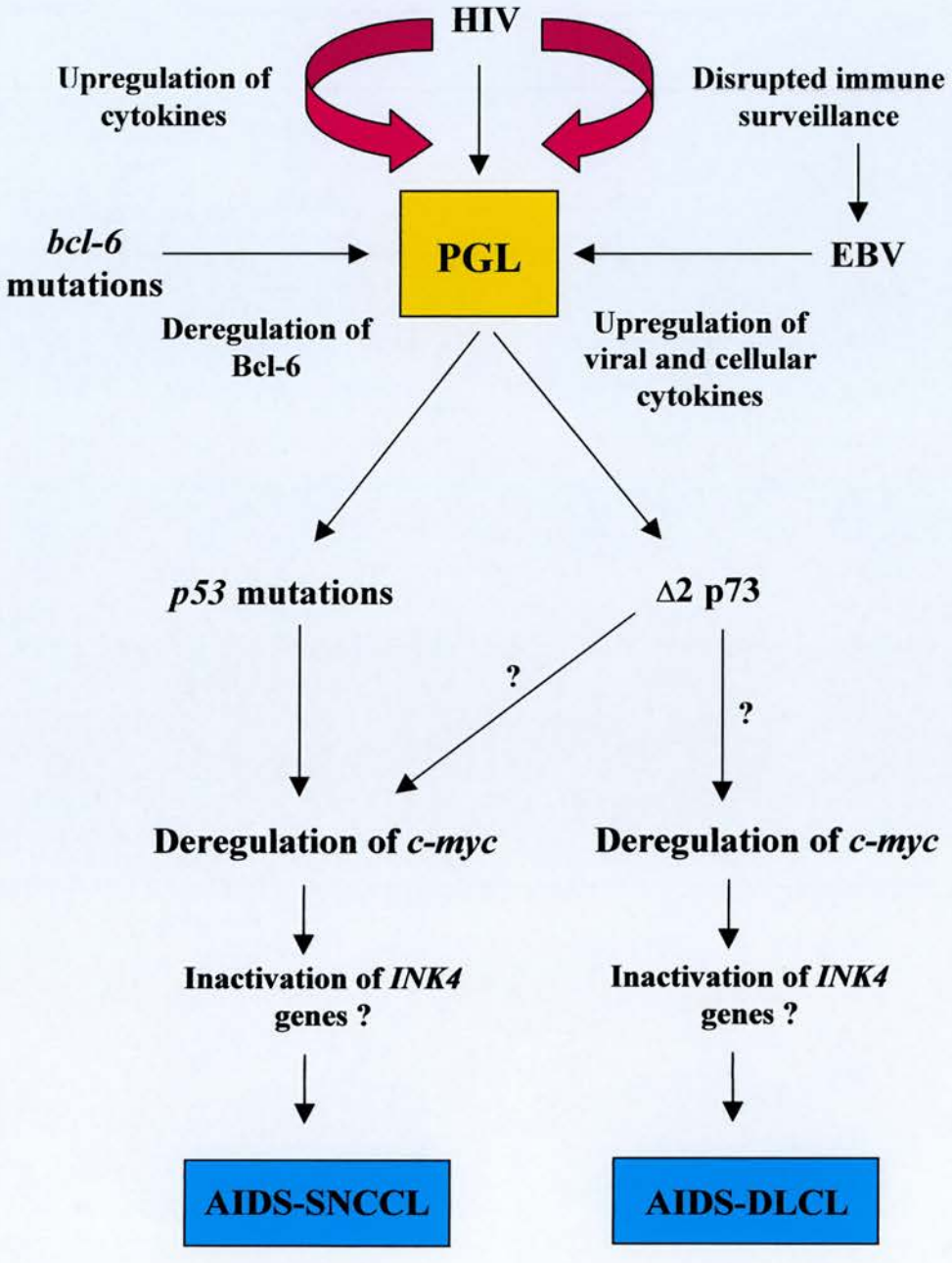

Lymphomagenesis in AIDS is believed to begin with the florid B cell hyperplasia that is characteristic of PGL. PGL results from the complex interplay of several factors of which the role of viruses such as HIV and EBV (either directly or through the disturbance of cytokine networks) and mutations in *bcl-6* are indicated. Inactivation of tumour suppressor genes such as p53, either through mutation or trans-dominant inhibition by Δ2 p73 is the second step. Deregulation of c-*myc* would then be an obligatory event in the case of AIDS-SNCCL, whereas this genetic event might not be required for the progression of all DLCLs. A third and possible questionable step perhaps involves inactivation of the *INK4* genes.
HIV, human immunodeficiency virus; **EBV**, Epstein-Barr virus; **SNCCL**, small non-cleaved cell lymphoma; **DLCL**, diffuse large cell lymphoma.

Apart from the known effects of viruses on B cell proliferation, a contributory role for *bcl-6* is also proposed in this model. Deregulation of *bcl-6* via alterations observed within the *cis*-acting negative regulatory elements present within the first intron, might relieve the inhibitory effects on Bcl-6 expression. Such constitutive or inappropriate expression of Bcl-6 within the germinal centre (GC) B cells would then impede B cell differentiation within the GC by repression of target genes (Shaffer *et al.*, 2000) and consequently sustain these cells in a permanent proliferative state.

Although a role for EBV and HIV in the pathogenesis of PGL cannot entirely be discounted, it is clearly apparent that other factors are required before a cell acquires a growth/clonal advantage. Inactivation of tumour suppressor genes and/or deregulation of oncogenes might provide a second crucial step in the cascade of events to lymphomagenesis. Mutation in the tumour suppressor, p53, as observed in the panel of PGL tissue examined, is one genetic event that would be predicted to have such a role. It is known that only a subset of AIDS-NHL harbour p53 mutations, in particular 60% of AIDS-BL, whereas such alterations are only occasionally observed in the other subtypes (Gaidano *et al.*, 1997b; Ballerini *et al.*, 1993). Therefore, one can predict that the p53 mutations observed in this study predispose to the development of AIDS-BL. However, although c-*myc* translocations are a consistent feature of BL, such findings were not validated in this study, leading to the premise that deregulation of c-*myc*, secondary to translocation might occur as a later event in lymphomagenesis. Such a scenario is certainly viable in light of the studies by Polack and co-workers wherein activation of c-*myc*, secondary to EBV-induced B cell immortalisation, is sufficient to maintain the immortalised state that is initially effected by EBV (Polack *et al.*, 1996).

It is interesting to speculate that in those tumours with absence of p53 mutations, other mechanisms of inactivation of p53 may exist. It is known that the N-terminal deleted variants of p63 and p73, ΔN p63 and Δ2 p73 respectively, can trans-dominantly inhibit wild-type p53 (Pozniak *et al.*, 2000; Crook *et al.*, 2000). Predominant high level expression of Δ2 p73 in the current series of HIV-PGL suggests that this mechanism of inactivation of wild-type p53 function might be

operative, at least in a subset of AIDS-NHL. Furthermore, inactivation of ARF and hMDM2, in tumours with wild type p53, could be proposed as an alternative to p53 mutation. Inactivation of the p53-ARF-hMDM2 pathway, by deletion and/or overexpression of ARF and hMDM2 respectively, in tumours that retain wild-type p53 function, has recently been shown to be an essential step in Burkitt's lymphomagenesis (Lindstrom et al., 2001; Eischen et al., 1999).

Lastly, the absence of genetic and epigenetic lesions in members of the INK4 locus, either predicts that these genes have no role in the pathogenesis of AIDS-NHL, or that they are altered late in lymphomagenesis.

An important consideration in the proposed speculative model is that it must be viewed in the light of the absence of micro-dissected PGL and lymphoma tissue. The availability and analysis of such tissue would help definitively to conclude whether the molecular genetic alterations observed in this study truly represent predictive markers of AIDS-NHL.

REFERENCES

Adams, J. M. and Cory, S. (1998). The Bcl-2 protein family: arbiters of cell survival. *Science* **281**, 1322-1326.

Adams, J. M., Gerondakis, S., Webb, E., Corcoran, L. M., and Cory, S. (1983). Cellular myc oncogene is altered by chromosome translocation to an immunoglobulin locus in murine plasmacytomas and is rearranged similarly in human Burkitt lymphomas. *Proceedings of the National Academy of Sciences of the United States of America* **80**, 1982-1986.

Agami, R., Blandino, G., Oren, M., and Shaul, Y. (1999). Interaction of c-Abl and p73alpha and their collaboration to induce apoptosis [see comments]. *Nature* **399**, 809-813.

Ahuja, H. G., Testa, M. P., and Cline, M. J. (1990). Variation in the protein coding region of the human p53 gene. *Oncogene* **5**, 1409-1410.

Aisenberg, A. C., Wilkes, B. M., and Jacobson, J. O. (1988). The bcl-2 gene is rearranged in many diffuse B-cell lymphomas. *Blood* **71**, 969-972.

Akasaka, T., Akasaka, H., Yonetani, N., Ohno, H., Yamabe, H., Fukuhara, S., and Okuma, M. (1998). Refinement of the BCL2/immunoglobulin heavy chain fusion gene in t(14;18)(q32;q21) by polymerase chain reaction amplification for long targets. *Genes Chromosomes Cancer* **21**, 17-29.

Akasaka, T., Muramatsu, M., Ohno, H., Miura, I., Tatsumi, E., Fukuhara, S., Mori, T., and Okuma, M. (1996). Application of long-distance polymerase chain reaction to detection of junctional sequences created by chromosomal translocation in mature B-cell neoplasms. *Blood* **88**, 985-994.

Allman, D., Jain, A., Dent, A., Maile, R. R., Selvaggi, T., Kehry, M. R., and Staudt, L. M. (1996). BCL-6 expression during B-cell activation. *Blood* **87**, 5257-5268.

Alonso, M. L., Richardson, M. E., Metroka, C. E., Mouradian, J. A., Koduru, P. R. K., Filippa, D., and Chaganti, R. S. K. (1987). Chromosome abnormalities in AIDS associated lymphadenopathy. *Blood* **69 No 3**, 855-858.

Amati, B. and Land, H. (1994). Myc-Max-Mad: a transcription factor network controlling cell cycle progression, differentiation and death. *Current Opinion in Genetics and Development* **4**, 102-108.

Amati, B., Littlewood, T. D., Evan, G. I., and Land, H. (1993). The c-Myc protein induces cell cycle progression and apoptosis through dimerization with Max. *EMBO Journal* **12**, 5083-5087.

Andrieu, J. M., Roithmann, S., Tourani, J. M., Levy, R., Desablens, B., le Maignan, C., Gastaut, J. A., Brice, P., Raphael, M., and Taillan, B. (1993). Hodgkin's disease during HIV1 infection: the French registry experience. French Registry of HIV-associated Tumors. *Annals of Oncology* **4**, 635-641.

Antman, K. and Chang, Y. (2000). Kaposi's sarcoma. *New England Journal of Medicine* **342**, 1027-1038.

Armstrong, J. A. and Horne, R. (1984). Follicular dendritic cells and virus-like particles in AIDS-related lymphadenopathy. *Lancet* **2**, 370-372.

Barillari, G., Sgadari, C., Fiorelli, V., Samaniego, F., Colombini, S., Manzari, V., Modesti, A., Nair, B. C., Cafaro, A., Sturzl, M., and Ensoli, B. (1999). The Tat protein of human immunodeficiency virus type-1 promotes vascular cell growth and locomotion by engaging the α5beta1 and αvbeta3 integrins and by mobilizing sequestered basic fibroblast growth factor. *Blood* **94**, 663-672.

Baron, B. W., Nucifora, G., McCabe, N., Espinosa, R., III, Le Beau, M. M., and McKeithan, T. W. (1993). Identification of the gene associated with the recurring chromosomal translocations t(3;14)(q27;q32) and t(3;22)(q27;q11) in B-cell lymphomas. *Proceedings of the National Academy of Sciences of the United States of America* **90**, 5262-5266.

Barre-Sinoussi, F., Chermann, J. C., Rey, F., Nugeyre, M. T., Chamaret, S., Gruest, J., Dauguet, C., Axler-Blin, C., Vezinet-Brun, F., Rouzioux, C., Rozenbaum, W., and Montagnier, L. (1983). Isolation of a T-lymphotropic retrovirus from a patient at risk for acquired immune deficiency syndrome (AIDS). *Science* **220**, 868-871.

Basso, K., Frascella, E., Zanesco, L., and Rosolen, A. (1999). Improved long-distance polymerase chain reaction for the detection of t(8;14)(q24;q32) in Burkitt's lymphomas. *American Journal of Pathology* **155**, 1479-1485.

Bates, S. and Vousden, K. H. (1999). Mechanisms of p53-mediated apoptosis. *Cellular and Molecular Life Sciences* **55**, 28-37.

Bates, S., Phillips, A. C., Clark, P. A., Stott, F., Peters, G., Ludwig, R. L., and Vousden, K. H. (1998). p14ARF links the tumour suppressors RB and p53 [letter]. *Nature* **395**, 124-125.

Battey, J., Moulding, C., Taub, R., Murphy, W., Stewart, T., Potter, H., Lenoir, G., and Leder, P. (1983). The human c-myc oncogene: structural consequences of translocation into the IgH locus in Burkitt lymphoma. *Cell* **34**, 779-787.

Baur, A. S., Shaw, P., Burri, N., Delacretaz, F., Bosman, F. T., and Chaubert, P. (1999). Frequent methylation silencing of p15(INK4b) (MTS2) and p16(INK4a) (MTS1) in B-cell and T-cell lymphomas. *Blood* **94**, 1773-1781.

Bejarano, M. T. and Masucci, M. G. (1998). Interleukin-10 abrogates the inhibition of Epstein-Barr virus-induced B-cell transformation by memory T-cell responses. *Blood* **92**, 4256-4262.

Bentley, D. L. and Groudine, M. (1986). Novel promoter upstream of the human c-myc gene and regulation of c-myc expression in B-cell lymphomas. *Molecular and Cellular Biology* **6**, 3481-3489.

Beral, V. (1991). The epidemiology of cancer in AIDS patients. *AIDS* **5 Suppl 2**, S99-103.

Beral, V. and Newton, R. (1998). Overview of the epidemiology of immunodeficiency-associated cancers. *Journal of the National Cancer Institute Monographs* **123**, 1-6.

Bernard, P., Gabant, P., Bahassi, E. M., and Couturier, M. (1994). Positive-selection vectors using the F plasmid ccdB killer gene. *Gene* **148**, 71-74.

Betz, A. G., Neuberger, M. S., and Milstein, C. (1993). Discriminating intrinsic and antigen-selected mutational hotspots in immunoglobulin V genes. *Immunology Today* **14**, 405-411.

Bhatia, K., Huppi, K., Spangler, G., Siwarski, D., Iyer, R., and Magrath, I. (1993). Point mutations in the c-Myc transactivation domain are common in Burkitt's lymphoma and mouse plasmacytomas. *Nature Genetics* **5**, 56-61.

Bhatia, K., Spangler, G., Gaidano, G., Hamdy, N., Dalla-Favera, R., and Magrath, I. (1994). Mutations in the coding region of c-myc occur frequently in acquired immunodeficiency syndrome-associated lymphomas. *Blood* **84**, 883-888.

Birx, D. L., Redfield, R. R., and Tosato, G. (1986). Defective regulation of Epstein-Barr virus infection in patients with acquired immunodeficiency syndrome (AIDS) or AIDS-related disorders. *New England Journal of Medicine* **314**, 874-879.

Bishop, J.M. (1991). Molecular themes in oncogenesis. *Cell* **64**, 235-48.

Blackwood, E. M. and Eisenman, R. N. (1991). Max: a helix-loop-helix zipper protein that forms a sequence-specific DNA-binding complex with Myc. *Science* **251**, 1211-1217.

Bonnet, M., Guinebretiere, J. M., Kremmer, E., Grunewald, V., Benhamou, E., Contesso, G., and Joab, I. (1999). Detection of Epstein-Barr virus in invasive breast cancers. *Journal of the National Cancer Institute* **91**, 1376-1381.

Bork, P., Doerks, T., Springer, T. A., and Snel, B. (1999). Domains in plexins: links to integrins and transcription factors. *Trends in Biochemical Sciences* **24**, 261-263.

Boshoff, C. and Weiss, R. A. (1998). Kaposi's sarcoma-associated herpesvirus. *Advances in Cancer Research* **75**, 57-86.

Boshoff, C., Gao, S. J., Healy, L. E., Matthews, S., Thomas, A. J., Coignet, L., Warnke, R. A., Strauchen, J. A., Matutes, E., Kamel, O. W., Moore, P. S., Weiss, R. A., and Chang, Y. (1998). Establishing a KSHV+ cell line (BCP-1) from peripheral blood and characterizing its growth in Nod/SCID mice. *Blood* **91**, 1671-1679.

Boshoff, C., Schulz, T. F., Kennedy, M. M., Graham, A. K., Fisher, C., Thomas, A., McGee, J. O., Weiss, R. A., and O'Leary, J. J. (1995). Kaposi's sarcoma-associated herpesvirus infects endothelial and spindle cells. *Nature Medicine* **1**, 1274-1278.

Bourboulia, D., Whitby, D., Boshoff, C., Newton, R., Beral, V., Carrara, H., Lane, A., and Sitas, F. (1998). Serologic evidence for mother-to-child transmission of Kaposi sarcoma-associated herpesvirus infection. *Journal of the American Medical Association* **280**, 31-32.

Boyle, M. J., Berger, M. F., Tschuchnigg, M., Valentine, J. E., Kennedy, B. G., Divjak, M., Cooper, D. A., Turner, J. J., Penny, R., and Sewell, W. A. (1993). Increased expression of interferon-gamma in hyperplastic lymph nodes from HIV-infected patients. *Clinical and Experimental Immunology* **92**, 100-105.

Boyle, M. J., Sculley, T. B., Cooper, D. A., Turner, J. J., Penny, R., and Sewell, W. A. (1992). Epstein-Barr virus and HIV play no direct role in persistent generalized lymphadenopathy syndrome. *Clinical and Experimental Immunology* **87**, 357-361.

Boyle, M. J., Swanson, C. E., Turner, J. J., Thompson, I. L., Roberts, J., Penny, R., and Cooper, D. A. (1990). Definition of two distinct types of AIDS-associated non-Hodgkin lymphoma. *British Journal of Hematology* **76**, 506-512.

Brooks, L., and Thomas, J.A. (1995). The significance of Epstein-Barr virus in the pathogenesis of lymphoid and epithelial neoplasia. *Current Diagnostic Pathology* **2**, 163-174.

Burri, N., Shaw, P., Bouzourene, H., Sordat, I., Sordat, B., Gillet, M., Schorderet, D., Bosman, F. T., and Chaubert, P. (2001). Methylation silencing and mutations of the p14ARF and p16INK4a genes in colon cancer. *Laboratory Investigation* **81**, 217-229.

Butler, M., Corbally, N., Dervan, P. A., and Carney, D. N. (1997). BCL-6 and other genomic alterations in non-Hodgkin's lymphoma (NHL). *British Journal of Cancer* **75**, 1641-1645.

Caelles, C., Helmberg, A., and Karin, M. (1994). p53-dependent apoptosis in the absence of transcriptional activation of p53-target genes [see comments]. *Nature* **370**, 220-223.

Camilleri-Broet, S., Davi, F., Feuillard, J., Seilhean, D., Michiels, J. F., Brousset, P., Epardeau, B., Navratil, E., Mokhtari, K., Bourgeois, C., Marelle, L., Raphael, M., and Hauw, J. J. (1997). AIDS-related primary brain lymphomas: histopathologic and immunohistochemical study of 51 cases. The French Study Group for HIV-Associated Tumors. *Human Pathology* **28**, 367-374.

Campomenosi, P., Monti, P., Aprile, A., Abbondandolo, A., Frebourg, T., Gold, B., Crook, T., Inga, A., Resnick, MA., Iggo, R., and Fronza, G. (2001). p53 mutants can often transactivate promoters containing a *p21* but not *Bax* or *PIG3* responsive elements. *Oncogene* **20**, 3573-3579.

Canman, C. E., Lim, D. S., Cimprich, K. A., Taya, Y., Tamai, K., Sakaguchi, K., Appella, E., Kastan, M. B., and Siliciano, J. D. (1998). Activation of the ATM kinase by ionizing radiation and phosphorylation of p53. *Science* **281**, 1677-1679.

Cannon, M. and Cesarman, E. (2000). Kaposi's sarcoma-associated herpes virus and acquired immunodeficiency syndrome-related malignancy. *Seminars in Oncology* **27**, 409-419.

Capello, D., Carbone, A., Pastore, C., Gloghini, A., Saglio, G., and Gaidano, G. (1997). Point mutations of the BCL-6 gene in Burkitt's lymphoma. *British Journal of Haematology* **99**, 168-170.

Capello, D., Vitolo, U., Pasqualucci, L., Quattrone, S., Migliaretti, G., Fassone, L., Ariatti, C., Vivenza, D., Gloghini, A., Pastore, C., Lanza, C., Nomdedeu, J., Botto, B., Freilone, R., Buonaiuto, D., Zagonel, V., Gallo, E., Palestro, G., Saglio, G., Dalla-Favera, R., Carbone, A., and Gaidano, G. (2000). Distribution and pattern of BCL-6 mutations throughout the spectrum of B-cell neoplasia. *Blood* **95**, 651-659.

Carbone, A., Dolcetti, R., Gloghini, A., Maestro, R., Vaccher, E., Di Luca, D., Tirelli, U., and Boiocchi, M. (1996b). Immunophenotypic and molecular analyses of acquired immune deficiency syndrome-related and Epstein-Barr virus-associated lymphomas: a comparative study. *Human Pathology* **27**, 133-146.

Carbone, A., Gaidano, G., Gloghini, A., Larocca, L. M., Capello, D., Canzonieri, V., Antinori, A., Tirelli, U., Falini, B., and Dalla-Favera, R. (1998). Differential expression of BCL-6, CD138/syndecan-1, and Epstein-Barr virus-encoded latent membrane protein-1 identifies distinct histogenetic subsets of acquired immunodeficiency syndrome-related non-Hodgkin's lymphomas. *Blood* **91**, 747-755.

Carbone, A., Gaidano, G., Gloghini, A., Pastore, C., Saglio, G., Tirelli, U., Dalla-Favera, R., and Falini, B. (1997). BCL-6 protein expression in AIDS-related non-Hodgkin's lymphomas: inverse relationship with Epstein-Barr virus-encoded latent membrane protein-1 expression. *American Journal of Pathology* **150**, 155-165.

Carbone, A., Gloghini, A., Gaidano, G., Cilia, A. M., Bassi, P., Polito, P., Vaccher, E., Saglio, G., and Tirelli, U. (1995). AIDS-related Burkitt's lymphoma. Morphologic and immunophenotypic study of biopsy specimens. *American Journal of Clinical Pathology* **103**, 561-567.

Carbone, A., Gloghini, A., Vaccher, E., Zagonel, V., Pastore, C., Dalla, Palma P., Branz, F., Saglio, G., Volpe, R., Tirelli, U., and Gaidano, G. (1996a). Kaposi's sarcoma-associated herpesvirus DNA sequences in AIDS-related and AIDS-unrelated lymphomatous effusions. *British Journal of Hematology* **94**, 533-543.

Carbone, A., Tirelli, U., Gloghini, A., Volpe, R., and Boiocchi, M. (1993). Human immunodeficiency virus-associated systemic lymphomas may be subdivided into two main groups according to Epstein-Barr viral latent gene expression. *Journal of Clinical Oncology* **11**, 1674-1681.

Carnero, A., Hudson, J. D., Price, C. M., and Beach, D. H. (2000). p16INK4A and p19ARF act in overlapping pathways in cellular immortalization. *Nature Cell Biology* **2**, 148-155.

Casciano, I., Ponzoni, M., Lo, Cunsolo C., Tonini, G. P., and Romani, M. (1999). Different p73 splicing variants are expressed in distinct tumour areas of a multifocal neuroblastoma [letter]. *Cell Death and Differentiation* **6**, 391-393.

Cattoretti, G., Chang, C. C., Cechova, K., Zhang, J., Ye, B. H., Falini, B., Louie, D. C., Offit, K., Chaganti, R. S., and Dalla-Favera, R. (1995). BCL-6 protein is expressed in germinal-center B cells. *Blood* **86**, 45-53.

Centers for Disease Control and Prevention (1985). Revision of the case definition of acquired immunodeficiency syndrome for national reporting--United States. Centers for Disease Control, Department of Health and Human Services. *Annals of Internal Medicine* **103**, 402-403.

Centers for Disease Control and Prevention (CDC). (1993). Revised classification system for HIV infection and expanded surveillance case definition for AIDS among adolescents and adults. *Morbidity and Mortality Weekly Reports* 1992, **41** (no. RR-17).

Cerimele, F., Curreli, F., Ely, S., Friedman-Kien, A. E., Cesarman, E., and Flore, O. (2001). Kaposi's sarcoma-associated herpesvirus can productively infect primary human keratinocytes and alter their growth properties. *Journal of Virology* **75**, 2435-2443.

Cesarman, E. and Knowles, D. M. (1999). The role of Kaposi's sarcoma-associated herpesvirus (KSHV/HHV-8) in lymphoproliferative diseases. *Seminars in Cancer Biology* **9**, 165-174.

Cesarman, E., Chadburn, A., Liu, Y. F., Migliazza, A., Dalla-Favera, R., and Knowles, D. M. (1998). BCL-6 gene mutations in posttransplantation lymphoproliferative disorders predict response to therapy and clinical outcome. *Blood* **92**, 2294-2302.

Cesarman, E., Chang, Y., Moore, P. S., Said, J. W., and Knowles, D. M. (1995). Kaposi's sarcoma-associated herpesvirus-like DNA sequences in AIDS-related body-cavity-based lymphomas. *New England Journal of Medicine* **332**, 1186-1191.

Cesarman, E., Dalla-Favera, R., Bentley, D., and Groudine, M. (1987). Mutations in the first exon are associated with altered transcription of c-myc in Burkitt lymphoma. *Science* **238**, 1272-1275.

Chadburn, A., Cesarman, E., Nador, R. G., Liu, Y. F., and Knowles, D. M. (1997). Kaposi's sarcoma-associated herpesvirus sequences in benign lymphoid proliferations not associated with human immunodeficiency virus. *Cancer* **80**, 788-797.

Chadburn, A., Metroka, C., and Mouradian, J. (1989). Progressive lymph node histology and its prognostic value in patients with acquired immunodeficiency syndrome and AIDS-related complex. *Human Pathology* **20**, 579-587.

Chan, J. K., Banks, P. M., Cleary, M. L., Delsol, G., Wolf-Peeters, C., Falini, B., Gatter, K. C., Grogan, T. M., Harris, N. L., Isaacson, P. G., *et al.* (1994). A proposal for classification of lymphoid neoplasms (by the International Lymphoma Study Group). *Histopathology* **25**, 517-536.

Chang, B. and Casali, P. (1994). The CDR1 sequences of a major proportion of human germline Ig VH genes are inherently susceptible to amino acid replacement. *Immunology Today* **15**, 367-373.

Chang, C. C., Ye, B. H., Chaganti, R. S., and Dalla-Favera, R. (1996). BCL-6, a POZ/zinc-finger protein, is a sequence-specific transcriptional repressor. *Proceedings of the National Academy of Sciences of the United States of America* **93**, 6947-6952.

Chang, Y., Cesarman, E., Pessin, M. S., Lee, F., Culpepper, J., Knowles, D. M., and Moore, P. S. (1994). Identification of herpesvirus-like DNA sequences in AIDS-associated Kaposi's sarcoma. *Science* **266**, 1865-1869.

Chen, W., Butler, M., Rao, P. H., Chaganti, S. R., Louie, D. C., Dalla-Favera, R., and Chaganti, R. S. (1998b). The t(2;3)(q21;q27) translocation in non-Hodgkin's lymphoma displays BCL6 mutations in the 5' regulatory region and chromosomal breakpoints distant from the gene. *Oncogene* **17**, 1717-1722.

Chen, W., Iida, S., Louie, D. C., Dalla-Favera, R., and Chaganti, R. S. (1998a). Heterologous promoters fused to BCL6 by chromosomal translocations affecting band 3q27 cause its deregulated expression during B-cell differentiation. *Blood* **91**, 603-607.

Cheng, S., Fockler, C., Barnes, W. M., and Higuchi, R. (1994). Effective amplification of long targets from cloned inserts and human genomic DNA. *Proceedings of the National Academy of Sciences of the United States of America* **91**, 5695-5699.

Chen-Levy, Z. and Cleary, M. L. (1990). Membrane topology of the Bcl-2 proto-oncogenic protein demonstrated in vitro. *Journal of Biological Chemistry* **265**, 4929-4933.

Chomczynski, P. and Sacchi, N. (1987). Single-step method of RNA isolation by acid guanidinium thiocyanate-phenol-chloroform extraction. *Analytical Biochemistry* **162**, 156-159.

Cinti, C., Leoncini, L., Nyongo, A., Ferrari, F., Lazzi, S., Bellan, C., Vatti, R., Zamparelli, A., Cevenini, G., Tosi, G. M., Claudio, P. P., Maraldi, N. M., Tosi, P., and Giordano, A. (2000). Genetic alterations of the retinoblastoma-related gene RB2/p130 identify different pathogenetic mechanisms in and among Burkitt's lymphoma subtypes. *American Journal of Pathology* **156**, 751-760.

Cleary, M. L., Smith, S. D., and Sklar, J. (1986). Cloning and structural analysis of cDNAs for bcl-2 and a hybrid bcl-2/immunoglobulin transcript resulting from the t(14;18) translocation. *Cell* **47**, 19-28.

Cline, J., Braman, J. C., and Hogrefe, H. H. (1996). PCR fidelity of pfu DNA polymerase and other thermostable DNA polymerases. *Nucleic Acids Research* **24**, 3546-3551.

Cole, M. D. (1986). The myc oncogene: its role in transformation and differentiation. *Annual Review of Genetics* **20,** 361-384.

Corbellino, M., Lusso, P., Gallo, R. C., Parravicini, C., Galli, M., and Moroni, M. (1993). Disseminated human herpesvirus 6 infection in AIDS. *Lancet* **342**, 1242.

Corn, P. G., Kuerbitz, S. J., van Noesel, M. M., Esteller, M., Compitello, N., Baylin, S. B., and Herman, J. G. (1999). Transcriptional silencing of the p73 gene in acute lymphoblastic leukemia and Burkitt's lymphoma is associated with 5' CpG island methylation. *Cancer Research* **59**, 3352-3356.

Cory, S. (1986). Activation of cellular oncogenes in hemopoietic cells by chromosome translocation. *Advances in Cancer Research* **47:189-234**, 189-234.

Cory, S., Vaux, D. L., Strasser, A., Harris, A. W., and Adams, J. M. (1999). Insights from Bcl-2 and Myc: malignancy involves abrogation of apoptosis as well as sustained proliferation. *Cancer Research* **59**, 1685s-1692s.

Crawford, D. H., Thomas, J. A., Janossy, G., Sweny, P., Fernando, O. N., Moorhead, J. F., and Thompson, J. H. (1980). Epstein Barr virus nuclear antigen positive lymphoma after cyclosporin A treatment in patient with renal allograft. *Lancet* **1**, 1355-1356.

Croce, C. M. and Nowell, P. C. (1985). Molecular basis of human B cell neoplasia. *Blood* **65**, 1-7.

Crook, T., Marston, N. J., Sara, E. A., and Vousden, K. H. (1994). Transcriptional activation by p53 correlates with suppression of growth but not transformation. *Cell* **79**, 817-827.

Crook, T., Nicholls, J. M., Brooks, L., O'Nions, J., and Allday, M. J. (2000). High level expression of deltaN-p63: a mechanism for the inactivation of p53 in undifferentiated nasopharyngeal carcinoma (NPC)? *Oncogene* **19**, 3439-3444.

Dalla-Favera, R., Bregni, M., Erikson, J., Patterson, D., Gallo, R. C., and Croce, C. M. (1982b). Human c-myc onc gene is located on the region of chromosome 8 that is translocated in Burkitt lymphoma cells. *Proceedings of the National Academy of Sciences of the United States of America* **79**, 7824-7827.

Dalla-Favera, R., Gelmann, E. P., Martinotti, S., Franchini, G., Papas, T. S., Gallo, R. C., and Wong-Staal, F. (1982a). Cloning and characterization of different human sequences related to the onc gene (v-myc) of avian myelocytomatosis virus (MC29).

Proceedings of the National Academy of Sciences of the United States of America **79**, 6497-6501.

Dalla-Favera, R., Migliazza, A., Chang, C. C., Niu, H., Pasqualucci, L., Butler, M., Shen, Q., and Cattoretti, G. (1999). Molecular pathogenesis of B cell malignancy: the role of BCL-6. *Current Topics in Microbiology and Immunology* **246**, 257-263.

Dang, C. V. (1999). c-Myc target genes involved in cell growth, apoptosis, and metabolism. *Molecular and Cellular Biology* **19**, 1-11.

Dang, C. V., Resar, L. M., Emison, E., Kim, S., Li, Q., Prescott, J. E., Wonsey, D., and Zeller, K. (1999). Function of the c-Myc oncogenic transcription factor. *Experimental Cell Research* **253**, 63-77.

Davi, F., Delecluse, H. J., Guiet, P., Gabarre, J., Fayon, A., Gentilhomme, O., Felman, P., Bayle, C., Berger, F., Audouin, J., Bryon, P. A., Diebold, J., and Raphaël, M. (1998). Burkitt-like lymphomas in AIDS patients: Characterization within a series of 103 human immunodeficiency virus-associated non-Hodgkin's Lymphomas. *Journal of Clinical Oncology* **16**, 3788-3795.

Davison, T. S., Vagner, C., Kaghad, M., Ayed, A., Caput, D., and Arrowsmith, C. H. (1999). p73 and p63 are homotetramers capable of weak heterotypic interactions with each other but not with p53. *Journal of Biological Chemistry* **274**, 18709-18714.

De Laurenzi, V. D., Catani, M. V., Terrinoni, A., Corazzari, M., Melino, G., Costanzo, A., Levrero, M., and Knight, R. A. (1999). Additional complexity in p73: induction by mitogens in lymphoid cells and identification of two new splicing variants epsilon and zeta [letter]. *Cell Death and Differentiation* **6**, 389-390.

de Stanchina, E., McCurrach, M. E., Zindy, F., Shieh, S. Y., Ferbeyre, G., Samuelson, A. V., Prives, C., Roussel, M. F., Sherr, C. J., and Lowe, S. W. (1998). E1A signaling to p53 involves the p19(ARF) tumor suppressor. *Genes and Development* **12**, 2434-2442.

De, Laurenzi, V, Costanzo, A., Barcaroli, D., Terrinoni, A., Falco, M., Annicchiarico-Petruzzelli, M., Levrero, M., and Melino, G. (1998). Two new p73 splice variants, gamma and delta, with different transcriptional activity. *Journal of Experimental Medicine* **188**, 1763-1768.

De, Laurenzi, V, Rossi, A., Terrinoni, A., Barcaroli, D., Levrero, M., Costanzo, A., Knight, R. A., Guerrieri, P., and Melino, G. (2000). p63 and p73 transactivate differentiation gene promoters in human keratinocytes. *Biochemical and Biophysical Research Communications* **273**, 342-346.

Decker, L. L., Shankar, P., Khan, G., Freeman, R. B., Dezube, B. J., Lieberman, J., and Thorley-Lawson, D. A. (1996). The Kaposi sarcoma-associated herpesvirus (KSHV) is present as an intact latent genome in KS tissue but replicates in the peripheral blood mononuclear cells of KS patients. *Journal of Experimental Medicine* **184**, 283-288.

Delecluse, H. J., Raphael, M., Magaud, J. P., and Felman, P. (1993b). Variable morphology of human immunodeficiency virus-associated lymphomas with c-myc rearrangements. *Blood* **82 (2)**, 552-563.

Delecluse, H. J., Raphael, M., Magaud, J. P., Felman, P., Alsamad, I. A., Bornkamm, G. W., and Lenoir, G. M. (1993a). Variable morphology of human immunodeficiency virus-associated lymphomas with c-myc rearrangements. The French Study Group of Pathology for Human Immunodeficiency Virus-Associated Tumors, I. *Blood* **82**, 552-563.

Di Como, C. J., Gaiddon, C., and Prives, C. (1999). p73 function is inhibited by tumor-derived p53 mutants in mammalian cells. *Molecular and Cellular Biology* **19**, 1438-1449.

Diehl, V., Henle, G., Henle, W., and Kohn, G. (1968). Demonstration of a herpes group virus in cultures of peripheral leukocytes from patients with infectious mononucleosis. *Journal of Virology* **2**, 663-669.

Dittmer, D., Lagunoff, M., Renne, R., Staskus, K., Haase, A., and Ganem, D. (1998). A cluster of latently expressed genes in Kaposi's sarcoma-associated herpesvirus. *Journal of Virology* **72**, 8309-8315.

Dolcetti, R., Di Luca, D., Carbone, A., Mirandola, P., De Vita, S., Vaccher, E., Sighinolfi, L., Gloghini, A., Tirelli, U., Cassai, E., and Boiocchi, M. (1996). Human herpesvirus 6 in human immunodeficiency virus-infected individuals: association with early histologic phases of lymphadenopathy syndrome but not with malignant lymphoproliferative disorders. *Journal of Medical Virology* **48**, 344-353.

Donehower, L. A., Harvey, M., Slagle, B. L., McArthur, M. J., Montgomery, C. A., Jr., Butel, J. S., and Bradley, A. (1992). Mice deficient for p53 are developmentally normal but susceptible to spontaneous tumours. *Nature* **356**, 215-221.

Drexler, H. G. (1998). Review of alterations of the cyclin-dependent kinase inhibitor INK4 family genes p15, p16, p18 and p19 in human leukemia-lymphoma cells. *Leukemia* **12**, 845-859.

Dupin, N., Gorin, I., Deleuze, J., Agut, H., Huraux, J. M., and Escande, J. P. (1995). Herpes-like DNA sequences, AIDS-related tumors, and Castleman's disease. *New England Journal of Medicine* **333**, 798-799.

Eischen, C. M., Weber, J. D., Roussel, M. F., Sherr, C. J., and Cleveland, J. L. (1999). Disruption of the ARF-Mdm2-p53 tumor suppressor pathway in Myc-induced lymphomagenesis. *Genes and Development* **13**, 2658-2669.

el Deiry, W. S. (1998). p21/p53, cellular growth control and genomic integrity. *Current Topics in Microbiology and Immunology* **227**, 121-137.

el Deiry, W. S., Kern, S. E., Pietenpol, J. A., Kinzler, K. W., and Vogelstein, B. (1992). Definition of a consensus binding site for p53. *Nature Genetics* **1**, 45-49.

Ensoli, B., Gendelman, R., Markham, P., Fiorelli, V., Colombini, S., Raffeld, M., Cafaro, A., Chang, H. K., Brady, J. N., and Gallo, R. C. (1994). Synergy between basic fibroblast growth factor and HIV-1 Tat protein in induction of Kaposi's sarcoma. *Nature* **371**, 674-680.

Epstein, M.A., Achong, B.G., and Barr, Y.M. (1964). Virus particles in cultured lymphoblasts from Burkitt's lymphoma. *The Lancet* **1**, 252-253.

Epstein, M.A., and Crawford, D.H., (1998). " Gammaherpesvirus: Epstein-Barr virus." 9th ed. Topley & Wilson's Microbiology & Microbial Infection (L.Collier, and B.W.J. Mahy, Eds.) **1**, 351-366. Arnold, London, UK.

Esteller, M., Tortola, S., Toyota, M., Capella, G., Peinado, M. A., Baylin, S. B., and Herman, J. G. (2000). Hypermethylation-associated inactivation of p14(ARF) is independent of p16(INK4a) methylation and p53 mutational status. *Cancer Research* **60**, 129-133.

Evan, G. I. and Littlewood, T. D. (1993). The role of c-myc in cell growth. *Current Opinion in Genetics and Development* **3**, 44-49.

Evan, G. I., Wyllie, A. H., Gilbert, C. S., Littlewood, T. D., Land, H., Brooks, M., Waters, C. M., Penn, L. Z., and Hancock, D. C. (1992a). Induction of apoptosis in fibroblasts by c-myc protein. *Cell* **69**, 119-128.

Ewen, M. E. (1994). The cell cycle and the retinoblastoma protein family. *Cancer Metastasis Review* **13**, 45-66.

Fanidi, A., Harrington, E. A., and Evan, G. I. (1992). Cooperative interaction between c-myc and bcl-2 proto-oncogenes. *Nature* **359**, 554-556.

Farrell, P. J., Allan, G. J., Shanahan, F., Vousden, K. H., and Crook, T. (1991). p53 is frequently mutated in Burkitt's lymphoma cell lines. *EMBO Journal* **10**, 2879-2887.

Fassone, L., Bhatia, K., Gutierrez, M., Capello, D., Gloghini, A., Dolcetti, R., Vivenza, D., Ascoli, V., Coco, F. L., Pagani, L., Dotti, G., Rambaldi, A., Raphael, M., Tirelli, U., Saglio, G., Magrath, I. T., Carbone, A., and Gaidano, G. (2000). Molecular profile of Epstein-Barr virus infection in HHV-8-positive primary effusion lymphoma. *Leukemia* **14**, 271-277.

Faulkner, G. C., Burrows, S. R., Khanna, R., Moss, D. J., Bird, A. G., and Crawford, D. H. (1999). X-Linked agammaglobulinemia patients are not infected with Epstein-Barr virus: implications for the biology of the virus. *Journal of Virology* **73**, 1555-1564.

Fearon, E. R., and Vogelstein, B. (1990). A genetic model for colorectal tumorigenesis. *Cell* **61**, 759-767.

Feigal, E. G. (1999). AIDS-associated malignancies: research perspectives. *Biochimica et Biophysica Acta* **1423**, C1-C9.

Feinberg, A. P. and Vogelstein, B. (1983). A technique for radiolabeling DNA restriction endonuclease fragments to high specific activity. *Analytical Biochemistry* **132**, 6-13.

Fillet, A. M., Raphael, M., Visse, B., Audouin, J., Poirel, L., and Agut, H. (1995). Controlled study of human herpesvirus 6 detection in acquired immunodeficiency syndrome-associated non-Hodgkin's lymphoma. The French Study Group for HIV-Associated Tumors. *Journal of Medical Virology* **45**, 106-112.

Fillippovich , I., Sorokina, N., Gatei, M., Haupt, Y., Hobson, K., Moallem, E., Spring, K., Mould, M., McGuckin, M. A., Lavin, M. F., and Khanna, K. K. (2001). Transactivation-deficient p73α (p73Δexon2) inhibits apoptosis and competes with p53. *Oncogene* **20**, 514-522.

Fingeroth, J. D., Weis, J. J., Tedder, T. F., Strominger, J. L., Biro, P. A., and Fearon, D. T. (1984). Epstein-Barr virus receptor of human B lymphocytes is the C3d receptor CR2. *Proceedings of the National Academy of Sciences of the United States of America* **81**, 4510-4514.

Francis, J. M., Heyworth, C. M., Spooncer, E., Pierce, A., Dexter, T. M., and Whetton, A. D. (2000). TGF-beta1-induces apoptosis independently of p53 and selectively reduces expression of bcl-2 in hematopoietic multipotent cells. *Journal of Biological Chemistry* **275**, 39137-39145.

Friborg, J., Kong, W., Hottiger, M. O., and Nabel, G. J. (1999). p53 inhibition by the LANA protein of KSHV protects against cell death. *Nature* **402**, 889-894.

Friedman-Kien, A. E. and Saltzman, B. R. (1990). Clinical manifestations of classical, endemic African, and epidemic AIDS-associated Kaposi's sarcoma. *Journal of the American Academy of Dermatology* **22**, 1237-1250.

Gaidano, G. and Dalla-Favera, R. (1993). Biologic and molecular characterization of non-Hodgkin's lymphoma. *Current Opinion in Oncology* **5**, 776-784.

Gaidano, G. and Dalla-Favera, R. (1995). Molecular pathogenesis of AIDS-related lymphomas. *Advances in Cancer Research* **67**, 113-153.

Gaidano, G., Capello, D., and Carbone, A. (2000). The molecular basis of acquired immunodeficiency syndrome-related lymphomagenesis. *Seminars in Oncology* **27**, 431-441.

Gaidano, G., Carbone, A., Pastore, C., Capello, D., Migliazza, A., Gloghini, A., Roncella, S., Ferrarini, M., Saglio, G., and Dalla-Favera, R. (1997d). Frequent mutation of the 5' noncoding region of the BCL-6 gene in acquired immunodeficiency syndrome-related non-Hodgkin's lymphomas. *Blood* **89**, 3755-3762.

Gaidano, G., Lo, Coco F., Ye, B. H., Shibata, D., Levine, A. M., Knowles, D. M., and Dalla-Favera, R. (1994). Rearrangements of the BCL-6 gene in acquired

immunodeficiency syndrome-associated non-Hodgkin's lymphoma: association with diffuse large-cell subtype. *Blood* **84**, 397-402.

Gaidano, G., Pastore, C., Capello, D., Migliazza, A., Gloghini, A., Saglio, G., Carbone, A., and Dalla-Favera, R. (1997c). Involvement of the bcl-6 gene in AIDS-related lymphomas. *Annals of Oncology* **8 Suppl 2**, 105-108.

Gaidano, G., Pastore, C., Gloghini, A., Canzonieri, V., Capello, D., Franceschi, S., Saglio, G., and Carbone, A. (1997b). Genetic heterogeneity of AIDS-related small non-cleaved cell lymphoma. *British Journal of Hematology* **98**, 726-732.

Gaidano, G., Volpe, G., Pastore, C., Chiarle, R., Capello, D., Gloghini, A., Perissinotto, E., Savinelli, F., Bosco, M., Mazza, U., Pileri, S., Palestro, G., Carbone, A., and Saglio, G. (1997a). Detection of BCL-6 rearrangements and p53 mutations in Malt-lymphomas. *American Journal of Hematology* **56**, 206-213.

Gaiddon, C., Lokshin, M., Ahn, J., Zhang, T., and Prives, C. (2001). A subset of tumor-derived mutant forms of p53 down-regulate p63 and p73 through a direct interaction with the p53 core domain. *Molecular and Cellular Biology* **21**, 1874-1887.

Gail, M. H., Pluda, J. M., Rabkin, C. S., Biggar, R. J., Goedert, J. J., Horm, J. W., Sondik, E. J., Yarchoan, R., and Broder, S. (1991). Projections of the incidence of non-Hodgkin's lymphoma related to acquired immunodeficiency syndrome. *Journal of the National Cancer Institute* **83**, 695-701.

Gallo, R. C., Salahuddin, S. Z., Popovic, M., Shearer, G. M., Kaplan, M., Haynes, B. F., Palker, T. J., Redfield, R., Oleske, J., Safai, B., and . (1984). Frequent detection and isolation of cytopathic retroviruses (HTLV-III) from patients with AIDS and at risk for AIDS. *Science* **224**, 500-503.

Gao, S. J., Kingsley, L., Hoover, D. R., Spira, T. J., Rinaldo, C. R., Saah, A., Phair, J., Detels, R., Parry, P., Chang, Y., and Moore, P. S. (1996b). Seroconversion to antibodies against Kaposi's sarcoma-associated herpesvirus-related latent nuclear antigens before the development of Kaposi's sarcoma. *New England Journal of Medicine* **335**, 233-241.

Gao, S. J., Kingsley, L., Li, M., Zheng, W., Parravicini, C., Ziegler, J., Newton, R., Rinaldo, C. R., Saah, A., Phair, J., Detels, R., Chang, Y., and Moore, P. S. (1996a). KSHV antibodies among Americans, Italians and Ugandans with and without Kaposi's sarcoma. *Nature Medicine* **2**, 925-928.

Garcia-Sanz, R., Gonzalez, M., Vargas, M., Chillon, M. C., Balanzategui, A., Barbon, M., Flores, M. T., and San Miguel, J. F. (1997). Deletions and rearrangements of cyclin-dependent kinase 4 inhibitor gene p16 are associated with poor prognosis in B cell non-Hodgkin's lymphomas. *Leukemia* **11**, 1915-1920.

Gascoyne, R. D., Krajewska, M., Krajewski, S., Connors, J. M., and Reed, J. C. (1997). Prognostic significance of Bax protein expression in diffuse aggressive non-Hodgkin's lymphoma. *Blood* **90**, 3173-3178.

Gazzeri, S., Della, Valle, V, Chaussade, L., Brambilla, C., Larsen, C. J., and Brambilla, E. (1998). The human p19ARF protein encoded by the beta transcript of the p16INK4a gene is frequently lost in small cell lung cancer. *Cancer Research* **58**, 3926-3931.

Genini, D., Sheeter, D., Rought, S., Zaunders, J. J., Susin, S. A., Kroemer, G., Richman, D. D., Carson, D. A., Corbeil, J., and Leoni, L. M. (2001). HIV induces lymphocyte apoptosis by a p53-initiated, mitochondrial-mediated mechanism. *FASEB Journal* **15**, 5-6.

Gerondakis, S., Cory, S., and Adams, J. M. (1984). Translocation of the myc cellular oncogene to the immunoglobulin heavy chain locus in murine plasmacytomas is an imprecise reciprocal exchange. *Cell* **36**, 973-982.

Gerstoft, J., Pallesen, G., Mathiesen, L., Dickmeiss, E., Lindhardt, B. O., Hofmann, B., Nielsen, C. M., Petersen, C. S., and Kroon, S. (1987). Stages in LAV/HTLV-III lymphadenitis. II. Correlation with clinical and immunological findings. *Scandinavian Journal of Immunology* **25**, 93-99.

Goedert, J. J., Cote, T. R., Virgo, P., Scoppa, S. M., Kingma, D. W., Gail, M. H., Jaffe, E. S., and Biggar, R. J. (1998). Spectrum of AIDS-associated malignant disorders. *Lancet* **351**, 1833-1839.

Gombart, A. F., Morosetti, R., Miller, C. W., Said, J. W., and Koeffler, H. P. (1995). Deletions of the cyclin-dependent kinase inhibitor genes p16INK4A and p15INK4B in non-Hodgkin's lymphomas. *Blood* **86**, 1534-1539.

Gong, J. G., Costanzo, A., Yang, H. Q., Melino, G., Kaelin, W. G., Jr., Levrero, M., and Wang, J. Y. (1999). The tyrosine kinase c-Abl regulates p73 in apoptotic response to cisplatin-induced DNA damage [see comments]. *Nature* **399**, 806-809.

Gonzalez-Zulueta, M., Bender, C. M., Yang, A. S., Nguyen, T., Beart, R. W., Van Tornout, J. M., and Jones, P. A. (1995). Methylation of the 5' CpG island of the p16/CDKN2 tumor suppressor gene in normal and transformed human tissues correlates with gene silencing. *Cancer Research* **55**, 4531-4535.

Gorina, S. and Pavletich, N. P. (1996). Structure of the p53 tumor suppressor bound to the ankyrin and SH3 domains of 53BP2 [see comments]. *Science* **274**, 1001-1005.

Gottlieb, T. M. and Oren, M. (1996). p53 in growth control and neoplasia. *Biochimica et Biophysica Acta* **1287**, 77-102.

Gottlieb, T. M. and Oren, M. (1998). p53 and apoptosis. *Seminars in Cancer Biology* **8**, 359-368.

Green, D. R. and Reed, J. C. (1998). Mitochondria and apoptosis. *Science* **281**, 1309-1312.

Greenspan, J. S., Greenspan, D., Lennette, E. T., Abrams, D. I., Conant, M. A., Petersen, V., and Freese, U. K. (1985). Replication of Epstein-Barr virus within the epithelial cells of oral "hairy" leukoplakia, an AIDS-associated lesion. *New England Journal of Medicine* **313**, 1564-1571.

Gribben, J. and Nadler, L. (1995). Detection of minimal residual disease. *Cancer Treatment and Research* **76**, 249-270.

Gronbaek, K., de Nully, Brown P., Moller, M. B., Nedergaard, T., Ralfkiaer, E., Moller, P., Zeuthen, J., and Guldberg, P. (2000). Concurrent disruption of p16INK4a and the ARF-p53 pathway predicts poor prognosis in aggressive non-Hodgkin's lymphoma. *Leukemia* **14**, 1727-1735.

Grossman, S. R., Perez, M., Kung, A. L., Joseph, M., Mansur, C., Xiao, Z. X., Kumar, S., Howley, P. M., and Livingston, D. M. (1998). p300/MDM2 complexes participate in MDM2-mediated p53 degradation. *Molecular Cell* **2**, 405-415.

Gu, W., Bhatia, K., Magrath, I. T., Dan, C. V., and Dalla-Favera, R. (1994). Binding and suppression of the myc transcriptional activation domain by p107. *Science* **264**, 251-254.

Gutierrez, M. I., Bhatia, K., Siwarski, D., Wolff, L., Magrath, I. T., Mushinski, J. F., and Huppi, K. (1992). Infrequent p53 mutation in mouse tumors with deregulated myc. *Cancer Research* **52**, 1032-1035.

Gutierrez, M. I., Cherney, B., Hussain, A., Mostowski, H., Tosato, G., Magrath, I., and Bhatia, K. (1999). Bax is frequently compromised in Burkitt's lymphomas with irreversible resistance to Fas-induced apoptosis. *Cancer Research* **59**, 696-703.

Halevy, O., Michalovitz, D., and Oren, M. (1990). Different tumor-derived p53 mutants exhibit distinct biological activities. *Science* **250**, 113-116.

Hamilton-Dutoit, S. J., Pallesen, G., Franzmann, M. B., Karkov, J., Black, F., Skinhoj, P., and Pedersen, C. (1991). AIDS-related lymphoma. *American Journal of Pathology* **138 No 1**, 149-162.

Hamilton-Dutoit, S. J., Rea, D., Raphael, M., Sandvej, K., Delecluse, H. J., Gisselbrecht, C., Marelle, L., van Krieken, H. J., and Pallesen, G. (1993). Epstein-Barr virus-latent gene expression and tumor cell phenotype in acquired immunodeficiency syndrome-related non-Hodgkin's lymphoma. Correlation of lymphoma phenotype with three distinct patterns of viral latency. *American Journal of Pathology* **143**, 1072-1085.

Hann, S. R., King, M. W., Bentley, D. L., Anderson, C. W., and Eisenman, R. N. (1988). A non-AUG translational initiation in c-myc exon 1 generates an N-terminally distinct protein whose synthesis is disrupted in Burkitt's lymphomas. *Cell* **52**, 185-195.

Hannon, G. J. and Beach, D. (1994). p15INK4B is a potential effector of TGF-beta-induced cell cycle arrest [see comments]. *Nature* **371**, 257-261.

Hanto, D. W., Frizzera, G., Gajl-Peczalska, K., and Simmons, R. L. (1985). Epstein-Barr virus, immunodeficiency, and B cell lymphoproliferation. *Transplantation* **39**, 461-472.

Hara, E., Smith, R., Parry, D., Tahara, H., Stone, S., and Peters, G. (1996). Regulation of p16CDKN2 expression and its implications for cell immortalization and senescence. *Molecular and Cellular Biology* **16**, 859-867.

Harrington, E. A., Fanidi, A., and Evan, G. I. (1994). Oncogenes and cell death. *Current Opinion in Genetics and Development* **4**, 120-129.

Hart, C., Schochetman, G., Spira, T., Lifson, A., Moore, J., Galphin, J., Sninsky, J., and Ou, C. Y. (1988). Direct detection of HIV RNA expression in seropositive subjects. *Lancet* **2**, 596-599.

Haupt, Y., Maya, R., Kazaz, A., and Oren, M. (1997). Mdm2 promotes the rapid degradation of p53. *Nature* **387**, 296-299.

Henle, G., and Henle, W. (1966). Immunofluorescence in cells derived from Burkitt's lymphoma. *Journal of Bacteriology* **91**, 1248-1256.

Henle, W., Henle, G., Andersson, J., Ernberg, I., Klein, G., Horwitz, C. A., Marklund, G., Rymo, L., Wellinder, C., and Straus, S. E. (1987). Antibody responses to Epstein-Barr virus-determined nuclear antigen (EBNA-1) and EBNA-2 in acute and chronic Epstein-Barr virus infection. *Proceedings of the National Academy of Sciences of the United States of America* **84**, 570-574.

Henriksson, M. and Luscher, B. (1996). Proteins of the Myc network: essential regulators of cell growth and differentiation. *Advances in Cancer Research* **68**, 109-182.

Herman, J. G., Civin, C. I., Issa, J. P., Collector, M. I., Sharkis, S. J., and Baylin, S. B. (1997). Distinct patterns of inactivation of p15INK4B and p16INK4A characterize the major types of hematological malignancies. *Cancer Research* **57**, 837-841.

Hinuma, Y., Konn, M., Yamaguchi, J., Wudarski, D. J., Blakeslee, J. R., and Grace, J. T. (1967). Immunofluorescence and herpes-type virus particles in the P3HR-1 Burkitt lymphoma cell line. *Journal of Virology* **1**, 1045-1051.

Hirao, A., Kong, Y. Y., Matsuoka, S., Wakeham, A., Ruland, J., Yoshida, H., Liu, D., Elledge, S. J., and Mak, T. W. (2000). DNA damage-induced activation of p53 by the checkpoint kinase Chk2. *Science* **287**, 1824-1827.

Ho, D. D., Neumann, A. U., Perelson, A. S., Chen, W., Leonard, J. M., and Markowitz, M. (1995). Rapid turnover of plasma virions and CD4 lymphocytes in HIV-1 infection. *Nature* **373**, 123-126.

Hoang, A. T., Lutterbach, B., Lewis, B. C., Yano, T., Chou, T. Y., Barrett, J. F., Raffeld, M., Hann, S. R., and Dang, C. V. (1995). A link between increased transforming activity of lymphoma-derived MYC mutant alleles, their defective regulation by p107, and altered phosphorylation of the c-Myc transactivation domain. *Molecular and Cellular Biology* **15**, 4031-4042.

Hockenbery, D. M., Zutter, m., Hickey, W., Nahm, M., and Korsmeyer, S. J. (1991). BCL2 protein is topographically restricted in tissues characterized by apoptotic cell death. *Proceedings of the National Academy of Sciences of the United States of America* **88**, 6961-6965.

Hockenbery, D., Nunez, G., Milliman, C., Schreiber, R. D., and Korsmeyer, S. J. (1990). Bcl-2 is an inner mitochondrial membrane protein that blocks programmed cell death. *Nature* **348**, 334-336.

Hollstein, M., Rice, K., Greenblatt, M. S., Soussi, T., Fuchs, R., Sorlie, T., Hovig, E., Smith-Sorensen, B., Montesano, R., and Harris, C. C. (1994). Database of p53 gene somatic mutations in human tumors and cell lines. *Nucleic Acids Research* **22**, 3551-3555.

Hollstein, M., Sidransky, D., Vogelstein, B., and Harris, C. C. (1991). p53 mutations in human cancers. *Science* **253**, 49-53.

Hu, Y., Benedict, M. A., Wu, D., Inohara, N., and Nunez, G. (1998). Bcl-XL interacts with Apaf-1 and inhibits Apaf-1-dependent caspase-9 activation. *Proceedings of the National Academy of Sciences of the United States of America* **95**, 4386-4391.

Huang, D. C., Adams, J. M., and Cory, S. (1998). The conserved N-terminal BH4 domain of Bcl-2 homologues is essential for inhibition of apoptosis and interaction with CED-4. *EMBO Journal* **17**, 1029-1039.

Huang, D. C., O'Reilly, L. A., Strasser, A., and Cory, S. (1997). The anti-apoptosis function of Bcl-2 can be genetically separated from its inhibitory effect on cell cycle entry. *EMBO Journal* **16**, 4628-4638.

Hueber, A. O. and Evan, G. I. (1998). Traps to catch unwary oncogenes. *Trends in Genetics* **14**, 364-367.

Hueber, A. O., Zornig, M., Lyon, D., Suda, T., Nagata, S., and Evan, G. I. (1997). Requirement for the CD95 receptor-ligand pathway in c-Myc-induced apoptosis. *Science* **278**, 1305-1309.

Hupp, T. R. and Lane, D. P. (1994). Allosteric activation of latent p53 tetramers. *Current Biology* **4**, 865-875.

Hupp, T. R. and Lane, D. P. (1995). Two distinct signaling pathways activate the latent DNA binding function of p53 in a casein kinase II-independent manner. *Journal of Biological Chemistry* **270**, 18165-18174.

Hussussian, C. J., Struewing, J. P., Goldstein, A. M., Higgins, P. A., Ally, D. S., Sheahan, M. D., Clark, W. H., Jr., Tucker, M. A., and Dracopoli, N. C. (1994). Germline p16 mutations in familial melanoma [see comments]. *Nature Genetics* **8**, 15-21.

Ichimiya, S., Nimura, Y., Kageyama, H., Takada, N., Sunahara, M., Shishikura, T., Nakamura, Y., Sakiyama, S., Seki, N., Ohira, M., Kaneko, Y., McKeon, F., Caput, D., and Nakagawara, A. (1999). p73 at chromosome 1p36.3 is lost in advanced stage neuroblastoma but its mutation is infrequent. *Oncogene* **18**, 1061-1066.

Iida, S., Akiyama, Y., Nakajima, T., Ichikawa, W., Nihei, Z., Sugihara, K., and Yuasa, Y. (2000). Alterations and hypermethylation of the p14(ARF) gene in gastric cancer. *International Journal of Cancer* **87**, 654-658.

Ikawa, S., Nakagawara, A., and Ikawa, Y. (1999). p53 family genes: structural comparison, expression and mutation. *Cell Death and Differentiation* **6**, 1154-1161.

Imai, S., Koizumi, S., Sugiura, M., Tokunaga, M., Uemura, Y., Yamamoto, N., Tanaka, S., Sato, E., and Osato, T. (1994). Gastric carcinoma: monoclonal epithelial malignant cells expressing Epstein-Barr virus latent infection protein. *Proceedings of the National Academy of Sciences of the United States of America* **91**, 9131-9135.

Ingvarsson, S. (1990). The myc gene family proteins and their role in transformation and differentiation. *Seminars in Cancer Biology* **1**, 359-369.

Irwin, M., Marin, M. C., Phillips, A. C., Seelan, R. S., Smith, D. I., Liu, W., Flores, E. R., Tsai, K. Y., Jacks, T., Vousden, K. H., and Kaelin, W. G., Jr. (2000). Role for the p53 homologue p73 in E2F-1-induced apoptosis. *Nature* **407**, 645-648.

Jäättela, M. (1999). Escaping cell death: survival proteins in cancer. *Experimental Cell Research* **248**, 30-43.

Jaffe, E. S., Clark, J., Steis, R., Blattner, W., Macher, A. M., Longo, D. L., and Reichert, C. M. (1985). Lymph node pathology of HTLV and HTLV-associated neoplasms. *Cancer Research* **45**, 4662s-4664s.

James, M. C. and Peters, G. (2000). Alternative product of the p16/CKDN2A locus connects the Rb and p53 tumor suppressors. *Progress in Cell Cycle Research* **4**, 71-81.

Jayaraman, L. and Prives, C. (1999). Covalent and noncovalent modifiers of the p53 protein. *Cellular and Molecular Life Sciences* **55**, 76-87.

Jin, M., Piao, Z., Kim, N. G., Park, C., Shin, E. C., Park, J. H., Jung, H. J., Kim, C. G., and Kim, H. (2000). p16 is a major inactivation target in hepatocellular carcinoma. *Cancer* **89**, 60-68.

Jones, J. F., Shurin, S., Abramowsky, C., Tubbs, R. R., Sciotto, C. G., Wahl, R., Sands, J., Gottman, D., Katz, B. Z., and Sklar, J. (1988). T-cell lymphomas

containing Epstein-Barr viral DNA in patients with chronic Epstein-Barr virus infections. *New England Journal of Medicine* **318**, 733-741.

Joos, S., Haluska, F. G., Falk, M. H., Henglein, B., Hameister, H., Croce, C. M., and Bornkamm, G. W. (1992). Mapping chromosomal breakpoints of Burkitt's t(8;14) translocations far upstream of c-myc. *Cancer Research* **52**, 6547-6552.

Jost, C. A., Marin, M. C., and Kaelin, W. G., Jr. (1997). p73 is a simian [correction of human] p53-related protein that can induce apoptosis [see comments] [published erratum appears in Nature 1999 Jun 24;399(6738):817]. *Nature* **389**, 191-194.

Kaghad, M., Bonnet, H., Yang, A., Creancier, L., Biscan, J. C., Valent, A., Minty, A., Chalon, P., Lelias, J. M., Dumont, X., Ferrara, P., McKeon, F., and Caput, D. (1997). Monoallelically expressed gene related to p53 at 1p36, a region frequently deleted in neuroblastoma and other human cancers. *Cell* **90**, 809-819.

Kalter, S. P., Riggs, S. A., Cabanillas, F., Butler, J. J., Hagemeister, F. B., Mansell, P. W., Newell, G. R., Velasquez, W. S., Salvador, P., Barlogie, B., Rios, A., and Hersh, E. M. (1985). Aggressive non-Hodgkin's lymphomas in immunocompromised homosexual males. *Blood* **66 (3)**, 655-659.

Kamb, A. (1995). Cell-cycle regulators and cancer. *Trends in Genetics* **11**, 136-140.

Kamb, A., Gruis, N. A., Weaver-Feldhaus, J., Liu, Q., Harshman, K., Tavtigian, S. V., Stockert, E., Day, R. S., III, Johnson, B. E., and Skolnick, M. H. (1994). A cell cycle regulator potentially involved in genesis of many tumor types [see comments]. *Science* **264**, 436-440.

Kamijo, T., Weber, J. D., Zambetti, G., Zindy, F., Roussel, M. F., and Sherr, C. J. (1998). Functional and physical interactions of the ARF tumor suppressor with p53 and Mdm2. *Proceedings of the National Academy of Sciences of the United States of America* **95**, 8292-8297.

Kamijo, T., Zindy, F., Roussel, M. F., Quelle, D. E., Downing, J. R., Ashmun, R. A., Grosveld, G., and Sherr, C. J. (1997). Tumor suppression at the mouse INK4a locus mediated by the alternative reading frame product p19ARF. *Cell* **91**, 649-659.

Kaplan, L. D., Abrams, D. I., Feigal, E., McGrath, M., Kahn, J., Neville, P., Ziegler, J., and Volberding, P. A. (1989). AIDS-associated non-Hodgkin's lymphoma in San Francisco. *JAMA* **261**, 719-724.

Kato, G. J., Barrett, J., Villa-Garcia, M., and Dang, C. V. (1990). An amino-terminal c-myc domain required for neoplastic transformation activates transcription. *Molecular and Cellular Biology* **10**, 5914-5920.

Kato, S., Shimada, A., Osada, M., Ikawa, S., Obinata, M., Nakagawara, A., Kanamaru, R., and Ishioka, C. (1999). Effects of p51/p63 missense mutations on transcriptional activities of p53 downstream gene promoters. *Cancer Research* **59**, 5908-5911.

Kawano, S., Miller, C. W., Gombart, A. F., Bartram, C. R., Matsuo, Y., Asou, H., Sakashita, A., Said, J., Tatsumi, E., and Koeffler, H. P. (1999). Loss of p73 gene expression in leukemias/lymphomas due to hypermethylation. *Blood* **94**, 1113-1120.

Kellam, P., Boshoff, C., Whitby, D., Matthews, S., Weiss, R. A., and Talbot, S. J. (1997). Identification of a major latent nuclear antigen, LNA-1, in the human herpesvirus 8 genome. *Journal of Human Virology* **1**, 19-29.

Kenney, J. L., Guinness, M. E., Curiel, T., and Lacy, J. (1998). Antisense to the epstein-barr virus (EBV)-encoded latent membrane protein 1 (LMP-1) suppresses LMP-1 and bcl-2 expression and promotes apoptosis in EBV-immortalized B cells. *Blood* **92**, 1721-1727.

Kern, S. E., Pietenpol, J. A., Thiagalingam, S., Seymour, A., Kinzler, K. W., and Vogelstein, B. (1992). Oncogenic forms of p53 inhibit p53-regulated gene expression. *Science* **256**, 827-830.

Kikuchi, M., Miki, T., Kumagai, T., Fukuda, T., Kamiyama, R., Miyasaka, N., and Hirosawa, S. (2000). Identification of negative regulatory regions within the first exon and intron of the BCL6 gene. *Oncogene* **19**, 4941-4945.

Klangby, U., Okan, I., Magnusson, K. P., Wendland, M., Lind, P., and Wiman, K. G. (1998). p16/INK4a and p15/INK4b gene methylation and absence of p16/INK4a mRNA and protein expression in Burkitt's lymphoma. *Blood* **91**, 1680-1687.

Klein, G. and Dombos, L. (1973). Relationship between the sensitivity of EBV-carrying lymphoblastoid lines to superinfection and the inducibility of the resident viral genome. *International Journal of Cancer* **11**, 327-337.

Klein, G., Giovanella, B., Westman, A., Stehlin, J. S., and Mumford, D. (1975). An EBV-genome-negative cell line established from an American Burkitt lymphoma; receptor characteristics. EBV infectibility and permanent conversion into EBV-positive sublines by in vitro infection. *Intervirology* **5**, 319-334.

Kliche, S., Kremmer, E., Hammerschmidt, W., Koszinowski, U., and Haas, J. (1998). Persistent infection of Epstein-Barr virus-positive B lymphocytes by human herpesvirus 8. *Journal of Virology* **72**, 8143-8149.

Knowles, D. M. (1997). Molecular pathology of acquired immunodeficiency syndrome-related non-Hodgkin's lymphoma. *Seminars in Diagnostic Pathology* **14**, 67-82.

Knudson, A. G. (1971). Mutation and cancer: statistical study of retinoblastoma. *Proceedings of the National Academy of Sciences of the United States of America* **68**, 820-823.

Knudson, C. M. and Korsmeyer, S. J. (1997). Bcl-2 and Bax function independently to regulate cell death. *Nature Genetics* **16**, 358-363.

Knudson, C. M., Johnson, G. M., Lin, Y., and Korsmeyer, S. J. (2001). Bax accelerates tumorigenesis in p53-deficient mice. *Cancer Research* **61**, 659-665.

Ko, L. J. and Prives, C. (1996). p53: puzzle and paradigm. *Genes and Development* **10**, 1054-1072.

Kocher, T. D., and Wilson, A. C. (1991). DNA amplification by the polymerase chain reaction. 1st ed. *In* "Essential molecular biology: A practical approach." (T.A. Brown, Ed.) **2**, 185-207. Oxford University Press, Oxford, UK.

Koduru, P. R., Zariwala, M., Soni, M., Gong, J. Z., Xiong, Y., and Broome, J. D. (1995). Deletion of cyclin-dependent kinase 4 inhibitor genes P15 and P16 in non-Hodgkin's lymphoma. *Blood* **86**, 2900-2905.

Koelle, D. M., Huang, M. L., Chandran, B., Vieira, J., Piepkorn, M., and Corey, L. (1997). Frequent detection of Kaposi's sarcoma-associated herpesvirus (human herpesvirus 8) DNA in saliva of human immunodeficiency virus-infected men: clinical and immunologic correlates. *Journal of Infectious Diseases* **176**, 94-102.

Korsmeyer, S. J. (1992). Bcl-2 initiates a new category of oncogenes: regulators of cell death. *Blood* **80**, 879-886.

Korsmeyer, S. J. (1999). BCL-2 gene family and the regulation of programmed cell death. *Cancer Research* **59**, 1693s-1700s.

Kovalev, S., Marchenko, N., Swendeman, S., LaQuaglia, M., and Moll, U. M. (1998). Expression level, allelic origin, and mutation analysis of the p73 gene in neuroblastoma tumors and cell lines. *Cell Growth and Differentiation* **9**, 897-903.

Krajewski, S., Tanaka, S., Takayama, S., Schibler, M. J., Fenton, W., and Reed, J. C. (1993). Investigation of the subcellular distribution of the bcl-2 oncoprotein: residence in the nuclear envelope, endoplasmic reticulum, and outer mitochondrial membranes. *Cancer Research* **53**, 4701-4714.

Kubbutat, M. H., Jones, S. N., and Vousden, K. H. (1997). Regulation of p53 stability by Mdm2. *Nature* **387**, 299-303.

Kubo, Y., Urano, Y., Matsumoto, K., Ahsan, K., and Arase, S. (1997). Mutations of the INK4a locus in squamous cell carcinomas of human skin. *Biochemical and Biophysical Research Communications* **232**, 38-41.

Kundu, R. K., Sangiorgi, F., Wu, L-Y., Pattengale, P. K., Hinton, D. R., Gill, P. S., and Maxson, R. (1999). Expression of the human immunodeficiency virus-tat gene in lymphoid tissues of transgenic mice is associated with B-cell lymphoma. *Blood* **94**, 275-282.

Lackovich, J. K., Lee, J. E., Chang, P., and Rashtchian, A. (2001). *Focus (2001)*, **23**. Molecular Biology Research and Development, Life Technologies, A Division of Invitrogen Corporation, Rockville, Maryland.

Lamb, P. and Crawford, L. (1986). Characterization of the human p53 gene. *Molecular and Cellular Biology* **6**, 1379-1385.

Land, H., Parada, L. F., and Weinberg, R. A. (1983). Cellular oncogenes and multistep carcinogenesis. *Science* **222**, 771-778.

Lane, D. P. and Crawford, L. V. (1979). T antigen is bound to a host protein in SV40-transformed cells. *Nature* **278**, 261-263.

Lang, W., Perkins, H., Anderson, R. E., Royce, R., Jewell, N., and Winkelstein, W. (1989). Patterns of T lymphocyte changes with human immunodeficiency virus infection: from seroconversion to the development of AIDS. *Journal of Acquired Immune Deficiency Syndromes and Human Retrovirology* **2**, 63-69.

Larocca, L. M., Capello, D., Rinelli, A., Nori, S., Antinori, A., Gloghini, A., Cingolani, A., Migliazza, A., Saglio, G., Cammilleri-Broet, S., Raphael, M., Carbone, A., and Gaidano, G. (1998). The molecular and phenotypic profile of primary central nervous system lymphoma identifies distinct categories of the disease and is consistent with histogenetic derivation from germinal center-related B cells. *Blood* **92**, 1011-1019.

Lazarus, P., Garewal, H. S., Sciubba, J., Zwiebel, N., Calcagnotto, A., Fair, A., Schaefer, S., and Richie, J. P. (1995). A low incidence of p53 mutations in pre-malignant lesions of the oral cavity from non-tobacco users. *International Journal of Cancer* **60**, 458-463.

Lee, J. T., Innes, D. J., Jr., and Williams, M. E. (1989). Sequential bcl-2 and c-myc oncogene rearrangements associated with the clinical transformation of non-Hodgkin's lymphoma. *Journal of Clinical Investigation* **84**, 1454-1459.

Lee, L. A., Dolde, C., Barrett, J., Wu, C. S., and Dang, C. V. (1996). A link between c-Myc-mediated transcriptional repression and neoplastic transformation. *Journal of Clinical Investigation* **97**, 1687-1695.

Lennette, E. T., Blackbourn, D. J., and Levy, J. A. (1996). Antibodies to human herpesvirus type 8 in the general population and in Kaposi's sarcoma patients. *Lancet* **348**, 858-861.

Levine, A. J. (1997). p53, the cellular gatekeeper for growth and division. *Cell* **88**, 323-331.

Levine, A. M. (1992). Acquired immunodeficiency syndrome-related lymphoma. *Blood* **80 (1)**, 8-20.

Levine, A. M. (1998). Hodgkin's disease in the setting of human immunodeficiency virus infection. *Journal of the National Cancer Institute Monographs* **73**, 37-42.

Levine, A. M., Gill, P. S., Meyer, P. R., Burkes, R. L., Ross, R., Dworsky, R. D., Krailo, M., Parker, J. W., Lukes, R. J., and Rasheed, S. (1985). Retrovirus and

malignant lymphoma in homosexual men. *Journal of the American Medical Association* **254**, 1921-1925.

Levine, A. M., Sullivan-Halley, J., Pike, M. C., Rarick, M. U., Loureiro, C., Bernstein-Singer, M., Willson, E., Brynes, R., Parker, J., Rasheed, S., *et al.* (1991). Human immunodeficiency virus-related lymphoma. Prognostic factors predictive of survival. *Cancer* **68**, 2466-2472.

Levrero, M., De, Laurenzi, V, Costanzo, A., Gong, J., Melino, G., and Wang, J. Y. (1999). Structure, function and regulation of p63 and p73 [see comments]. *Cell Death and Differentiation* **6**, 1146-1153.

Levy, J. A. (1993). Pathogenesis of human immunodeficiency virus infection. *Microbiological Reviews* **57**, 183-289.

Li, C. J., Wang, C., Friedman, D. J., and Pardee, A. B. (1995). Reciprocal modulations between p53 and Tat of human immunodeficiency virus type 1. *Proceedings of the National Academy of Sciences of the United States of America* **92**, 5461-5464.

Li, L. H., Nerlov, C., Prendergast, G., MacGregor, D., and Ziff, E. B. (1994b). c-Myc represses transcription in vivo by a novel mechanism dependent on the initiator element and Myc box II. *EMBO Journal* **13**, 4070-4079.

Li, Y., Nichols, M. A., Shay, J. W., and Xiong, Y. (1994a). Transcriptional repression of the D-type cyclin-dependent kinase inhibitor p16 by the retinoblastoma susceptibility gene product pRb. *Cancer Research* **54**, 6078-6082.

Liebowitz, D. (1998). Epstein-Barr virus and a cellular signaling pathway in lymphomas from immunosuppressed patients. *New England Journal of Medicine* **338**, 1413-1421.

Lilischkis, R., Sarcevic, B., Kennedy, C., Warlters, A., and Sutherland, R. L. (1996). Cancer-associated mis-sense and deletion mutations impair p16INK4 CDK inhibitory activity. *International Journal of Cancer* **66**, 249-254.

Limpens, J., de Jong, D., van Krieken, J. H., Price, C. G., Young, B. D., van Ommen, G. J., and Kluin, P. M. (1991). Bcl-2/JH rearrangements in benign lymphoid tissues with follicular hyperplasia. *Oncogene* **6**, 2271-2276.

Limpens, J., Stad, R., Vos, C., de Vlaam, C., de Jong, D., van Ommen, G. J., Schuuring, E., and Kluin, P. M. (1995). Lymphoma-associated translocation t(14;18) in blood B cells of normal individuals. *Blood* **85**, 2528-2536.

Lin, J., Teresky, A. K., and Levine, A. J. (1995). Two critical hydrophobic amino acids in the N-terminal domain of the p53 protein are required for the gain of function phenotypes of human p53 mutants. *Oncogene* **10**, 2387-2390.

Linz, U., Delling, U., and Rubsamen-Waigmann, H. (1990). Systematic studies on parameters influencing the performance of the polymerase chain reaction. *Journal of Clinical Chemistry and Clinical Biochemistry* **28**, 5-13.

Liu, Y., Cortopassi, G., Goedert, J. J., and Rabkin, C. S. (1997). Frequency of Bcl-2 rearrangements in peripheral blood of HIV-infected individuals. *British Journal of Haematology* **99**, 465-466.

Lo, Coco F., Ye, B. H., Lista, F., Corradini, P., Offit, K., Knowles, D. M., Chaganti, R. S., and Dalla-Favera, R. (1994). Rearrangements of the BCL6 gene in diffuse large cell non-Hodgkin's lymphoma. *Blood* **83**, 1757-1759.

Lohrum, M. A. and Vousden, K. H. (1999). Regulation and activation of p53 and its family members [see comments]. *Cell Death and Differentiation* **6**, 1162-1168.

Luciw, P. (1996). Human Immunodeficiency viruses and their replication. 3rd ed. *In* Fields Virology (B.N. Fields, D.M. Knipe, and P.M. Howley, Eds.) **2**, 1881-1952. Lippincott-Raven Publishers, Philadelphia, Pennsylvania, USA.

Lusso, P. and Gallo, R. C. (1994). Human herpesvirus 6 in AIDS. *Lancet* **343**, 555-556.

MacMahon, E. M., Glass, J. D., Hayward, S. D., Mann, R. B., Becker, P. S., Charache, P., McArthur, J. C., and Ambinder, R. F. (1991). Epstein-Barr virus in AIDS-related primary central nervous system lymphoma. *Lancet* **338**, 969-973.

Malumbres, M., Perez, de Castro, I, Santos, J., Fernandez, Piqueras J., and Pellicer, A. (1999). Hypermethylation of the cell cycle inhibitor p15INK4b 3'-untranslated region interferes with its transcriptional regulation in primary lymphomas. *Oncogene* **18**, 385-396.

Malumbres, M., Perez, de Castro, I, Santos, J., Melendez, B., Mangues, R., Serrano, M., Pellicer, A., and Fernandez-Piqueras, J. (1997). Inactivation of the cyclin-dependent kinase inhibitor p15INK4b by deletion and de novo methylation with independence of p16INK4a alterations in murine primary T-cell lymphomas. *Oncogene* **14**, 1361-1370.

Mao, E. J., Schwartz, S. M., Daling, J. R., Oda, D., Tickman, L., and Beckmann, A. M. (1996). Human papilloma viruses and p53 mutations in normal pre-malignant and malignant oral epithelia. *International Journal of Cancer* **69**, 152-158.

Marin, M. C., Jost, C. A., Brooks, L. A., Irwin, M. S., O'Nions, J., Tidy, J. A., James, N., McGregor, J. M., Harwood, C. A., Yulug, I. G., Vousden, K. H., Allday, M. J., Gusterson, B., Ikawa, S., Hinds, P. W., Crook, T., and Kaelin, W. G. (2000). A common polymorphism acts as an intragenic modifier of mutant p53 behaviour. *Nature Genetics* **25**, 47-54.

Martin, J. N., Ganem, D. E., Osmond, D. H., Page-Shafer, K. A., Macrae, D., and Kedes, D. H. (1998). Sexual transmission and the natural history of human herpesvirus 8 infection. *New England Journal of Medicine* **338**, 948-954.

Marutani, M., Tonoki, H., Tada, M., Takahashi, M., Kashiwazaki, H., Hida, Y., Hamada, J., Asaka, M., and Moriuchi, T. (1999). Dominant-negative mutations of the tumour suppressor p53 relating to early onset of Glioblastoma multiforme. *Cancer Research* **59**, 4765-4769.

Matolcsy, A., Casali, P., Warnke, R. A., and Knowles, D. M. (1996). Morphologic transformation of follicular lymphoma is associated with somatic mutation of the translocated Bcl-2 gene. *Blood* **88**, 3937-3944.

McClain, K. L., Leach, C. T., Jenson, H. B., Joshi, V. V., Pollock, B. H., Parmley, R. T., DiCarlo, F. J., Chadwick, E. G., and Murphy, S. B. (1995). Association of Epstein-Barr virus with leiomyosarcomas in children with AIDS. *New England Journal of Medicine* **332** , 12-18.

McDonnell, T. J. and Korsmeyer, S. J. (1991). Progression from lymphoid hyperplasia to high-grade malignant lymphoma in mice transgenic for the t(14; 18). *Nature* **349**, 254-256.

McGowan, J. P. and Shah, S. (1998). Long-term remission of AIDS-related primary central nervous system lymphoma associated with highly active antiretroviral therapy. *AIDS* **12**, 952-954.

Meijerink, J. P., Mensink, E. J., Wang, K., Sedlak, T. W., Sloetjes, A. W., de Witte, T., Waksman, G., and Korsmeyer, S. J. (1998). Hematopoietic malignancies demonstrate loss-of-function mutations of BAX. *Blood* **91**, 2991-2997.

Melendez, B., Malumbres, M., de Castro, I. P., Santos, J., Pellicer, A., and Fernandez-Piqueras, J. (2000). Characterization of the murine p19(ARF) promoter CpG island and its methylation pattern in primary lymphomas. *Carcinogenesis* **21**, 817-821.

Mellors, J. W., Rinaldo, C. R., Gupta, P., White, R. M., Todd, J. A., and Kingsley, L. A. (1996). Prognosis in HIV-1 infection predicted by the quantity of virus in plasma. *Science* **272**, 1167-1170.

Menezes, J., Leibold, W., Klein, G., and Clements, G. (1975). Establishment and characterization of an Epstein-Barr virus (EBC)-negative lymphoblastoid B cell line (BJA-B) from an exceptional, EBV-genome-negative African Burkitt's lymphoma. *Biomedicine* **22**, 276-284.

Merlo, A., Herman, J. G., Mao, L., Lee, D. J., Gabrielson, E., Burger, P. C., Baylin, S. B., and Sidransky, D. (1995). 5' CpG island methylation is associated with transcriptional silencing of the tumour suppressor p16/CDKN2/MTS1 in human cancers [see comments]. *Nature Medicine* **1**, 686-692.

Metroka, C. E., Cunningham-Rundles, S., Pollack, M. S., Sonnabend, J. A., Davis, J. M., Gordon, B., Fernandez, R. D., and Mouradian, J. (1983). Generalized lymphadenopathy in homosexual men. *Annals of Internal Medicine* **99**, 585-591.

Meyer, P. R., Yanagihara, E. T., Parker, J. W., and Lukes, R. J. (1984). A distinctive follicular hyperplasia in the acquired immune deficiency syndrome (AIDS) and the AIDS related complex. A pre-lymphomatous state for B cell lymphomas? *Hematological Oncology* **2**, 319-347.

Mietz, J. A., Unger, T., Huibregtse, J. M., and Howley, P. M. (1992). The transcriptional transactivation function of wild-type p53 is inhibited by SV40 large T-antigen and by HPV-16 E6 oncoprotein. *EMBO Journal* **11**, 5013-5020.

Migliazza, A., Martinotti, S., Chen, W., Fusco, C., Ye, B. H., Knowles, D. M., Offit, K., Chaganti, R. S., and Dalla-Favera, R. (1995). Frequent somatic hypermutation of the 5' noncoding region of the BCL6 gene in B-cell lymphoma. *Proceedings of the National Academy of Sciences of the United States of America* **92**, 12520-12524.

Milner, J. and Medcalf, E. A. (1991). Cotranslation of activated mutant p53 with wild type drives the wild-type p53 protein into the mutant conformation. *Cell* **65**, 765-774.

Miyashita, E. M., Yang, B., Lam, K. M., Crawford, D. H., and Thorley-Lawson, D. A. (1995). A novel form of Epstein-Barr virus latency in normal B cells in vivo. *Cell* **80**, 593-601.

Miyashita, T. and Reed, J. C. (1995). Tumor suppressor p53 is a direct transcriptional activator of the human bax gene. *Cell* **80**, 293-299.

Moore, P. S. and Chang, Y. (1998). Kaposi's sarcoma-associated herpesvirus-encoded oncogenes and oncogenesis. *Journal of the National Cancer Institute Monographs* **266**, 65-71.

Moses, A. V., Williams, S. E., Strussenberg, J. G., Heneveld, M. L., Ruhl, R. A., Bakke, A. C., Bagby, G. C., and Nelson, J. A. (1997). HIV-1 induction of CD40 on endothelial cells promotes the outgrowth of AIDS-associated B-cell lymphomas. *Nature Medicine* **3**, 1242-1249.

Moss, D. J., Rickinson, A. B., and Pope, J. H. (1978). Long-term T-cell-mediated immunity to Epstein-Barr virus in man. I. Complete regression of virus-induced transformation in cultures of seropositive donor leukocytes. *International Journal of Cancer* **22**, 662-668.

Mueller, N. (1999). Overview of the epidemiology of malignancy in immune deficiency. *Journal of Acquired Immune Deficiency Syndromes and Human Retrovirology* **21 Suppl 1**, S5-10.

Muller, J. R., Janz, S., Goedert, J. J., Potter, M., and Rabkin, C. S. (1995). Persistence of immunoglobulin heavy chain/c-myc recombination-positive lymphocyte clones in the blood of human immunodeficiency virus-infected homosexual men. *Proceedings of the National Academy of Sciences of the United States of America* **92**, 6577-6581.

Nador, R. G., Cesarman, E., Chadburn, A., Dawson, D. B., Ansari, M. Q., Sald, J., and Knowles, D. M. (1996). Primary effusion lymphoma: a distinct clinicopathologic entity associated with the Kaposi's sarcoma-associated herpes virus. *Blood* **88**, 645-656.

Nakamura, H., Said, J. W., Miller, C. W., and Koeffler, H. P. (1993). Mutation and protein expression of p53 in acquired immunodeficiency syndrome-related lymphomas. *Blood* **82 (3)**, 920-926.

Nakamura, Y., Saito, K., and Furusawa, S. (1999). Analysis of internal deletions within the BCL6 gene in B-cell non-Hodgkin's lymphoma. *British Journal of Haematology* **105**, 274-277.

Neale, G. A. and Kitchingman, G. R. (1991). mRNA transcripts initiating within the human immunoglobulin mu heavy chain enhancer region contain a non-translatable exon and are extremely heterogeneous at the 5' end. *Nucleic Acids Research* **19**, 2427-2433.

Neri, A., Barriga, F., Inghirami, G., Knowles, D. M., Neequaye, J., Magrath, I. T., and Dalla-Favera, R. (1991). Epstein-Barr virus infection precedes clonal expansion in Burkitt's and acquired immunodeficiency syndrome-associated lymphoma. *Blood* **77**, 1092-1095.

Neri, A., Knowles, D. M., Greco, A., McCormick, F., and Dalla-Favera, R. (1988). Analysis of RAS oncogene mutations in human lymphoid malignancies. *Proceedings of the National Academy of Sciences of the United States of America* **85**, 9268-9272.

Nesbit, C. E., Tersak, J. M., and Prochownik, E. V. (1999). MYC oncogenes and human neoplastic disease. *Oncogene* **18**, 3004-3016.

Ng, S. W., Yiu, G. K., Liu, Y., Huang, L. W., Palnati, M., Jun, S. H., Berkowitz, R. S., and Mok, S. C. (2000). Analysis of p73 in human borderline and invasive ovarian tumor. *Oncogene* **19**, 1885-1890.

Ngan, B. Y., Nourse, J., and Cleary, M. L. (1989). Detection of chromosomal translocation t(14;18) within the minor cluster region of bcl-2 by polymerase chain reaction and direct genomic sequencing of the enzymatically amplified DNA in follicular lymphomas. *Blood* **73**, 1759-1762.

Niederman, J. C., Evans, A. S., Subrahmanyan, L., and McCollum, R. W. (1970). Prevalence, incidence and persistence of EB virus antibody in young adults. *New England Journal of Medicine* **282 (17)**, 361-365.

Niedobitek, G., Young, L. S., and Herbst, H. (1997). Epstein-Barr virus infection and the pathogenesis of malignant lymphomas. *Cancer Surveys* **30**, 143-162.

Niu, H., Ye, B. H., and Dalla-Favera, R. (1998). Antigen receptor signaling induces MAP kinase-mediated phosphorylation and degradation of the BCL-6 transcription factor. *Genes and Development* **12**, 1953-1961.

Nosari, A., Cantoni, S., Oreste, P., Schiantarelli, C., Landonio, G., Alexiadis, S., Gargantini, L., Caggese, L., Gambacorta, M., and Morra, E. (1996). Anaplastic large cell (CD30/Ki-1+) lymphoma in HIV+ patients: clinical and pathological findings in a group of ten patients. *British Journal of Hematology* **95**, 508-512.

Offit, K., Lo, Coco F., Louie, D. C., Parsa, N. Z., Leung, D., Portlock, C., Ye, B. H., Lista, F., Filippa, D. A., and Rosenbaum, A. (1994). Rearrangement of the bcl-6 gene as a prognostic marker in diffuse large-cell lymphoma [see comments]. *New England Journal of Medicine* **331**, 74-80.

Okamoto, A., Hussain, S. P., Hagiwara, K., Spillare, E. A., Rusin, M. R., Demetrick, D. J., Serrano, M., Hannon, G. J., Shiseki, M., Zariwala, M., *et al.* (1995). Mutations in the p16INK4/MTS1/CDKN2, p15INK4B/MTS2, and p18 genes in primary and metastatic lung cancer. *Cancer Research* **55**, 1448-1451.

Oksenhendler, E., Duarte, M., Soulier, J., Cacoub, P., Welker, Y., Cadranel, J., Cazals-Hatem, D., Autran, B., Clauvel, J. P., and Raphael, M. (1996). Multicentric Castleman's disease in HIV infection: a clinical and pathological study of 20 patients. *AIDS* **10**, 61-67.

O'Leary, J. J., Kennedy, M., Luttich, K., Uhlmann, V., Silva, I., Russell, J., Sheils, O., Ring, M., Sweeney, M., Kenny, C., Bermingham, N., Martin, C., O'Donovan, M., Howells, D., Picton, S., and Lucas, S. B. (2000). Localisation of HHV-8 in AIDS related lymphadenopathy. *Molecular Pathology* **53**, 43-47.

Oltvai, Z. N., Milliman, C. L., and Korsmeyer, S. J. (1993). Bcl-2 heterodimerizes in vivo with a conserved homolog, Bax, that accelerates programmed cell death. *Cell* **74**, 609-619.

Ometto, L., Menin, C., Masiero, S., Bonaldi, L., Del Mistro, A., Cattelan, A. M., D'Andrea, E., De Rossi, A., and Chieco-Bianchi, L. (1997). Molecular profile of Epstein-Barr virus in human immunodeficiency virus type 1-related lymphadenopathies and lymphomas. *Blood* **90**, 313-322.

Osada, M., Ohba, M., Kawahara, C., Ishioka, C., Kanamaru, R., Katoh, I., Ikawa, Y., Nimura, Y., Nakagawara, A., Obinata, M., and Ikawa, S. (1998). Cloning and functional analysis of human p51, which structurally and functionally resembles p53 [see comments] [published erratum appears in Nat Med 1998 Sep 4(9): 982]. *Nature Medicine* **4**, 839-843.

Ozaki, T., Naka, M., Takada, N., Tada, M., Sakiyama, S., and Nakagawara, A. (1999). Deletion of the COOH-terminal region of p73alpha enhances both its transactivation function and DNA-binding activity but inhibits induction of apoptosis in mammalian cells. *Cancer Research* **59**, 5902-5907.

Palella, F. J., Delaney, K. M., Moorman, A. C., Loveless, M. O., Fuhrer, J., Satten, G. A., Aschman, D. J., and Holmberg, S. D. (1998). Declining morbidity and mortality among patients with advanced human immunodeficiency virus infection.

HIV Outpatient Study Investigators. *New England Journal of Medicine* **338**, 853-860.

Pallesen, G., Gerstoft, J., and Mathiesen, L. (1987). Stages in LAV/HTLV-III lymphadenitis. I. Histological and immunohistological classification. *Scandinavian Journal of Immunology* **25**, 83-91.

Palmero, I., Pantoja, C., and Serrano, M. (1998). p19ARF links the tumour suppressor p53 to Ras [letter]. *Nature* **395**, 125-126.

Pantaleo, G., Graziosi, C., Demarest, J. F., Butini, L., Montroni, M., Fox, C. H., Orenstein, J. M., Kotler, D. P., and Fauci, A. S. (1993). HIV infection is active and progressive in lymphoid tissue during the clinically latent stage of disease. *Nature* **362**, 355-358.

Parravicini, C., Chandran, B., Corbellino, M., Berti, E., Paulli, M., Moore, P. S., and Chang, Y. (2000). Differential viral protein expression in Kaposi's sarcoma-associated herpesvirus-infected diseases: Kaposi's sarcoma, primary effusion lymphoma, and multicentric Castleman's disease. *American Journal of Pathology* **156**, 743-749.

Pasqualucci, L., Migliazza, A., Fracchiolla, N., William, C., Neri, A., Baldini, L., Chaganti, R. S., Klein, U., Kuppers, R., Rajewsky, K., and Dalla-Favera, R. (1998). BCL-6 mutations in normal germinal center B cells: evidence of somatic hypermutation acting outside Ig loci. *Proceedings of the National Academy of Sciences of the United States of America* **95**, 11816-11821.

Pastore, C., Carbone, A., Gloghini, A., Volpe, G., Saglio, G., and Gaidano, G. (1996). Association of 6q deletions with AIDS-related diffuse large cell lymphoma. *Leukemia* **10**, 1051-1053.

Pelicci, P. G., Knowles, D. M., Magrath, I., and Dalla-Favera, R. (1986a). Chromosomal breakpoints and structural alterations of the c-myc locus differ in endemic and sporadic forms of Burkitt lymphoma. *Proceedings of the National Academy of Sciences of the United States of America* **83**, 2984-2988.

Pelicci, P-G., Knowles, D. M., Arlin, Z. A., Wieczorek, R., Luciw, P., Dina, D., Basilico, C., and Dalla-Favera, R. (1986b). Multiple monoclonal B cell expansions and c-myc oncogene rearrangements in acquired immune deficiency syndrome-related lymphoproliferative disorders. *Journal of Experimental Medicine* **164**, 2049-2076.

Pescarmona, E., De, Sanctis, V, Pistilli, A., Pacchiarotti, A., Martelli, M., Guglielmi, C., Mandelli, F., Baroni, C. D., and Le Coco, F. (1997). Pathogenetic and clinical implications of Bcl-6 and Bcl-2 gene configuration in nodal diffuse large B-cell lymphomas. *Journal of Pathology* **183**, 281-286.

Pezzella, F., Gatter, K. C., Mason, D. Y., Bastard, C., Duval, C., Krajewski, A., Turner, G. E., Ross, F. M., Clark, H., and Jones, D. B. (1990). Bcl-2 protein

expression in follicular lymphomas in absence of 14;18 translocation [letter] [see comments]. *Lancet* **336**, 1510-1511.

Pinyol, M., Cobo, F., Bea, S., Jares, P., Nayach, I., Fernandez, P. L., Montserrat, E., Cardesa, A., and Campo, E. (1998). p16(INK4a) gene inactivation by deletions, mutations, and hypermethylation is associated with transformed and aggressive variants of non-Hodgkin's lymphomas. *Blood* **91**, 2977-2984.

Pinyol, M., Hernandez, L., Martinez, A., Cobo, F., Hernandez, S., Bea, S., Lopez-Guillermo, A., Nayach, I., Palacin, A., Nadal, A., Fernandez, P. L., Montserrat, E., Cardesa, A., and Campo, E. (2000). INK4a/ARF locus alterations in human non-Hodgkin's lymphomas mainly occur in tumors with wild-type p53 gene. *American Journal of Pathology* **156**, 1987-1996.

Poi, M. J., Yen, T., Li, J., Song, H., Lang, J. C., Schuller, D. E., Pearl, D. K., Casto, B. C., Tsai, M. D., and Weghorst, C. M. (2001). Somatic INK4a-ARF locus mutations: a significant mechanism of gene inactivation in squamous cell carcinomas of the head and neck. *Molecular Carcinogenesis* **30**, 26-36.

Polack, A., Hörtnagel, K., Pajic, A., Christoph, B., Baier, B., Falk, M., Mautner, J., Geltinger, C., Bornkamm, G. W., and Kempkes, B. (1996). *c-myc* activation renders proliferation of Epstein-Barr virus (EBV)-transformed cells independent of EBV nuclear antigen 2 and latent membrane protein 1. *Proceedings of National Academy of Sciences* **96**, 10411-10416.

Polito, P., Cilia, A. M., Gloghini, A., Cozzi, M., Perin, T., De Paoli, P., Gaidano, G., and Carbone, A. (1995). High frequency of EBV association with non-random abnormalities of the chromosome region 1q21-25 in AIDS-related Burkitt's lymphoma-derived cell lines. *International Journal of Cancer* **61**, 370-374.

Pomerantz, J., Schreiber-Agus, N., Liegeois, N. J., Silverman, A., Alland, L., Chin, L., Potes, J., Chen, K., Orlow, I., Lee, H. W., Cordon-Cardo, C., and DePinho, R. A. (1998). The Ink4a tumor suppressor gene product, p19Arf, interacts with MDM2 and neutralizes MDM2's inhibition of p53. *Cell* **92**, 713-723.

Pope, J.H., Horne, M.K., and Scott, W. (1968). Transformation of foetal human leukocytes *in vitro* by filtrates of a human leukaemic cell line containing herpes-like virus. *International Journal of Cancer* **3**, 857-866.

Popescu, N. C., Chen, M. C., Simpson, S., Solinas, S., and DiPaolo, J. A. (1993). A Burkitt lymphoma cell line with integrated Epstein-Barr virus at a stable chromosome modification site. *Virology* **195**, 248-251.

Pozniak, C. D., Radinovic, S., Yang, A., McKeon, F., Kaplan, D. R., and Miller, F. D. (2000). An anti-apoptotic role for the p53 family member, p73, during developmental neuron death [see comments]. *Science* **289**, 304-306.

Prives, C. and Hall, P. A. (1999). The p53 pathway. *Journal of Pathology* **187**, 112-126.

Pulvertaft, R.J.V (1965). A study of malignant tumours in Nigeriaby short term tissue culture. *Journal of Clinical Pathology* **18**, 261-273.

Purtilo, D. T., Cassel, C. K., Yang, J. P., and Harper, R. (1975). X-linked recessive progressive combined variable immunodeficiency (Duncan's disease). *Lancet* **1**, 935-940.

Quelle, D. E., Cheng, M., Ashmun, R. A., and Sherr, C. J. (1997). Cancer-associated mutations at the INK4a locus cancel cell cycle arrest by p16INK4a but not by the alternative reading frame protein p19ARF. *Proceedings of the National Academy of Sciences of the United States of America* **94**, 669-673.

Quelle, D. E., Zindy, F., Ashmun, R. A., and Sherr, C. J. (1995). Alternative reading frames of the INK4a tumor suppressor gene encode two unrelated proteins capable of inducing cell cycle arrest. *Cell* **83**, 993-1000.

Raab-Traub, N., Rajadurai, P., Flynn, K., and Lanier, A. P. (1991). Epstein-Barr virus infection in carcinoma of the salivary gland. *Journal of Virology* **65**, 7032-7036.

Rabbitts, T. H., Hamlyn, P. H., and Baer, R. (1983). Altered nucleotide sequences of a translocated c-myc gene in Burkitt lymphoma. *Nature* **306**, 760-765.

Radkov, S. A., Kellam, P., and Boshoff, C. (2000). The latent nuclear antigen of Kaposi sarcoma-associated herpesvirus targets the retinoblastoma-E2F pathway and with the oncogene Hras transforms primary rat cells. *Nature Medicine* **6**, 1121-1127.

Ratner, L., Lee, J., Tang, S., Redden, D., Hamzeh, F., Herndier, B., Scadden, D., Kaplan, L., Ambinder, R., Levine, A., Harrington, W., Grochow, L., Flexner, C., Tan, B., and Straus, D. (2001). Chemotherapy for Human Immunodeficiency Virus-Associated Non-Hodgkin's Lymphoma in Combination With Highly Active Antiretroviral Therapy. *Journal of Clinical Oncology* **19**, 2171-2178.

Ratovitski, E. A., Patturajan, M., Hibi, K., Trink, B., Yamaguchi, K., and Sidransky, D. (2001). p53 associates with and targets Delta Np63 into a protein degradation pathway. *Proceedings of the National Academy of Sciences of the United States of America* **98**, 1817-1822.

Raycroft, L., Wu, H. Y., and Lozano, G. (1990). Transcriptional activation by wild-type but not transforming mutants of the p53 anti-oncogene. *Science* **249**, 1049-1051.

Reed, J. C. (1997). Double identity for proteins of the Bcl-2 family. *Nature* **387**, 773-776.

Reed, J. C., Cuddy, M., Slabiak, T., Croce, C. M., and Nowell, P. C. (1988). Oncogenic potential of bcl-2 demonstrated by gene transfer. *Nature* **336**, 259-261.

Riboldi, P., Gaidano, G., Schettino, E. W., Steger, T. G., Knowles, D. M., Dalla-Favera, R., and Casali, P. (1994). Two acquire immunodeficiency syndrome-

associated Burkitt's lymphomas produce specific anti-i IgM cold agglutinins using somatically mutated VH4-21 segments. *Blood* **83 (10)**, 2952-2961.

Rickinson, A. B., and Kieff, E. (1996). "Epstein-Barr virus." 3rd ed. *In* Fields Virology (B.N. Fields, D.M. Knipe, and P.M. Howley, Eds.) **2**, 2397-2446. Lippincott-Raven Publishers, Philadelphia, Pennsylvania, USA.

Rizos, H., Darmanian, A. P., Mann, G. J., and Kefford, R. F. (2000). Two arginine rich domains in the p14ARF tumour suppressor mediate nucleolar localization. *Oncogene* **19**, 2978-2985.

Roschke, V., Kopantzev, E., Dertzbaugh, M., and Rudikoff, S. (1997). Chromosomal translocations deregulating c-myc are associated with normal immune responses. *Oncogene* **14**, 3011-3016.

Rosenblum, M. L., Levy, R. M., Bredesen, D. E., So, Y. T., Wara, W., and Ziegler, J. L. (1988). Primary central nervous system lymphomas in patients with AIDS. *Annals of Neurology* **23 Suppl**, S13-S16.

Roussel, M. F. (1999). The INK4 family of cell cycle inhibitors in cancer. *Oncogene* **18**, 5311-5317.

Rowan, S., Ludwig, R. L., Haupt, Y., Bates, S., Lu, X., Oren, M., and Vousden, K. H. (1996). Specific loss of apoptotic but not cell-cycle arrest function in a human tumor derived p53 mutant. *EMBO Journal* **15**, 827-838.

Rowe, M., Lear, A. L., Croom-Carter, D., Davies, A. H., and Rickinson, A. B. (1992). Three pathways of Epstein-Barr virus gene activation from EBNA1-positive latency in B lymphocytes. *Journal of Virology* **66**, 122-131.

Ruas, M. and Peters, G. (1998). The p16INK4a/CDKN2A tumor suppressor and its relatives. *Biochimica et Biophysica Acta* **1378**, F115-F177.

Rubio, R. (1994). Hodgkin's disease associated with human immunodeficiency virus infection. A clinical study of 46 cases. Cooperative Study Group of Malignancies Associated with HIV Infection of Madrid. *Cancer* **73**, 2400-2407.

Russo, J. J., Bohenzky, R. A., Chien, M. C., Chen, J., Yan, M., Maddalena, D., Parry, J. P., Peruzzi, D., Edelman, I. S., Chang, Y., and Moore, P. S. (1996). Nucleotide sequence of the Kaposi sarcoma-associated herpesvirus (HHV8). *Proceedings of the National Academy of Sciences of the United States of America* **93**, 14862-14867.

Sahota, S. S., Davis, Z., Hamblin, T. J., and Stevenson, F. K. (2000). Somatic mutation of bcl-6 genes can occur in the absence of V(H) mutations in chronic lymphocytic leukemia. *Blood* **95**, 3534-3540.

Saiki, R. K., Gelfand, D. H., Stoffel, S., Scharf, S. J., Higuchi, R., Horn, G. T., Mullis, K. B., and Erlich, H. A. (1988). Primer-directed enzymatic amplification of DNA with a thermostable DNA polymerase. *Science* **239**, 487-491.

Saiki, R. K., Scharf, S., Faloona, F., Mullis, K. B., Horn, G. T., Erlich, H. A., and Arnheim, N. (1985). Enzymatic amplification of beta-globin genomic sequences and restriction site analysis for diagnosis of sickle cell anemia. *Science* **230**, 1350-1354.

Salghetti, S. E., Kim, S. Y., and Tansey, W. P. (1999). Destruction of Myc by ubiquitin-mediated proteolysis: cancer-associated and transforming mutations stabilize Myc. *EMBO Journal* **18**, 717-726.

Sambrook, J., Fritsch, E. F., and Maniatis, T. (1989). "Molecular cloning: A laboratory manual." 2nd ed. Cold Spring Harbour Laboratory Press, New York, USA.

Sanchez-Cespedes, M., Reed, A. L., Buta, M., Wu, L., Westra, W. H., Herman, J. G., Yang, S. C., Jen, J., and Sidransky, D. (1999). Inactivation of the INK4A/ARF locus frequently coexists with TP53 mutations in non-small cell lung cancer. *Oncogene* **18**, 5843-5849.

Sangfelt, O., Erickson, S., Einhorn, S., and Grander, D. (1997). Induction of Cip/Kip and Ink4 cyclin dependent kinase inhibitors by interferon-alpha in hematopoietic cell lines. *Oncogene* **14**, 415-423.

Sarid, R., Flore, O., Bohenzky, R. A., Chang, Y., and Moore, P. S. (1998). Transcription mapping of the Kaposi's sarcoma-associated herpesvirus (human herpesvirus 8) genome in a body cavity-based lymphoma cell line (BC-1). *Journal of Virology* **72**, 1005-1012.

Schmale, H. and Bamberger, C. (1997). A novel protein with strong homology to the tumor suppressor p53. *Oncogene* **15**, 1363-1367.

Schwab, M., Varmus, H. E., and Bishop, J. M. (1985). Human N-myc gene contributes to neoplastic transformation of mammalian cells in culture. *Nature* **316**, 160-162.

Serrano, M., Hannon, G. J., and Beach, D. (1993). A new regulatory motif in cell-cycle control causing specific inhibition of cyclin D/CDK4 [see comments]. *Nature* **366**, 704-707.

Seto, M., Jaeger, U., Hockett, R. D., Graninger, W., Bennett, S., Goldman, P., and Korsmeyer, S. J. (1988). Alternative promoters and exons, somatic mutation and deregulation of the Bcl-2-Ig fusion gene in lymphoma. *EMBO Journal* **7**, 123-131.

Seyfert, V. L., Allman, D., He, Y., and Staudt, L. M. (1996). Transcriptional repression by the proto-oncogene BCL-6. *Oncogene* **12**, 2331-2342.

Shaffer, A. L., Yu, X., He, Y., Boldrick, J., Chan, E. P., and Staudt, L. M. (2000). BCL-6 represses genes that function in lymphocyte differentiation, inflammation, and cell cycle control. *Immunity* **13**, 199-212.

Sheiness, D. and Bishop, J. M. (1979). DNA and RNA from uninfected vertebrate cells contain nucleotide sequences related to the putative transforming gene of avian myelocytomatosis virus. *Journal of Virology* **31**, 514-521.

Shen, H. M., Peters, A., Baron, B., Zhu, X., and Storb, U. (1998). Mutation of BCL-6 gene in normal B cells by the process of somatic hypermutation of Ig genes. *Science* **280**, 1750-1752.

Shen-Ong, G. L., Keath, E. J., Piccoli, S. P., and Cole, M. D. (1982). Novel myc oncogene RNA from abortive immunoglobulin-gene recombination in mouse plasmacytomas. *Cell* **31**, 443-452.

Sherr, C. J. (1996). Cancer cell cycles. *Science* **274**, 1672-1677.

Sherr, C. J. and Roberts, J. M. (1995). Inhibitors of mammalian G1 cyclin-dependent kinases. *Genes and Development* **9**, 1149-1163.

Sherr, C. J. and Weber, J. D. (2000). The ARF/p53 pathway. *Current Opinion in Genetics and Development* **10**, 94-99.

Shibata, D., Weiss, L. M., Nathwani, B. N., Brynes, R. K., and Levine, A. M. (1991). Epstein-Barr virus in benign lymph node biopsies from individuals infected with the human immunodeficiency virus is associated with concurrent or subsequent development of non-Hodgkin's lymphoma. *Blood* **77**, 1527-1533.

Shieh, S. Y., Ikeda, M., Taya, Y., and Prives, C. (1997). DNA damage-induced phosphorylation of p53 alleviates inhibition by MDM2. *Cell* **91**, 325-334.

Shuman, S. (1994). Novel approach to molecular cloning and polynucleotide synthesis using vaccinia DNA topoisomerase. *Journal of Biological Chemistry* **269**, 32678-32684.

Siebert, R., Willers, C. P., and Opalka, B. (1996). Role of the cyclin-dependent kinase 4 and 6 inhibitor gene family p15, p16, p18 and p19 in leukemia and lymphoma. *Leukemia and Lymphoma* **23**, 505-520.

Silvestrini, R., Veneroni, S., Daidone, M. G., Benini, E., Boracchi, P., Mezzetti, M., Di Fronzo, G., Rilke, F., and Veronesi, U. (1994). The Bcl-2 protein: a prognostic indicator strongly related to p53 protein in lymph node-negative breast cancer patients. *Journal of the National Cancer Institute* **86**, 499-504.

Smith, D. B., Pathirana, S., Davidson, F., Lawlor, E., Power, J., Yap, P. L., and Simmonds, P. (1997). The origin of hepatitis C virus genotypes. *Journal of General Virology* **78**, 321-328.

Soulier, J., Grollet, L., Oksenhendler, E., Cacoub, P., Cazals-Hatem, D., Babinet, P., d'Agay, M. F., Clauvel, J. P., Raphael, M., Degos, L., *et al.* (1995). Kaposi's sarcoma-associated herpesvirus-like DNA sequences in multicentric Castleman's disease. *Blood* **86**, 1276-1280.

Soussi, T., Caron, de Fromentel, and May, P. (1990). Structural aspects of the p53 protein in relation to gene evolution. *Oncogene* **5**, 945-952.

Southern, E. M. (1975). Detection of specific sequences among DNA fragments separated by gel electrophoresis. *Journal of Molecular Biology* **98**, 503-517.

Spencer, C. A. and Groudine, M. (1991). Control of c-myc regulation in normal and neoplastic cells. *Advances in Cancer Research* **56:1-48**, 1-48.

Spruck, C. H., Gonzalez-Zulueta, M., Shibata, A., Simoneau, A. R., Lin, M. F., Gonzales, F., Tsai, Y. C., and Jones, P. A. (1994). p16 gene in uncultured tumours. *Nature* **370**, 183-184.

Srivastava, S., Zou, Z. Q., Pirollo, K., Blattner, W., and Chang, E. H. (1990). Germ-line transmission of a mutated p53 gene in a cancer-prone family with Li-Fraumeni syndrome [see comments]. *Nature* **348**, 747-749.

Stamatatos, L. and Cheng-Mayer, C. (1993). Evidence that the structural conformation of envelope gp120 affects human immunodeficiency virus type 1 infectivity, host range, and syncytium-forming ability. *Journal of Virology* **67**, 5635-5639.

Staskus, K. A., Sun, R., Miller, G., Racz, P., Jaslowski, A., Metroka, C., Brett-Smith, H., and Haase, A. T. (1999). Cellular tropism and viral interleukin-6 expression distinguish human herpesvirus 8 involvement in Kaposi's sarcoma, primary effusion lymphoma, and multicentric Castleman's disease. *Journal of Virology* **73**, 4181-4187.

Steven, N. M. Infectious Mononucleosis. Epstein-Barr virus Report 3, 91-95. 1996.

Stone, S., Dayananth, P., Jiang, P., Weaver-Feldhaus, J. M., Tavtigian, S. V., Cannon-Albright, L., and Kamb, A. (1995). Genomic structure, expression and mutational analysis of the P15 (MTS2) gene. *Oncogene* **11**, 987-991.

Stott, F. J., Bates, S., James, M. C., McConnell, B. B., Starborg, M., Brookes, S., Palmero, I., Ryan, K., Hara, E., Vousden, K. H., and Peters, G. (1998). The alternative product from the human CDKN2A locus, p14(ARF), participates in a regulatory feedback loop with p53 and MDM2. *EMBO Journal* **17**, 5001-5014.

Strasser, A., Harris, A. W., Bath, M. L., and Cory, S. (1990). Novel primitive lymphoid tumours induced in transgenic mice by cooperation between myc and bcl-2. *Nature* **348**, 331-333.

Strasser, A., Harris, A. W., Jacks, T., and Cory, S. (1994). DNA damage can induce apoptosis in proliferating lymphoid cells via p53-independent mechanisms inhibitable by Bcl-2 [see comments]. *Cell* **79**, 329-339.

Straus, D. J., Huang, J., Testa, M. A., Levine, A. M., and Kaplan, L. D. (1998). Prognostic factors in the treatment of human immunodeficiency virus-associated non-Hodgkin's lymphoma: analysis of AIDS Clinical Trials Group protocol 142--low-dose versus standard-dose m-BACOD plus granulocyte-macrophage colony-stimulating factor. National Institute of Allergy and Infectious Diseases. *Journal of Clinical Oncology* **16**, 3601-3606.

Strauss, B. S. (2000). Role in tumorigenesis of silent mutations in the TP53 gene. *Mutation Research* **457**, 93-104.

Subar, M., Neri, A., Inghirami, G., Knowles, D. M., and Dalla-Favera, R. (1988). Frequent c-myc oncogene activation and infrequent presence of Epstein-Barr virus genome in AIDS-associated lymphoma. *Blood* **72**, 667-671.

Subler, M. A., Martin, D. W., and Deb, S. (1994). Activation of the human immunodeficiency virus type 1 long terminal repeat by transforming mutants of human p53. *Journal of Virology* **68**, 103-110.

Summers, K. E., Goff, L. K., Wilson, A. G., Gupta, R. K., Lister, T. A., and Fitzgibbon, J. (2001). Frequency of the Bcl-2/IgH rearrangement in normal individuals: implications for the monitoring of disease in patients with follicular lymphoma. *Journal of Clinical Oncology* **19**, 420-424.

Susin, S. A., Zamzami, N., Castedo, M., Hirsch, T., Marchetti, P., Macho, A., Daugas, E., Geuskens, M., and Kroemer, G. (1996). Bcl-2 inhibits the mitochondrial release of an apoptogenic protease. *Journal of Experimental Medicine* **184**, 1331-1341.

Takada, N., Ozaki, T., Ichimiya, S., Todo, S., and Nakagawara, A. (1999). Identification of a transactivation activity in the COOH-terminal region of p73 which is impaired in the naturally occurring mutants found in human neuroblastomas. *Cancer Research* **59**, 2810-2814.

Takagi, M., Nishioka, M., Kakihara, H., Kitabayashi, M., Inoue, H., Kawakami, B., Oka, M., and Imanaka, T. (1997). Characterization of DNA polymerase from Pyrococcus sp. strain KOD1 and its application to PCR. *Applied and Environmental Microbiology* **63**, 4504-4510.

Takahashi, T., Nau, M. M., Chiba, I., Birrer, M. J., Rosenberg, R. K., Vinocour, M., Levitt, M., Pass, H., Gazdar, A. F., and Minna, J. D. (1989). p53: a frequent target for genetic abnormalities in lung cancer. *Science* **246**, 491-494.

Talbot, S. J., Weiss, R. A., Kellam, P., and Boshoff, C. (1999). Transcriptional analysis of human herpesvirus-8 open reading frames 71, 72, 73, K14, and 74 in a primary effusion lymphoma cell line. *Virology* **257**, 84-94.

Tanaka, H., Shimada, Y., Imamura, M., Shibagaki, I., and Ishizaki, K. (1997). Multiple types of aberrations in the p16 (INK4a) and the p15(INK4b) genes in 30 esophageal squamous-cell-carcinoma cell lines. *International Journal of Cancer* **70**, 437-442.

Tanaka, S., Louie, D., Kant, J., and Reed, J. C. (1992). Application of a PCR-mismatch technique to the BCL-2 gene: detection of point mutations in BCL-2 genes of malignancies with a t(14,18). *Leukemia* **6 Suppl 3**, 15S-19S.

Taub, R., Moulding, C., Battey, J., Murphy, W., Vasicek, T., Lenoir, G. M., and Leder, P. (1984). Activation and somatic mutation of the translocated c-myc gene in burkitt lymphoma cells. *Cell* **36**, 339-348.

Taylor, G. R. (1991). Polymerase chain reaction: Basic principles and automation. *In* "PCR: A practical approach." (M.J. McPherson, P. Quirke, and G.R. Taylor, Eds.), 1-14. Oxford University Press, Oxford, UK.

Tenner-Racz, K., Racz, P., Bofill, M., Schulz-Meyer, A., Dietrich, M., Kern, P., Weber, J., Pinching, A. J., Veronese-Dimarzo, F., Popovic, M., and . (1986). HTLV-III/LAV viral antigens in lymph nodes of homosexual men with persistent generalized lymphadenopathy and AIDS. *American Journal of Pathology* **123**, 9-15.

Theodorakis, P., D'Sa-Eipper, C., Subramanian, T., and Chinnadurai, G. (1996). Unmasking of a proliferation-restraining activity of the anti-apoptosis protein EBV BHRF1. *Oncogene* **12**, 1707-1713.

Thomas, J. A., Allday, M. J., and Crawford, D. H. (1991). Epstein-Barr virus-associated lymphoproliferative disorders in immunocompromised individuals. *Advances in Cancer Research* **57**, 329-380.

Thomas, J. A., Brookes, L. A., McGowan, I., Weller, I., and Crawford, D. H. (1996). HHV8 DNA in normal gastrointestinal mucosa from HIV seropositive people. *Lancet* **347**, 1337-1338.

Tibbetts, R. S., Brumbaugh, K. M., Williams, J. M., Sarkaria, J. N., Cliby, W. A., Shieh, S. Y., Taya, Y., Prives, C., and Abraham, R. T. (1999). A role for ATR in the DNA damage-induced phosphorylation of p53. *Genes and Development* **13**, 152-157.

Trink, B., Okami, K., Wu, L., Sriuranpong, V., Jen, J., and Sidransky, D. (1998). A new human p53 homologue [letter] [see comments] [published erratum appears in Nat Med 1998 Sep 4(9): 982]. *Nature Medicine* **4**, 747-748.

Trovato, R., Luppi, M., Barozzi, P., Da Prato, L., Maiorana, A., Lico, S., Marasca, R., Torricelli, P., Torelli, G., and Ceccherini-Nelli, L. (1999). Cellular localization of human herpesvirus 8 in nonneoplastic lymphadenopathies and chronic interstitial pneumonitis by in situ polymerase chain reaction studies. *Journal of Human Virology* **2**, 38-44.

Tsujimoto, Y. and Croce, C. M. (1986). Analysis of the structure, transcripts, and protein products of bcl-2, the gene involved in human follicular lymphoma. *Proceedings of the National Academy of Sciences of the United States of America* **83**, 5214-5218.

Tsujimoto, Y., Finger, L. R., Yunis, J., Nowell, P. C., and Croce, C. M. (1984). Cloning of the chromosome breakpoint of neoplastic B cells with the t(14;18) chromosome translocation. *Science* **226**, 1097-1099.

Tsujimoto, Y., Gorham, J., Cossman, J., Jaffe, E., and Croce, C. M. (1985). The t(14;18) chromosome translocations involved in B-cell neoplasms result from mistakes in VDJ joining. *Science* **229**, 1390-1393.

Uccini, S., Monardo, F., Vitolo, D., Faggioni, A., Gradilone, A., Agliano, A. M., Manzari, V., Ruco, L. P., and Baroni, C. D. (1989). Human immunodeficiency virus (HIV) and Epstein-Barr virus (EBV) antigens and genome in lymph nodes of HIV-positive patients affected by persistent generalized lymphadenopathy (PGL). *American Journal of Clinical Pathology* **92**, 729-735.

Uchida, T., Watanabe, T., Kinoshita, T., Murate, T., Saito, H., and Hotta, T. (1995). Mutational analysis of the CDKN2 (MTS1/p16ink4A) gene in primary B-cell lymphomas. *Blood* **86**, 2724-2731.

Ueda, Y., Hijikata, M., Takagi, S., Chiba, T., and Shimotohno, K. (1999). New p73 variants with altered C-terminal structures have varied transcriptional activities. *Oncogene* **18**, 4993-4998.

UNAIDS/WHO (2000). Global summary of the HIV/AIDS epidemic, December 2000.

Vaux, D. L., Cory, S., and Adams, J. M. (1988). Bcl-2 gene promotes haemopoietic cell survival and cooperates with c-myc to immortalize pre-B cells. *Nature* **335**, 440-442.

Veis, D. J., Sorenson, C. M., Shutter, J. R., and Korsmeyer, S. J. (1993). Bcl-2-deficient mice demonstrate fulminant lymphoid apoptosis, polycystic kidneys, and hypopigmented hair. *Cell* **75**, 229-240.

Villuendas, R., Sanchez-Beato, M., Martinez, J. C., Saez, A. I., Martinez-Delgado, B., Garcia, J. F., Mateo, M. S., Sanchez-Verde, L., Benitez, J., Martinez, P., and Piris, M. A. (1998). Loss of p16/INK4A protein expression in non-Hodgkin's lymphomas is a frequent finding associated with tumor progression. *American Journal of Pathology* **153**, 887-897.

Visscher, D. W., Sarkar, F. H., Shimoyama, R. K., and Crissman, J. D. (1996). Correlation between p53 immunostaining patterns and gene sequence mutations in breast carcinoma. *Diagnostic Molecular Pathology* **5**, 187-193.

Vitolo, U., Gaidano, G., Botto, B., Volpe, G., Audisio, E., Bertini, M., Calvi, R., Freilone, R., Novero, D., Orsucci, L., Pastore, C., Capello, D., Parvis, G., Sacco, C., Zagonel, V., Carbone, A., Mazza, U., Palestro, G., Saglio, G., and Resegotti, L. (1998). Rearrangements of bcl-6, bcl-2, c-myc and 6q deletion in B-diffuse large-cell lymphoma: clinical relevance in 71 patients. *Annals of Oncology* **9**, 55-61.

Vogelstein, B., Fearon, E. R., Hamilton, S. R., Kern, S. E., Preisinger, A. C., Leppert, M., Nakamura, Y., White, R., Smits, A. M., and Bos, J. L. (1988). Genetic alterations during colorectal-tumor development. *New England Journal of Medicine* **319**, 525-532.

Vonlanthen, S., Heighway, J., Tschan, M. P., Borner, M. M., Altermatt, H. J., Kappeler, A., Tobler, A., Fey, M. F., Thatcher, N., Yarbrough, W. G., and Betticher, D. C. (1998). Expression of p16INK4a/p16alpha and p19ARF/p16beta is frequently altered in non-small cell lung cancer and correlates with p53 overexpression. *Oncogene* **17**, 2779-2785.

Wang, Y., Reed, M., Wang, P., Stenger, J. E., Mayr, G., Anderson, M. E., Schwedes, J. F., and Tegtmeyer, P. (1993). p53 domains: identification and characterization of two autonomous DNA-binding regions. *Genes and Development* **7**, 2575-2586.

Weber, J. D., Jeffers, J. R., Rehg, J. E., Randle, D. H., Lozano, G., Roussel, M. F., Sherr, C. J., and Zambetti, G. P. (2000). p53-independent functions of the p19(ARF) tumor suppressor. *Genes and Development* **14**, 2358-2365.

Weber, J. D., Taylor, L. J., Roussel, M. F., Sherr, C. J., and Bar-Sagi, D. (1999). Nucleolar Arf sequesters Mdm2 and activates p53. *Nature Cell Biology* **1**, 20-26.

Weinberg, R. A. (1994). Oncogenes and tumor suppressor genes. *CA: A Cancer Journal for Clinicians* **44**, 160-170.

Weiss, L. M., Movahed, L. A., Warnke, R. A., and Sklar, J. (1989). Detection of Epstein-Barr viral genomes in Reed-Sternberg cells of Hodgkin's disease. *New England Journal of Medicine* **320**, 502-506.

Weiss, L. M., Warnke, R. A., Sklar, J., and Cleary, M. L. (1987). Molecular analysis of the t(14;18) chromosomal translocation in malignant lymphomas. *New England Journal of Medicine* **317**, 1185-1189.

Whitby, D., Howard, M. R., Tenant-Flowers, M., Brink, N. S., Copas, A., Boshoff, C., Hatzioannou, T., Suggett, F. E., Aldam, D. M., Denton, A. S., and . (1995). Detection of Kaposi sarcoma associated herpesvirus in peripheral blood of HIV-infected individuals and progression to Kaposi's sarcoma. *Lancet* **346**, 799-802.

Wilson, V. L., Yin, X., Thompson, B., Wade, K. R., Watkins, J. P., Wei, Q., and Lee, W. R. (2000). Oncogenic base substitution mutations in circulating leukocytes of normal individuals. *Cancer Research* **60**, 1830-1834.

Wiman, K. G., Clarkson, B., Hayday, A. C., Saito, H., Tonegawa, S., and Hayward, W. S. (1984). Activation of a translocated c-myc gene: role of structural alterations in the upstream region. *Proceedings of the National Academy of Sciences of the United States of America* **81**, 6798-6802.

Wolf, H., Hausen, H.z., and Becker, V. (1973). EB viral genomes in epithelial nasopharyngeal carcinoma cells. *Nature New Biology* **244**, 245-247.

Wu, X., Bayle, J. H., Olson, D., and Levine, A. J. (1993). The p53-mdm-2 autoregulatory feedback loop. *Genes and Development* **7**, 1126-1132.

Wyke, J. (1997). Viruses and cancer. *In* "Introduction to the cellular and molecular biology of cancer." 3rd ed. (L.M. Franks and N.M. Teich, Eds.), 151-167. Oxford University Press, Oxford, UK.

Yabumoto, K., Akasaka, T., Muramatsu, M., Kadowaki, N., Hayashi, T., Ohno, H., Fukuhara, S., and Okuma, M. (1996). Rearrangement of the 5' cluster region of the BCL2 gene in lymphoid neoplasm: a summary of nine cases. *Leukemia* **10**, 970-977.

Yamaguchi, K., Wu, L., Caballero, O. L., Hibi, K., Trink, B., Resto, V., Cairns, P., Okami, K., Koch, W. M., Sidransky, D., and Jen, J. (2000). Frequent gain of the p40/p51/p63 gene locus in primary head and neck squamous cell carcinoma. *International Journal of Cancer* **86**, 684-689.

Yamamura, M., Uyemura, K., Deans, R. J., Weinberg, K., Rea, T. H., Bloom, B. R., and Modlin, R. L. (1991). Defining protective responses to pathogens: cytokine profiles in leprosy lesions. *Science* **254**, 277-279.

Yang, A., Kaghad, M., Wang, Y., Gillett, E., Fleming, M. D., Dotsch, V., Andrews, N. C., Caput, D., and McKeon, F. (1998). p63, a p53 homolog at 3q27-29, encodes multiple products with transactivating, death-inducing, and dominant-negative activities. *Molecular Cell* **2**, 305-316.

Yang, A., Schweitzer, R., Sun, D., Kaghad, M., Walker, N., Bronson, R. T., Tabin, C., Sharpe, A., Caput, D., Crum, C., and McKeon, F. (1999). p63 is essential for regenerative proliferation in limb, craniofacial and epithelial development. *Nature* **398**, 714-718.

Yang, A., Walker, N., Bronson, R., Kaghad, M., Oosterwegel, M., Bonnin, J., Vagner, C., Bonnet, H., Dikkes, P., Sharpe, A., McKeon, F., and Caput, D. (2000). p73-deficient mice have neurological, pheromonal and inflammatory defects but lack spontaneous tumours. *Nature* **404**, 99-103.

Yang, E. and Korsmeyer, S. J. (1996). Molecular thanatopsis: a discourse on the BCL2 family and cell death. *Blood* **88**, 386-401.

Yano, T., van Krieken, J. H., Magrath, I. T., Longo, D. L., Jaffe, E. S., and Raffeld, M. (1992). Histogenetic correlations between subcategories of small noncleaved cell lymphomas. *Blood* **79**, 1282-1290.

Yao, Q. Y., Rickinson, A. B., and Epstein, M. A. (1985). A re-examination of the Epstein-Barr virus carrier state in healthy seropositive individuals. *International Journal of Cancer* **35**, 35-42.

Yao, Q. Y., Rowe, M., Morgan, A. J., Sam, C. K., Prasad, U., Dang, H., Zeng, Y., and Rickinson, A. B. (1991). Salivary and serum IgA antibodies to the Epstein-Barr virus glycoprotein gp340: incidence and potential for virus neutralization. *International Journal of Cancer* **48**, 45-50.

Ye, B. H. (2000). BCL-6 in the pathogenesis of non-Hodgkin's lymphoma. *Cancer Investigation* **18**, 356-365.

Ye, B. H., Cattoretti, G., Shen, Q., Zhang, J., Hawe, N., de Waard, R., Leung, C., Nouri-Shirazi, M., Orazi, A., Chaganti, R. S., Rothman, P., Stall, A. M., Pandolfi, P. P., and Dalla-Favera, R. (1997). The BCL-6 proto-oncogene controls germinal-centre formation and Th2-type inflammation. *Nature Genetics* **16**, 161-170.

Ye, B. H., Chaganti, S., Chang, C. C., Niu, H., Corradini, P., Chaganti, R. S., and Dalla-Favera, R. (1995a). Chromosomal translocations cause deregulated BCL6 expression by promoter substitution in B cell lymphoma. *EMBO Journal* **14**, 6209-6217.

Ye, B. H., Lista, F., Lo, Coco F., Knowles, D. M., Offit, K., Chaganti, R. S., and Dalla-Favera, R. (1993). Alterations of a zinc finger-encoding gene, BCL-6, in diffuse large-cell lymphoma. *Science* **262**, 747-750.

Ye, B. H., Lo, Coco F., Chang, C. C., Zhang, J., Migliazza, A., Cechova, K., Knowles, D. M., Offit, K., Chaganti, R. S., and Dalla-Favera, R. (1995b). Alterations of the BCL-6 gene in diffuse large-cell lymphoma. *Current Topics in Microbiology and Immunology* **194**, 101-108.

Yen-Moore, A., Hudnall, S. D., Rady, P. L., Wagner, R. F., Moore, T. O., Memar, O., Hughes, T. K., and Tyring, S. K. (2000). Differential expression of the HHV-8 vGCR cellular homolog gene in AIDS-associated and classic Kaposi's sarcoma: potential role of HIV-1 Tat. *Virology* **267**, 247-251.

Yin, X. M., Oltvai, Z. N., and Korsmeyer, S. J. (1994). BH1 and BH2 domains of Bcl-2 are required for inhibition of apoptosis and heterodimerization with Bax. *Nature* **369**, 321-323.

Yunis, J. J., Frizzera, G., Oken, M. M., McKenna, J., Theologides, A., and Arnesen, M. (1987). Multiple recurrent genomic defects in follicular lymphoma. A possible model for cancer. *New England Journal of Medicine* **316**, 79-84.

Yunis, J. J., Oken, M. M., Kaplan, M. E., Ensrud, K. M., Howe, R. R., and Theologides, A. (1982). Distinctive chromosomal abnormalities in histologic subtypes of non-Hodgkin's lymphoma. *New England Journal of Medicine* **307**, 1231-1236.

Zaika, A., Irwin, M., Sansome, C., and Moll, U. M. (2001). Oncogenes induce and activate endogenous p73 protein. *Journal of Biological Chemistry* **276**, 11310-11316.

Zan, H., Li, Z., Yamaji, K., Dramitinos, P., Cerutti, A., and Casali, P. (2000). B cell receptor engagement and T cell contact induce Bcl-6 somatic hypermutation in human B cells: identity with Ig hypermutation. *Journal of Immunology* **165**, 830-839.

Zhang, S. Y., Klein-Szanto, A. J., Sauter, E. R., Shafarenko, M., Mitsunaga, S., Nobori, T., Carson, D. A., Ridge, J. A., and Goodrow, T. L. (1994). Higher frequency of alterations in the p16/CDKN2 gene in squamous cell carcinoma cell lines than in primary tumors of the head and neck. *Cancer Research* **54**, 5050-5053.

Zhang, Y. and Xiong, Y. (1999). Mutations in human ARF exon 2 disrupt its nucleolar localization and impair its ability to block nuclear export of MDM2 and p53. *Molecular Cell* **3**, 579-591.

Zhu, J., Jiang, J., Zhou, W., and Chen, X. (1998). The potential tumor suppressor p73 differentially regulates cellular p53 target genes. *Cancer Research* **58**, 5061-5065.

Zindy, F., Eischen, C. M., Randle, D. H., Kamijo, T., Cleveland, J. L., Sherr, C. J., and Roussel, M. F. (1998). Myc signaling via the ARF tumor suppressor regulates p53-dependent apoptosis and immortalization. *Genes and Development* **12**, 2424-2433.

APPENDIX 1

Overview of the genetic, epigenetic and virological analysis in HIV-PGL

Case No.	*p53* mutation	p73			p63		$p16^{INK4a}$		$p15^{INK4b}$		$p14^{ARF}$	c-*myc*	*bcl-2*	*bcl-6* mutation	Viral status	
LN		C-term	ΔN	Meth	TA	ΔN	Expn	Meth	Expn	Meth	Expn				EBV	KSHV
1	+	ND	ND	-	ND	ND	ND	-	ND	-	ND	-	-	+	+	+
2	-	+	+	-	+	-	+	-	+	-	+	-	-	-	+	-
3	-	+	+	-	+	-	+	-	+	-	+	-	-	-	+	-
4	-	+	+	-	+	-	+	-	+	-	+	-	-	-	+	-
5	+	+	+	-	+	-	+	-	+	-	+	-	-	+	+	-
6	-	+	+	-	+	-	+	-	+	-	+	-	-	+	+	-
8	-	+	ND	-	-	-	ND	-	ND	-	+	-	-	-	+	-
9	+	+	+	-	+	-	+	-	+	-	+	-	-	+	+	-
10	-	+	+	-	+	-	+	-	+	-	+	-	-	-	+	-
12	-	+	ND	-	-	-	ND	-	ND	-	+	-	-	+	+	-
14	-	+	ND	-	-	-	ND	-	ND	-	+	-	-	+	+	-
15	+	+	+	-	+	-	+	-	+	-	+	-	-	+	+	+
16	+	+	+	-	+	-	+	-	+	-	+	-	-	-	+	-
17	-	+	+	-	+	-	+	-	+	-	+	-	-	-	+	-
18	-	+	+	-	+	-	+	-	+	-	+	-	-	-	+	-
19	-	+	+	-	+	-	+	-	+	-	+	-	-	+	+	-
20	+	+	+	-	+	-	+	-	+	-	+	-	-	+	+	-

APPENDIX 1 continued

Case No.	*p53* mutation	p73			p63		$p16^{INK4a}$		$p15^{INK4b}$		$p14^{ARF}$	c-*myc*	*bcl-2*	*bcl-6* mutation	Viral status	
		C-term	ΔN	Meth	TA	ΔN	Expn	Meth	Expn	Meth	Expn				EBV	KSHV
21	-	+	+	-	-	-	+	-	+	-	+	-	-	-	+	-
22	-	+	+	-	-	-	+	-	+	-	+	-	-	-	+	-
23	-	+	+	-	+	-	+	-	+	-	+	-	-	+	+	-
24	-	ND	ND	-	ND	ND	ND	-	ND	-	ND	-	-	+	+	-
25	-	ND	ND	-	ND	ND	ND	-	ND	-	ND	-	-	-	+	-
27	-	ND	ND	-	ND	ND	ND	-	ND	-	ND	-	-	-	+	-

+, positive; -, negative; ND, Not done; C-term, C terminus; Meth, methylation; Expn, Expression; EBV, Epstein-Barr virus; KSHV, Kaposi's-sarcoma associated herpes virus.

APPENDIX 2

Overview of the genetic, epigenetic and virological analysis in HIV-uninfected lymph nodes and tonsils

Case No.	*p53* mutation	p73			p63		$p16^{INK4a}$		$p15^{INK4b}$		$p14^{ARF}$	c-*myc*	*bcl-2*	*bcl-6* mutation	Viral status	
		C-term	ΔN	Meth	TA	ΔN	Expn	Meth	Expn	Meth	Expn				EBV	KSHV
T1	-	+	+	ND	-	+	+	ND	ND	ND	+	-	-	-	+	-
T2	-	-	-	ND	-	+	+	ND	+	ND	+	-	-	-	+	-
T3	-	+	+	ND	-	+	+	ND	+	ND	+	-	-	-	ND	-
T4	-	+	+	ND	-	+	+	ND	+	ND	+	-	-	-	+	-
T5	-	+	+	ND	-	+	+	ND	+	ND	+	-	-	-	+	-
T6	+	-	-	ND	-	-	+	ND	+	ND	+	-	-	-	+	-
T7	-	+	+	ND	+	+	+	ND	+	ND	+	-	-	-	+	-
2425	-	+	+	ND	-	-	+	ND	-	ND	ND	-	-	-	ND	-
2435	-	+	+	ND	+	-	+	ND	-	ND	+	+	-	-	-	-
2437	-	-	-	ND	-	-	+	ND	-	ND	+	-	-	-	+	-
2462	-	+	+	ND	+	-	+	ND	+	ND	+	-	-	-	+	-
2478	-	-	-	ND	-	-	+	ND	-	ND	+	-	-	-	+	-
2495	-	-	-	ND	+	-	+	ND	-	ND	-	-	-	+	+	-
2498	-	+	+	ND	+	-	+	ND	-	ND	+	-	-	-	+	-
2499	-	+	+	ND	+	-	+	ND	-	ND	+	-	-	+	+	-
2512	-	ND	-	ND	-	-	+	ND	-	ND	+	-	-	-	-	-

+, positive; -, negative; ND, Not done; C-term, C terminus; Meth, methylation; Expn, Expression; EBV, Epstein-Barr virus; KSHV, Kaposi's-sarcoma associated herpes virus.

APPENDIX 3

Commercial Suppliers

Amersham Pharmacia Biotec (UK) Ltd, Little Chalfont, Buckinghamshire, UK

Anachem/Scotlab, Luton, Bedforshire, UK

Beckman Instruments, High Wycombe, Bucks, UK

Beckton-Dickinson (UK) Ltd, Cowley, Oxford, UK

Bibby Sterilin Ltd, Stone, Staffordshire, UK

Biogenesis, Yeomans Way, Bournemouth, UK

Bio-Rad Laboratories Ltd, Hemel Hempstead, Hertfordshire, UK

BioWhittaker, Wokingham, Berkshire, UK

Clontech Laboratories, Basingstoke, Hampshire, UK

CP Laboratories, Saffron Walden, Essex, UK

Cryotechnics, Edinburgh, Lothian, UK

Dynal AS, Wirral, Merseyside, UK

Flowgen, Lichfield, Staffordshire, UK

Fred Baker, Runcorn, Cheshire, UK

Fuji Photo (UK) Ltd, London, UK

Harlan SeraLab, Hill Crest, Belton, Loughborough, UK

Heraeus, Brentwood, Essex, UK

Hybaid Ltd, Ashford, Middlesex, UK

ICN Biomedicals Ltd, Basingstoke Hampshire, UK

Intergen Company, Oxford Science Park, Oxford, UK

Invitrogen Corporation, NV Leek, Holland

Jencons, Leighton Buzzard, Bedfordshire, UK

Jet X-ray, London, UK

Leitz, Wild Leitz UK Ltd, Knowlhill, Milton Keynes, Buckinghamshire, UK

Life Technologies, Paisley, Scotland, UK

Merck EuroLab Ltd, Poole, Dorset, UK

Millipore (UK) Ltd, Watford, Hertfordshire, UK

National Diagnostics, Hessle, Hull, UK

Oswel DNA Services, Southampton, Hampshire, UK

PE Biosystems, Warrington, Cheshire, UK

Philip Harris, London, UK

Promega, Southhampton, UK

Qiagen, Crawley, West Sussex

Roche, Welwyn Garden City, Herts, UK

Sanyo Gallenkamp PLC, Loughborough, Leicestershire, UK

Scientific Lab Supplies Ltd, Coatbridge, Lanarkshire, UK

Shandon Scientific, Runcorn, Cheshire, UK

Sigma Chemical Company, Poole, Dorset, UK

Stratagene, Cambridge, UK

Stuart Scientific, Poole, Dorset, UK

Ultra Violet Products Ltd., Science Park, Cambridge, UK

Whatman, Maidstone, Kent, UK

APPENDIX 4

Clinical data on HIV-infected individuals with PGL

No.	DOB	Total lymphocyte count ($x10^9$/L)	HIV Viral load (viral RNA copies/ml)	Clinical presentation	Other viruses	ARV	Dead/Alive
1	26.1.47	0.8	nk	Multiple cutaneous KS Presumptive PCP	CMV, HSV, Adenovirus	nk	Died 25.9.83
2	nk	nk	nk	nk	nk	nk	nk
3	10.1.48	3.7	nk	Cutaneous KS	HepB, CMV, HSV	nk	Last seen 8.88
4	25.7.55	1.4	nk	Cryptococcal meningitis and pneumonia Cerebral atrophy on MRI OHL	Perianal oral warts, Perianal HSV, Hep B	AZT	Last FU 3.94
5	21.7.49	1.3	500,000	Hepatosplenomegaly OHL Shingles	HepB, Hep A, HSV, CMV, Adenovirus, measles	nk	Transferred to King's 11.94
6	3.9.45	1.5	nk	Oral KS	Hep B, CMV	AZT, DDC, D4T SQV, NFV	Alive under care MMC
8	3.4.48	2.6	nk	Cutaneous KS Hepatosplenomegaly	HepA, HepB, CMV	nk	nk
9	3.12.55	2.4	nk	Lung lobectomy Presumptive PCP CMV retinitis Cutaneous KS Cerebral Toxoplasmosis?	HepB	AZT	Died 4.89
10	1.9.56	1.2	nk	Cryptococcal meningitis (Treated), PCP Spastic paraparesis MRI brain atrophy	nk	AZT	Died

No.	DOB	Total lymphocyte count ($x10^9$/L)	HIV Viral load (viral RNA copies/ml)	Clinical presentation	Other viruses	ARV	Dead/Alive
12	18.3.48	nk	nk	nk	nk	nk	Transferred to St Stephens C&W 2.12.86
14	27.7.51	1.3	105,500	No AIDS defining diagnosis	HepB	nk	Alive and well (MMC)
15	nk	nk	nk	Typical KS, cutaneous, palatal, lymphedema Left pleural effusion	Herpes, CMV, HepB	nk	? Death
16	24.6.53	1.1	nk	Shingles, PCP CMV retinitis, MAI spleen and mesenteric LNs, cardiomegaly	HepB, VZV, CMV	AZT	Died 15.11.92
17	13.7.50	nk	nk	Cutaneous, palatal KS Thrombocytopenia, Presumptive PCP Hepatosplenomegaly HIV encephalopathy	HepB, Genital HSV	nk	Died 10.6.87
18	12.11.54	2.4	nk	Shingles	CMV, HSV	nk	Emigrated to Australia
19	10.4.63	1.8	nk	nk	HepB, HepA, CMV, HSV, Perianal warts	nk	Last seen 1.91
20	31.3.55	nk	nk	Thrombocytopenia PCP 21.9.86	HepB, Perianal warts, CMV, Measles	nk	Died
21	4.3.46	2	nk	PGL only	HepA, HepB, CMV, HSV, Measles, Adenovirus, Molluscum contagiosum, Perianal warts	nk	Transferred
22	12.7.53	1.9	60,300	KS palate	CMV, HSV, Measles	d4T, DDI, NFV, NVP	Alive (MMC)

No.	DOB	Total lymphocyte count ($x10^9$/L)	HIV Viral load (viral RNA copies/ml)	Clinical presentation	Other viruses	ARV	Dead/Alive
23	nk	nk	nk	nk	nk	nk	nk
24	30.3.56	1.6	nk	Cutaneous KS AIDS defining	HepB, CMV	nk	Last FU 5.91
25	12.8.50	nk	nk	PCP Pulmonary TB	Perianal warts, Genital HSV, Measles positive	nk	Last seen C&W 8.85
27	5.11.63	3.3	nk	Splenectomy Bacterial pneumonia OHL	HepB, Perinanal warts, Genital HSV	nk	Last FU 1992

HIV, Human immunodeficiency virus; PGL, persistent generalised lymphadenopathy; DOB, date of birth; nk, not known; pos, positive; FU, follow up; KS, Kaposi's sarcoma; PCP, pneumocystic carinii pneumonia; OHL, oral hairy leukoplakia; CMV, cytomegalovirus; HSV, herpes simplex virus; HepB; Hepatitis B; HepA, Hepatitis A; MRI, Magnetic resonance imaging; ARV, antiretrovirals; AZT, zidovudine (azidothymidine); DDC, zalcitabine (dideoxycytidine); DDI, dideoxyinosine; d4T, stavudine; SQV, saquinavir mesylate; NFV, nelfinavir mesylate; NVP, nevirapine; MAI, Mycobacterium avium intracellulare; LN, lymph node; MMC, Mortimer Market Centre; C&W; Chelsea and Westminster Hospital